Distribution of Virulence Factors among Multidrug Resistant Isolates of Uropathogenic *Escherichia coli*

By

Zara Rafaque

PhD Thesis

in

Microbiology

Department of Microbiology

Faculty of Biological Sciences

Quaid-i-Azam University

Islamabad

2019

Distribution of Virulence Factors among Multidrug Resistant Isolates of Uropathogenic *Escherichia coli*

A thesis submitted to Department of Microbiology, Quaid-i-Azam University, Islamabad, Pakistan in the partial fulfillment of the requirements for the degree of

Doctor of Philosophy in Microbiology

By

Zara Rafaque

Department of Microbiology

Faculty of Biological Sciences

Quaid-i-Azam University

Islamabad

2019

Dedicated to

ABU, AMMI & CHACHI

For their unprecedented love, support and trust

Author's Declaration

I Ms. Zara Rafaque hereby state that my Ph.D. thesis titled **"Distribution of Virulence Factors among Multidrug Resistant Isolates of Uropathogenic *Escherichia coli"*** is my own work and has not been submitted previously by me for taking any degree from Quaid-i-Azam University, Islamabad, Pakistan.

At any time if my statement is found to be incorrect even after I Graduate, the University has the right to withdraw my Ph.D. degree.

Ms. Zara Rafaque
Date: 02-01-2020

Plagiarism Undertaking

"**Distribution of Virulence Factors among Multidrug Resistant Isolates of Uropathogenic** *Escherichia coli*" is solely my research work with no significant contribution from any other person. Small contribution / help wherever taken has been duly acknowledged and that complete thesis has been written by me.

I understand the zero tolerance policy of the HEC and Quaid-i-Azam University towards plagiarism. Therefore I as an Author of the above titled thesis declare that no portion of my thesis has been plagiarized and any material used as reference is properly referred/cited.

I undertake that if I am found guilty of any formal plagiarism in the above titled thesis even after award of Ph.D degree and that HEC and the University has the right to publish my name on the HEC/University Website on which names of students are placed who submitted plagiarized thesis.
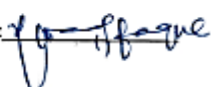
Student / Author Signature: _____

Name: **Ms. Zara Rafaque**

Certificate of Approval

This is to certify that the research work presented in this thesis, entitled titled "**Distribution of Virulence Factors among Multidrug Resistant Isolates of Uropathogenic *Escherichia coli*"** was conducted by **Ms. Zara Rafauqe** under the supervision of **Dr. Javid Iqbal Dasti**. No part of this thesis has been submitted anywhere else for any other degree. This thesis is submitted to the Department of Microbiology, Quaid-i-Azam University, Islamabad in partial fulfillment of the requirements for the degree of Doctor of Philosophy in field of **Microbiology**.
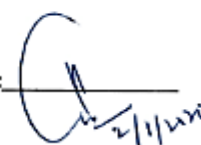
Student Name: <u>**Ms. Zara Rafaque**</u>   Signature: _____
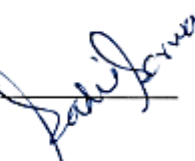
Examination Committee:

a) External Examiner 1:   Signature: _____

Dr. Naeem Akthar
Professor & Head of Department of Pathology
Rawalpindi Medical University, Rawalpindi

b) External Examiner 2:   Signature: _____

Dr. Sadia Sarwar
Associate Professor
Riphah Institute of Pharmaceutical Sciences
Dental Hospital, Near ISI Head Office
G-7/4, Islamabad

Supervisor Name: <u>**Dr. Javid Iqbal Dasti**</u>   Signature: _____

Name of HOD: <u>**Prof. Dr. Rani Faryal**</u>   Signature: _____

Table of Contents

LIST OF FIGURES

LIST OF TABLES

LIST OF ABBREVIATIONS

ABU   Asymptomatic bacteriuria

AMR   Antimicrobial resistance

APEC   Avian pathogenic *E coli*

ARDB   Antibiotic Resistance Database

ASB   Asymptomatic bacteriuria

AUC   Acute uncomplicated cystitis

AUP   Acute uncomplicated pyelonephritis

BAP   Blood agar plate

BHI   Brain heart infusion

BLAST   Basic Local Alignment Search Tool

CARD   Comprehensive Antibiotic Resistance Database

CAS   Chrome azurol S- agar

CAUTI   Community-acquired urinary tract infection

CA-UTI   Catheter associated urinary tract infection

CFU   Colony forming unit

CLED   Cytosine Lactose Electrolyte Deficient

CLSI   Clinical lab standard international

CNF-1   Cytotoxin necrotizing factor

CNS   Central nervous system

CRA   Congo red agar

CSH   Cell surface hydrophobicity

CV   Crystal violet

DAEC   Diffusely adherent *E. coli*

DAF   Decay accelerating factor

DDST   Double disc synergy test

DGE   Diglucosyl-C-enterobactin

dNTP   Deoxynucleotide Triphosphate

DTPA   Ddiethylenetriaminepentaacetic acid

EA	*ΔentBECiucABCD::cat*
EAEC	enteroaggregative *E. coli*
EH	*ΔentBEChemRT::cat*
EHEC	Enterohemorrhagic *E. coli*
EIEC	Enteroinvasive *E. coli*
EPEC	Enteropathogenic *E. coli*
ESBL	Extended spectrum *β* lactamase
ESCMID	European Society of Clinical Microbiology and Infectious Diseases
ETEC	Enterotoxigenic *E. coli*
EUCAST	European Committee for Antimicrobial Susceptibility Testing
Ex-PEC	Extraintestinal pathogenic *E coli*
EY	*ΔentBECirp1_2::cat*
EYA	*ΔentBECirp1_2iucABCD::cat*
FBS	Fetal bovine serum
FDA	Food and Drug Administration
FQ	Fluoroquinolone
FQR	Fluoroquinolone resistance
GPI	Glycosylphosphatidylinositol
HA	*ΔhemRTiucABCD::cat*
HAUTI	Hospital-acquired urinary tract infections
HPI	High pathogenicity island
HY	*ΔhemRTirp1_2::cat*
IBCs	Intracellular bacterial communities
IDC	Islamabad Diagnostic Centre
IDSA	Infectious Diseases Society of America
IS	Insertion sequence
IV	Intravenous
KO	Knock out
MBC	Minimum bactericidal concentration
MBEC	Minimum biofilm eradication concentration

MBIC	Minimum biofilm inhibitory concentration.
MBV	membrane bound vacuoles
MDR	Multi drug resistant
MEE	Multilocus enzyme electrophoresis
MGE	Monoglucosyl-C-enterobactin
MHB	Mueller-Hinton broth
MIC	minimal inhibitory concentration
MIC-b	Minimum inhibitory concentration-biofilm
MIC-p	Minimum inhibitory concentration-planktonic
MM	Minimal medium
MOI	Multiplicity of infection
MRHA	Mannose resistant haemagglutination
MSHA	Mannose sensitive haemagglutination
MSU	Midstream sample of urine
NDARO	National Database of Antibiotic Resistant Organisms
NMEC	Neonatal meningitis *E. coli*
OD	Optical density
OM	Outer membrane
PAI	Pathogenicity associated islands
PATRIC	The Pathosystems Resource Integration Centre
PBS	Phosphate buffer saline
PCR	Polymerase chain reaction
PFGE	pulsed-field gel electrophoresis
PIMS	Pakistan Institute of Medical Sciences
QIRs	Quiescent intracellular reservoirs
RPMI	Roswell Park Memorial Institute (culture medium)
rpm	Revolution per minute
RUTI	Recurrent urinary tract infections
SBA	Serum bactericidal activity
SD	Standard deviation

SEM	Scanning electron microscopy
TCP	Tissue culture plate
TGE	Triglucosyl-C-enterobactin
TM	Tube method
TSI	Triple Sugar Iron
UPEC	Uropathogenic *E. coli*
UTI	Urinary tract infections
UV	Ultra violet
VF	Virulence factors
VFDB	Virulence Factor Database
VRE	vancomycin-resistant *Enterococci*
WGS	Whole genome sequencing
WT	Wild type
YA	*Δirp1_2iucABCD::cat*

Acknowledgements

The ultimate praise and the deepest gratitude to the Almighty, the creator of the heavens and earth, the sole provider and nourisher – without his will nothing could be done. Thousands of salutations to all the messengers and Muhammad (PBUH) the greatest example for all the human beings, ever existed or would exist among humanity. I would like to express my heartfelt gratitude to my research supervisor **Dr. Javid Iqbal Dasti**, Quaid-i-Azam University, Islamabad, Pakistan. His scholastic guidance, continuous encouragement, sincere criticism and moral support has helped me throughout this study. I have great reverence and admiration for my co-supervisor **Prof. Simon Andrews** at School of Biological Sciences, University of Reading, UK. I am highly indebted for his supervision in fulfilling my research endeavors and enriching my research experience in University of Reading. I am also obliged to **Dr. Rani Faryal**, Chairperson Department of Microbiology, QAU, Islamabad, for her support during my Ph.D. studies. I am extremely grateful to the entire faculty at the Department of Microbiology, Quaid-i-Azam University, Islamabad.

I must express my gratitude to Higher Education Commission (HEC), Pakistan for providing financial support for my study under "Indigenous Ph. D scholarship" program. I would also like to thank "Commonwealth Scholarship Commission" for providing me Split-site PhD scholarship at University of Reading and introducing me to the vibrant scientific community abroad. Furthermore, I would like to express my gratitude to my senior **Dr. Ihsan Ali** for encouragement and scientific discussions. I am also highly indebted to my friends and colleagues at QAU and UoR. I would like to offer my heartfelt gratitude to **Safia, Faiza, Sehrish, Pashmina, Saima, Faiza, Mehwish, Sana, Zurva, Nasira** and **Nida** for their contributions and support in this project. I would also extend my thanks to my UoR family **Shaema, Fauzia, Aida, Afrah, Dama, Louis, Kang and Salem.** I owe my gratitude to my flat mate and friend **Yao Deng,** for sharing quality time with me. My sincerest gratitude to my travel buddies **Amna, Telma, Sabeen, Shar**i and **Ornisaa**. All the non-academic and technical staff of the Department of Microbiology is acknowledged for their services and support. I feel thankful to **Mr. Shabbir, Mr. Sharjeel, Mr. Shafaqat, Jordan, Harriet and Ross** for their kind assistance.

Words are inadequate to pay my thanks to my **Chachu** and **Chachi** for providing me home away from home for 6 years and counting. Their affection, care and love were the only things that kept me going. I can never pay back the love and support of my brothers **Assad** and

Abstract

Urinary tract infections (UTIs) are frequently encountered bacterial infections treated with antibiotics. Extraintestinal *Escherichia coli* is responsible for majority of the UTIs. Infections associated with particular clonal lineages such as fluoroquinolone resistant ST-131 are becoming increasingly challenging to treat. The notion that the acquisition of MDR factors have the fitness cost associated in terms of compromise on virulence potential has led to the scrutiny of the MDR strains of UPEC across different continents. However, there is very scarce knowledge about the clonal types and genetic characteristics of UPEC strains associated with UTIs in Pakistan region. In this study, we scrutinized genetically distinct MDR UPEC strains for number of virulence factors, however particular focus was the role of iron acquisition system in invasion process. Furthermore, by Whole Genome Sequencing genetic blueprint of 20 different UPEC strains was assembled. PCR screening of 155 UPEC isolates, confirmed presence of *fimH* (100%), *iutA* (55%), *feoB* (49%), *papC* (48%), *papGII* (45%), *kpsMTII* (26%), *papEF* (24%), *fyuA* (24%), *usp* (14%), *papA* (13%), *sfa/foc* (13%), *hlyA* (12%), *afa* (10%), *cdtB* (7%), *papGI* (4%), *papGIII* (4%), *kpsMTIII* (3%) and *bma*E2 (1%). Certain VF factors such as cell surface hydrophobicity, mannose resistant hemagglutination, *papGII, sfa/foc* and *feoB* were frequently distributed among MDR strains, while these strains were resistant to the major frontline antibiotics including trimethoprim and cephalosporins. WGS was performed using next generation MiSeq and HiSeq 2500 platforms. SPAdes v.3.11 was used for the De novo assembly of the reads, whereas genomic features were determined using PATRIC and RASTtk. Mutants were produced by λ-Red recombination and invasion assays were performed to determine the virulence potential *in-vitro*. Among different sequence types, VF were uniformly distributed, whereas, some VF such as *papEF, sfa/foc, fyuA and iutA* occurred frequently among ST131 strains. Selected MDR-virulent strains were tested for their invasion ability which was dependent on the presence or the absence of different iron acquisition genes such as enterobactin (*entABCDEFH, fepA*), yersiniabactin (*ybtPQirp1irp2, fyuA*), aerobactin (*iucABCD, iutA*), and the heme uptake systems (*hmuRSTUV*). Strains having all three siderophores along with the heme uptake systems were significantly more invasive when compared to their counterparts having either of three siderophore genes. The gene knock out experiments confirmed that the loss of yersiniabactin and aerobactin has the most profound effect on the invasive ability of UPEC. WGS sequencing of the MDR virulent clone of ST131-O25b-H30 lead to the identification of an array of molecular factors, including $bla_{CTX-M-15}$, bla_{OXA-1}, bla_{CMY-2}, *sul2*, *catB*, *dfrA17*, *mph* (A) a class 1 integron, 77 insertional sequences

(IS elements), a Tn*3*-like transposon, multiple virulence markers and 7 intact prophage loci. Likewise, WGS of another clone, ST38-O1:H15 identified *bla*_{TEM-1}, *CMY-2, sul1, sul2, dfrA17, tetA, mphA* and mobile elements *int1,* two transposons, 30 insertion sequence elements, one integrative conjugative element, four plasmids and five prophages. A comparative genomic analysis of twenty MDR-virulent UPEC isolates identified multitude of VF, resistance genes, plasmids and prophages. Certain VF (*papI, papC, papE, papH,* RTX, *cnf*) resistance genes (*bla*_{CTXM-15,} *bla*_{OXA-1,} *catB, dfrA17*) and plasmid incompatibility groups (IncFIA and IncI1) were significantly associated with the clonal group ST131. In conclusion, this study confirms an array of VF and MDR factors in UPEC strains. Moreover, invasion assays confirmed that the invasion ability of tested strains directly depend on their ability to sequester iron and the loss of siderophore genes significantly impairs invasion ability. WGS and comparative genomic analysis of MDR UPEC strains revealed their diverse virulence and MDR profile which indicates a successful acquisition of MDR factors by the virulent UPEC strains circulating in this part of the world. Among these the predominant clonal group ST131 showed diverse virulence and MDR profile postulated as a significant fitness advantage to these strains.

List of Publications

Publications

1. Ali I**, Rafaque Z**, Ahmed I, Tariq F, Graham SE, Salzman E, Foxman B, Dasti JI. Phylogeny, sequence-typing and virulence profile of uropathogenic Escherichia coli (UPEC) strains from Pakistan. *BMC Infectious Diseases*. 2019;19(1):620.

2. **Rafaque Z**, Dasti JI, Andrews SC. Draft genome sequence of a uropathogenic *Escherichia coli* isolate (ST38 O1: H15) from Pakistan, an emerging multidrug-resistant sequence type with a high virulence profile. *New Microbes and New Infections* 2019; 1(27):1-2.

3. **Rafaque Z**, Dasti JI, Andrews SC. Draft genome sequence of a multidrug-resistant CTX-M-15 β-lactamase-producing uropathogenic *Escherichia coli* isolate (ST131-O25b-H30) from Pakistan exhibiting high potential virulence. *Journal of Global Antimicrobial Resistance.*2018; 1(15):164-5.

4. Ali I, **Rafaque Z**, Dasti JI, Graham SE, Salzman E, Foxman B. Uropathogenic *E. coli* from Pakistan have high prevalence of multidrug resistance, ESBL, and O25b-ST131. *Open Forum Infectious Diseases* 2016; 3 (1): 2008-2008.

5. Ali I, **Rafaque Z**, Ahmed S, Malik S, Dasti JI. Prevalence of multi-drug resistant Uropathogenic *Escherichia coli* in Potohar region of Pakistan. *Asian Pacific Journal of Tropical Biomedicine,* 2016; *6*(1): 60-66.

Abstracts

1. **Rafaque Z**, Salunkhe A, Dasti JI, Andrews SC. Impact of iron availability and iron-acquisition on the virulence of Uropathogenic *E. coli*. Poster presentation at PhD Symposium -June 24th, 2018, University of Reading, UK.

2. **Rafaque Z**, Liaqat N, Abid N, Andrews SC, Dasti JI. Phenotypic and genotypic attributes of multi-drug resistant UPEC isolates involved in urinary tract infections in Pakistan. Abstract submission at ASM Microbe June 8th -10th 2018, Atlanta, GA, USA.

3. Ali I, **Rafaque Z**, Ahmed S, Malik S, Dasti JI. Prevalence of multi-drug resistant Uropathogenic *Escherichia coli* in Potohar region of Pakistan. Poster presentation   at One day International symposium on **"Burden of Antibiotic Resistance in Neonates",** March 29, 2016. Quaid-i-Azam University, Islamabad, Pakistan, **1st Prize in Poster Presentation**).

CHAPTER 1:   INTRODUCTION

1.1.   Background

UTI are estimated to cause infections among 40-50% of the women and 5% of the men during their entire life span (Ulett et al., 2013). These infections not only cause significant morbidity in women of all ages but also affect elderly, infants, people having prolonged hospitalization (catheters associated infection), obstructed urinary tract and spinal cord injury (O'Brien et al., 2016). Serious complications may include recurrent UTI, pyelonephritis, renal sepsis, pre-term birth and bacteremia. It is estimated that annually around 150 million people suffer from UTI around the globe. In United States (US) alone UTI accounts for an estimated 10.5 million clinic visits (constituting 0.9% of all ambulatory visits). Only in the year 2007, 2–3 million visits of the emergency department were recorded because of UTIs. In Europe this constitutes 19.6% of all the infections reported, similarly for the developing countries figure is 24% of all the infections reported (Tandogdu and Wagenlehner, 2016b). In economic terms, in US alone UTI cause an annual burden of \$3.5 billion and more than \$6 billion around the globe (Flores-Mireles et al., 2015a, Foxman, 2014a, Terlizzi et al., 2017b).

Uropathogenic *E. coli* (UPEC) is the leading cause of UTIs and is associated with 80-90% of the community-acquired (CAUTI) and hospital-acquired (HAUTI) urinary tract infections (Terlizzi et al., 2017b, Foxman, 2014a, Flores-Mireles et al., 2015a). Besides, UPEC, other major bacterial causes of UTIs include *Klebsiella pneumoniae* (~7%) and *Proteus mirabilis* (~5%). While *Enterococcus faecalis, Pseudomonas aeruginosa, Candida albicans, Enterobacter cloacae* and *Streptococcus bovis* account for the remaining UTIs across the globe (Parish and Holliday, 2012, Hof, 2017, Terlizzi et al., 2017b).

UPEC is categorized into four phylogroups "A, B1, B2 and D" (Bien et al., 2012c). UPEC usually requires multiple VF in order to cause an infection. The process of UPEC pathogenesis

1

involves colonization, adherence biofilm formation, invasion/replication to form intracellular bacterial communities (IBCs) and quiescent intracellular reservoirs (QIRs) for the persistence in urothelium. The severe consequences of UPEC infection include kidney colonization and the host tissue damage leading to the septicemia and bacteremia (Terlizzi et al., 2017b).

UPEC was not considered a true intracellular pathogen, until late 1970's. However, recent studies based on the "gentamicin protection assays" and microscopic analysis of the mouse and rat bladders along with bladder epithelial cell lines suggest that UPEC can successfully invade bladder tissue (Fukushi et al., 1979, Martinez et al., 2000a, Lewis et al., 2016). Although, most of the studies investigated UPEC invasion on the bladder cells, other studies based on the renal epithelial cell lines demonstrated their ability to invade kidney cells (Warren et al., 1988, Donnenberg et al., 1994, Bens et al., 2014). UPEC invasion of the host cells facilitates its survival by protecting against the host immune defenses. It not only provides access to the nutrients but also enhances the chances of UPEC to invade deeper tissues (Mulvey, 2002, Lewis et al., 2016). The process of formation of the intracellular bacterial communities (IBCs) has been frequently associated with the recurrent UTIs (RUTIs) (Rosen et al., 2007, Blango and Mulvey, 2010, Robino et al., 2013). The role of the IBCs in RUTI suggests that the bladder cells serve as a staging ground for the UPEC intracellular bacterial growth and a shelter for the persistent bacterial reservoirs against hostile UT niche. UPEC harbors a plethora of virulence factors, which helps in successful colonization of UT amidst the presence of the various host factors. Fimbriae, primarily type-1 fimbriae are the most important adhesins which are assembled by chaperone-usher pathway and bind to the D-mannosylated surface receptors such as uroplakins via the cognate FimH adhesin (Nielubowicz and Mobley, 2010). FimH is involved in biofilm formation and has been shown to activate host immune pathways in mouse UTI model (Sokurenko et al., 2008). Other surface associated factors involved in UPEC colonization include P-fimbriae (associated with pyelonephritis), F1C, S and Afa (afimbrial

adhesin) and lately characterized factors such as Ag43, UpaH (autotransporter proteins), afimbrial adhesins (TosA, FdeC), curli and flagella (reviewed by; (Totsika et al., 2012a, Terlizzi et al., 2017b). Additionally, UPEC secretes multiple toxins that causes damage to the host epithelial cells. Alpha-hemolysin is an important cytolytic toxin encoded by UPEC and mediates host cell lysis, eventually releasing iron that is vital for the UPEC. It is also associated with renal scarring by inducing Ca^{+2} oscillations in kidney epithelial cells (Nagamatsu et al., 2015). Besides, another toxin which mediates UPEC invasion by disrupting the cytoskeleton is cytotoxic necrotizing factor 1 (CNF1) (Dhakal et al., 2008). Virulence factors such as type 1 pili, Afa/Dr adhesins and OmpT are also shown to help in invasion process (He et al., 2015, Kakkanat et al., 2015b, Saldaña et al., 2014). Other than that, the role of iron acquisition systems particularly siderophores in invasion process of UPEC has not been studied. However, one study reported the role *iroN* receptor in invasion of UPEC in which *iroN* loss resulted in impaired invasion (Feldmann et al., 2007). Iron is a crucial element/mineral required for the bacterial survival and its availability in UT is limited. UPEC produces four different iron (Fe^{3+}) chelating siderophores including enterobactin, salmochelin, aerobactin and yersiniabactin. UPEC may encode variety of siderophores molecules while some strains may exhibit all four above enlisted molecules (Watts et al., 2012, Henderson et al., 2009). These systems facilitate UPEC persistence in the iron-restricted milieu of UT by scavenging iron from the host and are established as an important virulence factor in UTI (Gao et al., 2012b, Hagan, 2009, Henderson et al., 2009, Johnson et al., 2018, Peralta et al., 2016, Watts et al., 2012). Additionally, UPEC also expresses heme receptors such as ChuA and HmA which enable UPEC to sequester host iron sources (heme, hemoglobin) and are shown to enhance UPEC virulence (Hagan, 2009, Hagan et al., 2010). Besides the distinct role of these iron acquisition systems, certain siderophores such as yersiniabactin have been shown to sequester host-associated copper (Chaturvedi et al., 2012). However, further work is required to understand the vitality of

siderophores in uptake of other transition elements such as manganese, zinc and copper. This area has a potential to unravel some novel concept about UPEC virulence and nutritional immunity. Iron acquisition systems are also an attractive choice as potential vaccine candidate, with an ever-rising resistance in UPEC against the antibiotics.

UPEC utilizes different mechanisms to evade stress such as immune responses, starvation and antibiotic treatment. Extracellular DNA (eDNA), exopolysaccharides (EPS), pili, curli and flagella, creates a framework of multicellular bacterial communities that protects UPEC from antimicrobial agents, immune responses and nutritional stress (Kostakioti et al., 2013b). Biofilm provides a physical barrier to the antibiotic's entry; thus, level of resistance increases with biofilm maturation (Flores-Mireles et al., 2015a, González et al., 2017a). Therefore, understanding the species-specific biofilm formation, administration of appropriate antibiotics at right stage of the biofilm formation and dispersal mechanism of biofilm is necessary for the development of anti-biofilm targets.

UTIs are the second most common reason for the prescription of antibiotics globally, other than otitis media (Foxman, 2010). Currently antibiotics such as trimethoprim sulfamethoxazole, ampicillin, fluoroquinolones and cephalosporins are used as the treatment options against UTI (Gupta et al., 2011b). However, in the last decade an alarming increase in resistance against antibiotics has been observed. With an increase in the resistance, emergence of multi-drug resistant (MDR) clones such as ST131 of *E. coli* has been reported across different contents (Nicolas-Chanoine et al., 2014). Emerging clones can be MDR and may possess a multitude of virulence factors (reviewed by (Beceiro et al., 2013). Clonal group ST131 is particularly associated with CTX-M-15, β-lactamases, rendering it resistant to all generations of cephalosporins (Nicolas-Chanoine et al., 2014). Studies suggest different prevalence of ST131 across different countries. For example, it counts for the 21% and 25% of the ESBL producing *E. coli* responsible for the CAUTI in France (2006) and Mexico (2006-2007) (Arpin et al.,

2009, Reyna-Flores et al., 2013). A national survey (2007-2011) in Sweden reports prevalence of ST131 up to 34% of the community and hospital acquired UTI (HAUTI) (Brolund et al., 2014). In India (2009) ST131 are reported to count for 70% ESBL producing *E. coli* in HAUTI (Hussain et al., 2012). Our study in Pakistan (2016) reports 46% of *E. coli* from UTI belonging to ST131 and about half of these were ST131-O25b-H30-R (Ali et al., 2016c). No other study regarding ST131 prevalence in UPEC has been reported from Pakistan.

Antimicrobial resistance (AMR) is a clear threat to the public health worldwide. It is estimated that by 2050 around the globe the mortality could reach 10 million deaths/year at a current resistance rate and the net economic loss could reach up to $100 trillion (de Kraker et al., 2016, Brown et al., 2017). *E. coli* is a versatile/unique bacterium having multiple mechanisms of resistance towards antibiotics. It has been placed in most critical group of "priority pathogens", by World Health Organization (WHO), based on their MDR nature and urgency of novel antibiotics against their treatment (World Health Organization, WHO; Geneva, 2017). Many of these resistance genes are located on conjugative plasmids that also carry virulence factors (VF) which might get selected under antibiotic pressure (da Silva and Mendonça, 2012). However, the genetic mechanisms leading to co-evolution of VF and antibiotic resistance are not well understood. Pandemic clone of UPEC-ST131, isolates of enterohaemorrhagic *E. coli* (EHEC) *E. coli* a O104 and O157, are not only virulent but are also resistant towards multitude of antibiotics (penicillins, fluoroquinolones and cephalosporins). Additionally, *Enterococcus faecium* clone CC17, *Streptococcus pneumoniae clone* PMEN1, *Clostridium difficile* ribotype NAP1/027 are also reported to have higher virulent and resistant nature (Beceiro et al., 2013; Schroeder et al., 2017a). Previously, most of the studies focused on single aspect of either virulence or resistance, which limits the solutions to the global challenge of antibiotic resistance. An approach considering the interdependence of both, the transmission and the regulation of resistance and virulence must be considered equally important and the

investigations should be probed in the view of phenotypic and genotypic diversity of UPEC

clonal groups.

1.2.   Aims and objectives

To investigate the virulence attributes of MDR strains of UPEC and particularly the impact of iron and iron acquisition systems on the invasion of UPEC was the major aim of this study.

Following objectives were achieved by conducting outlined study

1. Genetic determinants responsible for the molecular mechanisms of drug resistance were scrutinized in MDR strains of UPEC.

2. Genetic determinants responsible for the virulence of UPEC strains were scrutinized in MDR strains of UPEC.

3. Evaluated was the invasion potential of MDR UPEC strains having multitude of VF genes.

4. Investigated was the role of iron acquisition genes in invasion process.

5. Complete genetic profile of the MDR virulence strains was determined by WGS sequencing.

CHAPTER 2:   LITERATURE REVIEW

2.1   Urinary tract infections

Generally, an infection of any part of the urinary tract (UT) system (including bladder, kidneys and the tubules connected to them) is considered as UTI and may refer to a condition with the presence of significant numbers of pathogens inside urinary tract. However, pertaining to the conditions like frequent urination, pus or blood in urine along with pain in suprapubic region, count of as few as 100 uropathogens per milliliter may be considered significant (Stamm, 1982). UT is normally sterile, however bacteria may ascend from pre-anal region of excretory system, invade the urinary tract and develop complications like urinary tract infections (Al-Badr and Al-Shaikh, 2013)**.** Inside the bladder pathogens may remain inert or silent (asymptomatic bacteriuria) or could lead to the development of severe consequences like septicemia, shock and less often death (Mignini et al., 2009, Rizvi and Siddiqui, 2010). Bacteria reside around the urethral opening and routinely colonize the urine in the urethra but are washed out during micturition. However, shorter the urethra in women provides more opportunities for bacterial colonization before they could be removed by micturition. Moreover, the shorter distance between vaginal cavity and rectum that harbors large bacterial communities makes it possible for bacteria to ascend towards bladder.

2.2   Epidemiology of UTI

UTIs are one of the most frequent infections encountered in community and hospital-settings (Flores-Mireles et al., 2015b, Foxman, 2010). According to an estimate approximately 150 million people around the globe suffer from UTI. In United States (US) alone UTI were responsible for 10.5 million hospital visits in year 2007 alone. In Europe UTI count for 19.6% of all the infections reported, similarly for the developing countries these infections are reported to be 24% of all the infections (Tandogdu and Wagenlehner, 2016b). It is estimated

that UTI put an annual financial constraint of US$3.5 billion to US alone, and 6 billion dollars per year around the globe, due to the higher health care costs and aftermath of sick leaves associated with them (Hasan et al., 2007, Flores-Mireles et al., 2015b, Foxman, 2010, Tandogdu and Wagenlehner, 2016b).

Apparently, the disease is not life threatening in immunocompetent adults, but they are a source of higher infection rate among infants, older men and women of all ages. The distribution of asymptomatic bacteriuria has somewhat J-shaped, with higher incidence among the infants, a gradual increase with age in both genders. However, at age of 60 and above they tend to be more common in women than men. The prevalence of symptomatic UTI is significantly higher in young women (15-29 yrs.), approaching to 20% (Foxman, 2010). Overall, they are more frequent among women than men, with a proportionate of 8:1 and one report suggests about 50% of the women may have had undergone the infection by their late 20's (Rahn, 2008, Foxman et al., 2000a). Furthermore, about 20–30% of the women with a first UTI have a recurrence defined as three reports of infections in total twelve months or two in six months of time (Guglietta, 2017). In Pakistan the ratio of UTI symptoms is 24.4% and 20.0% among the pregnant and control women (Sheikh et al., 2000). Similarly a study based on individuals of Gilgit Baltistan reported a high incidence of UTI that was 60.18% and 39.83% in females and males respectively in the age group 21-50 years (Ahmed and Imran, 2008). In a report by Khan *et al*., 2010 prevalence of nosocomial UTI was found to be 20.43% (Khan et al., 2010). Among children the cases of UTI are reported as 37.5% (375 out of 1000) among them 36 (9.6%) were male patients and 339 (90.4%) were female patients (Anis-ur-Rehman et al., 2008). Akram et al., 2014 performed a nationwide analysis of micro-organisms involved in UTI in Pakistan and found 56% prevalence of UTI in female, when compared to male 44% (Kausar et al., 2014). Our previous data suggests similar trends where the occurrence of UTI in women is reported to be higher than their male counterparts (Ali et al., 2014)

2.3   Clinical manifestations of Urinary Tract Infection

It is important to classify UTI for better clinical decisions, scientific research and teaching. Identification of UTIs is usually relies on signs and symptoms, microbiological findings, and laboratory data. The current classification of UTI is forwarded by US Centers for Disease Control and Prevention (CDC) in 1988 (update: 2008), the Infectious Diseases Society of America (IDSA) and the US Food and Drug Administration (FDA) in 1992 (update: 2010) and the guidelines provided by European Society of Clinical Microbiology and Infectious Diseases (ESCMID) in 1993; update: 2010 and 2016 (Smelov et al., 2016a). Based on the clinical representation and microbiological analysis, UTI are broadly classified into; asymptomatic bacteriuria (ABU) and symptomatic bacteriuria (Figure 2.1).

2.3.1   Asymptomatic bacteriuria

A variety of non-pathogenic or commensal bacteria are capable of growth in urine. According to the current guidelines ABU refers to a midstream sample of urine (MSU) showing significant ($\geq 10^5$ CFU/ml) of a potential uropathogenic bacteria in two successive samples in case of women and single sample in case of men, in any person without any apparent sign and symptoms of UTI (Gleckman et al., 1979). However, in catheterized persons, a bacterial count as low as 10^2 CFU/ml can be considered significant (bacteriuria) in both men and women (Smelov et al., 2016a).

2.3.2   Symptomatic bacteriuria

Symptomatic bacteriuria is further classified into acute uncomplicated cystitis (AUC) or acute uncomplicated pyelonephritis (AUP). Invasion of the normal urinary system by uropathogens is referred as uncomplicated urinary tract infection. In cystitis infection is localized to bladder while in pyelonephritis the infections reaches up to the kidneys (Hooton, 2012). In healthy

individuals, cystitis usually ends without serious complications while pyelonephritis may be fatal. Clinical symptoms of cystitis include dysuria (pain during urination), frequent urination, urgency, suprapubic pain, burning sensation and cloudy or/and bloody urine, often with foul smell, without any urinary symptoms in 4 weeks before this infection. Bacterial growth of $\geq 10^3$ CFU/ml are considered clinically relevant bacteriuria (Kunin, 1997, Smelov et al., 2016a). The symptoms of pyelonephritis are bacteriuria, pyuria, fever, chills and flank pain, without any clinical evidence of urological abnormalities. Bacterial counts of $\geq 10^4$ CFU/ml are considered clinically significant (Najar et al., 2009, Rubin et al., 1992, Smelov et al., 2016a).

Complicated UTI: Patients with an obstructed and structurally abnormal genitourinary tract or with an underlying ailment are at a higher risk of attaining UTI with even higher risk of failing therapy. This UTI is referred as complicated UTI (Najar et al., 2009, Rubin et al., 1992). Clinically they will have any combination of symptoms of ABU, cystitis and pyelonephritis, further complicated by dysfunctionality or obstruction in their tract. In complicated UTI, bacterial growth of $\geq 10^4$ and $\geq 10^5$ CFU/ml in men and women respectively are considered clinically relevant (Kunin, 1997, Smelov et al., 2016a, Rubin et al., 1992). Recurrent UTI (RUTI) are more prevalent in healthy young women without any structural or functional abnormality in their genitourinary tracts. Clinically they are represented by at least three recurrent episodes of uncomplicated UTI in past 12 months. A colony count of $\geq 10^3$ CFU/mL should be considered significant. In certain cases, when host immune system is compromised the infection can ascend to the kidneys via the urethra and ultimately disseminates to cause

systemic   infection   (bacteremia).

```
                        ┌─────────────────┐
                        │  Urinary Tract  │
                        │   Infection     │
                        │     (UTI)       │
                        └─────────────────┘
```

Figure (flowchart):

- Urinary Tract Infection (UTI)
  - Asymptomatic
    - Asymptomatic Bacteriuria (ABU)
  - Symptomatic
    - Cystisis (bladder infection)
    - Pyelonephritis (kidney infection)
    - Complicated UTI
    - Recurrent UTI (RUTI)
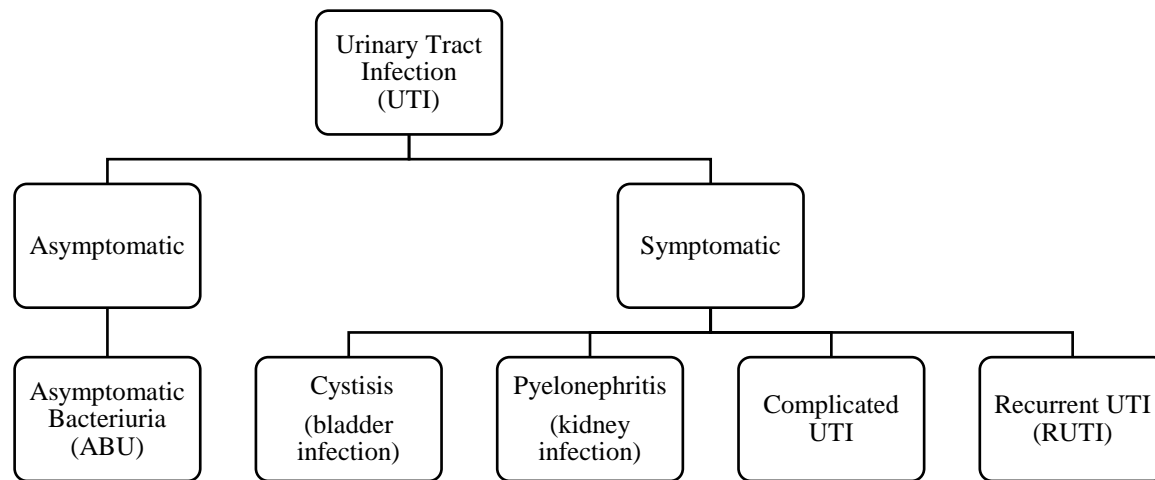
Figure 2.1   Classification of UTI based on clinical, microbiological and diagnostic representation

2.4   Major risk factors and etiological agents

Uncomplicated UTI like cystitis are triggered by numerous factors such as gender (anatomical differences), a history of UTI, obesity, diabetes, sexual activity, vaginal infection, hormonal changes, dietary imbalance (excessive intake of calcium), enlarged prostrate (in case of men) (Ramzan et al., 2004). Complicated UTI are due to obstruction of the urinary tract, renal transplant, prolonged hospitalization, kidney stones, urinary retention, renal failure, pregnancy and dwelling catheters. Indeed 70-80% of complicated UTI are caused due to indwelling devices and urinary catheters (Flores-Mireles et al., 2015b, Guglietta, 2017, McLellan and Hunstad, 2016).

Other factors that predispose development of UTI include use of spermicides, immune suppression, anxiety and genetic vulnerability (maternal history of UTI). The maternal history of UTI being a risk factor of UTI shows that the genetic makeup and other vertically transmitted traits like normal flora play an important role towards the development of UTI. In

postmenopausal women the recurrent cystitis and bladder voiding abnormalities are factors

contributing in causing UTI (Raz et al., 2000a, McLellan and Hunstad, 2016).

Urine provides a good medium for the growth of certain bacteria. Since host has many effective

methods of eradicating bacteria from the urinary tract most of the bacteria colonizing it, do not

cause disease. However, bacteria that successfully infect urinary niche have special virulence

features like adhesins, invasins, toxins, biofilm formation and siderophores that enable them to

successfully invade the host. Another factor that helps to successfully colonize the host is host's

incompetency to remove the bacteria due to indwelling devices like catheters. This fact answers

the higher incidence rate of UTI in hospitalized and catheter dwelling patients, since 50-70%

of the hospital associated UTI cases reported are due to the catheters (Foxman, 2014b,

McLellan and Hunstad, 2016). The causative agents of UTI include bacteria, as well as some

fungi. The uropathogenic *Escherichia coli* (UPEC) is responsible for 70-90% of all UTIs

reported. Besides UPEC, the organisms responsible for complicated UTI include *Klebsiella*

pneumoniae, *Staphylococcus. aureus*, *Pseudomonas aeruginosa, Proteus mirabilis* and group

B *Streptococcus* and others (Ronald, 2002). For uncomplicated UTI, UPEC is followed is by

Klebsiella pneumoniae, *Proteus mirabilis*, *Enterococcus faecalis, Pseudomonas aeruginosa*,

Staphylococcus aureus, *Staphylococcus saprophyticus*, GBS and *Candida* spp., (Flores-

Mireles et al., 2015b, Foxman, 2010).

However, the type and the prevalence of uropathogens may vary according to the health status

and the debility of the individuals. For instance, in diabetic patients GBS and *K. pneumoniae*

are reported to be the major agents, whilst *Pseudomonas* infections are found more common in

chronically-catheterized patients (Amna et al., 2013). Multiple studies executed within the

South Asian region especially Pakistan, also place *E. coli* as the most common etiological agent

of UTI's (Ahmed et al., 2015, Ali et al., 2014, Ali et al., 2016a, Kalsoom et al., 2012, Sabir et

al., 2014). Besides UPEC, other bacterial species that frequently caused UTI in Pakistani population include: *K. pneumoniae, P. aeruginosa, Enterococcus* spp., and *S. aureus*. Akram et al., 2014 performed a nationwide analysis of micro-organisms that cause UTI in Pakistan. Out of the 1050 samples analyzed, the largest frequency was for Extended Spectrum β-lactamases (ESBL) producing *E. coli* followed by *P. aeruginosa, Klebsiella* and *Proteus* spp. Overall disease prevalence was more frequent among females when compared to the males population (Kausar et al., 2014).

2.5   *Escherichia coli*

German pediatrician, 'Theodor Escherich', isolated this bacterium from the feces of neonates. Initially it was named as "*Bacterium coli commun"e* and was later renamed to "*Escherichia coli*". It's a facultatively anaerobic Gram-negative rod with a length of 2.0 μm, a diameter of 0.25–1.0 μm, and cell volume about 0.6–0.7 μm^3. It's a motile and non-spore forming bacterium and belongs to the family *Enterobacteriaceae* (enteric bacteria) Class Gammaproteobacteria and Phylum Proteobacteria (Harvey, 2007). It has the ability to survive in diverse environments including reptilian, avian and mammalian intestines, inside plant cells, water bodies and moist soil (Harvey, 2007). Thus, it has become the permanent part of the microbiota of all mammals and resides as a harmless and commensal microorganism (Kaper et al., 2004, Harvey, 2007). It can grow well under oxygen rich, as well as oxygen deficient environments. Under oxygen deficient conditions, it switches to anaerobic mode and acquires energy via fermentation. Besides, it can utilize NO_3^{-1}, NO_2^{-1} and fumarate as a final electron acceptor under anaerobic conditions. Such versatility enables to thrive successfully in anaerobic (intestinal) and aerobic (extra-intestinal) environments (Krussel et al., 2005). The harmless nature of *E. coli* was not debated until 1945 when it was found to cause diarrheic outbreak among neonates (Harvey, 2007, Lesage, 1897, Bray, 1945). It is an opportunistic

pathogen and causes disease in its host under immune-compromised conditions. Under such conditions it can cause life-threatening infections such as dysentery, diarrhea, hemolytic uremic syndrome (HUS), septicemia and UTIs. The fact that it exists in two forms; commensal and pathogenic was first postulated in 1897 by Lesage, whose hypothesis was supported by Bray when he isolated Enteropathogenic *E. coli* (EPEC) strains from neonates suffering from diarrhea (Bray, 1945). The fact that it can successfully exist in two distinct phenotypes (commensal and pathogenic) is evident by its genome plasticity and is amenability to genetic recombination (Dobrindt et al., 2003). Dobrindt and his colleagues compared commensal *E. coli* K-12 strain MG1655 with 26 pathogenic strains and found that there is great heterogeneity among *E. coli* strains. *E. coli* K-12 was found to be missing several virulence factors as compared to its pathogenic counterparts. Whereas pathogenic strains were equipped with pathogenicity islands, integrated phage genomes and an arsenal of virulence factors. Molecular events responsible for the diversity of *E. coli* strains include recombination within the genome; lysogenic phages carrying virulence genes; pathogenicity islands which are regions of the foreign DNA from another bacterial species and via conjugation (Dobrindt et al., 2003, Zdziarski et al., 2008).

2.6   Phylogenetic groups of *Escherichia coli*

Based on the genomic information, *Escherichia coli* strains are largely assigned into six phylogenetic groups; A, B1, B2, C, D and E (Herzer et al., 1990) as given in Table 2.1. According to the Lecointre et al., groups A and B1 fall into sister groups while group B2 falls into an ancestral branch. These phylogenetic groups differ from each other regarding their life history, ecological niches, biochemical characteristics such as the ability to utilize different sugar sources, growth rates as well as their antibiotic resistance profiles (Lecointre et al., 1998). Furthermore, phylogroups A and B1 have comparatively smaller genome sizes when compared

with B2 and D groups. The groups A and B1 are usually commensal *E. coli* and persist in environment, while B2 and D are found to encode more virulence factors (VF) than A and B1 (Johnson et al., 2001, Walk et al., 2007). Extraintestinal *E. coli* usually belongs to the group B2 and D, intestinal to A, B1 and B2 whereas commensal fall in A and B1 phylogroup. Clermont *et al*., have developed a PCR based method for identification of phylogroups using *yjaA, chuA* and the DNA fragment TspE4.C2 as genetic markers (Clermont et al., 2000).

Table 2.1   A brief overview of the major genotypes and associated pathotypes of *E. coli*.

	Phylogenetic Group	Habitat and Phenotype
1.	A	Intestinal Pathogenic *E. coli*, Commensal Strains
2.	B1	Environmental Strains, Intestinal Pathogenic *E. coli*, Commensal Strains
3.	B2	Extra-intestinal Pathogenic *E. coli*
4.	D	Extra-intestinal Pathogenic *E. coli*, Intestinal Pathogenic *E. coli*

2.7   Classification of pathogenic *Escherichia coli*

Based on the site of infection, the type of VF and the host, pathogenic *E. coli* are categorized into: (a) intestinal/enteric or diarrheagenic strains (b) and extra-intestinal strains. Within these two groups are the strains that share similar VF and induce infection of similar nature. This subset of strains is referred as pathotypes (Wiles et al., 2008a). The pathotypes of enteric pathogenic *E. coli* origin infect mucosal lining of the intestine and cause dysentery, diarrhea, and related outcomes. On the other hand, extra-intestinal pathogenic *E. coli* (ExPEC) maintain a friendly niche inside intestine and causes infections in extra-intestinal niche of central nervous system (CNS), blood, respiratory tract (in birds), urinary tract (Figure 2.2). Diarrheagenic pathogenic *E. coli* is comprised of total six different pathotypes (given in Table

2.2). Among the Ex-PEC pathotypes include uropathogenic *E. coli* (UPEC) along with others(Kaper et al., 2004) discussed in forthcoming chapter.
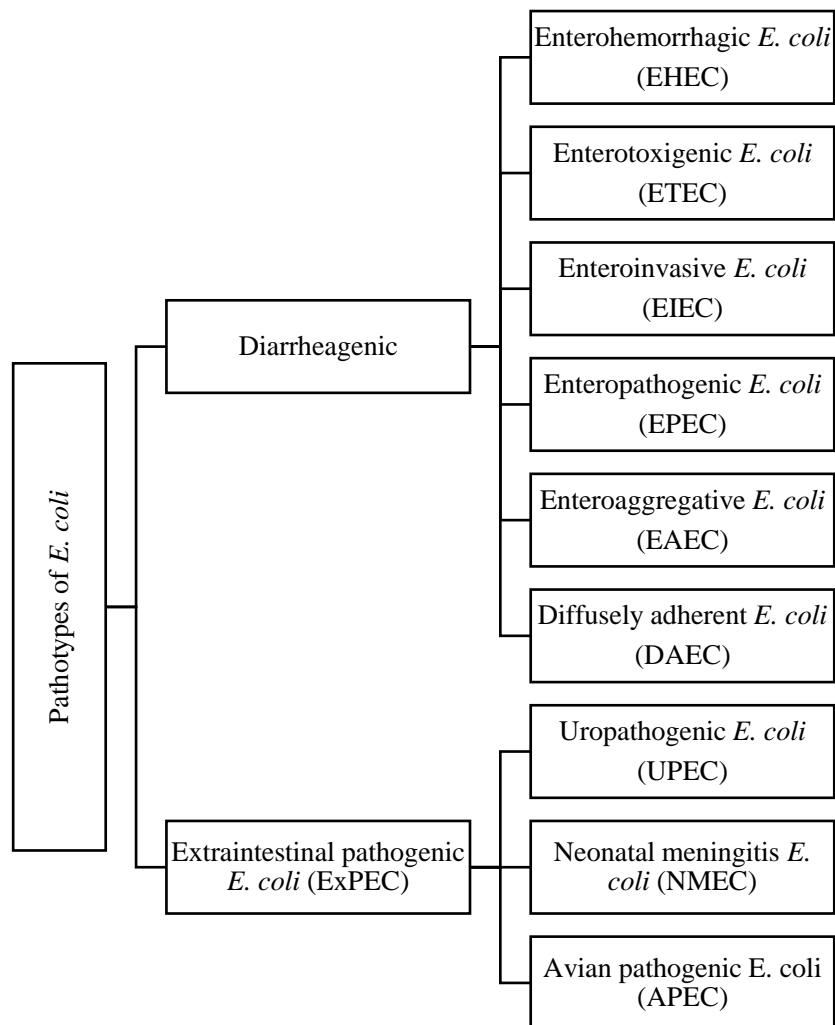
Figure 2.2 Various pathotypes of *E. coli* associated with intestinal and extra-intestinal infections.

E. coli can cause a myriad of diseases which can either be confined to the gastrointestinal tract or sites other than the gut. The figure explains the types of infections caused by eight pathotypes of *E. coli.*

Table 2.2 A brief overview of diarrheagenic (intestinal) *E. coli*

Name	Description
Enterohemorrhagic *E. coli* **(EHEC)**	EHEC in 1982, was first documented as a human pathogen. Major causative agent of hemolytic uremic syndrome (HUS), hemorrhagic colitis (bloody diarrhea) and non-bloody diarrhea. The prominent strain of this pathotype is *E. coli* O157:H7 which causes HUS. The key virulence factor of this strain is Stx also referred to as verotoxin (VT) (Kaper et al., 2004).
Enterotoxigenic *E. coli* **(ETEC)**	ETEC is the etiological agent of watery diarrhea also referred to as travelers' diarrhea. It colonizes the surface of small bowel of using its fimbrial proteins. It is non-invasive in nature. Key virulence factor includes 2 enterotoxins; ST (heat stable) and LT (heat labile), which share their homology with cholera toxin secreted by *Vibrio cholera* (Spangler, 1992).
Enteroinvasive *E. coli* **(EIEC)**	EIEC has high resemblance with *Shigella spp.*in terms genetics and pathogenesis. It causes watery diarrhea, inflammatory colitis and dysentery.
Enteropathogenic *E. coli* **(EPEC)**	EPEC adheres to intestinal epithelial cells and is known for infant's diarrhea. Clinical manifestations of EPEC include acute diarrhea, fever, malaise and vomiting (Deborah Chen and Frankel, 2005).
Enteroaggregative *E. coli* **(EAEC)**	EAEC are typically noninvasive and carry hemolysin and an ST enterotoxin like that of ETEC. They cause watery diarrhea without vomiting (Okhuysen and DuPont, 2010).
Diffusely adherent *E. coli* **(DAEC)**	DAEC are characterized by their adherence to bowel enterocytes that displays as the growth of long finger-like cellular projections and are associated with diarrhea in children >12 months. They have special adhesins called Dr/Afa that help them to adhere to bowel (Scaletsky et al., 2002).

2.8   Uropathogenic *E. coli* (UPEC)

Uropathogenic *E. coli* is an extra intestinal *E. coli* that has an ability to invade mucosal lining of urinary tract, bladder and kidneys. By far it is one of the predominant etiological agent involved in UTI and are involved in 80-90% of community acquired UTIs (CAUTI) (Terlizzi et al., 2017a, Flores-Mireles et al., 2015b, Foxman, 2014b). As mentioned earlier the *E. coli* strain responsible for cystitis and acute pyelonephritis differs from its commensal counterpart that colonizes the lower part of the intestine. A total of six 'O' serogroups are responsible for 75% of the UTI's (pyelonephritis and cystitis). Most of the UPEC strains express hemolysin, P-fimbriae, serum resistance, aerobactin and encapsulation (Terlizzi et al., 2017a, Bien et al., 2012b, Klemm et al., 2006). However, there is no established-set of virulence factors (VF) which is common in all UPEC strains. UPEC typically belong to phylogenetic group B2 and D (Mobley et al., 2009).

2.9   UPEC classification and genome structure

UPEC can be classified on the basis of the type and severity of the infection caused by them. Urosepsis or pyelonephritis isolates infect kidney and allow the access to bloodstream, thus cause the most severe UTI. Cystitis strains progress infections in bladder, whereas asymptomatic bacteriuria (ABU) strains colonize the UT without any apparent signs and symptoms (Donnenberg, 2013). Complete genome sequencing of UPEC strain CFT073 was performed Welch et al., 2002. A three-way genome comparison between among CFT073, *E. coli* EDL933 (entero-hemorrhagic strain) and MG1655 (a laboratory strain) revealed that only 39.2% of the coding region is shared by all three strains This suggest that pathogens differ from each other in a similar pattern as they differ from their commensal counterparts. For instance,

O157:H7 and CFT073 differ from each other due to the presence of type III secretion systems and phage/plasmid encoded toxins in CFT073 while they are absent in O157:H7. The CFT073 genome is enriched with genes encoding iron-acquisition systems, auto-transporters, recombinases and fimbrial adhesins. Similarly, striking differences were observed in pathogenicity islands (PAI) of CFT073 and other UPEC strains; J96 and 536. (Welch et al., 2002).

In another study, genomic comparison of ten UPEC and four fecal commensals revealed that in UPEC CFT073 13% of the genome is comprised of 10 pathogenicity associated islands (PAI). Three of these PAI encoded P-fimbriae. Moreover, 52% of genomic characteristics were common among UPEC and commensal isolates and only 131 genes (out of 5379) present in CFT073 were specific to UPEC. The study also reports that ABU isolates have an expanded genome in comparison to commensal isolates (Lloyd et al., 2009). However, a study conducted by Salvador *et al*., 2012, revealed that ABU isolates have gone through reductive evolution. Deletions and points mutations in VF of ABU has led to reduced virulence in such isolates. (Salvador et al., 2012). Henceforth, UPEC has acquired virulence over by acquisition of PAI via horizontal gene transfer, whilst reductive evolution has resulted in the impaired virulence in case of ABU isolates.

2.10   Virulence repertoire of UPEC

VF is referred as any part/feature of an organism that enhances its potential to embark an infection/disease. Genetically UPEC encodes many VF, however on the basis of functionality they are grouped into adhesins, toxins, iron uptake system and defense systems against host immunity (Johnson and Stell, 2000b)

2.10.1 Adhesins

Adhesins are among the first VF that impart their role in the initiating an infection. Besides, they also act as invasins, promote biofilm formation, and transmit signals to the epithelial cells that result in inflammation. UPEC encode diverse group of adhesins, some of which are characterized and some are yet to be characterized (Spurbeck et al., 2011, Zhang and Foxman, 2003). The genome of prototypical pyelonephritis strain CFT073 encodes 12 fimbrial operons including 10 chaperone-usher fimbriae and 2 putative type IV pili (Donnenberg, 2013). Fimbriae and pili are encoded by chaperone-usher pathway. The gene cluster responsible for chaperone-usher also encodes the major and minor pilin subunits (Sauer et al., 2004). Among chaperone-usher encoded fimbrial adhesins Type-1 and P-fimbriae are the best characterized fimbriae.

Type 1 fimbriae are encoded by almost 99% of the *E. coli* strains and are crucial for intestinal colonization (Vigil et al., 2011). These fimbriae are comprised of a main structural subunit (FimA), several minor subunits and the adhesin (FimH) found at the tip of the fimbriae as well as sporadically throughout the shaft (Klemm et al., 1990). Although they have been found to enhance colonization and host immune response in animal models but their role in human pathology still remains unclear (Bergsten et al., 2007, Snyder et al., 2004, Connell et al., 1996, Hultgren et al., 1985). Their role in human infection is difficult to reconcile because they are expressed both in commensal and pathogenic strains, particularly there is no remarkable difference in *fim* gene expression in both virulent and less virulent strains in urinary tract (Hultgren et al., 1985, Hagberg et al., 1981, Hagberg et al., 1983, Plos et al., 1995).

Type1 fimbriae are an important VF of UPEC as demonstrated by Connell and co-workers in mouse models. According to Connell and colleagues deleting *fimH* gene leads to reduced virulence, colonization and inflammation**.** Besides**,** restoration of *fimH* gene by expressing the

respective gene over a plasmid led to reinstatement of inflammatogenecity and colonization, hence satisfying Koch's postulates (Connell et al., 1996). They have been shown to enhance bacterial survival, to increase the invasion and growth as biofilm, and to trigger mucosal inflammation (Martinez et al., 2000b, Anderson et al., 2003b, Connell et al., 1996, Oelschlaeger et al., 2002, Schembri and Klemm, 2001, Struve and Krogfelt, 1999). They bind to the mannose moieties of glycoproteins present on the urothelial via FimH subunit localized at the fimbrial tip. This binding results in initiation of a molecular cascade of phosphorylation which is prerequisite for the pathways involved in the processes of invasion and apoptosis (Martinez et al., 2000b, Wiles et al., 2008b ,Thumbikat et al., 2009).

P-fimbriae among the first VF of UPEC to get characterized (Svanborg Eden et al., 1976). The pyelonephritis associated pili *(pap)* encoding P-fimbriae is comprised of 11 genes. Pap operon is comprised of a fimbrial subunit (*papA*) and a tip (*papG*) (Hull et al., 1981). Unlike type 1 fimbriae the P-fimbriae mediated adherence mannose-resistant and is more specific P blood group antigen (Källenius et al., 1981). P fimbriae bind to α-D-galactopyranosyl-(1-4)-β-D-galactopyranoside receptor, a key epitope of P blood group antigen, and triggers immune response in different models (Roberts et al., 1994, Bergsten et al., 2007, Bergsten et al., 2005). Another factor, PapG is present in the form of three alleles, PapG1, PapG2 and PapG3*,* each having substrate specificity to a distinct domain of Gal-Gal disaccharide, containing glycosphingolipid (Strömberg et al., 1991). P-fimbriae are reportedly encoded by 54-70% of UPEC as opposed to fecal *E. coli*, only 20-25% of fecal *E. coli* encode P-fimbriae (Spurbeck et al., 2011, Johanson et al., 1993, Johnson et al., 1998). P-fimbriae enhance the pathogenesis of UPEC by strongly promoting their adherence to vascular endothelium and muscular layer in contrast to bladder epithelial barrier (Virkola et al., 1988). These fimbriae also result in high inflammatory response leading to increasing severity of UTI. Studies have reported a positive association between P-fimbriae presence and intensity of infection (Spurbeck et al., 2011,

Vigil et al., 2011). Anti-P-fimbriae antibodies have been detected in the serum of infected (De Ree and Van den Bosch, 1987). However, P-fimbriae mutant in a murine model showed no defect in colonization. (Mobley et al., 1993)**.** In contrast a pyelonephritis model in cynomolgus monkey *pap* mutant resulted in reduced colonization as compared to the wildtype (WT),(Roberts et al., 1994). Although P-fimbriae display a subtle role in uropathogenesis, they have been found to be strongly associated with acute pyelonephritis ascending UT. Also the presence of *pap* operon is linked to highly virulent strains (Leffler and Svanborg-Eden, 1981, Väisänen et al., 1981, Plos et al., 1995, Donnenberg, 2013).

F1C and S fimbriae: F1C are found in 16% of UPEC as compared to 10% fecal strains (Spurbeck et al., 2011), and the difference is not significant, they have been positively associated with pyelonephritis strains of UPEC (Johnson et al., 2005b). Likewise, S fimbriae are prevalent in reported to be in 15% and 5% of UPEC and fecal *E. coli* isolates respectively. S fimbriae are strongly correlated with ABU and cystitis isolates (Spurbeck et al., 2011). F1C and S fimbriae are genetically identical, and both are often grouped within F1C class of adhesins in epidemiological studies (Ott et al., 1988). However, difference in tip adhesin between these two fimbriae confers distinct adhesive properties and thus they are considered as separate virulence entities (Donnenberg, 2013). Both have been shown to adhere to epithelial and vascular endothelial cell lines derived from the lower human UT and renal cells. The S fimbriae are also found associated with *E. coli* strains causing sepsis, ascending UTI and meningitis. They are also involved in dissemination of the infection within host tissues (Bien et al., 2012a).

The afimbrial Afa and fimbrial Dr adhesins of *E. coli* have been found involved in UTI especially in cases like gestational pyelonephritis and recurrent cystitis. They bind to Dr Blood group antigen, also referred to as decay-accelerating factor (Nowicki et al., 1990).

2.10.2 Autotransporter adhesins

Autotransporter (AT) adhesins is an important class of adhesins, associated with UPEC virulence. It represents the largest group of AT proteins that undergo type-V secretion system. AT proteins share homology in general features as they encode N-terminal signal sequence, a passenger domain (α-domain) attached to either cell surface or released into external locale, and a translocation domain (β-domain) lying in outer membrane (OM) (Jose et al., 1995), (Henderson et al., 2000). Differences in the passenger domain of AT proteins determines the unique functional characteristics associated virulence properties. Most of AT proteins remain anchored to bacterial membrane some others are secreted out of cell. So far about eleven AT-encoding genes have been identified in UPEC strain CFT073 (Parham et al., 2004, Allsopp et al., 2010). Among the characterized AT proteins, include **Sat** (a secreted toxin), **Antigen Ag43a** (surface-associated adhesin). Antigen Ag43a reportedly undergoes phase variation and is associated with urovirulence. It is also involved in cell aggregation and intra cellular biofilm formation (Anderson et al., 2003b). The trimeric AT protein UpaG is associated with adherence to human uroepithelial cells of bladder, fibronectin and laminin. Similarly, it plays role in biofilm formation and cell aggregation (Valle et al., 2008, Totsika et al., 2012b). The surface associated UpaB, UpaC, UpaH**,** AT proteins have been shown to contribute towards the colonization of bladder in mouse model (Allsopp et al., 2010).

2.10.3 Toxins

In order to thrive better, UPEC encodes certain toxins. Among others, **α-hemolysin (HlyA) toxin** is secreted by nearly 50% of the UPEC and its expression found to be strongly associated with symptomatic UTI (Johnson, 1991a). Epidemiologically it is linked with highly virulent strains, as and is found more frequent in urosepsis and pyelonephritis isolates (Johnson et al., 2005b, Blanco et al., 1996, Opal et al., 1990). The toxin results in cell lysis, resulting in the

release of nutrients and growth factors such as heme-iron, to be utilized by bacteria for successful survival inside host. Sublytic concentration of HlyA also may enhance virulence by inactivating serine/threonine kinase Akt, which is associated with cell transduction pathways and cytic cycle progression (König and König, 1993, Uhlén et al., 2000, Hilbert et al., 2012).

Cytonecrotizing factor-1 (CNF-1) is an important toxin produced by nearly one third of UPEC strains. Epidemiological evidences associate CNF-1 to urovirulent strains. It modulates cytoskeleton by de-amination of glutamine and activating small GTPases. The Rho-GTPases thus then promote bacterial invasion through endocytosis (Falzano et al., 1993, Visvikis et al., 2011a). Besides, activation of RhoA result in actin polymerization and cell-cell bacterial dissemination. (Hofman et al., 2000). **Sat** and **Vat** toxins are the AT proteins, secreted by some of UPEC strains. They are involved in the induction of variety of cytopathic pathways (Totsika et al., 2012b).

2.10.4 Iron acquisition systems — virulence factors that pull their weight

Iron is vital nutrient for almost all forms of life, exceptions exist in case of *Borrelia burgdorferi* (causative agent of Lyme disease) and certain lactobacilli (Posey and Gherardini, 2000, Johnstone and Nolan, 2015a). Iron is the fourth most abundant element on earth and exists in two readily inter-convertible states, Ferrous (Fe^{+2}) and Ferric (Fe^{+3}) respectively. Its ability to exist in different redox states allows it to play a pivotal role as electron acceptor and biocatalyst. (Johnstone and Nolan, 2015a). It is involved in numerous biological and biochemical processes including tri-chloroacetic acid (TCA) cycle, respiration, oxygen transport, DNA biosynthesis, photosynthesis, nitrogen fixation, hydrogen production and assimilation, gene regulation and methanogenesis (Andrews et al., 2003a). Iron cannot be used in its free state; its biological functionality is dependent upon its chelation to proteins either as mono/bi-nuclear species or in a more complex assembly as heme groups or part of iron sulfur clusters. Such incorporations

allow iron to adopt necessary redox potential, spin and geometry needed for the distinct biological functions (Neilands, 1981b, Neilands, 1981a). However due to its high oxidizing potential, under aerobic conditions and neutral pH, most of the iron exists as oxyhydroxide, a state which makes iron unavailable to the bacteria. Although it is essential for almost all life forms, iron is toxic at higher concentration, both eukaryotic and prokaryotic cells have evolved mechanisms to maintain a balance between iron scavenging and induced iron toxicity (Touati, 2000).

2.10.4.1 Mechanisms of iron acquisition

In the mammals, free iron concentration is very low, $\sim 10^{-25}$ M in the blood and even lower at other sites. Bacteria require $\sim 10^{-6}$ M cytoplasmic iron concentration for normal growth. (Andrews et al., 2003a). For commensal and pathogenic bacteria that colonize humans, available iron concentration is even lower due to presence of human proteins such as lactoferrin, heme, transferrin, and lipocalin-2 that sequester iron. However, bacteria have evolved multiple strategies to acquire iron under such iron limited conditions. As a result, pathogenic bacteria, including ExPEC, have evolved various strategies for scavenging iron from the host. These mechanisms include: (i) solubilizing ferric oxides via active secretion of acids (ii) oxidizing soluble Fe^{+2} to the insoluble Fe^{+3} and (iii) using specialized iron chelators (siderophores) to actively bind ferric ions A proficient mechanism for iron sequestration is through the production of low molecular iron (Fe^{+3}) chelating compounds, the siderophores (Chu et al., 2010, Miethke and Marahiel, 2007)

2.10.4.2 Siderophore iron acquisition systems

Siderophores are chelator molecules with a mass of around 200–2000 Dalton. They have high specificity and affinity for ferric (Fe^{+3}) iron and thus are capable of quenching iron from host

iron storage proteins; ferritins and transferrin (Garénaux et al., 2011). They are produced by bacteria, fungi and monocotyledons under low iron concentration. UPEC synthesizes three classes of siderophores; catecholates (enterobactin, salmochelin), hydroxamates (aerobactin) and mixed type of siderophores (yersiniabactin) (Mobley et al., 2009). Despite the chemical differences in the structure of these siderophores, typically each system mediates iron uptake in specific steps including; (i) synthesis (ii) export (iii) binding of iron-siderophore complex at the OM surface (iv) internalization and (v) iron release into the cytoplasm (Figure 2.3) (Garénaux et al., 2011). Bacteria synthesize and secrete molecules known as siderophores that have a high affinity for binding ferric iron. This ferric-siderophore complex is then up taken by specific siderophore receptors present on the OM, whereby the energy for the uptake of these complexes comes from machinery located in the inner membrane (IM) known as the TonB-ExbB-ExbD system. Periplasmic binding proteins are responsible for shuttling the ferric-siderophore complexes from their receptors (present in the OM) to the ATP-binding cassette (ABC) (present in the IM); that in turn dispenses it into the cytoplasm. Once inside the cytosol iron the complex may be dissociated through chemical breakdown of the iron ligand. Enzymes may also be employed to catalyze this chemical breakdown, for example, enterobactin-iron complexes are broken down by an esterase enzyme that hydrolyzes the iron and releases it into the cytosol. In the final step of the release ferric (Fe^{+3}) is reduced to ferrous (Fe^{+2}) state in order to avoid re-association with siderophores. Siderophores not only support bacteria in growth and metabolism through iron acquisition, but also help them to enhance their virulence. Siderophores hence are frequently expressed by pathogenic strains of *E. coli*. For pathogenic bacteria iron limitation acts as line between survival and death. As a host defense mechanism host binds their iron in high affinity iron proteins such as transferrin, lactoferrin or in intracellular forms such as a starvation tactic. On other hand, in order to survive in iron deficient environment such as bladder, bacteria produce high level of siderophores. UPEC can express

four kinds of "siderophores" such as "enterobactin, salmochelin, aerobactin and yersiniabactin" (Figure 2.4). Enterobactin is the most common type of siderophore produced by *E. coli,* however it is easily recognized and degraded by host innate immunity protein Lipocalin 2. Salmochelin is a glycosylated enterobactin that evades host recognition and degradation. Similarly, aerobactin and yersiniabactin are also not recognized by host lipocalin 2 and thus help bacteria to harness iron from the environment.
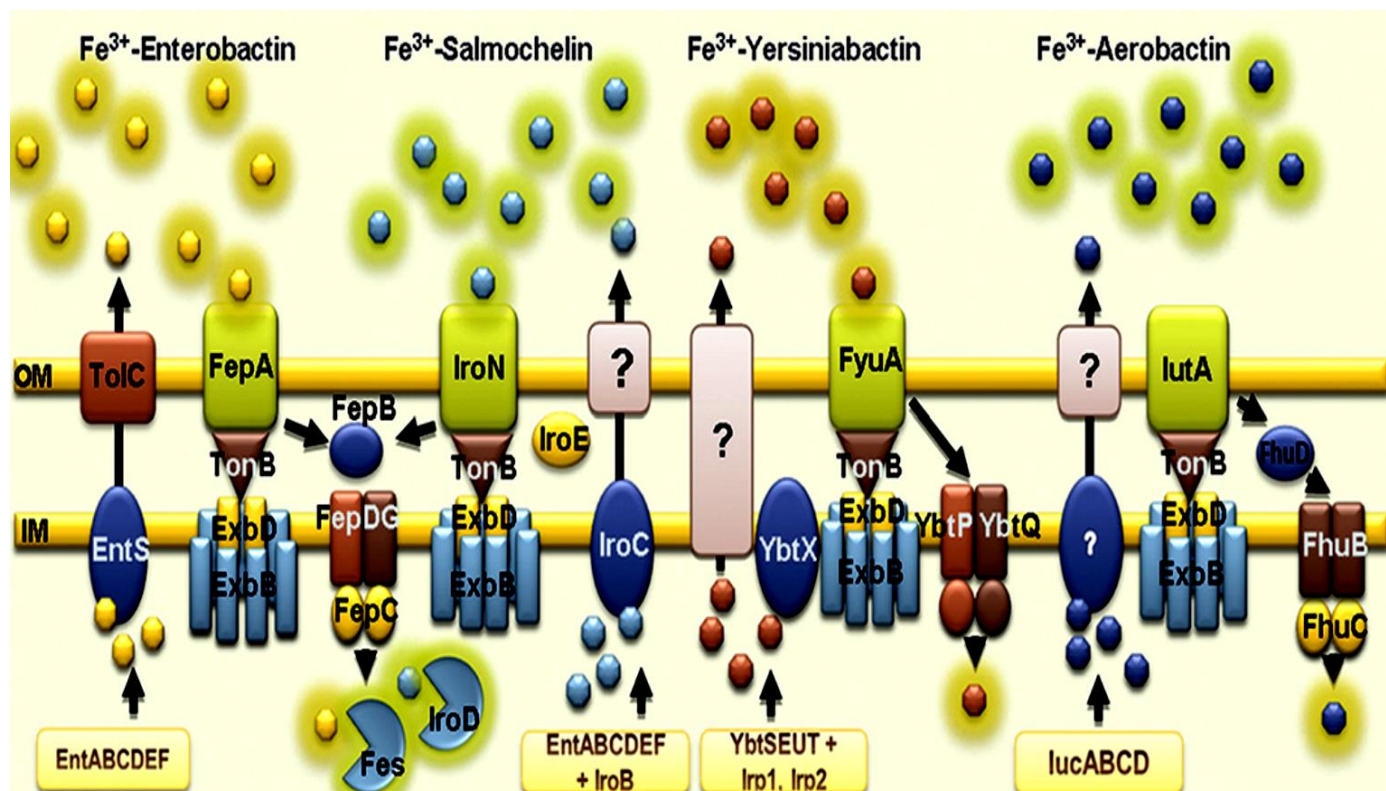
Figure 2.3 An overview of multiple systems playing role in siderophore-associated uptake of iron in *E. coli.*

Figure shows different systems contributing in synthesis, uptake, transfer, internalization and processing of enterobactin, salmochelin, yersiniabactin and aerobactin. Yellow rectangles indicate proteins involved in biosynthesis, dark blue ovals represent integral membrane exporters, light green indicate OM receptors, while light blue color indicate TonBExbDB complex used for energy transduction. ATP-binding cassette (ABC) are indicated on inner membrane (IM) adjacent to them are periplasmic binding proteins. Esterases (FeS and IroD) involved in breakdown of catecholates from enterobactin and salmochelin are shown inside cytoplasm. Proteins with unknown mechanism are indicated as question marks Source: (Garénaux et al., 2011).

2.10.4.3 Enterobactin

Enterobactin is produced by both commensal and pathogenic strains. The enterobactin gene cluster is encodes 15 genes responsible for biosynthesis, uptake and transport (Figure 2.5) (Crosa and Walsh, 2002). Out of 15 genes, 6 are involved in enterobactin biosynthesis and the process is completed in two steps. In the primary step synthesis of <u>2,3- dihydroxybenzoate (2,3-DHB)</u> from chorismate takes place, involving EntC (isochorismate synthetase), EntB (isochorismatase) and EntA (dihydroxybenzoate dehydrogenase respectively (Ozenberger et al., 1989, Liu et al., 1989). In the second stage 2,3-DHB and serine are processed by a non-ribosomal peptide synthetase (NRPS) enzymatic complex constituted of EntB, EnE and EntF to synthesize the final enterobactin molecule <u>2,3-dihydroxybenzoyl serine, (a cyclized DHBS)</u> (Roche and Walsh, 2003). In this stage activation of thiolation domain of NRPS and 2, 3-DHB mediated by EntD (phosphopantetheinyltransferase) also takes place. The role of enterobactin in case of ExPEC virulence is relatively negligible as compared to aerobactin and yersiniabactin. It was shown that a mutant strain lacking aerobactin and salmochelin while producing enterobactin was outcompeted in chicken infection model (Dozois et al., 2003). The inefficacy of enterobactin in successful pathogenesis is attributed to the fact that it can be readily scavenged by the host immune defense proteins lipocalin 2 or siderocalin. In order to overcome this host barrier, a glycosylated version of enterobactin, salmochelin, is produced, which are found to successfully evade host immune system. Salmochelins are vital virulence factors in the infection process of *Salmonella* and *E. coli* (Fischbach et al., 2006, Edwards and Massey, 2011).

2.10.4.4 Salmochelins

Salmochelins were first identified in *Salmonella enterica*, and they differ from enterobactin because of the glycosylation at C5 residues of enterobactin 2, 3-DHB. IroA locus responsible

for salmochelin biosynthesis was also identified in *Salmonella spp* and is comprised of two convergent regions. One region carries the *iroBCDE* genes involved in biosynthesis and transport of salmochelins, whilst the other region encodes the *iroN* gene for salmochelin receptor (Garénaux et al., 2011, Bäumler et al., 1998). Although only IroB is reported to be required for generation of salmochelin from enterobactin, Fes, IroD, IroE esterases can be used to produce six other linear forms of salmochelins (Caza et al., 2008, Johnson et al., 2000). IroB is a glycosyltransferase that is used to transfer glycosyl groups from uridine-5'-diphosphoglucose to C5 residues of enterobactin 2,3-DHB and generates three types of cyclic salmochelins; diglucosyl-C-enterobactin (DGE), triglucosyl-C-enterobactin (TGE) and monoglucosyl-C-enterobactin (MGE) (Fischbach et al., 2005). In UPEC salmochelin associated genes are usually encoded by ColVor ColBM virulence plasmids, although they have been reportedly found on chromosomally encoded pathogenicity-associated islands (PAI) in few strains (Johnson et al., 2006). They count for 77% of UPEC strains, and their receptor iroN is reported to enhance virulence of UTI strain CP9 and NMEC strain 588. UPEC strain UTI89 is reported to have increased expression of *iroN* inside intracellular bacterial communities (IBC) in a mouse model (Reigstad et al., 2007a, Peigne et al., 2009).

2.10.4.5 Yersiniabactin

Yersiniabactin is a mixed-type siderophore, first identified in *Yersinia entercolitica* in the year 1993 (Jürgen et al., 1993). Yersinibactin synthesis occurs through a NRPS/PKS (polyketide synthase) system (Miller et al., 2010). Yersiniabactin encoding gene cluster is present on a high pathogenicity island (HPI) and is comprised of 13 genes. All the 11 genes responsible for yersiniabactin biosynthesis are grouped in a single gene cluster except *fur* and *ybtD* (putative phosphopantetheinyl (P-pant) transferase) (Miller et al., 2010). The 5' end of the HPI consists of the core gene cluster and contains 12 genes, namely: *int* (P4 integrase) and genes for

biosynthesis and uptake of yersiniabactin (*irp* 1 – 9, *ybt*A and *fyu*A). The *fyu*A gene of *E. coli* is 99.6% identical to the *Y. pestis* gene (Schubert et al., 2000a). Briefly, *irp9* (*ybtS*) a salicylate synthetase, synthesis salicylate from chorismate, followed by its adenylation by YbtE and transferred to the NRPS/PKS complex. Next, the two thiazoline rings are synthesized by NRPS system (encoded by *irp2*) cysteines. On the PKS (encoded by *irp1*), a monolinker is incorporated and reduction of thiazoline ring to thiazolidine is executed by YbtU. YbtT (putative thioesterase) performs editing by removing unnecessary molecules. In the final step the newly synthesized siderophore molecule is released from the enzyme complex by PKS (Miller et al., 2010).

Yersiniabactin has been shown to play significant role in the establishment of UTI. It plays a critical role in iron uptake and aids in biofilm formation in human urine (Garcia et al., 2011, Hancock et al., 2008). Yersiniabactin reduce reactive oxygen species (ROS) formation from macrophages, monocytes and polymorphonuclear leukocytes by sequestering iron and inhibiting Haber–Weiss reactions (Paauw et al., 2010). They hold pivotal part in successful pathogenesis of UPEC in cystitis and pyelonephritis. Yersiniabactin import mutants were reportedly attenuated in UPEC isolates, to progress the infection (Brumbaugh et al., 2015).

2.10.4.6 Aerobactin

Aerobactin was first identified in *Aerobacter aerogenes,* grown under iron deficient medium (Gibson and Magrath, 1969). It is reportedly found on ColV plasmid and carries four biosynthesis genes (*iucABCD*) and one transport gene (*iutA*) (de Lorenzo et al., 1986). IucD (monooxygenase)   synthesizes   N6-hydroxy-L-lysine   from   L-lysine.   Next,   IucB (acetyltransferase) converts N6-hydroxy-L-lysine and acetyl-CoA to N6-acetyl-N6-hydroxy-Llysine. Acylation and condensation of to N6-acetyl-N6-hydroxy-Llysine is aided by IucA and IucC, respectively to produce final product aerobactin (de Lorenzo et al., 1986, Garénaux et

al., 2011, Garcia et al., 2011). Aerobactin are found more associated with pathogenic strains as compared to non-pathogenic strains. In UTI mouse model aerobactin helps in iron uptake and **Δ***iucD* mutants have been shown to have reduced colonization in several internal organs (Gao et al., 2012a). Moreover in an aerobactin deficient APEC strain, virulence potential was compromised as compared to the WT strain, in a chicken systemic infection model (Dozois et al., 2003).
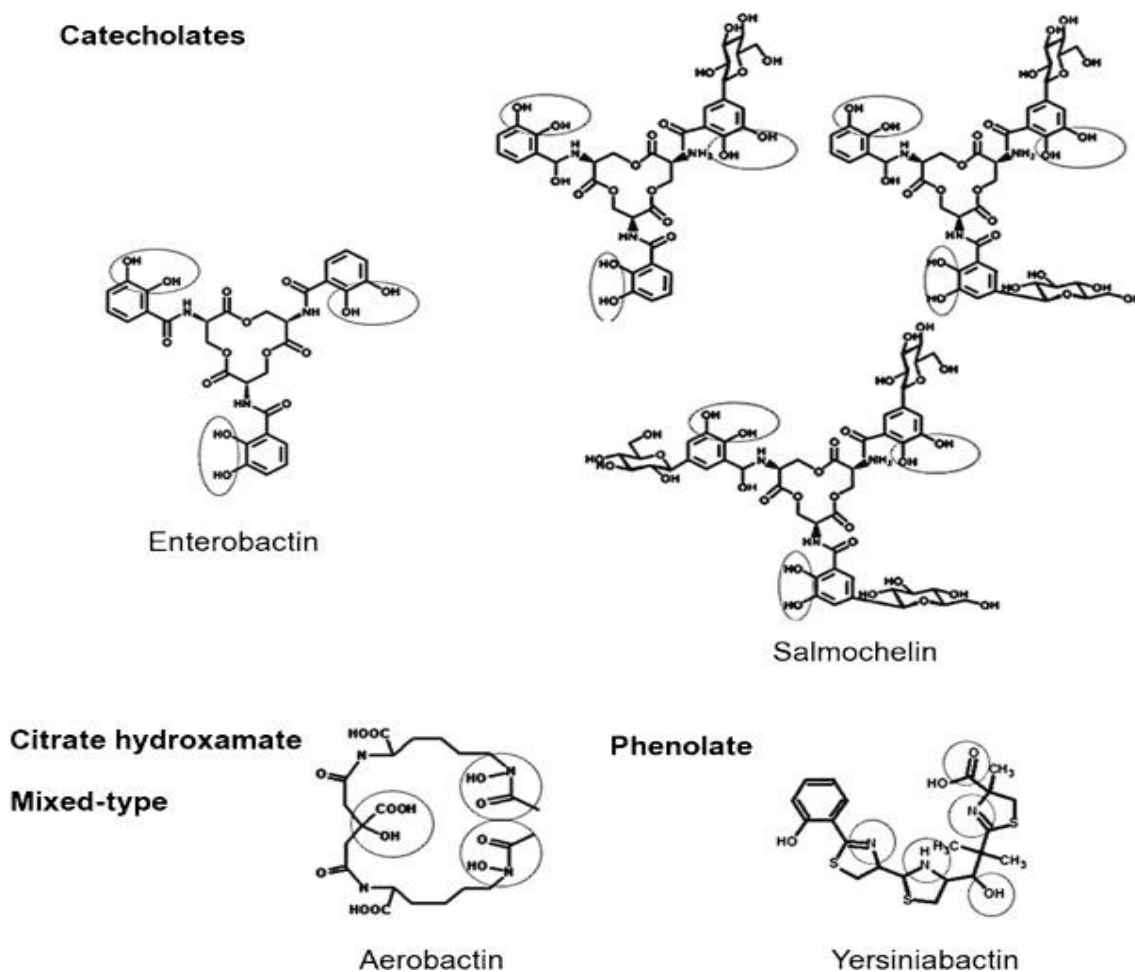
Figure 2.4 Siderophores produced by pathogenic *E. coli*.

Catecholates include enterobactin (non-glycosylated) and salmochelins-the (glycosylated) derivatives (MGE, DGE, TGE) and are produced by ExPEC. Aerobactin (mixed-type hydroxamates) and yersiniabactin (phenolates) are also more frequent among ExPEC. Encircled zones indicate the iron-binding domains of siderophores. Source (Garénaux et al., 2011).
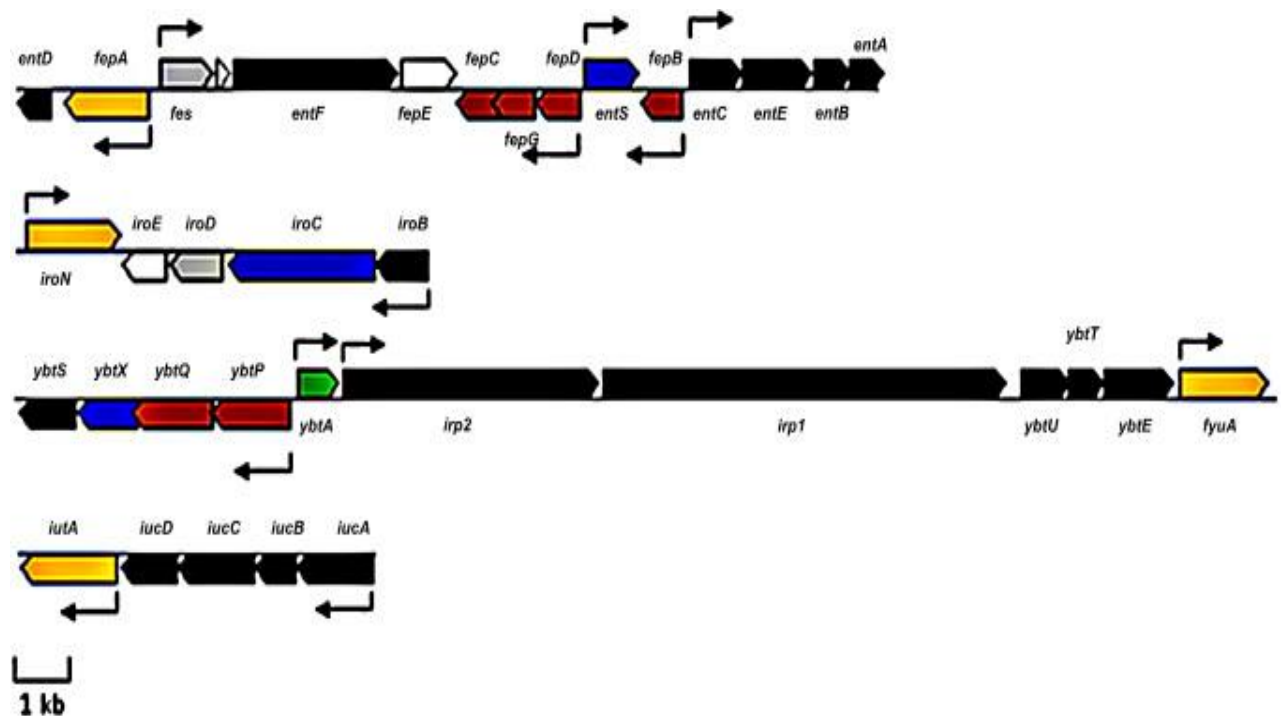
Figure 2.5 Gene clusters responsible for synthesis of enterobactin, yersiniabactin and aerobactin.

Black arrows indicate gene clusters responsible for biosynthesis, blue indicate, yellow indicate, reception, brown indicate import and grey arrows indicate degradation of siderophores. Thin black arrows represent promoters containing a fur box. Source (Garénaux et al., 2011).

2.10.4.7 Acquisition of host iron sources

In addition to the siderophore mediated iron uptake, bacterial pathogens have devised mechanisms/strategies to scavenge iron directly from the host iron resources. Bacteria like *Haemophilus, Neisseria, Moraxella and Pasteurella spp.,* bind to host's transferrin proteins remove its iron via a TonB dependent OM receptor and lipoprotein (Cornelissen, 2003). Similar mechanism is deployed to sequester lactoferrin-bound iron. However, most widespread mechanism of iron acquisition from host is in the form of heme. Most of the pathogenic bacteria, sequester heme either directly through TonB dependent OM receptors or indirectly by removing heme from hemoproteins then transporting it into periplasm, from where it is transferred to cytoplasm through specific ABC transporters (Hagan, 2009). Certain species

such as *Yersinia pestis*, *Pseudomonas aeruginosa* and *Serratia marcescens* are reported to secrete hemophores. Hemophores are small proteins that scavenge heme and transfer it to OM receptors like siderophores(Wandersman and Stojiljkovic, 2000). In pathogenic *E. coli* heme utilization is mediated by *chu* locus, which is homologous to *shu* locus of *Shigella,* involved in heme utilization. The *chu* locus is an eight gene cluster and encodes proteins involved in transport as well subsequent processing (Mills and Payne, 1995) (**Figure 2.6**).

ChuA is a 69 kDa TonB dependent OM receptor bearing 99% similarity to ShuA receptor of *S. dysenteriae* (Torres and Payne, 1997). The *chuTUV* gene encodes an ABC transporter involved in heme (Burkhard and Wilks, 2008) while *chuS* is described as heme oxygenase that uses cellular electron donors to catalyzed degradation of heme into biliverdin, carbon monoxide, and free iron (Suits et al., 2005). Crystal structure of *chuS* revealed a unique fold in its structure unlike other bacterial heme oxygenases, which is speculated to enable *chuS* to utilize a wider range of electron donors (Suits et al., 2005). Although functionality of remaining *chu* genes has not been elucidated yet, however *chuX* is shown to have a role in heme binding and *chuW* is speculated as a potential porphyrin oxidase (Suits et al., 2009).
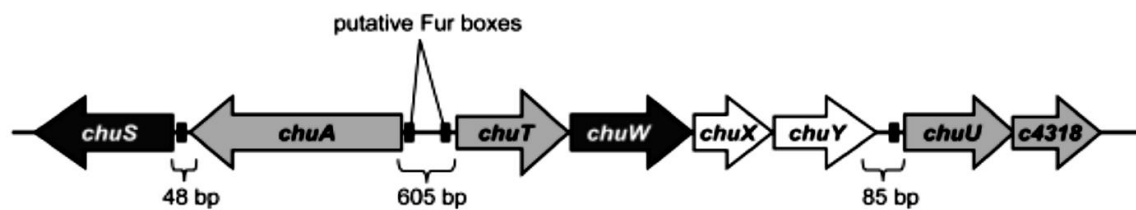
Figure 2.6 *E. coli chu* **heme utilization locus.**

Black arrows represent genes involved in heme processing (*chuS, chuW),* gray arrows represent genes involved in heme transport (*chuA, chuT, chuU, c4318*); c4318 role is not identified yet, it is homologous to *shuV S. dysenteriae.* White arrows (*chuX, chuY*) indicate gene with unknown function. Source (Hagan, 2009).

2.11   Molecular mechanisms of UPEC pathogenesis

The human UT is normally sterile. The shear flow of urine, secretion of tissue-associated antimicrobial factors and bactericidal activity of immune cells prevent contamination of urine from pathogens (Foxman et al., 2000b). Despite a continuous check by immune system, UPEC successfully evades the host defense barriers and successfully colonizes UT. Therefore, it is necessary to understand the molecular mechanisms of pathogenesis in order to introduce novel and effective therapeutic options (Bergstrom et al., 1999). Numerous studies have been conducted to understand the cellular and molecular basis of infection. Recent advances in new mouse models have also enabled to study the infection basis of recurrent UTI (RUTI) and complicated UTIs such as catheter associate UTI (CAUTI), pyelonephritis and renal abscess. Such advances have further elucidated the role of host and pathogenic virulence factors in the progression of UTI.

2.11.1 Entry

Initiation of UTI begins with UPEC entry into UT niche, which is likely to get introduced after colonization of peri-urethral space by GIT flora (Raz et al., 2000b). UPEC ascends toward urethra by overcoming the challenge of moving against the urine flow, in a relatively undetermined mechanism.

2.11.2 Adherence

After entering bladder, UPEC adheres to bladder superficial umbrella (facet) cells prevents itself from being flushed out by urine. Facet cells are terminally differentiated, large epithelial cells (Wu et al., 2009). Plasma membrane of facet cells contains a quasicrystalline array of uroplakin integral membrane proteins. These uroplakin cells are comprised of four uroplakin proteins, "UPIa, UPIb, UPII and UPIIIa", which constitute a permeability barrier for adherence of bacteria (Xie et al., 2006). Urothelium is further coated by proteoglycan mucin layer and prevents bacterial colonization due to the presence of higher negatively charged, sulfated and carboxylated glucosaminoglycans as well as the reduced availability of the receptors (Xie et al., 2006, Wu et al., 2009).

Despite all these barriers, UPEC adhere to bladder epithelial cells due to its ability to express mannose-binding type 1 pili. UPEC binds to high mannose glycoprotein uroplakin (UP1a) via type 1 pili adhesion protein, FimH (Wu et al., 2009). Soluble host factors such as Tamm-Horsfall protein protect the bladder by competing with type 1 pili (Bates Jr et al., 2004), once UPEC successfully binds to the urothelium the virulent cycle of infection is ready to begin.

2.11.3 Invasion

UPEC encodes several factors to invade host cell. The surface mediated adhesins are involved in both adherence and invasion of host bladder cells (Mulvey et al., 1998).

The Afa/Dr are recognized by host surface receptors, CD55 and $\alpha5\beta1$ integrins. Once Afa/Dr bind to host surface receptor they trigger internalization of UPEC by host cells. Internalization of UPEC occurs in a zipper like mechanism and involves additional receptors such as CD66e and decay accelerating factor (DAF). CD66e receptors carry glycosylphosphatidylinositol (GPI) regions, which facilitate clustering of receptors around adherent UPEC. Receptor clustering results in modulation of cytoskeleton, which induces a phagocytic cup to envelop UPEC, allowing it to enter the host cell(Peiffer et al., 1998). Afa-III mediates UPEC internalization through a DAF and CD66e independent pathway that involves binding to $\alpha5\beta1$ integrins (Plançon et al., 2003). Once UPEC is internalized it is enclosed into membrane bound vacuoles (MBV). Cytotoxin necrotizing factor (CNF-1) is also reported to induce internalization into host cell by modulating cytoskeleton (Visvikis et al., 2011b).

FimH mediated invasion occurs through receptors such as UP1a and CD48, both of which are localized within lipid raft domains (Wu et al., 2009). The binding of type 1 fimbriae with UPIa results in activation of focal adhesion kinase (FAK) and protein tyrosine kinases. FAK creates binding site for phosphoinositide-3 kinase (PI3K) at protein tyrosine kinases, leading to the activation of PI3K. P13K catalyzes synthesis of phosphatidylinositol 3-phosphate (PI3P), which acts as a messenger and results in the activation of RhoGTPase Rac 1. RhoGTPase then modulates actin cytoskeleton rearrangement (Visvikis et al., 2011b).

Once internalized, UPEC becomes enclosed in MBVs and prevents fusion of these vacuoles with lysosomes. MBVs help bacteria to get nutrients from host and shields from host innate and adaptive immune responses. The fate of UPEC within MBVs depends upon differentiation status of bladder cells. Entering the cytosol of facet cells, they have been reported to replicate rapidly forming a loose collection of bacteria called intracellular bacterial communities (IBCs) (Mulvey et al., 2000).

2.11.4 Intracellular bacterial community (IBC)

After reaching cytosol of facet cells, it starts multiplying rapidly to form IBCs. During early stages of IBCs UPEC are loosely attached, rod-shaped and non-motile. However, in the middle stage they become closely packed and adapt coccoid morphology and by the end of mature stage IBCs are in the form of dense and an organized community. At the outer edge of the middle stage IBCs the coccoid UPEC differentiate into rod form, become motile and flux out into the bladder lumen (Anderson et al., 2003a). This fluxing out leads to bacteriuria and helps spread into other cells as a result of exfoliation

2.11.5 Exfoliation

After the IBC formation, bacteria start effacing out into bladder lumen. The infected cells undergo apoptosis as a result of the interaction between bacterial ligands and host receptors. As a result, membrane integrity is lost causing release of motile bacteria. Exfoliation is triggered by the engagement of FimH with UPIa. Other bacterial virulence factors like CNF-1, hemolysin and the death receptors of factor receptor (TNFR) superfamily are also involved in induction of apoptosis (Mysorekar et al., 2002, Mysorekar and Hultgren, 2006).

2.11.6 Quiescent intracellular reservoir (QIR)

As a result of exfoliation and apoptosis facet cells are damaged which lets UPEC to gain entry into underlying immature bladder cells. Within these underlying cells UPEC are often entangled within actin fibers as a result of which bacterial replication is limited. In response to limited replication bacteria establish quiescent intracellular reservoirs (QIRs), where it can stay undetected from host immune system for longer periods of time. It has been shown that facet cell exfoliation can revert QIRs into active form, leading to recurrent UTI (Mysorekar and Hultgren, 2006).

2.12   Treatment options for UTI

The foremost step for U'Tis' treatment is accurate diagnosis of type and nature of infection such as, "acute uncomplicated cystitis or pyelonephritis, acute complicated cystitis or pyelonephritis, catheter associated UTI (CA-UTI), prostatitis or asymptomatic bacteriuria (ASB)". (Beahm et al., 2017). According to IDSA, the empiric treatment for uncomplicated UTI should be led by local susceptibility pattern. It further recommends prescription of trimethoprim/sulfamethoxazole (TMP-SXT) only if the local antibiotic resistance prevalence is less than 20%, likewise for fluoroquinolones (FQ) the suggested level is 10% (Gupta et al., 2011b). Similarly, for complicated UTI the empiric regimen should be recommended according to the local susceptibility trends of uropathogens (Helen S. Lee, 2018, Bennett et al., 2014). Collateral damage is another important criterion for treatment of uncomplicated UTIs (Gupta et al., 2011b). Collateral damage is regarded as an ecological adverse effect, such as selection of drug resistant microorganisms, subsequent colonization of MDR organisms as a result of the selected antimicrobial therapy. For instance, use of broad spectrum cephalosporins have been associated with successive infections vancomycin-resistant enterococci (VRE), β-lactam resistant *Acinetobacter spp.* and ESBL producing *K pneumoniae.* Likewise the use of FQ has been associated with subsequent infection of "methicillin-resistant *S. aureus* (MRSA)" and increased resistance in *Pseudomonas aeruginosa* (Paterson, 2004). Other parameters for antibiotic recommendation include safety and evaluation of possible adverse actions of the treatment, costs and market availability of certain compounds in consideration with local or country wise antibiotic susceptibility patterns (Bartoletti et al., 2016). UTI treatment guidelines issued by IDSA, ESCMID and European Association of Urology (EAU) are summarized below. For the acute uncomplicated cystitis (AUC) nitrofurantoin monohydrate/macrocrystals (100mg) twice daily for 5 days is recommended due its minimal resistance level and tendency for collateral damage. Alternatively, TMP-SXT DS twice daily for 3 days is recommended

when the strain causing AUC is susceptible or the local antibiotic resistance profile for AUC does not exceeds 20%. Otherwise, Pivmecillinam 400 mg twice daily for 3 days or fosfomycin 3 gm single oral dose should be recommended due to minimal risk of resistance and collateral damage or, If the above recommended antibiotics cannot be used amoxicillin-clavulanate or cefdinir or cefpodoxime-proxetil or cefaclor for 3-7 days are recommended. Likewise, fluoroquinolone (ciprofloxacin (250 mg, twice daily) /levofloxacin (250-500mg, once a day) for 3 days is also recommended. For the acute uncomplicated pyelonephritis (AUP) susceptibility, testing is recommended.

Oral ciprofloxacin (500 mg twice daily) for 7 days, OR, ciprofloxacin ER (1000 mg once daily) for 7 days is recommended when patients does not require hospitalization or levofloxacin (750 mg once daily) for 5 days is recommended where local resistance profile for fluoroquinolones does not exceed 10%. OR. If the prevalence of fluoroquinolones resistance exceeds 10% initial 1-time intravenous (IV) dose of a long-acting parenteral antibiotic agent such as ceftriaxone or combined with 24-h dose of an aminoglycoside, is recommended. Alternative choice of drug after susceptibility is confirmed could be trimethoprim/sulfamethoxazole (160/800 mg, twice daily) for 14 days or Cefpodoxime proxetil (200 mg-twice daily) for 10–14 days or amoxicillin/clavulanate (500mg thrice a day) for 10-14 days (Gupta et al., 2011a).

For UTIs and asymptomatic bacteriuria (ABU) in pregnant women following drugs should be recommended. Nitrofurantoin monohydrate/ macrocrystals 100 mg (twice daily) for 5–7 day- (except during first trimester or near term) or amoxicillin 500 mg (thrice daily) for 3–7 days or amoxicillin/clavulanate 500 mg (thrice a day) for 3–7 days. Or cephalexin 500 mg (4 times a day) for 3–7 days or cefpodoxime 100 mg (twice daily) for 3–7 day. For prevention of recurrent UTIs (RUTI), nitrofurantoin 50 mg (at night) or Trimethoprim/sulfamethoxazole 40/200 mg (once daily) is recommended. For complicated infections like acute bacterial prostatitis,

ceftriaxone 1–2 g (IV) every 24-hours followed by oral fluoroquinolones for 2–4 week or ciprofloxacin 400 mg (IV) every 12 hours. Or levofloxacin 500 mg (IV) every 24 hours should be administered. For chronic bacterial prostatitis, ciprofloxacin 500 mg (twice daily) for 4–6 weeks levofloxacin 500 mg (once daily) for 4–6 weeks or trimethoprim 100 mg (twice daily) for 4–12 weeks. Or Doxycycline 100 mg (twice daily) for 4 weeks should be recommended.

2.13   Challenge of antibiotic resistance in UPEC- an overview

Antibiotics are lifesaving drugs and are considered a standard for treatment of life-threatening infections caused by bacteria. However, the practice of prescribing antibiotics without prior diagnosis has resulted in increased resistance among bacteria particularly uropathogens. This has led physicians to recommend last line of drugs for growing common infections and thus have decreased the efficacy of the treatment. The challenge of antibiotic resistance is growing at such a pace that recently a study published by leading economist funded by UK government reports that as a result of growing AMR 700,000 deaths every year across the globe. They have further warned of this figure to reach 10 million/year by 2050, if rapid and proactive solution is not found (de Kraker et al., 2016) The suggested death toll is more than the current death rate of cancer. Moreover, World Bank suggests an estimated loss of $100 trillion by 2050 in combating such infections (Brown et al., 2017, O'Neill, 2014).

Uropathogenic *E. coli* is the leading cause of UTI and is increasingly becoming resistant to the frontline drugs administered against it. It is on high risk priority pathogen due to its association with carbapenem and broad spectrum β-lactam (3rd generation cephalosporin) drugs (World Health Organization, 2017). There are differences in global data e.g., studies report FQ resistance in UPEC from China, Vietnam and India as high as 70% and around 60% of these FQ resistant are also co-expressing ESBLs (Jean et al., 2016). However, a national survey conducted in Australia in 2012 reports significantly lower level of resistance in UPEC. The

study reports 4.2% and 6.9% of *E. coli* resistant to third-generation cephalosporins and FQ respectively (Turnidge et al., 2014).   Similarly, across Europe countries like Netherlands have as low as 0.2% resistance against carbapenems and in Greece its reported to be around 59.4%. Similarly, in USA the resistance rate against carbapenems, cephalosporins and FQ is less than 10% (Zowawi et al., 2015). A global survey conducted by Study for Monitoring Antimicrobial Resistance Trends (SMART) 2002-2011 reports a high level (~40%) of ESBL mediated resistance in uropathogens (*E. coli*, *K. pneumoniae* and *P. mirabilis*) across Asia, Middle East and Latin America. However, across Europe, North America and Africa its prevalence was about 8-12% in 2011(Morrissey et al., 2013).

The most common ESBL associated with UPEC is CTX-M-type. About 97% of ESBL producing *E. coli* from Europe and North America are reported to carry CTX-M (Hoban et al., 2012). Among CTX-M, CTX-M-15 is the most prevalent type and is found associated with sequence type 131 (ST131). ST131 is a globally endemic clone of *E. coli* which is known for its multidrug resistance and high virulence profile and is frequently associated with extra-intestinal infections (Nicolas-Chanoine et al., 2014). Studies suggest varying level of ST131 prevalence in different countries. It counts for 21 and 25% of ESBL producing *E. coli* responsible for CAUTI in France (2006) and Mexico (2006-2007) (Arpin et al., 2009,Reyna-Flores et al., 2013). A national survey (2007-2011) in Sweden reports 34% prevalence of ST131 UPEC in CAUTI and HAUTI (Brolund et al., 2014). In India (2009) they are reported to count for 70% ESBL positive *E. coli* in HAUTI (Hussain et al., 2012). Our study in Pakistan (2016) reports 46% of *E. coli* from UTI belonging to ST131 and about half of them were ST131-O25b-H30-R (Ali et al., 2016c). Another study from Pakistan (2013) reports 18% prevalence of ST131 in *E. coli* isolates from blood and urine (Habeeb et al., 2014).

2.14   **Correlation between antimicrobial resistance (AMR) and virulence**

Increasing use of antibiotics in human/animal medicines, livestock, agriculture and improved understanding of underlying mechanisms of HGT between bacterial strains and species have led the focus towards previously unaddressed question of "association between AMR and virulence". Hosts and bacteria have co-evolved over millions of years, during which pathogenic-bacteria have modified their VF to successfully cause infection and evade host immune system (Beceiro et al., 2013). Although with the advent of antibiotics in the scale of infections has been controlled, however improper use of antibiotics has led to global surge in antibiotic resistance. Thus, the spread and evolution of antibiotic resistance occurred mainly in last 60 years after the discovery of first antibiotic in 1928. Despite the difference in time scale of evolution, both virulence and resistance share some common features. i) Both are required for successful survival of pathogen under hostile conditions. Whilst VF are required to overcome host defense barriers, resistance is necessary to avoid antimicrobial therapies and to survive in competitive and hostile niches (Martínez and Baquero, 2002). ii) Both characteristics are commonly acquired between species and genera through HGT, although other mechanisms such as adaptive or compensatory mutations may also occur. iii) Antimicrobial resistance is often associated with infections such as biofilm formation or intracellular infections and is therefore a virulence mechanism as well. iv) Other common characteristics shared by virulence and resistance are contribution of efflux pumps, cell wall modifications, two-component systems involved in regulation of resistance and virulence genes (Beceiro et al., 2013). Given the complexity of the topic itself because of diversity of resistance and virulence mechanism, host and bacterial species, it is difficult to comment on it. However successful dissemination of high-risk clones of both animal and human origins have opened a new question to address upon.

Enterococcus faecium **clonal complex 17 (CC17)**, is an epidemic-virulent clone reported across all the five continents and is reportedly associated with most of nosocomial and clinical infections of *Enterococcus spp.* The clone is characterized by its resistance to quinolones and ampicillin along with the presence of a putative PAI (Galloway-Peña et al., 2009, Leavis et al., 2006). Some authors speculate that clone has been circulating around the globe for about 30 years and have co-evolved resistance and virulence determinants leading to the recent successful spread (Beceiro et al., 2013). It has been demonstrated that a strong correlation between (*P*<0.01) the presence of Esp (enterococcal surface protein, involved in virulence) and resistance to ciprofloxacin, ampicillin and imipenem was found (Billström et al., 2008).

Streptococcus pneumoniae **clone PMEN1 (Spain23FST81)**, is a globally disseminated clonal group belonging to ST81. The clone is estimated to have originated around year 1970 is widely disseminated across Asia, Africa, Europe and America. It is resistant to penicillin, chloramphenicol and tetracycline. Additionally, it is resistant to macrolides and fluoroquinolones (Throup et al., 2000). The clone also encodes several VF at bacteriocin locus (*blp*). The loss of this locus has been demonstrated to lead towards loss of virulence in mouse pneumoniae model (Throup et al., 2000).

Clostridium difficile **ribotype NAP1/027,** is an epidemic quinolone resistant and hyper-virulent clone. It is believed that high production of toxins "TcdA and TcdB, protease Cwp84" along with the antibiotic resistance, has contributed to its global spread (Denève et al., 2009).

ExPEC *E. coli* **clone ST131**, *E. coli* ST131 (O25:H4) id frequently associated with CTX-M-15 ESBLs. This clone is also widely resistant to fluoroquinolones and is reported to harbour various virulence factors such as *iutA, traT, fyuA* (Da Silva and Mendonca, 2012). Pitout *et al*. 2017 found that in general the VF were more frequent among CTX-M producers, similarly *usp* gene (uropathogenic-specific protein) was more prevalent in CTX-M-15 β-lactamase producers (Pitout and DeVinney, 2017). Other studies report co-selection of CTX-M genes and

virulence genes in IncFII group plasmids (such as pEK499) as the driving force for successful distribution of ST131 (Woodford et al., 2009).

2.15 Novel drug targets and approaches regarding UTI treatment

Antibiotics have been used for decades for treatment of UTIs, however due to increased threat of antibiotic resistance and recurrent UTI, efforts are needed to work on novel therapeutic targets. As a matter of urgency novel approaches for UTI treatment are being explored.

2.15.1 Pilicides and mannosides

As discussed previously in section 2.10.1, UPEC type-1 pili is assembled through the chaperone usher pathway. It relies on periplasmic chaperone FimC for folding, stabilization, transport and assembly of pilus assembly (Thanassi et al., 2012). Small artificially synthesized molecules known as pelicides are designed to target FimC chaperones, thus interfering with pilus assembly. This in turn blocks bacterial adhesion to urothelial cells, preventing its colonization. *In vitro* experiments have shown pilicides to effectively inhibit pilus synthesis leading to reduced adherence and biofilm formation (Pinkner et al., 2006, Chorell et al., 2012b). Mannosides are used as soluble receptor analogues to target FimH adhesin. These molecules bind FimH adhesin thus preventing FimH dependent adherence and colonization. Recently developed orally available mannosides derivatives have shown promising results to be used as a new therapeutic agent. They are also shown to reduce UPEC invasion into bladder cells (Chorell et al., 2012a, Han et al., 2010). However, one potential adverse effect associated with pelicides and mannosides is undifferentiated harm to commensal *E. coli* and normal flora of GIT expressing type 1 pili (Barber et al., 2013).

2.15.2 Vaccinology

Another approach to combat recurrent and chronic UTIs is the development of mucosal or systemic vaccines. In the last two decades several vaccination approaches have been explores, including bacterial cell extracts, the use of heat-killed whole bacteria and the purified UPEC associated proteins such as antigens. Solco Urovac is a multivalent vaccine formulation and contains 6 *E. coli* strains plus 1 strain each of *K. pneumoniae, P. mirabilis, E. faecalis* and *Morganella morgani* passed phase II clinical trials (Hopkins et al., 2007). Although some patients showed increase in anti-*E. coli* antibody levels, however no statistically significant difference between vaccinated and placebo control groups were found. That's the reason probably the reason for the lack of any follow-up phase III trials. Other than that, specific bacterial factors have also been tested as potential candidates for vaccine against UTI. Like mannosides and pelicides, antibodies against FimH can disrupt functional hierarchy of type 1 pili, preventing UPEC to colonize the UT. Murine and primate models of cystitis were protected against UPEC when vaccinated with purified FimH coupled to its periplasmic chaperone FimC (Langermann et al., 2000). A similar vaccine containing a truncated version of FimH when inoculated intramuscularly or intranasally with CpG oligonucleotides as adjuvants, protected mice from cystitis (Poggio et al., 2006).As previously discussed in detail in section 2.10.4 iron is crucial/vital element for bacterial survival. While it is present in ample quantities in human body it is in not readily available to bacteria. UPEC have evolved several mechanisms to sequester iron from host through iron chelating molecules and receptors. Iron receptors appear as a promising candidate for vaccine development. Out of 7 UPEC siderophores cognate receptors IreA and IutA have shown to provide protection against induced cystitis. Hma receptor has shown to protect against kidney infection but not for cystitis (Alteri et al., 2009). Further studies are yet to be performed in order to elucidate their vaccine potential.

CHAPTER 3:   MATERIALS AND METHODS

3.1   Sample collection

A total of 250 urine samples were collected from the patients suspected for urinary tract infection from outpatient department (OPD) of Islamabad Diagnostic Centre (IDC) and Pakistan Institute of Medical Sciences (PIMS). Patients were provided with sterile and screw capped containers for collection of midstream urine. Samples were labeled with patient ID, gender and date. Within 30 minutes of the collection, the samples were sent for microbiological analysis.

3.1.1   Inclusion criteria and exclusion criteria

Both male and female patients of all age groups having sign and symptoms of urinary tract infections, patients with colony count $> 10^5$ colony-forming units CFU/ml and patients with pyuria (Pus cell>10-12/HPF) were included in the current study. All the patients using antibiotics, samples collected in non-sterile and unclean container, inadequate sample and colony count, less than10^5 CFU/ml were excluded from present study.

3.2   Microbiological analysis

3.2.1   Isolation and identification

In order to make an estimate about colony forming unit (CFU) sterile and calibrated loops of 01 µl (0.001mm) were used. The specimen was inoculated on Cytosine Lactose Electrolyte Deficient (CLED Agar, Oxoid England) agar and incubated for overnight at 37°C under aerobic conditions. The primary culture so obtained was then grown over MacConkey agar (Oxoid England). Pure cultures obtained were preserved on MacConkey plates and nutrient agar slants for shorter period of time, whilst for longer time preservation glycerol preservation was used, later stored at low temperature conditions(-20°C). Identification was made on morphological and biochemical attributes. Moreover molecular identification was done by amplifying 16s ribosomal gene.

3.2.1.1   Colony morphology and Gram-staining

Initially *E. coli* isolates were screened by checking their growth over selective media (CLED and MacConkey agar). Morpho-cultural characteristics of *E. coli* colonies such as color (yellow, pink), shape (round, irregular), size (small, moderate, large), margin and elevation (concave, convex, raised) were kept into consideration, whilst picking up colonies for further identification. Carefully selected colonies from either CLED or MacConkey agar were then processed for Gram-staining for further confirmation. For smear preparation, a small part of isolated colony was transferred to the normal saline by using a sterile loop and a thin smear was made. To make a uniform smear circular movement was used. Smear was air-dried and then gently heat fixed. After fixation, slide was allowed to cool down. Fixed smear was then generously covered with crystal violet (CV) dye for one minute that was subsequently washed/rinsed off with tap water and the water was tipped off. It was covered with iodine stain for ~1 min. Slide was rinsed/washed with tap water and water was tipped off. After decolorizing step with alcohol for few seconds slide was rinsed with tap water. The smear was counter stained with safranin dye for 30 seconds and washed subsequently. Slide was air-dried and then observed under oil-immersion(100X) lens.

3.2.1.2   Biochemical analysis

Biochemical identification of *E. coli* isolates was performed by using five tests. Triple sugar iron (TSI), indole, citrate, urease and lactose-fermentation (LF) tests were performed.

(a) *Triple sugar iron test*

In order to differentiate members of Enterobacteriaceae from non-Enterobacteriaceae TSI was performed. Principle is based on the utilization of carbohydrates, amino acids (a.a) and the presence ferrous ions in the medium. Due to inoculation of microorganism into TSI agar slant, color changes are observed in slant and butt. A sterile inoculating needle was used to touch the

center of a well isolated colony from freshly grown colonies over Mackonkey plates. Then slant was stabbed into within 3-5mm from bottom. After stabbing needle was withdrawn and entire surface of the slant was streaked. Loosely tightened the cap of the test-tube and incubated under aerobic conditions at 37°C for 18-24 hours. After overnight incubation results were recorded.

(b) *Indole test*

This test is used to confirm *Enterobacteriaceae* species. Its principle is based on the ability of utilization of indole from amino acid tryptophan due to the presence of an enzyme tryptophanase. Utilization of indole results in the formation of red to brown colour ring in peptone water. No ring formation indicates absence of indole utilization. Isolated colony of test organism was inoculated into peptone water (2 ml) and test tubes were incubated overnight at 37°C. Following day 1-2 drops (~0.5 ml) of Kovac's reagent were added, test tubes were shaken gently and then were allowed to settle for few moments. Results were noted.

(c) *Citrate hydrolysis test*

Initial differentiation between *Enterobacteriaceae* and non-*Enterobacteriaceae* was followed by citrate test. This is used to differentiate among members of *Enterobacteriaceae*. Principle is based on the utilization of citrate present in medium. Utilization of citrate results in the degradation of ammonium salts into ammonia resulting in an increased pH due to alkalinity. This shift in pH leads to the colour change of bromothymol indicator in medium from green to blue. If there is no citrate utilization no colour change is observed. A sterile inoculating needle was used to pick inoculums from the center of an isolated colony. Then the citrate agar slant was streaked back and forth. Test tubes were capped loosely. Test tubes were incubated at 37°C under aerobic conditions for 18-24 hours. After overnight incubation color changes were observed and noted.

(d) *Urea hydrolysis test*

This test is used to differentiate *E. coli* from *Proteus vulgaris* and *Klebsiella pneumoniae* based on urea hydrolysis. Urea is produced as result of de-carboxylation of certain amino acids. It can be hydrolyzed into CO_2 and ammonia gas by the action of urease. As a result of this hydrolysis pH of agar is increased resulting in a change of colour of phenol-red (an indicator) to red. Organisms that lack this particular enzyme will experience no change in color of media. A sterile inoculating needle is used to pick up freshly grown and isolated colonies of test organism. The test organism is inoculated into Christensen's urea agar slants and incubated at 37° under aerobic conditions for 18-24 hours. Next day colour change was observed and results were noted.

(e) *Lactose fermentation test*

This test is used to differentiate coliforms from non-coliforms. This test is based on the ability of certain group of bacteria to assimilate carbohydrates, present in the media like MacConkey and CLED agar. A color change in indicator is observed. Tested organism is streaked upon MacConkey and agar plates, incubated at 37°C under aerobic conditions for 18-24 hours. The shift/change in color of medium is observed.

3.2.1.3   Molecular identification

Molecular identification of biochemically identified *E. coli* isolates was performed to further ensure the authenticity of screened isolates. All the biochemically confirmed isolates were subjected to DNA extraction (phenol-chloroform method) followed by PCR using *E. coli* specific primers as previously mentioned by Ali *et al*., 2014.

3.3   **Genomic DNA extraction**

Briefly, a single colony was inoculated into 5ml of L-broth and incubated at 37°C overnight. Next day the bacterial suspension was centrifuged at 10,000 rpm for 5 minutes, to collect the pellet. L-broth was discarded, and pellet was further proceeded fore genomic DNA extraction. Bacterial pellet was again suspended in 450µl TE buffer further followed by the addition of 45µl of 10% SDS and 5 µl of Proteinase K (20mg/ml). The mixture was gently mixed until all the pellet was dissolved until no clumps were visible and incubated at 37°C for 1 hour. After incubation 500 µl of phenol-chloroform (1:1) was added and suspension was mixed completely by gentle vertexing. The resultant suspension was centrifuged at 10,000 rpm for 2 minutes. The upper aqueous phase was carefully separated and transferred into a new 1. 5ml microcentrifuge eppendorf tube. To this aqueous phase again 500 µl phenol-chloroform and centrifuged at 10,000 rpm for 5 minutes. After centrifugation, again the aqueous layer was separated and transferred it into new 1.5ml microcentrifuge eppendorf tube. To this aqueous layer was added 50 µl of 3M sodium acetate and 300 µl of isopropanol, mixed well until DNA precipitates were formed and again centrifugation at 10,000 rpm was performed for ~5 minutes. Liquid phase was removed/discarded, and the microcentrifuge tube was washed with 1 ml 70% ethanol and centrifuged at 10,000 rpm for 01 minute. Ethanol was carefully removed, and tube (s) were inverted over a sterile blotting paper under sterile conditions to dry off the moisture from tube (s). Finally, 100- 200 µl of TE buffer+RNase was added, and DNA was stored at -20 °C after confirmation by agarose gel electrophoresis (AGE).

3.3.1   **Polymerase chain reaction (PCR)**

The "*E. coli* identification primers" (E.C) targeting proximal and distal conserved flanking regions of 16s ribosomal RNA were used (Table 3.3). PCR reaction mixture was prepared by in 25 µl volume using, 0.2 ml thin walled PCR tubes. DNA polymerase, 25 mM $MgCl_2$, 100mM

dNTPS and 10X reaction buffer were purchased from Thermo Fisher Scientific™. PCR

reaction mixture and amplification conditions are given in Table 3.1 and 3.2 respectively.

Table 3.1 Concentrations of reagents used in the polymerase chain reaction for UPEC identification

Reaction Components (Thermo Scientific)	Volume	Final Concentrations
DNA Template	2μL	~ 100 ng
Taq Polymerase	0.25μL	1.25 Units
Forward Primers (10 μM)	1 μL	0.4 μM
Reverse Primers (10 μM)	1 μL	0.4 μM
MgCl$_2$ (25 mM)	1.5μL	1.5 mM
10X Taq Buffer ((NH$_4$)$_2$SO$_4$ – MgCl$_2$)	2.5μL	1X
dNTP's	0.5μL	200 μMole
PCR Water	10.75μL	
Total Reaction Volume	25μL	

Table 3.2 Thermocycler conditions used for PCR amplification of E. C primer

Initial denaturation	95° C 5 min	
Denaturation	95° C 45 sec	
Annealing	57 ° C 1 min	X 35 cycles
Extension	72 ° C 1 min	
Final extension	72 ° C 1 min	

3.3.2 Agarose gel electrophoresis

The resulting 450 bp PCR fragment was run on 1 % agarose gel, prepared in 1X TBE buffer.

The gel was run at 80 V for 60 min in BIO-RAD™ gel electrophoresis equipment. The gel was

observed under UV-transilluminator and photographed by BIO-RAD^{TM} gel documentation

system.

Table 3.3 List of primers used in this study

Primer	PS	Nucleotide sequence (5'→ 3')	Size of product (bp)	Source
E.C	F	CAATTTTCGTCTCCCCTTCG	450 bp	(Khan et al., 2007)
E. C	R	GTTAATGATAGTGTGTCGA		
TEM-1	F	TTGGGTGCACGAGTGGGT	503 bp	(del Castillo et al., 2013)
TEM-1	R	TAATTGTTGCCGGGAAGC		
OXA-1	F	AGCAGCGCCAGTGCATCA	708 bp	(del Castillo et al., 2013)
OXA-1	R	ATTCGACCCCAAGTTTC		
PSE-1	F	CGCTTCCCGTTAACAAGTAC	419 bp	(del Castillo et al., 2013)
PSE-1	R	CTGGTTCATTTCAGATAGCG		
SHV	F	TCGGGCCGCGTAGGCATG	606 bp	(del Castillo et al., 2013)
SHV	R	AGCAGGGCGACAATCCC		
PapA	F	ATGGCAGTGGTGTTTTGGTG	720 bp	(Johnson and Stell, 2000a)
PapA	R	CGTCCCACCATACGTGCTCTTC		
PapC	F	GTGGCAGTATGAGTAATGACCGTTA	200 bp	(Johnson and Stell, 2000a)
PapC	R	ATATCCTTTCTGCAGGGATGCAATA		
PapEF	F	GCAACAGCAACGCTGGTTGCATCAT	336 bp	(Yamamoto et al., 1995)
PapEF	R	AGAGAGAGCCACTCTTATACGGACA		
PapGI	F	TCGTGCTCAGGTCCGGAATTT	461 bp	(Yamamoto et al., 1995)
PapGI	R	TGGCATCCCCCAACATTATCG		
PapGII	F	GGGATGAGCGGGCCTTTGA	190 bp	(Yamamoto et al., 1995)
PapGII	R	CGGGCCCCCAAGTAACTCG		
PapGIII	F	GGCCTGCAATGGATTTACCTGG	258 bp	(Yamamoto et al., 1995)
PapGIII	R	CCACCAAATGACCATGCCAGAC		
Sfa/foc	F	CTCCGGAGAACTGGGTGCATCTTAC		

Sfa/foc	R	CGGAGGAGTAATTACAAACCTGGCA	410 bp	(Yamamoto et al., 1995)
FimH	F	TGCAGAACGGATAAGCCGTGG	508 bp	(Johnson and Stell, 2000a)
FimH	R	GCAGTCACCTGCCCTCCGGT		
Afa	F	GGCAGAGGGCCGGCAACAGGC	559 bp	(Johnson and Stell, 2000a)
Afa	R	CCCGTAACGCGCCAGCATCTC		
BmaE	F	ATGGCGCTAACTTGCCATGCTG	507 bp	(Johnson and Stell, 2000a)
BmaE	R	AGGGGGACATATAGCCCCCTTC		
HlyA	F	AACAAGGATAAGCACTGTTCTGGCT	1177 bp	(Yamamoto et al., 1995)
HlyA	R	ACCATATAAGCGGTCATTCCCGTCA		
CdtB	F	AAATCACCAAGAATCATCCAGTTA	430 bp	(Johnson and Stell, 2000a)
CdtB	R	AAATCTCCTGCAATCATCCAGTTTA		
IutA	F	GGCTGGACATCATGGGAACTGG	300 bp	(Yamamoto et al., 1995)
IutA	R	CGTCGGGAACGGGTAGAATCG		
FeoB	F	AATTGGCGTGCATGAAGATAACTG	470 bp	(Yamamoto et al., 1995)
FeoB	R	AGCTGGCGACCTGATAGAACAATG		
FyuA	F	TGATTAACCCCGCGACGGGA	880 bp	(Johnson and Stell, 2000a)
FyuA	R	CGCAGTAGGCACGATGTTGTA		
KpsmtII	F	GCGCATTTGCTGATACTGTTG	272 bp	(Johnson and Stell, 2000a)
KpsmtII	R	CATCCAGACGATAAGCATGAGCA		
KpsmtIII	F	TCCTCTTGCTATTATTCCCCCT	392 bp	(Johnson and Stell, 2000a)
KpsmtIII	R	AGGCGTATCCATCCCTCCTAAC		
Usp	F	ATGCTACTGTTTCCGGGTAGTGTGT	1000 bp	(Johnson and Stell, 2000a)
Usp	R	CATCATGTAGTCGGGGCGTAACAAT		

3.4 Antibiotic susceptibility profiling (AST)

3.4.1 Disc diffusion method

Antibiotic susceptibility profiling of UPEC isolates was performed against 23 antibiotics belonging to 8 different classes such as penicillins, cephalosporins, fluoroquinolones, monobactams, tetracyclines, sulfonamides, aminoglycosides and carbapenems. ATCC 25922 (*E. coli*) and ATCC 25923 (*S. aureus*) was used as a control while performing disc diffusion for UPEC isolates. Antibiotic susceptibility profiling was performed according to the Clinical laboratories Standard International (CLSI) guidelines 2013 using Modified Kirby Bauer Disc Diffusion Method. Extended spectrum beta lactamase (ESBL) detection was performed by using double disc synergy test (DDST). This part of the study was performed by Ihsan *et al.,* 2016 as a part of his research and is already published with Rafaque Z as the co- author (Ali et al., 2016a).

3.4.2 Minimum inhibitory concentration

In order to get a quantitative estimation of antibiotic resistance against routine antibiotics (**Table 3.4**) recommended against UTI, their minimal inhibitory concentration (MIC) and minimum bactericidal concentration (MBC) were determined. MIC was determined using broth dilution method as recommended by CLSI and European Committee for Antimicrobial Susceptibility Testing (EUCAST) (Microbiology et al., 2003). MIC (broth dilution) works on the principle of preparation of a regime of antibiotic concentrations, followed by the addition of a known volume of inoculum containing known number of bacterial cells.

3.4.2.1   Antibiotic stock preparation

Stock solution of antibiotics was prepared using formula;

$$\text{Weight of powder (mg)} = \frac{\text{Volume of solvent (mL) x Concentration (mg/L)}}{\text{Potency of powder (mg/g)}}$$

Antibiotics stock solution were stored as aliquots at -20 °C.

3.4.2.2   McFarland standard

McFarland standard 0.5 was used to standardize the approximate number of bacterial cells in the suspension by visually comparing the turbidity of bacterial suspension with 0.5 McFarland standard. The standard was prepared by mixing 9.95 ml of 1% (v/v) H_2SO_4 with 0.5 ml of 1.175% (w/v) $BaCl_2$ $.2H_2O$, to give a total volume of 10 ml. OD_{600} of 0.5 McFarland equilibrates approximately 0.5×10^8 CFU/ml of bacterial cells.

3.4.2.3   Antibiotic dilution preparation for MIC

For each antibiotic to be tested twelve dilutions of 2x concentration were prepared in Mueller-Hinton broth (MHB) and the dilution range was kept from 512 µg/ml to 0.125 µg/ml.

3.4.2.4   Inoculum preparation

A freshly streaked O/N culture was used to pick 3-5 isolated colonies and suspended in 3-5 ml of normal saline. The suspension was vortexed and compared with 0.5 McFarland standard to attain 0.5×10^8 CFU/ml of bacterial cells. This suspension was further diluted in MHB to 1: 100 to get a final cell count of 5×10^5 to 1×10^6 CFU/ml. Equal volume (1:1) of 2x antibiotic concentration and the bacterial suspension were mixed in test tubes/tissue culture plates and incubated overnight at 37°C. Sterile media without antibiotic (sterility control) and bacterial

suspension without antibiotics (inoculum control) were used as two internal controls to maintain the fidelity of experiment.

3.4.2.5   MIC interpretation

After overnight incubation test tubes/wells were observed and results were noted as turbid, slightly turbid and non-turbid based on the appearance of tubes. MIC was determined as the lowest visible concentration that completely inhibited growth.

3.4.2.6   Minimum bactericidal determination

In order to determine minimum bactericidal concentration (MBC), test tubes/wells showing no visible growth were used for transferring 0.01ml (10 µl) of samples into Mueller-Hinton agar, which were incubated at 18h at 37°C. MBC was interpreted as the lowest concentration which produced 99.9% of killing of 10 µl inoculum (five colonies or less).

Table 3.4 List of antibiotics used for MIC determination

Antibiotic	Solvent	Storage
Ceftriaxone	Water	-20 °C
Ceftazidime	Saturated sodium bicarbonate solution	-20 °C
Gentamicin	Water	-20 °C
Trimethoprim	Half volume water, a minimum volume of 0.1 M lactic acid or 0.1 M HCl to dissolve, then make up to total volume with water	-20 °C

3.5   Molecular characterization of UPEC isolates

In order to molecularly characterize the UPEC isolates, they were subjected for the screening of ESBL mediated resistance markers (*bla*TEM-1, *bla*OXA-1, *bla*PSE, *bla*SHV) and eighteen virulence factors (enlisted in **Table 3.3**).

3.5.1 Screening of plasmid mediated resistance (PMR) markers

Plasmid mediated resistance genes (bla_{TEM-1}, bla_{OXA-1}, bla_{PSE}, bla_{SHV}) were screened in ESBL producer strains, as indicated by DDST. Prior to PCR based screening of plasmid mediated resistance genes, plasmids were extracted using "Thermo Scientific™ Gene JET Plasmid Miniprep Kit #K0503".

3.5.1.1 Plasmid extraction

A single colony from freshly streaked plate was inoculated into 7-10ml of LB supplemented with selected antibiotic and incubated for overnight at 37°C with shaking at 200rpm. Next day, the culture was centrifuged at 8000 rpm for 2 min at room temperature. Supernatant was removed, and pellet was proceeded for plasmid extraction according to the manufacturers' instructions. Pellet was re-suspended in 250 µl of the resuspension solution. Cell suspension was re-suspended by vortexing and transferred to 1.5 ml micro centrifuge tube. About 250µl of the lysis solution was added and tube was gently inverted 4-6 times until the solution became viscous and then slightly clear. After this step, 350µl of neutralization solution was added and tube was immediately inverted 4-6 times, to avoid local precipitation. After these steps, tube was centrifuged at 10,000 rpm for 5 min to remove cell-debris along with chromosomal-DNA. Supernatant was shifted to "Gene JET" spin column and centrifuged at 10000 rpm for ~1 min. Discarded the flow through added 500µl of the wash solution that followed centrifugation step for 30-60 seconds (this step was repeated twice). To remove remans of ethanol the column (without any solution) was centrifuged for 30-60 seconds. The column was transferred to a new 1.5ml micro centrifuge tube (collection tube was discarded). Finally, 50µl of elution buffer (or water when used for transformation or electroporation) was added to the center of the column. After incubation centrifugation was done and purified plasmid was visualized on 0.7% agarose gel (run at 60 V for 100 min) and stored at -20°C.

3.5.1.2   Polymerase chain reaction for plasmid mediated resistance genes

PCR reaction mixture was prepared as described previously (Table 3.1), while the reaction conditions were set as given below (Table 3.5). Reactions were carried out in Labnet ® MultiGene OptiMax thermocycler.

Table 3.5 Thermocycler conditions used for PCR amplification of plasmid mediated resistance genes

Initial denaturation	95° C 5 min	
Denaturation	95° C 45 sec	
Annealing	55 ° C 1 min	X 35 cycles
Extension	72 ° C 1 min	
Final extension	72 ° C 1 min	

3.5.1.3   Sequencing of PMR genes

PCR product were purified using commercially available PCR purification kit (Thermo Scientific™ GeneJET). DNA sequencing was performed by automated DNA sequencer (AB3730. 48 capillary) at Centre of Excellence in Molecular Biology (CEMB) Lahore, Pakistan. BLAST tool was used for alignment and sequences were submitted to NCBI gene bank.

3.5.2   Screening of virulence markers in UPEC isolates

A total of eighteen virulence factors encoding adhesins (*fimH, papA, papC, papEF, papGI, papGII, papGIII, sfa/focG, afa, bmaE*), toxins (*hlyA, cdtB*), capsule (*kpsmtII, kpsmtIII*), iron acquisition system (*fyuA, iutA, feoB*) and UPEC specific protein (*usp*) were screened in all the 155 UPEC isolates. PCR reaction mixture was prepared as described previously (Table 3.1),

while the reaction conditions were same as given in Table 3.5. Reactions were carried out in Labnet ® MultiGene OptiMax thermocycler.

3.6   Phenotypic screening of virulence factors in UPEC

All 155 UPEC isolates were screened for phenotypic virulence markers including cell surface hydrophobicity (CSH), hemagglutination, hemolysin and serum resistance. All the assays were repeated at least twice to validate the results.

3.6.1   Cell surface hydrophobicity

Cell surface hydrophobicity (CSH) is important for mediating attachment and detachment from abiotic and abiotic surfaces. It also contributes in biofilm formation and penetration into the host tissues, hence is an important virulence factor. CSH was determined as described previously (Siegfried et al., 1994). Briefly, a single colony was picked from a freshly streaked *E. coli* culture and inoculated into ~2 ml phosphate buffer (PBS) (pH 6.8). Turbidity of the suspension was compared with McFarland's standard 6. Ammonium sulphate solutions of three different molar concentrations (1M, 1.4M and 2M) were also prepared. About 40µl of *E. coli* cell suspension was mixed separately with equal volume of ammonium sulphate solutions of different molarities on a VDRL (venereal diseases research laboratory – test) slide and rotated for 3-4 minutes. Strains were considered hydrophobic if they aggregated in the presence PBS ≤1.4M. *E. coli* strain ATCC 25922 was used as a negative control.

3.6.2   Haemagglutination

Fimbriae are an important virulence factors and aid UPEC in colonizing the urinary tract lining. Hemagglutination test is based upon the ability of *E. coli* isolates to cause agglutination of erythrocytes in the presence (P-fimbriae) or absence (type-1 fimbriae) of D-mannose. Initially a 3% erythrocyte suspension was made in PBS, pH 7.4, by collecting 5 ml of group O$^+$ blood

and adding it into 5 ml of Alsever's solution and centrifuging for 3-5 minutes at 1500rpm. Resulting supernatant was aspirated leaving RBCs undisturbed. About ¾ of this tube was filled with normal saline and inverted 2-3 times. This tube was then centrifuged for 1 min 3500 rpm. Normal saline was decanted, and RBCs were washed 3 times with normal saline. 3 % erythrocyte suspension was made by mixing 20 µl RBC with 970 µl PBS (pH 7.4). In parallel, UPEC isolates were inoculated into 5-7 ml of MHB and incubated for 48 h to achieve fimbriae enriched *E. coli* growth. Forty µl of broth culture was added to 40 µl of 3% RBC suspension both in the presence and absence of 40 µl 3 % w/v D-mannose on VDRL slide. Slide was rocked to and fro for 5 min to facilitate the process. If hemagglutination occurred in the presence of D-mannose it was considered mannose resistant haemagglutination (MRHA) , whereas if no hemagglutination occurred in the presence of D-mannose but occurred in the absence of D-mannose, it was considered mannose sensitive haemagglutination (MSHA) (Jadhav et al., 2011).

3.6.3   Hemolysin

This test is used to determine the ability of strains to produce hemolysin. Hemolysin is cytolytic protein which causes the lysis of erythrocytes. Hemolysin production was detected by streaking a single colony of test organism on blood agar plate (BAP) and incubating it overnight. BAP was prepared by supplementing blood agar base (Oxoid^{TM}) with 5% sheep blood. A clear zone of lysis of the erythrocytes around the colony and clearance of the medium indicated the hemolysin production by the test strain.

3.6.4   Serum bactericidal activity (SBA)

Serum resistance is an important virulence attribute, which helps bacteria to evade the lytic activity of human serum. This test determines the serum resistance of strains against human serum. SBA was determined by suspending a freshly cultured *E. coli* growth in Hank's balanced

salt solution (HBSS). The turbidity of this suspension was then matched with 0.5 MacFarland standard. Then 0.05 mL (50 μl) of the bacterial suspension was incubated with equal volume of serum in a sterile test tube, at 37°C in a shaker incubator. A tube with only HBSS was used as a negative control. A 10 μl of samples was taken at 0, 60 and 120 min, on three separate plates of nutrient agar and viable count was determined, by inoculating/spreading. An isolate was termed sensitive if viable count declined to 1% of the original inoculum and was termed resistant if the count remained >90% of the initial inoculum (Siegfried et al., 1994).The isolates with consistent serum resistance were used as an internal positive control.

3.7   Investigation of biofilm formation

All UPEC isolates were further screened for biofilm potential by means of three methods i.e. Congo red agar (CRA), tube method (TM) and tissue culture plate (TCP) method. CRA and TM are the qualitative methods of determining biofilm production, while TCP is a gold standard method for quantitative determination of biofilm production.

3.7.1   Congo red agar method

Congo red agar is a simple qualitative method for estimating biofilm production ability as previously described (Triveda and Gomathi, 2016). The principle of assay lies in the ability of Congo red dye to stain the bacterial polysaccharide layer black. Congo red agar medium was prepared by adding Congo red stain (0.8g/L) and sucrose (50g/L) in brain heart infusion (BHI) agar. Once the media plates were prepared, a single colony was picked from freshly streaked culture and sub-cultured onto Congo red agar plates and incubated at 37°C for 24 hrs. Next day, plates were observed for the formation of black crystalline colonies (strong biofilm producers), black colonies without crystalline morphology (moderate biofilm producer), dark

pink colonies (weak biofilm producers) and orange/red colonies (non-biofilm producers). Experiment was repeated twice to confirm the results.

3.7.2   Tube method

Tube method is another qualitative method to determine the biofilm production ability as described previously (Christensen et al., 1985). The test is based on the principle of ring formation at the bottom of test tube by biofilm forming isolates after staining with 0.1% crystal violet (CV).

Isolates were inoculated in 5 ml BHI broth supplemented with 2% sucrose and incubated at 37°C for overnight. Next day, media was discarded, and test tubes were washed thrice with 7-8 ml of PBS. Tubes were air dried and then stained with 5-7 ml of 0.1% CV for 30 min. Excess stain was removed by subsequently washing with deionized water, at least twice. Tubes were air dried by inverting and biofilm formation was observed. Isolates were categorized as strong, moderate and weak biofilm producer, by estimating the amount of ring formation at the bottom of test tube. Ring formation only at the liquid interface was categorized as non-biofilm producer. Experiments were performed thrice to validate the results.

3.7.3   Tissue culture plate (TCP) method

TCP is another quantitative method of biofilm determination and is considered as gold standard for biofilm estimation. Microtiter plate assay was performed as determined by Rossi and colleagues (de Rossi et al., 2009). Assay was performed in triplicates and performed at least twice. An overnight culture was standardized to 0.5 McFarland by diluting it (1:100) in fresh MHB. Aliquots (200 µl) of this standardized inoculum were inoculated into sterile 96-well flat-bottomed TCP and incubated at 37°C for 24hrs. Next day, media was discarded, and wells were washed thrice with PBS. Wells were stained with 0.1% CV for 15 min. Excess stain

was removed by again washing with PBS. The stained biofilms were dissolved with 95% (v/v)

ethanol and optical density (OD) was measured at 540 nm using ELISA plate reader (Bio-

Rad^{TM} model 680). Cutoff value of 0.1% CV (negative control) was calculated by: Optical

density cut-off value (ODc) = average OD of negative control + 3x standard deviation (SD) of

negative control. Similarly, estimation of biofilm formation at different time intervals; 2hrs,

4hrs, 10hrs, 18hrs and 24hrs was also measured according to previously described TCP

method. Isolates were categorized as weak, moderate and strong biofilm producers according

to following formula.

Table 3.6 Optical density cut-off value (ODc) calculated from crystal violet control

OD $\leq OD_c$	Non-biofilm producer
OD > OD_c or OD $\leq 2xOD_c$ (0.056-0.11)	Weak biofilm producer
OD > $2xOD_{c \text{ or }}$ OD $\leq 4xOD_c$ (0.11-0.22)	Moderate biofilm producer
OD>$4xOD_C$ (0.22 or above)	Strong biofilm producers

3.8   Topographical examination of UPEC biofilm

Biofilm of UPEC was also examined by performing scanning electron microscopy (SEM) on

selected isolates. SEM was used to determine the morphological changes occurred in biofilm

forms of UPEC at three different time intervals (4 h, 10 h and 18 h). Biofilm was allowed to

grow in 6 well flat-bottomed polystyrene plate as described by (Wang et al., 2016). The fresh

MHB media was used as a negative control and samples were processed and analyzed by SEM.

3.9   Antimicrobial susceptibility test of planktonic bacteria (MIC-p)

Further 21 strains were selected, based on their sensitivity to all the frontline antibiotics such

as trimethoprim, ceftazidime, ceftriaxone, levofloxacin, ciprofloxacin and gentamicin. These

strains were further scrutinized for biofilm formation at different time intervals and *in-vitro*

efficacy of trimethoprim, ceftazidime, levofloxacin and gentamicin for biofilm treatment.

MIC of these 21 isolates was carried out/performed as described previously in section 3.4.2

3.10   Antimicrobial susceptibility testing of biofilm

After initial determination of MIC of planktonic forms (MIC-p), all the 21 strains were further screened for MIC of biofilm forms. Experiments were performed in triplicates and repeated at least twice. Briefly, 75µl of standardized (as described in section 3.7.3) bacterial suspensions were inoculated in a sterile 96-well flat-bottomed polystyrene TCP and incubated at 37°C for 24 hrs to allow biofilm formation. Following 24 hrs, MHB discarded and wells were washed at least twice with PBS to remove non-adherent bacteria. Next, 100 µl of two-fold (1:2) dilutions (ranging from 2048ug/ml to 0.5ug/ml) of antibiotics (trimethoprim, ceftazidime, levofloxacin and gentamicin) prepared separately in fresh MHB were added to these preformed biofilms in the respective plates and incubated at 37°C for 24 hrs. The MIC-b was measured as minimum concentration of antibiotic that inhibited the growth of planktonic bacteria of their shedding from biofilm. Sterile MHB was use as negative control.

3.11   Growth experiments for iron acquisition and utilization

This experiment aims of determining effect of iron source and iron levels on growth capacity of UPEC strains; investigation of those iron-uptake systems that are specific for the UT niche. For iron restricted growth experiments, all the glassware was washed with 6 M HCl and rinsed with deionized water. All the reagents were ultrapure.

3.11.1 Growth on solid medium

In order to determine effect of iron on growth pattern of UPEC isolates, isolates were grown on iron deficient M9 salts medium (no added iron) and "iron-sufficient" M9 medium (MM) containing 10 µM ferric citrate. Briefly a single isolated colony was picked for each of the 20

strains and streaked on iron deficient and iron-sufficient M9 medium. Plates were incubated at 37 ^{o}C for 24-48 h.

3.11.2 Growth in liquid medium

To determine the effect of iron source and iron levels on growth capacity of UPEC strains they were grown in liquid MM in the presence and absence of iron. Briefly a single colony was picked from agar plates and inoculated to 5 ml L-broth in test tubes. Test tubes were incubated overnight in shaker incubator with 200 rpm at 37 ^{o}C. Next day, about 500 µl of O/N bacterial culture was taken carefully and inoculated to ~50 ml of MM media with and without iron. Each strain was found to have a starting OD of 0.05. OD_{600nm} was measured after every two hours. All the experiments were performed in duplicates and experiments were repeated twice at least, to validate the findings.

3.11.3 Siderophore detection Assay

Chrome Azurol S (CAS) plate assays were performed to investigate those iron uptake systems that are specific to urinary tract niche.

3.11.3.1 Preparation of CAS agar plates

The CAS agar plates were prepared as described by Louden and colleagues (Louden et al., 2011). Briefly 20 ml of 1 mM $FeCl_{3.}6H_2O$ were prepared in 10 mM HCl. To prepare the dark blue solution; 60.5 mg CAS was dissolved in 50 ml water, following the addition of 10 ml of 1 mM $FeCl_3$ solution. In another Duran bottle, 72.9 mg HDTMA (hexadecyltrimethylammonium bromide) was dissolved in 40 ml of water. Followed by the addition of 60 ml $FeCl_3$/CAS solution to the HDTMA solution, with slow continuous stirring. The resultant solution was a "dark blue solution" (final volume; 100ml). The base culture

medium was prepared by adding 15 g agar, 30.24 g PIPES, ~12 ml 50% w/w NaOH solution (to raise pH to 6.8), into 750 ml deionized water. In a separate Duran bottle, 10X M9 salts were dissolved in 100 ml of deionized water. All the three solutions (dark blue solution, base culture medium and 10X M9 salts) were autoclaved at 121 °C for 15 min. Once M9-salts/agar was cooled, 100 ml dark blue solution, 30 ml of 10% casamino acids, 1 ml of 20% glucose, 1 ml of 0.1 M $CaCl_2$, 1 ml of 1 M $MgSO_4$ and 0.5 ml 1% thiamine to make a total volume of 1 L. All the solutions were mixed uniformly, and plates were poured, each containing ~20 ml medium.

3.11.3.2   Chrome Azurol S (CAS) plate assay

Briefly, 3-5 ml of overnight (O/N) cultures were prepared the night before the assay. CAS agar plates were punctured using a gel puncher to make 5 mm diameter wells. After that 0.5 ml of O/N cultures were introduced/added into 50 ml M9 medium (MM) with and without 10 μM ferric citrate. The cultures were incubated at 37 °C and 250 rpm for 24 h. Cultures were taken at various times (after every 2 h) and growth curves were measured. Cultures were then centrifuged at 14000 rpm for 2 minutes and supernatants were separated. About 35 μl of culture supernatants were added to the wells on the CAS agar plate, after observing the complete diffusion of the supernatant added, another 35 μl of supernatants were added into the wells to make up a total of 70 μl in each well. Plates were incubated for 4-8 h and yellow-golden halos were observed, and their diameter was measured. Supernatants were stored in -20 ˚C till further use. Controls – Iron chelators such as DTPA was used as control.

3.11.4 Arnow's assay for detection of catecholates

If siderophore production was indicated on CAS plate, the supernatant was further processed for catecholates detection using Arnow's assay (Arnow, 1937). Arnow's assay was performed

by adding 1 ml of culture supernatant in a sterile test tube, then 1 ml of 0.5M HCl was added and mixed. Next 1 ml of nitrite-molybdate reagent (prepared by adding 10 g sodium nitrite + 10 g sodium molybdate dissolved in 100 ml ddH2O) was added and mixed. Catechol presence was indicated by the formation of yellow color. Next, 1 ml of 1 M NaOH was added and mixed. The presence of catechol-type siderophore is indicated by the development of a pink color, while the negative control remains colorless. The principal of Arnow's method is that when catechol reacts with nitrous acid, it gives a yellow color. Upon the addition of NaOH, the yellow color turns into orange-red. Since the assay is colorimetric, the test tubes were allowed to incubate for 5 min at RT, to let the color fully develop. After 5 min absorbance of the solution was measured at 500 nm using SpectraMax® Plus 384 Microplate Reader. Supernatants of bacterial cultures grown under iron-sufficient conditions were used as negative controls.

3.11.5 Atkin's assay for the detection of hydroxamates

The culture supernatant was also tested for the presence of hydroxamate-type siderophore using Atkin's assay (Atkin et al., 1970). The assay was performed my mixing 0.5ml supernatant from the culture with 2.5ml of 0.1771 g $Fe(ClO_4)3$ that was suspended in 100 ml qH_2O and 1.43 ml perchloric acid). To develop the colour mixture was incubated for five min and absorbance was taken subsequently at 480 nm while uninoculated minimal media along with reagents was used as blank. The supernatant prepared in higher iron concentrations was used as a control. Finally, the interpretation of the assay was made according to the standard colour scheme.

3.12   Infection of urothelial cell lines

3.12.1 Materials:

Human bladder epithelial cell lines 5637 (ATCC HTB-9), RPMI 1640 (Gibco^{TM}), Fetal bovine serum (Sigma Aldrich ^{TM}), Gentamicin 10 mg/ml (Sigma Aldrich ^{TM}), Triton X-100 (Sigma Aldrich ^{TM}), T-24 tissue culture plates (Nunclon ^{TM}).

3.12.2 Preparation of bacterial cultures:

All the 5 strains exhibiting different siderophore production potential were grown under iron deficient and iron sufficient (10 µM) M9 minimal media. Briefly a single colony was carefully picked from M9 minimal agar medium and inoculated into the 50 ml media for overnight growth at 37°C with 200 rpm. Next day OD600 of each strain was measured and was adjusted to OD=1, that contains ~ 10^9 cells, was also confirmed by plating the culture on L-agar pates. Bacteria were washed 3-times with PBS by alternate rounds of centrifugation at 10000rpm for 5 minutes. Finally, pellet was suspended in RPMI 1640 medium, supplemented with 10% FBS.

3.12.3 Mammalian cell culture

Bladder epithelial cell lines (HTB-9) were purchased from ATCC under Lot# T-95637 (62761993). Cell cultures were grown in RPMI-1640 supplemented with 10% FBS and maintained at 37°C in 5% CO_2. Briefly, wells were seeded with 0.5 $\times 10^5$ cells (in 500 µl per well) with RPMI 1640 supplemented with 10% fetal bovine serum in 24 wells tissue culture plates. Cells were maintained at 37°C in a 5% CO_2 environment for 24 h. Once cells became confluent with 1.2x10^6 cells per well, the culture medium was removed, and cells washed three times with PBS/RPMI.

3.12.4 Infection of cell lines

Bacterial cultures were vortexed to avoid clumps. Cell lines were infected with a multiplicity of infection (MOI) 10. A 10 µl culture of washed bacteria (resulting in approximately $2x10^7$cfu/ml) to each well in 490 µl RPMI medium containing 10% FBS as previously described by (Martinez et al., 2000b, Kakkanat et al., 2015a, Edwards and Massey, 2011). A 500 µl of RPMI containing 10% FBS were kept as control wells without addition of any inoculum. Tissue culture plates were incubated at 37°C in 5% CO_2 for 1 h. After 1 h, media was carefully removed, and plates were washed 3 times with PBS to remove unbound bacteria. A 500 µl of 100µg/ml gentamicin solution in RPMI supplemented with 10% FBS was added to each well (including control wells) to kill all the extracellular bacteria and incubated for 1h at 37°C in 5% CO_2.

3.12.5 Enumeration of intracellular bacteria (gentamicin protection assay)

After 1 h of the incubation with gentamicin, medium was removed from each well the wells were washed 3 times with PBS. Wells were added a 500 µl solution of 0.1% Triton X-100 and left for 5 min, to lyse the cells. In order to ensure complete lysis of mammalian cells and release of intracellular bacteria, wells were pipetted several times. Lysate from each well was then serially diluted with 1: 10 and plated on to the L-agar plates. Plates were incubated at 37 ^{o}C and bacterial counts were done using Syngene^{TM} G; Box, colony counter. Wells containing only bladder cell lines were used as negative controls. The assays were performed in triplicate. The invasion ratio was determined by dividing the number of invading bacteria by the initial inoculation bacterial number.

3.13   Mutant construction by λ-Red recombination

3.13.1 Primer design

Deletion primers were designed against four iron-acquisition systems; enterobactin (*entBEC*), yersiniabactin (*irp1_2*), aerobactin (*iucABCD*) and heme (*hemRT*) using pKD3 (*cat* cassette) as a template to generate mutants. Primers were 80 nucleotides long for each system comprising of a 20 bp *cat* cassette and 60 bp homologous site. In addition, 20 bp confirmation primers were designed approximately 100 bp upstream of the homologous site.

3.13.1.1 Primer designing for *entBEC* gene
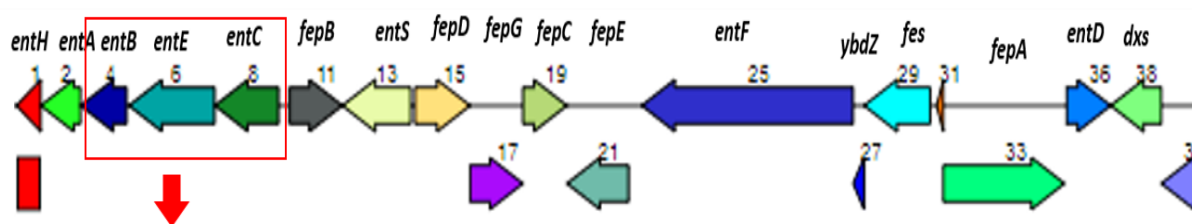
TGTAACCACAACCAGATGCAACCCCGAGTTGCAGATTGCGTTACCTCAAGAGTTGACATAGTGCGCGTTTGCT TTTAGGTTAGCGACCGAAAATATAAATGATAATCATTATTAAAGCCTTTATCATTTTGTGGAGGATGATATGGATAC GTCACTGGCTGAGGAAGTACAGCAGACCATGGCAACACTTGCGCCCAATCGCTTTTTCTTTATGTCGCCGTACC GCAGTTTTACGACGTCAGGATGT..GGCGGCGCGCTGG CGCAAAGTGCATGGCGATATCGACTTTGTCATGCTGGCGAAAAACCCGACCATCGACGCCTGGTGGAAGCTACT CTCCCGCGAGGTGAAATAATGGATTTCAGCGGTAAAAATGTCTGGGTAACTGGCGCGGGGAAAGGTATAGGCTA CGCCACGGCGCTGGCATTTGTTGAGGCGGGGGCGAAAGTTACAGGTTTTGATCAAGCGTTTAGTCAGGAGCAA TATCCTTTTGCGACCGAAGTAATGGATGTTGCCGATGCTGCGCAGGT**GGCGCAGGTATGTCAGCGACTGTTA**

i. **PCR primer used to generate UPEC deletion mutants**

Primer	Sequence 5'-3'	Length (bp)	Melting T°C
entBEC-del_for	ATATAAATGATAATCATTATTAAAGCCTTTATCATTTTGTGGAGGATGAT ATGGATACGT*GTGTAGGCTGGAGCTGCTTC*	80	74.9
entBEC -del_rev	CGTAGCCTATACCTTTCCCCGCGCCAGTTACCCAGACATTTTTACCGCT GAAATCCATTA*ATGGGAATTAGCCATGGTCC*	80	81.3

ii. **Post deletion confirmation primers**

Primer	Sequence 5'-3'	Length (bp)	Melting T°C
entBEC-con_F	**TGTAACCACAACCAGATGCAACCCC**	25bp	62
entBEC-con_R	**TAACAGTCGCTGACATACCTGCGCC**	25bp	63

72

3.13.1.2 Primer designing for *irp1_2* genes

i. **PCR primer used to generate UPEC deletion mutants**

Primer	Sequence 5'-3'	Length (bp)	Melting T°C
irp1_2-del_for	ATTCTCATATGAGTAATGCTTTTCGGTAAGACGTGCCATCAGGAGGAAGA*ATG*ATTTCTG*GTGTAGGCTGGAGCTGCTTC*	80	79.2
irp1_2 -del_rev	TTTCGCCAAATTTGGCGCCCACAATCAGTACGCGTTGTTTTGGGGAGGCGGACGGCATCA*ATGGGAATTAGCCATGGTCC*	80	85.1

ii. **Post deletion confirmation primers**

Primer	Sequence 5'-3'	Length (bp)	Melting T°C
irp1_2-con_for	**TACCCCATCAGGGCCTCTGTTCTTT**	25	62
irp1_2 -con_rev	**TTCCGGCGAGGTATACAGCGGAATG**	25	64

73

3.13.1.3 Primer designing for *iucABCD* gene
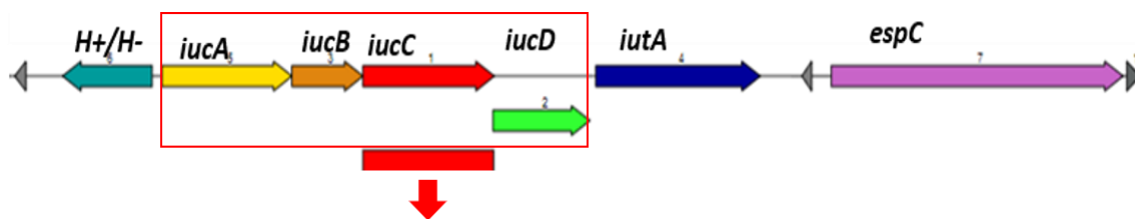
TTTTTGGGGCGTATCTTCGATCCCTGGTGACATTATAATGTTTCAACTCCATGTATTAATTGTGTTTATTTGTA
AAAATTAATTTATCTGACAATAACATTTATTATTGATAATGAGAATCATTATTGACATAATTGTTATTATTTTGCT
GTGTGGGAGCTGTTTGACTATGACCCTGCCCTCTGAAAAACCAGCCACAGATGTGGCTGCGCAGTGCTTCCTGA
ATGCACTGATTCGTGAAACCACAGACTGGAAACTG...
........TAAAGTGCGTGATGACTTCACTCTGGAATGGAGTGGCCCGAAAGAGAACAACATCTTCGTGGTCAACGCC
AGTATGCAAACCCATGGCATCGCCGAACCCCAGCTCAGCCTGATGGCATGGAGATCTGCACGTATTCTTAATC
GCGTAATGGGACGTGATTTATTCGATCTCAGTATGCCGCCCGCCCTGATTCAGTGGCGCAGCGGCACCTAGGG
AAAACGCAGCCGGAGGCTGCTTCTTTAACTCGCTACACAGCATCTTTGGGCTGATTTTTTCCGCCCGTATGGAG
GAATAATGATGATAAGCAAAAAGTATACGCTTTGGGCTCTCAACCCACTGCTTCTTACCATGATGGCGCCAGC
AGTC**GCTCAACAAACCGATGATGAAACGT**

i. PCR primer used to generate UPEC deletion mutants

Primer	Sequence 5'-3'	Length (bp)	Melting T°C
iucABCD-del_for	TCATTATTGACATAATTGTTATTATTTTGCTGTGTGGGAGCTGTTTGACTATGACCCTGC*GTGTAGGCTGGAGCTGCTTC*	80	75.7
iucABCD -del_rev	ATCAGCCCAAAGATGCTGTGTAGCGAGTTAAAGAAGCAGCCTCCGGCTGCGTTTTCCCTA*ATGGGAATTAGCCATGGTCC*	80	77

ii. Post deletion confirmation primers

Primer	Sequence 5'-3'	Length (bp)	Melting T°C
iucABCD-con_for	**TTTTTGGGGCGTATCTTCGATCCCT**	25	62
iucABCD -con_rev	**ACGTTTCATCATCGGTTTGTTGAGC**	25	60

3.13.1.4 Primer designing for *hemRT* gene

i. **PCR primer used to generate UPEC deletion mutants**

Primer	Sequence 5'-3'	Length (bp)	Melting T°C
hemRT-del_for	GCGTGAGATCCAGGGTGTTATTTGTGTTCATTCGTCTGATTTAAATCCATTT ATTGCGGC*GTGTAGGCTGGAGCTGCTTC*	80	75.7
hemRT-del_rev	GTGGTTCATTGTCTCTCTTCCTTCCAGATAAATGCCCCGAAATATCGGGGCA GATGATTA*ATGGGAATTAGCCATGGTCC*	80	77

ii. **Post deletion confirmation primers**

Primer	Sequence 5'-3'	Length (bp)	Melting T°C
hemRT-con_for	**CGTTTGATTGATCATCTCTTGCCAG**	25bp	58
hemRT-con_rev	**AAATGCCAGTTCTGCTTCGCTGATA**	25bp	61

3.13.2 PCR amplification of target gene (s)

PCR amplification of pKD3 (*cat* cassette) was performed for each of the afore mentioned deletion primers (see 3.13.1) using "Thermo Scientific™ Phusion High-Fidelity PCR kit (F553S)". The reaction was set as follows.

Component	Volume (20 µl)	Final concentration
Nuclease free water	Added to 20 µl	
5X Phusion HF Buffer	4 µl	1X
10 mM dNTPs	0.4 µl	200 µM each
Primer_forward	1 µl	0.5 µM
Primer_reverse	1 µl	0.5 µM
Template DNA	0.5 µl	
DMSO	0.6 µl	3%
Phusion DNA Polymerase	0.2 µl	0.02 U/µl

The reaction was set at room temperature as per providers instructions. PCR reaction was then set in BIO-RAD T100™ thermal cycler with these temperature condition; Initial denaturation at 93°C for 1 min, final denaturation at 93 °C for 30 sec, annealing at a gradient temperature of 58-66 °C for 30 sec, initial extension at 72 °C for 30 sec (35 cycles) and a final extension at 72 °C for 1 min. After completion of PCR cycle amplified products were run on 0.7% agarose at 60 V and 60 min in BIO-RAD gel electrophoresis equipment. The products were visualized by GeneSys™ G: Box.

3.13.3 PCR product purification and quantification

PCR products were purified using Thermo Scientific™ GeneJET PCR Purification Kit. The concentration of DNA was measured using NanoDrop®ND-1000 spectrophotometer and recorded.

3.13.4 Transformation of UEC59 with pACBSR-*hyg*.

In order to transform UEC59 (the target strain) with pACBSR-*hyg* (plasmid Expresses lambda-red system with *hyg* selection marker), 1 mL of the O/N culture was inoculated into 100 mL of fresh LB in a 250 mL "Erlenmeyer flask" (conical flask) and was incubated at 37°C with shaking at 180rpm. When the observed25 OD600 reached 0.4 – 0.6 (~2.5 hours), strain was made chemically competent as follows. Everything was kept ice cold after this stage. Cell culture was centrifuged for 5 min at 6,500 rpm (7,000 x g). LB media was carefully decanted and cells were gently resuspended in 10 mL ice-cold 0.1M $CaCl_2$. Incubated on ice for 10 min and again centrifuged for 5 min at 6,500 rpm. Supernatant was carefully decanted, and cells were gently resuspended in 10 mL ice-cold 0.1M $CaCl_2$., centrifuged for 5 min at 6,500 rpm. Supernatant was discarded, and cells were gently resuspended in 5mL cold 0.1M $CaCl_2$ /15% glycerol. Cells (300 µl/tube) were dispensed in pre- chilled 1.5 mL microcentrifuge tubes and stored at -80 °C. About 2 µl of plasmid were added to competent cells and kept on ice for 30 min, followed by heat shock at 42 °C for 2.5 min. Cells were kept on ice for another 5 min and after that 1 mL prewarmed LB- medium was added and cells were incubated at 30 °C for 1 h with gentle shaking. After 1 h cells were centrifuged 900 µL of supernatant was discarded and 100 µL of cell suspension was plated onto low-salt L gar plates containing hygromycin (200 µg/mL). Plates were incubated overnight at 30 °C.

3.13.5 Electroporation of UEC59 (transformed with pACBSR-Hyg) with PCR-amplified knockout cassette

After successful transformation of UEC59 with pACBSR-Hyg, a single colony of UEC59+pACBSR-Hyg was inoculated in 3 mL low salt LB broth + hygromycin at 30°C overnight. Next day 1 mL of the overnight culture was inoculated into a 250 mL Erlenmeyer containing 90 mL low-salt LB, 9 mL of a 1 M L-arabinose solution, and hygromycin. Incubated

at 30°C with shaking at 180 RPM. When the OD600 reached 0.4 – 0.6 (4 – 5 hours), electrocompetent cells were prepared as follows. Culture was centrifuged for 5 min at 6,500 rpm (7,000 x g). LB media was carefully decanted and discarded. Cells were washed with 50 mL of ice-cold 10% glycerol and pellet was re-suspended by slight vortexing. Re-suspended and centrifugation was carried out again at 6,500 rpm for ~5 min. Centrifuge tube was placed into ice immediately after removal from the centrifuge. Supernatant was carefully decanted and another 50 mL of ice-cold 10% glycerol was added into the cells and re-suspended by pipetting up and down. Cells were centrifuged again at 6,500 rpm for 5 min. Supernatant was carefully decanted and another 50 mL of ice-cold 10% glycerol was added into the cells and re-suspended by pipetting up and down. Centrifuged again at 6,500 rpm for 5 min. Supernatant was carefully decanted and the pellet was re-suspended in the residual glycerol by pipetting up and down with a 1000 µl pipet. Electroporation was carried out in BIO-RAD^{TM} electroporator at voltage of 1.8 kV. Reaction was set on ice and everything was pre-chilled. Briefly 100 µl of the electrocompetent cells were dispensed into pre-chilled 1.5ml microcentrifuge tubes and ~1 µg of PCR product (gene knock out *cat* cassette) was added to these electrocompetent cells. The mixture was shifted into a cold "electroporation cuvette VWR^{TM} (0.1 cm gap)" using a gel loading tip. Cuvette was slightly tapped to bring all the cells to bottom and electroporated (Pulse time around 5-6 seconds). Quickly, 500 µl of SOC medium were added and the mixture was transferred using a sterile long gel-loading tip to a sterile 2 mL microfuge tube. Tubes were incubated at 37°C with gentle shaking for 60–90 min. Cells were plated onto L-agar plates with 25 µg/mL chloramphenicol and incubated at 37°C for overnight. A control without any addition of PCR product was used to ensure the fidelity of protocol.

3.13.6 Screening of mutants

After successful knock out 5 to 6 colonies were marked. Each colony was dabbed with a sterile toothpick and suspended in 20 µl sterile water. About 2 µl of each suspension was used as template DNA to confirm the correct insertion of KO cassette, and 3 µl of this suspension was streaked onto L-agar plates containing chloramphenicol (25 µg/mL) and incubated at 37°C for overnight. Note: Control was recorded to have no colonies on chloramphenicol plates confirming the fidelity of procedure.

3.13.7 Genotypic confirmation of mutants *entBEC, hemRT, irp1_2* and *iucABCD* mutants

In order to confirm mutants, confirmation primers (as descried under section 1) were used for each of mutants. Briefly 2 µl of each suspension was used as template DNA for PCR. The PCR protocol was performed as in section 3.13.2. The *ΔentBEC::cat, ΔhemRT::cat, Δirp1_2::cat* and *ΔiucABCD::cat* was expected to give a PCR product of ~1.5kb this being the *cat* cassette plus the gene fragments adjacent to the gene of interest amplified by confirmation primers. The gene size for *entBEC, hemRT, irp1_2* and *iucABCD* of wild type UEC59 is expected to be 4009 bp, 3909 bp, 16015 bp and 6035 bp, this being the gene of interest plus the gene fragments adjacent to the gene of interest amplified by confirmation primers.

3.13.8 Phenotypic confirmation of mutants

After genotypic confirmation of mutants, they were further confirmed by CAS plate assay to determine the difference in siderophore production capability and zone size. In order to detect catecholates and hydroxamate production Arnow's and Atkin's assays were performed. A detailed procedure for these assays has been discussed before in previous section (section 3.11).

3.13.9 Growth analysis of *ΔentBEC, ΔhemRT, Δirp1_2* and *ΔiucABCD*

All the glassware used in these experiments were acid washed. Initially mutants were sub cultured from L-agar plates containing chloramphenicol (25 µg/mL) to M9 minimal medium with 10 µM iron and incubated at 37 °C. Carefully a colony was picked from M9 plate and inoculated onto 3 ml of M9 medium supplemented with 10 µM iron incubated at 37 °C in a shaker incubator at 180 RPM. Next day, the culture was centrifuged at 5000 RPM, 4 °C for 5 min in Sorvall RC-3B centrifuge to pellet the cells. The cells were then re-suspended in 5 ml of 1X M9 salts and recentrifuged to wash remaining iron. The procedure was repeated 2 to 3 times. Finally, the pellets were suspended in 1X M9 salts and their OD_{600} was measured.

Growth curves were monitored in Bioscreen-C Automated Growth Curve Analysis System. The working volume of the medium in Bioscreen 100-honeycomb well microplate (Oy Growth Curves AB, Helsinki, Finland) was 250 µl. Mutants were grown under different range of conditions such as "0 µM, 10 µM and 20 µM iron"; "0 µM, 0.5 µM and 5 µM heme"; "0 µM, 1 µM and 2 µM diethylenetriaminepentaacetic acid (DTPA)". The final OD_{600} of cultures was then adjusted to 0.01 in M9 medium containing above conditions. The growth conditions in Bioscreen-C were; plate temperature: 37 °C, lid temperature: 38 °C, shaking: continuous, reading interval: every 30 min, wavelength: 600nm brown, incubation time: 24 h. Each strain was tested in three biological and two experimental replicates. Data was exported to MS excel for graph generation and statistical analysis.

3.13.10 Removal of *cat* cassette

Before removal of *cat* cassette, mutants were screened for the loss of pACBSR-Hyg by streaking on to chloramphenicol plates and low salt + hygromycin plates at 37/42 °C for 2 to 3 days. Once the mutants lost pACBSR-Hyg they wouldn't grow on low salt + hygromycin plates. Then mutants were inoculated into 3 ml LB (chloramphenicol) at 37 °C overnights and

electrocompetent cells were made as discussed in 3.14.4. Electrocompetent cells were than transformed with pFLP-*hyg* as described previously (section 3.14.4) and incubated at 30 °C overnight. Next day, mutants were heat shocked at 43°C overnight by streaking them onto LB plates. Following day, mutants were screened for the loss of *cat* cassette by streaking them onto L-agar plates with and without chloramphenicol and incubating them at 37 °C overnight. Chloramphenicol sensitive colonies were then sub cultured 2-3 times and incubated at 37/42 °C to lose pFLP-*hyg*. Loss of pFLP-*hyg* was confirmed by checking their sensitivity on low salt + hygromycin plates. Loss of *cat* cassette was confirmed by PCR, resulting in a shorter fragment of ~ 100 bp

3.13.11 Construction of double and triple mutants

Once *cat* cassette was removed double and subsequently triple mutants were constructed as described in section 3.13.2 to 3.13.9.

3.13.12 *in-vitro* invasion assays in bladder epithelial cell lines

Invasion assays for single, double and triple mutants under different iron conditions low-low (Fe-/Fe-), high-low (Fe+/Fe-), low-high (Fe-/Fe+) and high-high (Fe+/Fe+) as described previously (section 3.13.4).

3.14   Whole genome sequence analysis of twenty (20) UPEC isolates

Chromosomal DNA was isolated and submitted for complete sequencing, assembly and annotation. DNA sequences (gene composition) was compared with reference strains, with a focus on loci involved in virulence, antibiotic resistance and iron uptake.

3.14.1 Sample preparation for whole genome sequencing (WGS)

Each of the selected 20 strains were streaked subsequently 3-4 times to reduce chances of cross contamination. A single colony was picked mixed in 100 μl sterile 1x PBS for each strain separately. Then the culture was streaked out on L-agar plates, by making 1/3 of the plate a lawn of bacteria and streaking in rest of plate. Plates were incubated overnight at 37 ºC. Next day all bacterial culture was taken off from the plate using a large sterile loop and was mixed into the representative barcoded bead tube/tubes supplied by MicrobesNG.

3.14.2 DNA Extraction/ Illumina library preparation

DNA extraction was performed by MicrobesNG (IMI- School of Biological Sciences, University of Birmingham), by loading the bead tubes onto the robots. These automatic DNA extraction plates then extracted respective DNA and prepared Illumina library to proceed genome sequencing.

3.14.3   Genome sequencing

Next-generation genome sequencing (NGS) technology was used to determine the complete DNA sequence of the selected strains. NGS facility was provided by MicrobesNG (IMI- School of Biological Sciences, University of Birmingham), funded by BBSRC (grant number BB/L024209/1). The sequencing was performed on the MiSeq and HiSeq 2500 platforms (Illumina, UK) and sequence coverage of 30X was used.

3.14.4   Genome assembly

BWA-MEM software (Burrows-Wheeler Aligner http://bio-bwa.sourceforge.net/) was used for mapping low-divergent sequences against large reference genome to assess the quality of the data. The reads were trimmed using Trimmomatic by identification of adapter sequences

and quality filtering (Bolger et al., 2014a). The quality of trimmed reads was assessed using in-house scripts combined with the Samtools, BedTools ad BWA-MEM software (Li and Durbin, 2009). Kraken taxonomic sequence classification system (https://ccb.jhu.edu/software/kraken/) was used to assign taxonomic labels to the short DNA reads using exact alignment of *k-mers*. *De novo* assembly of reads was done by SPAdes v.3.11 (Genome Assembler http://bioinf.spbau.ru/spades) and map the reads back to the resultant contigs again to get more quality metrics (Bankevich et al., 2012).

3.14.5 Quality assurance

The assembly metrics and quality were calculated using QUAST (http://bioinf.spbau.ru/quast). The assemblies of draft genome were aligned to a reference genome and were evaluated metrics depending on alignments (Gurevich et al., 2013).

3.14.6 Mapping against reference genome

Mapping of the contigs against the reference genome was carried out using an online tool CONTIGuator (http://combo.dbe.unifi.it/contiguator). This tool combines the routines of one of the most commonly used tool ABACAS (BLAST and MUMmer) and allows the visualization of a map of contigs with Artemis comparison tool (ACT) (Galardini et al., 2011).

3.14.7 Genome annotation

Annotation is the process of finding "genes" and identification of ribosomal and transfer RNAs encoded in the genome. Once the ordered set of contigs was obtained, next the draft genome was annotated using "The Pathosystems Resource Integration Center (PATRIC)" database (**https://www.patricbrc.org**) (Wattam et al., 2014, Wattam et al., 2016). This database derives information from two basic annotation tools RAST tool kit (RASTtk) and BLAST. RASTtk

offers users a standard software pipeline for identifying genomic features (i.e., protein-encoding genes and RNA) and annotating their functions (Brettin et al., 2015). While BLAST performs comparison with several externally curated 'Specialty Genes' databases such as virulence factors databases like Virulence Factor Database (**VFDB**) and Victors (Mao et al., 2014). It also derives information from databases for antimicrobial resistance such as; National Database of Antibiotic Resistant Organisms (**NDARO),** the Comprehensive Antibiotic Resistance Database (**CARD**) and Antibiotic Resistance Database (**ARDB**) (Wattam et al., 2016).

3.14.8 Plasmid identification

Plasmid identification was performed using **PLACNETw,** PLAsmid Constellation NETwork web (https://castillo.dicom.unican.es/upload/). PLACNET is a graph-based tool that reconstructs plasmids from whole genome sequencing (WGS) pair-end datasets (Vielva et al., 2017). The software PLACENT is able to perform three different tasks (i) information about scaffold links and coverage is the WGS (ii) alignments to regrence extrachromosomal bacterioal DNA (iii) and identification of plasmid-diagnostic sequence. After successful manual pruning each plasmid becomes a separate connected component subgraph. It integrates information from periodically updated databases like NCBI comprised of all complete genomes and plasmids that helps it to align the contigs with closest reference.

3.14.9 Comparative genome analysis

In silico analysis of the complete genome sequence of strains was proceeded to reveal significant similarities and differences between this strain and other published UPEC strains. Command-line search tools such as BLAST was used for comparison of sequences locally through the web server. Mauve software was used for genome comparison to identify

conserved genomic regions and to determine rearrangements structure (Darling et al., 2004). CRISPRs finder server (http://crispr.i2bc.paris-saclay.fr/) was used to identify CRISPR system that represent an acquired adaptive system providing protection against mobile genetic elements such as viruses, conjugative plasmids, and transposable elements (Grissa et al., 2007). Prophages were identified in the chromosome using PHAST web server (http://phast.wishartlab.com) (Arndt et al., 2016).

RESULTS

CHAPTER 4: **Molecular characterization of multi-drug resistant (MDR) UPEC isolates**

4.1 **Biochemical and molecular identification**

A total of 250 bacterial samples were collected from non-hospitalized patients, out of which 155 samples were confirmed as *E. coli.* Upon Gram-staining isolates appeared Gram-negative pink rods of moderate size (Figure 4.1). Upon culturing on CLED agar *E. coli* colonies appeared as opaque yellow, medium sized and slightly deeper yellow center (Figure 4.2A). After initial identification on CLED agar, selected colonies were sub-cultured on Mackonkey Agar (Oxoid™). *E. coli* appeared pink (lactose fermenter) moderate/large, and slightly elevated colonies (Figure 4.2B). Biochemical identification of these isolates was performed using triple sugar iron test (TSI) urease test, indole test and citrate test. Isolates with yellow butt/yellow slant (indicative of glucose, lactose and/or sucrose fermenter), urease negative (no color change), indole positive (reddish brown ring) and citrate negative (no color change) were considered as *E. coli* isolates (Figure 4.2 C-D; 4.3 A-B).
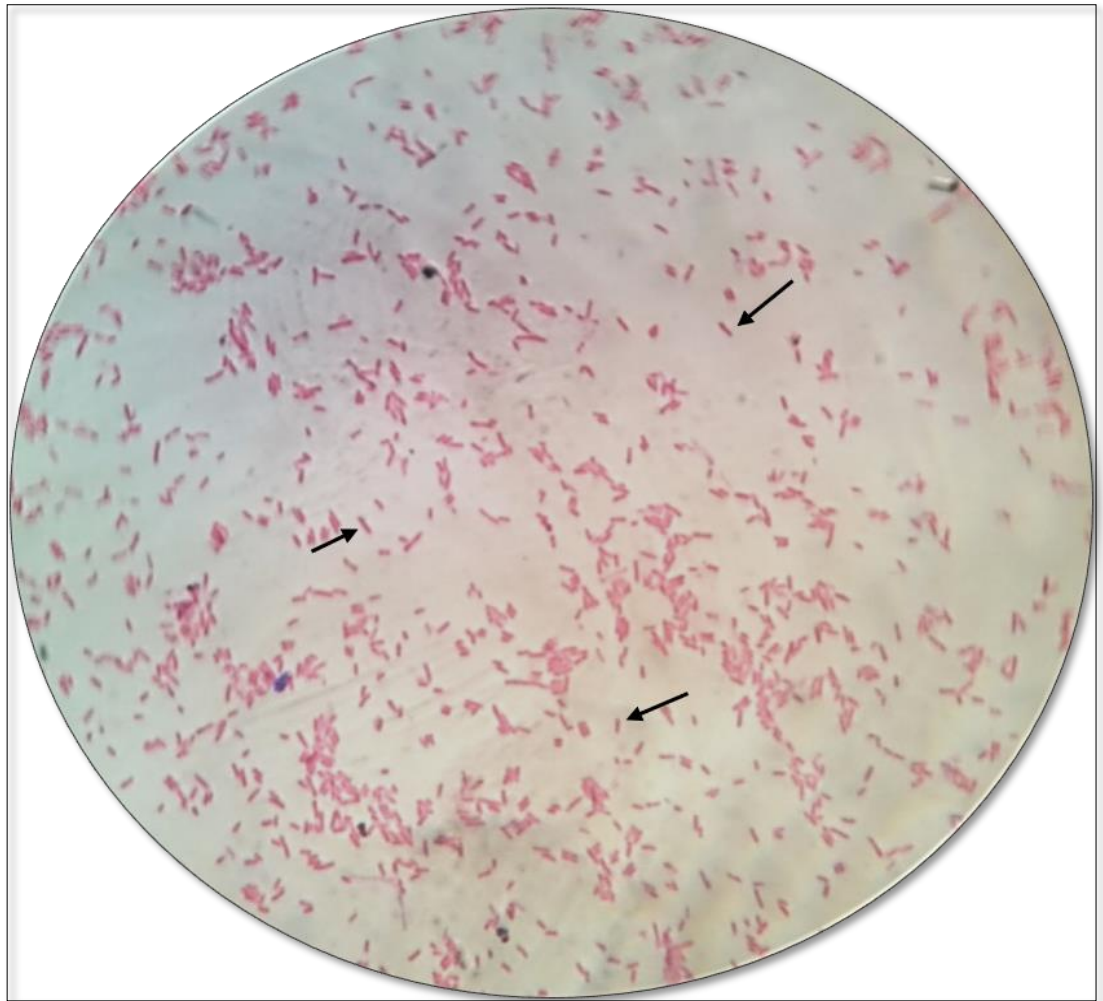
Figure 4.1 Gram stain of a UPEC isolated from patient.

Arrow indicate characteristic Gram negative (pink) rods of an *E. coli* isolated from urine.
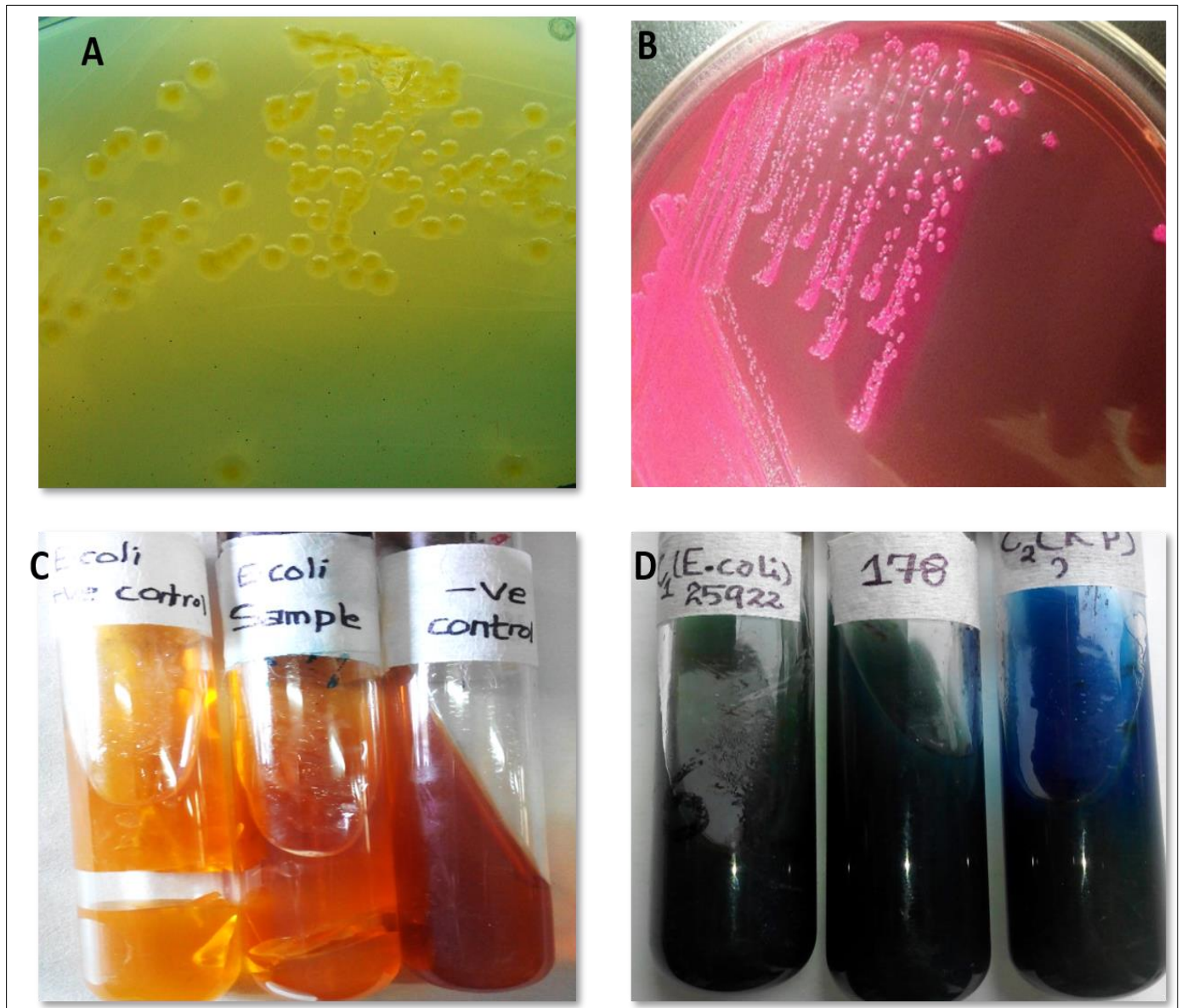
Figure 4.2. Microbiological and biochemical identification of clinical isolates of *E. coli*

(A&B). Isolated colonies of clinical samples of *E. coli* on CLED and MacConkey agar, yellow (CLED) and pink (MacConkey) colonies suggest that the organism is lactose fermenter. (C) *E. coli* (left and middle) showing yellow butt and yellow slant with gas production while on right is media control. (D) *E. coli* appears negative for the citrate hydrolysis (left and middle), hence there is no color change in the slant or media, while *K. pneumoniae* (on right) is citrate positive hence blue in the color.
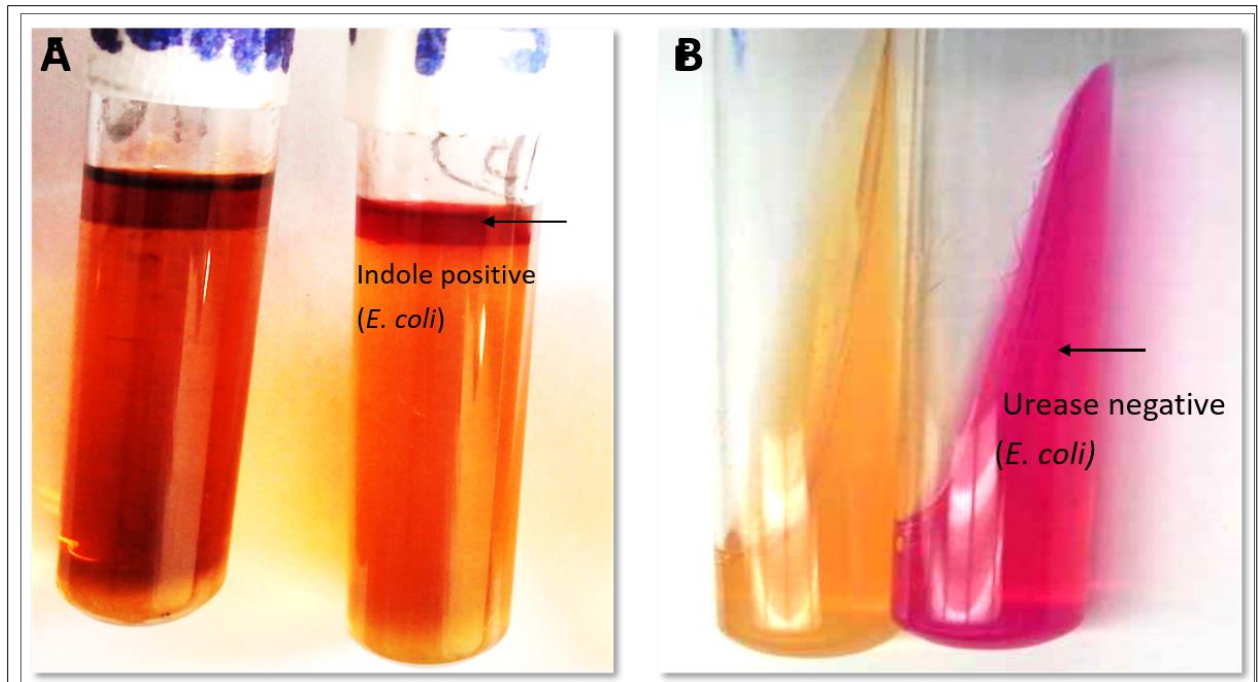
Figure 4.3. Microbiological and biochemical identification of clinical isolates of *E. coli*

(A) Indole test for *E. coli* is positive (right) and there is a formation of a reddish-brown ring on the surface of the peptone water. (B) Urease test for *E. coli* is negative (on the right side), while *Proteus vulgaris* is positive for urease (on the left side).

4.1.1 Molecular identification

In order to validate biochemical identification, all the 155 (tentatively identified as *E. coli*) isolates were tested by PCR. *E. coli* were identified by their unique 16S ribosomal RNA sequence yielding a PCR product of 450 bp (Figure 4.5). A total of 155 isolates were confirmed as *E. coli* both biochemically and molecularly. ATCC strain 25923 of *S. aureus* was used as a negative control.
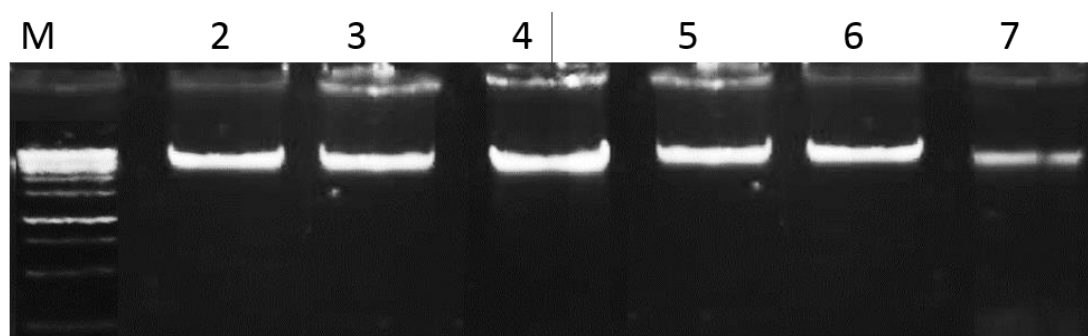
Figure 4.4 Detection of genomic DNA of *E. coli* (UPEC) on 1% agarose gel.

Figure shows M (l kb ladder Thermofisher scientific^{TM}, lane 2-7 represent quality of DNA as obtained.
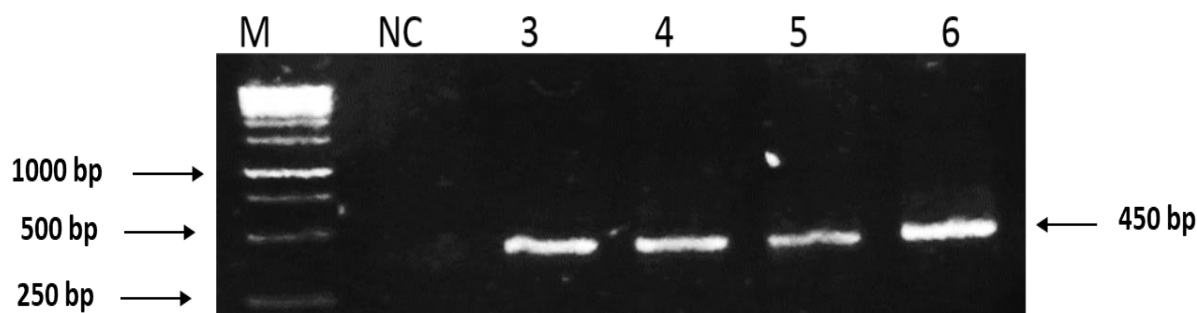
Figure 4.5 PCR amplification of 16S rRNA fragment of *E. coli* (UPEC).

The 16S rRNA fragment of *E. coli* is 450bp long which is depicted in this gel picture. The fragment length was compared to a standard DNA ladder (lane M, 1 kb ladder Thermofisher Scientific ^{TM}), NC is negative control, lane 3-6 are *E. coli* positive samples each showing a 450bp PCR fragment.

4.2   Antibiotic sensitivity profiling

All the confirmed 155 UPEC isolates were screened for the antibiotic sensitivity profiling against 23 antibiotics belonging to 8 different classes such as penicillins, cephalosporins, fluoroquinolones, monobactams, tetracyclines, sulfonamides, aminoglycosides and carbapenems. ATCC 25922 and ATCC 25923 was used as a control while performing disc diffusion for UPEC isolates. Among antibiotics sulfonamide-trimethoprim (SXT) was found least effective with 84% of the total isolates resistant to it, followed by cephalothin (KF, 81%)

amoxicillin-calvulanic acid (AMC, 72%) cefixime (CFM, 65%) cefotaxime (CTX, 65%) ceftriaxone (CRO, 64%) levofloxacin (LEV, 63%) ceftazidime (CAZ, 62%) ciprofloxacin (CIP, 61%) sparfloxacin (SPX, 61%) norfloxacin (NOR, 59%) aztreonam (ATM, 54%) gentamicin (CN, 32%) fosfomycin (FF, 10%) minocycline (MH, 8%) sulbactam (SUL, 6%) nitrofurantoin (F, 6%) tazobactam (TZP, 5%) amikacin (AK, 5%) meropenem (MEM, 1%) cefepime (FEP, 1%) and tigecycline (TGC, 1%) Figure 4.6). Out of 155 samples 65 (42%) were found positive for the extended spectrum β-lactamase production ESBL production, through double disc synergy testing (Figure 4.7). A total of 124 (80%) of the samples were resistant to 3 or more antibiotics belonging to 3 different classes, hence were considered multi-drug resistance (MDR).
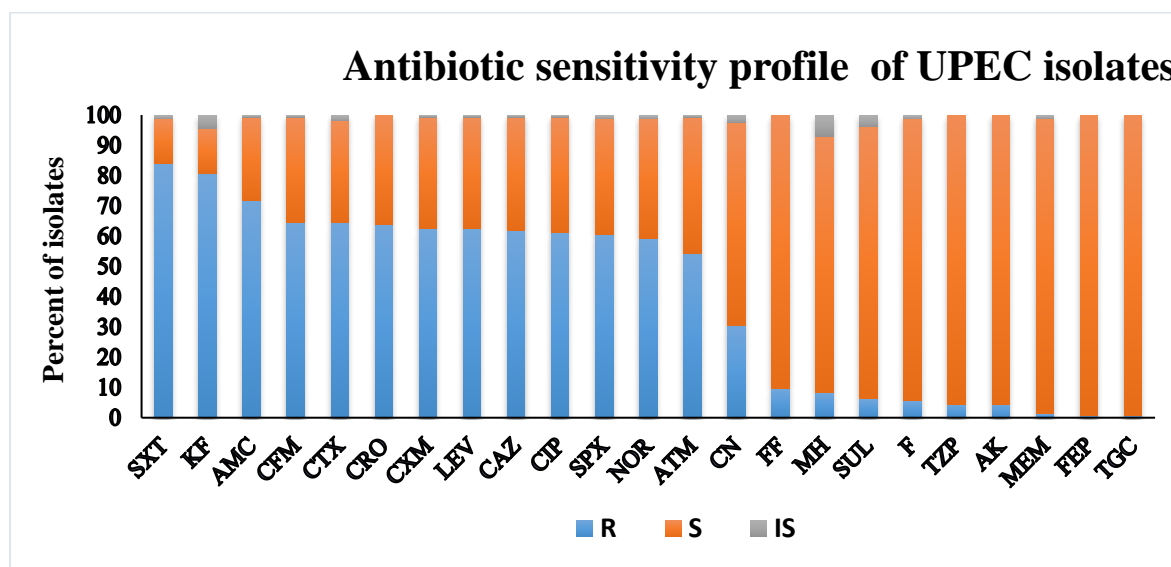
Figure 4.6 Antibiogram of 155 UPEC isolates against 23 antibiotics.

Highest level of resistance was observed against sulfamethoxazole-trimethoprim (SXT, 84%), cephalothin (KF, 81%), while gentamicin (CN, 32%) and least resistance was observed against meropenem (MEM, 1%), cefepime (FEP, 1%) and tigecycline (TGC, 1%).
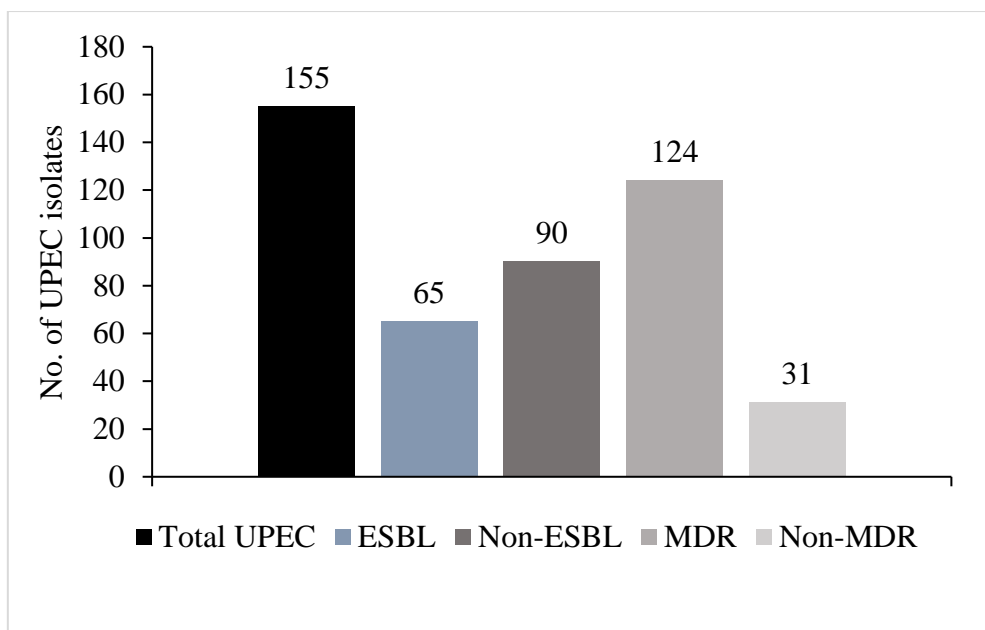
Figure 4.7 Resistance attributes of UPEC isolates.

Out of 155 isolates 65 (42%) of the isolates were found positive for ESBL while 90 (58%) ESBL negative 124 (80%) as MDR 31 (20%) were regarded as non-MDR.

4.3   Minimum inhibitory concentrations of selected antibiotics

In order to determine the quantitative level of resistance of frontline antibiotics recommended against UTI, their MICs and MBCs were performed. Six antibiotics (trimethoprim, ceftazidime, ceftriaxone, gentamicin, levofloxacin and ciprofloxacin), usually recommended against UTI were selected for this purpose. Over all higher level (≥256 µg/ml) of resistance was observed against majority of the antibiotics except levofloxacin and ciprofloxacin. In case of trimethoprim a total of 132 (resistant) isolates were scrutinized to determine *in-vitro* MICs and MBCs. Out of 132 total 89 (67%) and 31 (23%) of the isolates had shown very high MICs of >256 and 256 µg/ml respectively. Similarly, about 12 (10%) of the isolates had a MIC of ≤128 µg/ml and ≥32 µg/ml. In a similar way extended spectrum cephalosporins (ESC) such as ceftazidime had 77% of isolates with MIC >256 µg/ml and ceftriaxone had 87% of the isolates

with very high MIC of >256 µg/ml. Gentamicin was found to have 44% of the isolates with very high MIC of >256 µg/ml while its 15 (32%) of the isolates ≥8 µg/ml. However, in case of levofloxacin 72% of the isolates had MIC in range of ≤32 µg/ml, while ciprofloxacin had 50% of the isolates with high MICs of ≥256 µg/ml and 34 (35%) had MICs of ≤64 µg/ml (Table 4.1). Over all these result show very high level of resistance against the common antibiotics recommended against UPEC isolates, circulating in Pakistani population. In case of MBCs, all the drugs except levofloxacin had higher MICs in range of ≥256 µg/ml validating our results (Table 4.2). Moreover, our results showed no significance difference of MICs between ESBL and non-ESBL isolates (data not shown).

Table 4.1 "Minimum inhibitory concentrations" (MICs) of frontline drugs recommended against UTI.

Antibiotic	N	>256 µg/ml	256 µg/ml	128 µg/ml	64 µg/ml	32 µg/ml	16 µg/ml	8 µg/ml	4 µg/ml	2 µg/ml	1 µg/ml	≤0.5 µg/ml
TMP	132	89 (67%)	31 (23%)	5 (4%)	6 (5%)	1 (1%)	-	-	-	-	-	-
CAZ	97	75 (77%)	4 (4%)	5 (5%)	3 (3%)	4 (6%)	3 (3%)	-	-	-	-	-
CRO	99	86 (87%)	3 (3%)	3 (3%)	1 (1%)	-	4 (4%)	1 (1%)	1 (1%)	-	-	-
CN	51	22 (44%)	7 (15%)	4 (9%)	9 (20%)	2 (4%)	2 (4%)	2 (4%)	-	-	-	-
LEV*	75	3 (4%)	4 (5%)	5(7%)	7 (9%)	18 (24%)	16 (21%)	14 (19%)	2 (3%)	1 (1%)	2 (3%)	3 (4%)
CIP*	89	22 (25%)	22 (25%)	13 (15%)	15 (17%)	9 (10%)	4 (4%)	-	-	-	2 (2%)	2 (2%)

Table 4.2 Minimum bactericidal concentrations (MBCs) of frontline drugs recommended against UTI.

Antibiotic	N	>256 µg/ml	256 µg/ml	128 µg/ml	64 µg/ml	32 µg/ml	16 µg/ml	8 µg/ml	4 µg/ml	2 µg/ml	1 µg/ml	≤0.5 µg/ml
CAZ	97	82 (85%)	5 (5%)	4 (4%)	2 (2%)	-	1 (1%)	-	-	-	-	-
CRO	99	90 (91%)	3 (3%)	1 (1%)	3 (3%)	1 (1%)	1 (1%)	-	-	-	-	-
CN	51	21 (46%)	9 (20%)	5 (11%)	7 (15%)	2 (4%)	2 (4%)	-	-	-	-	-
LEV*	75	12 (16%)	4 (5%)	10 (13%)	15 (20%)	13 (17%)	10 (13%)	7 (9%)	-	1 (1%)	1 (1%)	2 (3%)
CIP*	89	44 (49%)	16 (18%)	10 (11%)	10 (11%)	3 (3%)	2 (2%)	-	-	-	2 (2%)	2 (2%)

*, ** Previously done by Ihsan *et al.,* 2016

A

B
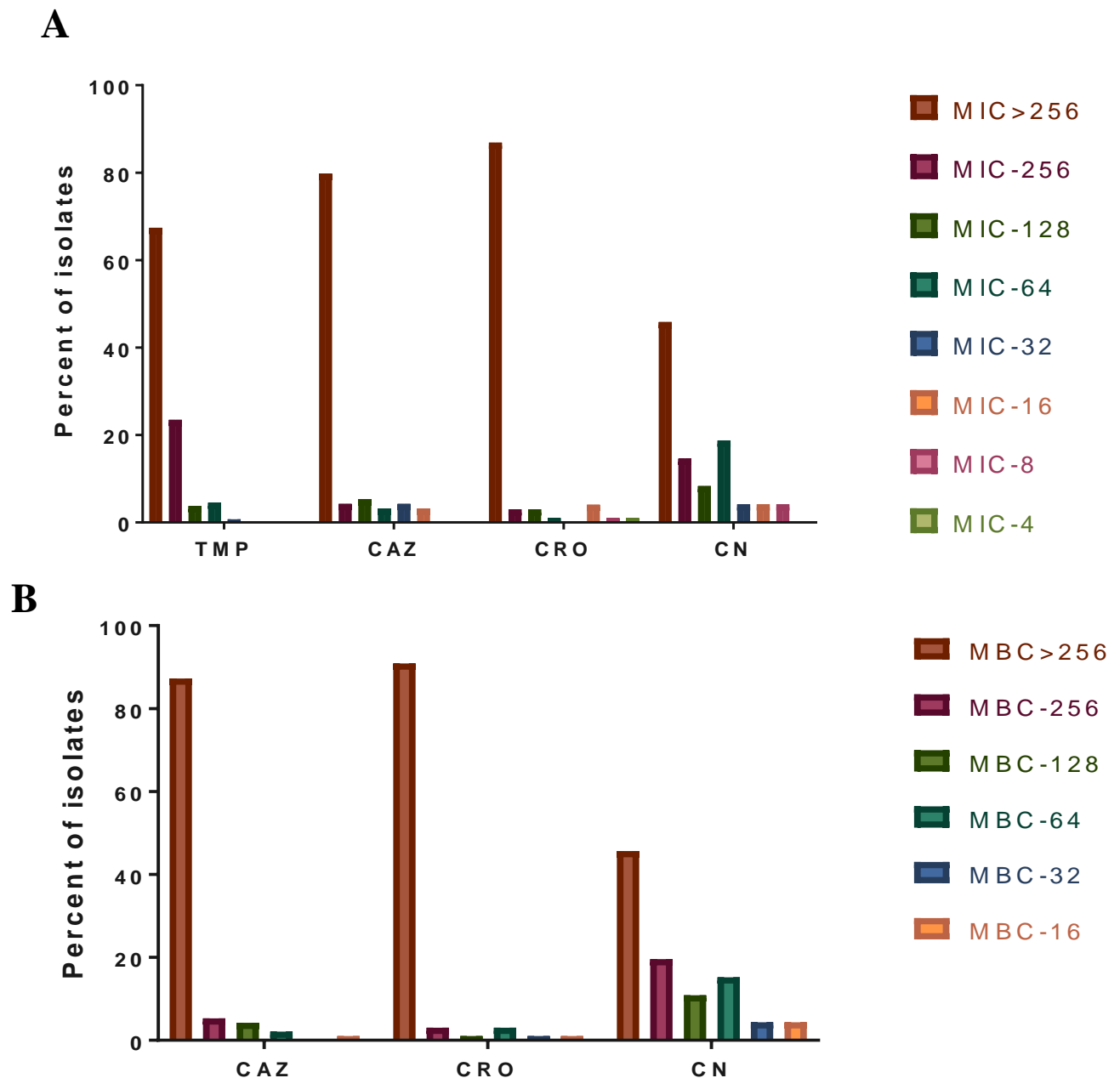
Figure 4.8. MICs (A) and MBCs (B) of trimethoprim*, ceftazidime, ceftriaxone and gentamicin against UPEC isolates.

Bar graph shows MIC and MBC values of trimethoprim, ceftazidime and ceftriaxone as compared to gentamicin, against antibiotic resistant UPEC isolates.

*Trimethoprim is a bacteriostatic drug hence MBC values are not possible for it.

4.4   Genetic screening of plasmid mediated resistance genes in ESBL⁺ UPEC strains

After phenotypic detection (DDST) of ESBLs, genetic screening of ESBL mediated resistance genes was performed. Apart from $bla_{CTX-M-15}$, amplification of all four genes (bla_{TEM-1}, bla_{SHV}, bla_{OXA-1}, bla_{PSE-1}) were performed in this study. Details of primers is given in Table 3.3. The gene $bla_{CTX-M-15}$ was screened by another colleague Ihsan *et al.*,2016 (Ali et al., 2016b) as a part of his research. The data regarding $bla_{CTX-M-15}$ shown here is with his consent and agreement.

Out of 65 ESBL producing isolates, $bla_{CTX-M-15}$ was found in 57 (88%) of the isolates. Additionally, bla_{TEM-1} was found in 23 (36%), bla_{SHV} in 6 (7%), bla_{OXA-1} in 12 (15%) and bla_{PSE-1} in 1 (1%) of the isolates (Figure 4.10). Selected DNA sequences were reported to the GenBank database and the following accession numbers were assigned (KX171170-171195). (https://www.ncbi.nlm.nih.gov/nuccore/KX171170;

http://getentry.ddbj.nig.ac.jp/getentry/na/KX171170-KX171195/?filetype=html&limit=26)

Majority of the isolates were found in the presence of other genes (Table 4.3). Certain genes such as $bla_{CTX-M-15}$ and bla_{TEM-1} were observed to have a significant ($P<0.05$) co-prevalence. Likewise, another significant ($P<0.01$) association was noted between $bla_{CTX-M-15}$ and bla_{SHV}. Similarly, $bla_{CTX-M-15}$, bla_{TEM-1} and bla_{OXA-1} were found statistically significant ($P<0.01$) co-prevalent.
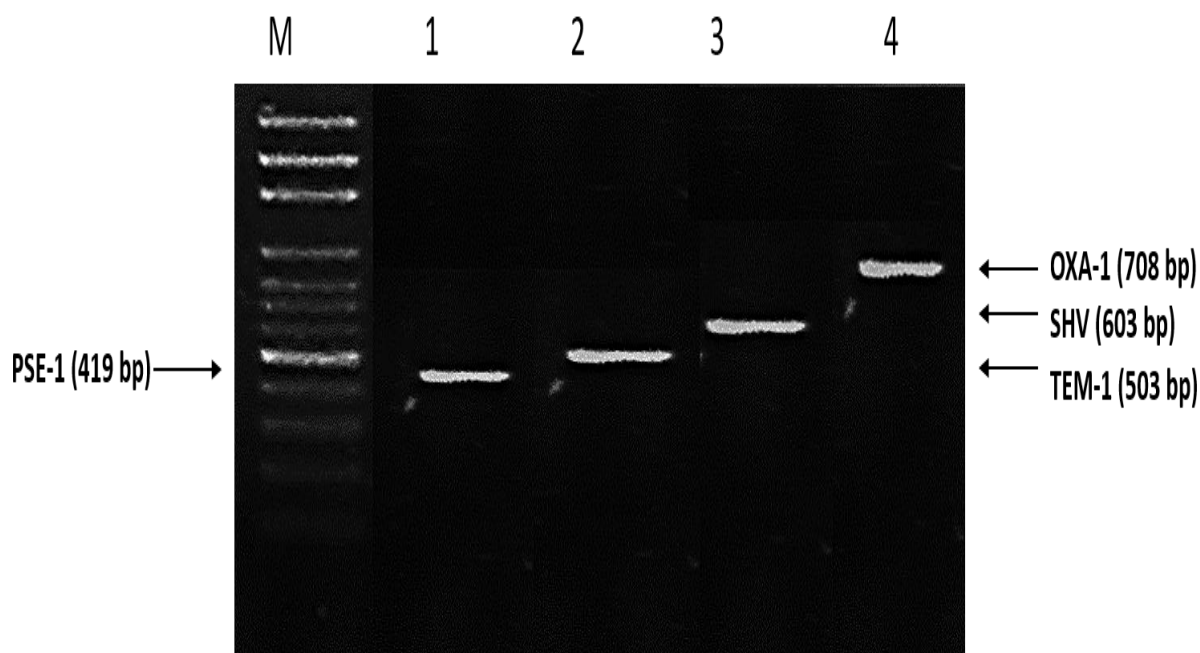
Figure 4.9. Molecular screening of ESBL factors in UPEC isolates.

Agarose gel picture shows Thermofisher Scientific ™, 100 bp ladder (M), followed by 419 bp gene fragment of bla_{PSE-1} (lane 1), 503 bp gene fragment of bla_{TEM-1} (lane 2), 603 bp gene fragment of bla_{SHV} (lane 3) and 708 bp gene fragment of bla_{OXA-1} (lane 4).
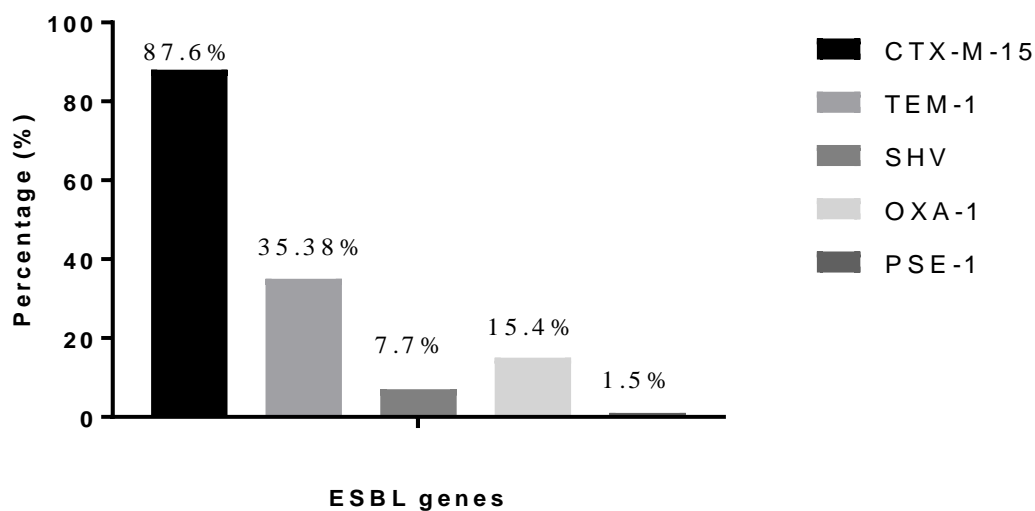
Figure 4.10 Prevalence of plasmid mediated ESBL genes.

Bar graph shows relative prevalence of plasmid ESBL genes $bla_{CTX-M-15}$, bla_{SHV}, bla_{TEM-1}, bla_{OXA-1} and bla_{PSE-1}.

Table 4.3 Co-prevalence of multiple resistance genes

Genes	Number (%)	*P* value[*]
bla_{CTXM}-bla_{TEM}	11 (17%)	0.0137
bla_{CTXM} - bla_{SHV}	3 (5%)	0.0049
bla_{CTXM}- bla_{OXA-}	2	0.1029
bla_{TEM-1}- bla_{SHV}	0	-
bla_{TEM-1}- bla_{OXA-}	0	-
bla_{OXA-1} - bla_{SHV}	1	0.1029
bla_{CTXM} - bla_{TEM-1}- bla_{SHV}	0	-
bla_{CTXM} - bla_{TEM-1}- bla_{OXA-}	5 (8%)	0.0041
bla_{CTXM}-bla_{SHV} - bla_{OXA-}	1	-
bla_{CTXM} - bla_{TEM-} bla_{SHV} - bla_{OXA-}	1	-
bla_{CTXM} bla_{TEM-1}- bla_{SHV-} bla_{OXA-}- bla_{PSE-1}	1	<0.0001
$bla_{CTXM-15}$	31	-
bla_{TEM-1}-1	5	-

- *P* **value was calculated using chi-square**

4.5   Virulence profiling of UPEC isolates

After the MDR status of strains was confirmed through disc diffusion, MIC and molecular screening of resistance genes, next they were scrutinized for their virulence profiling through phenotypic and genotypic assays.

4.5.1   Phenotypic profiling of virulence factors and their correlation to resistance

4.5.1.1   Frequency of virulence phenotypes

Phenotypic assays such as hemagglutination, cell surface hydrophobicity, hemolysis and serum bactericidal resistance were performed to determine the phenotypic virulence markers. An isolate was considered to have mannose resistant hemagglutination (MRHA), if hemagglutination occurred in the presence of D-mannose, whereas it was considered mannose sensitive hemagglutination (MSHA), if no hemagglutination occurred in the presence of D-mannose (Figure 4.11A). Out of 155 isolates, 37 (24%) isolates showed MRHA and 3 (2%) isolates showed MSHA, remaining 115 (74%) isolates did not show hemagglutination. An

isolate was considered positive for cell surface hydrophobicity (CSH) if it aggregated in the presence of ammonium sulphate solution of concentration $\leq 1.4M$ (Figure 4.11B). Out of 155 isolates 48 (31%) were found positive for CSH. Among the hemolysin positive isolates, 67(43%) were alpha hemolysin producers and 3(2%) isolates were found positive β-hemolysin (Figure 4.11C). Additionally, 48 (31%) were found positive for CSH and 70 (45%) isolates showed hemolysis on BAP. Our results further indicated that 28% hemolytic strains were also positive for haemagglutination test. In serum bactericidal assay (SBA) 132 (85%) of isolates showed resistance to the serum bactericidal effect (Figure 4.11D).
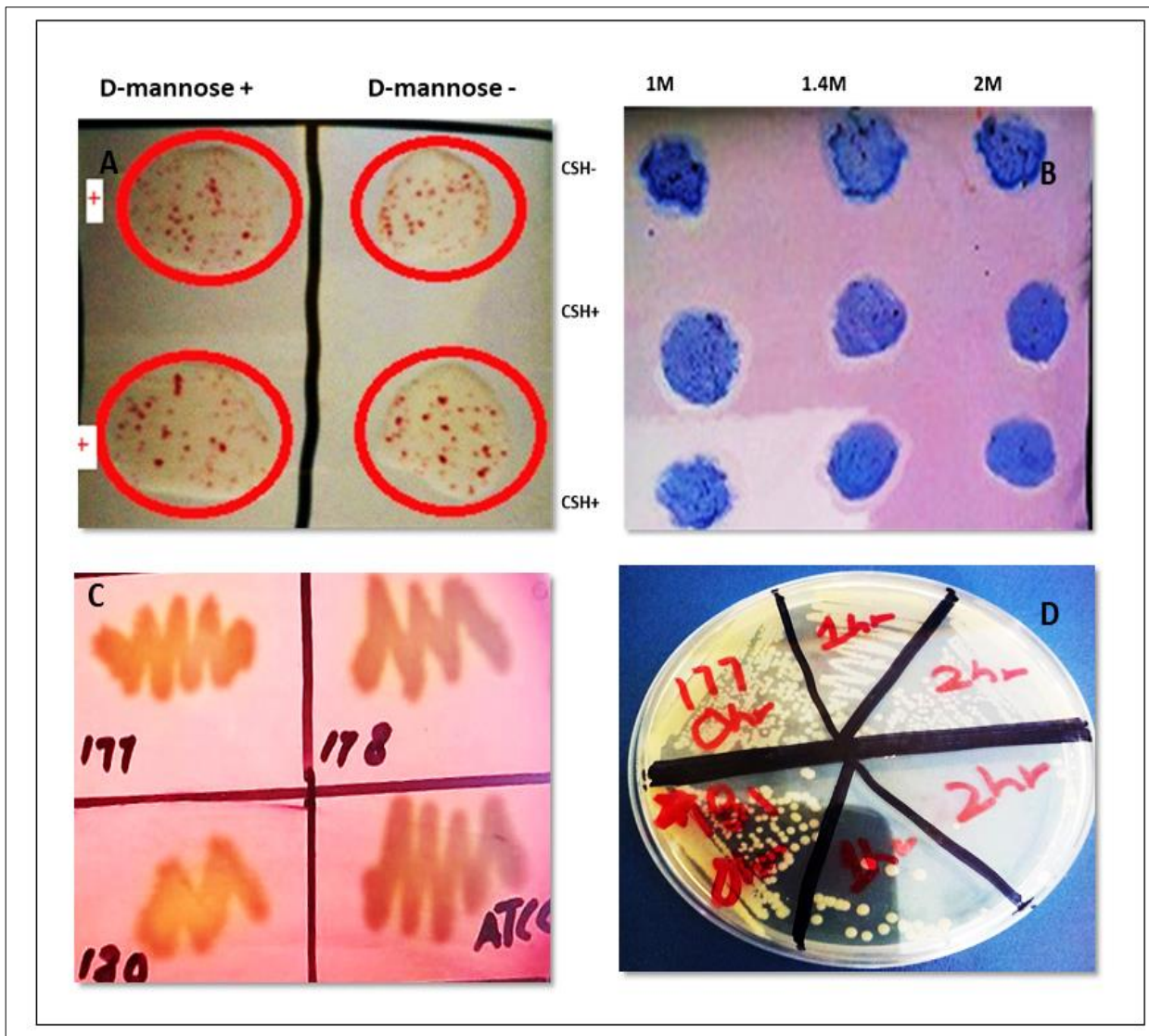
Figure 4.11 Phenotypic screening of virulence factors.

 (A) Hemagglutination test in the presence and absence of D-mannose, MRHA positive isolates show hemagglutination under both conditions. (B) CSH, top isolate is CSH negative (shows agglutination in all 3 concentrations), bottom two are positive (agglutination at ≤1.4M) (C) Hemolysis on BAP, isolate 177 and 180 are positive for α-hemolysis, while isolate 178 and ATCC 25922 negative for hemolysis (γ hemolysis). (D) Serum bactericidal assay, isolate 177 is resistant to SBA, isolate 181 is sensitive to SBA shows no growth after 2 hours.
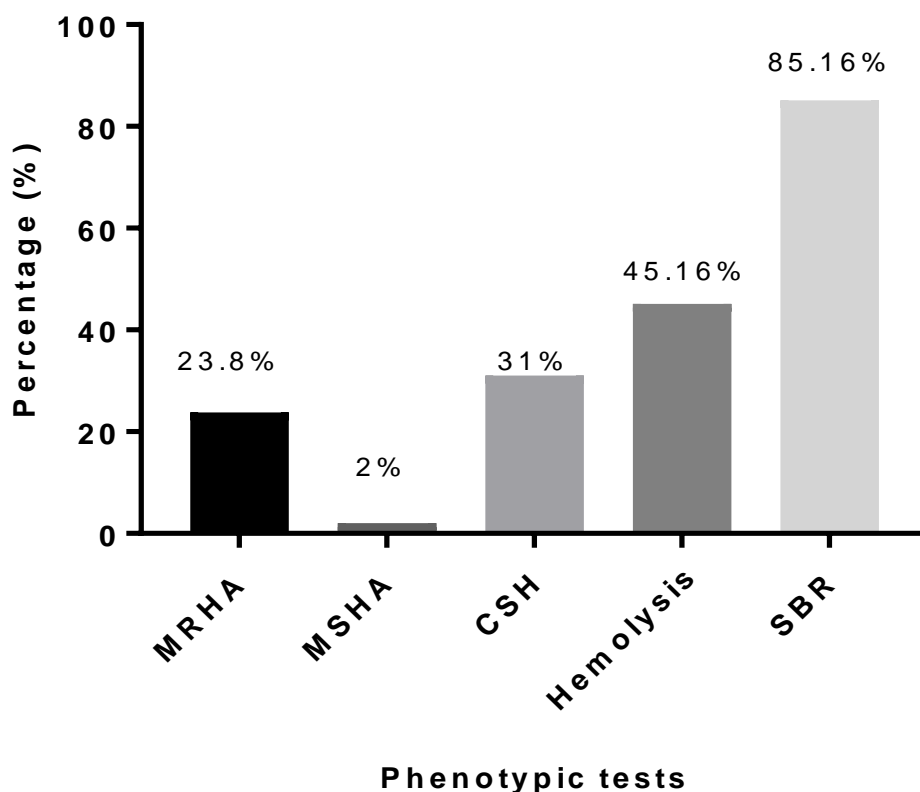
Figure 4.12 Phenotypic characteristics of UPEC

Bar graph shows frequency of phenotypic attributes of UPEC, with serum bactericidal resistance (SBR) having the highest frequency (85%) and mannose resistant hemagglutination (MSHA) with the lowest frequency (2%).

4.5.1.2   Virulence phenotype and their association with antimicrobial resistance

In an attempt to determine a link between resistance and virulence in our UPEC strains, phenotypic virulence characteristics were analyzed in the presence and absence of ESBLs, MDR and resistance to individual antibiotics (Table 4.4 - 4.7). Fisher-exact test was used to compare the given datasets.

None of the virulence phenotypes showed any significant association between ESBL and non-ESBL phenotypes (Table 4.4). All the virulence factors were uniformly distributed among both phenotypes (ESBL and non-ESBL). However, a significant relationship ($P<0.05$) was found

between $bla_{\text{CTX-M-15}}$ and SBR with 88% of $bla_{\text{CTX-M-15}}$ isolates found resistant to serum bactericidal activity (Table 4.5). When compared with MDR and non-MDR, virulence factors such as CSH and MRHA were found significantly associated with MDR phenotype (Table 4.6). Our results showed that hemolysis was significantly associated ($P<0.05$) with gentamicin sensitive isolates (51%) as compared to gentamicin resistant isolates (33%). Our results also showed a highly significant association of serum resistance with $bla_{\text{CTX-M-15}}$ producing and trimethoprim resistance isolates (Table 4.7). MRHA positive isolates were found significantly ($P<0.05$) with trimethoprim, ceftriaxone and ceftazidime resistant isolates.

Table 4.4 Association of virulence phenotypes with ESBL production

Virulence Factors	ESBL⁺ (n=65)	Non-ESBL (n=90)	*P* value
Hemolysis	28 (43%)	42 (47%)	0.7441
CSH	20 (31%)	28 (31%)	>0.9999
SBA	56 (86%)	76 (84%)	0.8224
MRHA	17 (26%)	20 (22%)	0.4589
MSHA	2 (3%)	1 (1%)	0.5723

Table 4.5 Association of virulence phenotypes with *bla*$_{CTX-M-15}$

Virulence Factors	*bla*$_{CTX-M-15}$ (n=57)	Non-*bla*$_{CTX-M-15}$ (n=98)	*P* value
Hemolysis	25 (44%)	45 (46%)	0.8677
CSH	18 (32%)	30 (31%)	>0.9999
SBA	50 (88%)	72 (73%)	0.0426
MRHA	16 (28%)	21 (22%)	0.4348
MSHA	2 (4%)	1 (1%)	0.5549

Table 4.6 Association of virulence phenotypes with multidrug-resistance

Virulence Factors	MDR (n=124)	Non-MDR (n=31)	*P* value
Hemolysis	55 (44%)	15 (48%)	0.6923
CSH	44 (35%)	4 (13%)	0.0165
SBA	104 (84%)	28 (90%)	0.5720
MRHA	35 (28%)	2 (6%)	0.0094
MSHA	2 (2%)	1 (4%)	0.4905

Table 4.7 Association of virulence phenotypes with antibiotic resistance

Virulence trait	TMP-SXT-R (n=132)	TMP-SXT-S (n=23)	CN-R (n=51)	CN-S (n=104)	CAZ-R (n=97)	CAZ-S (n=58)	CRO-R (n=99)	CRO-S (n=56)	LEV-R (n=98)	LEV-S (n=57)	CIP-R (n=96)	CIP-S (n=59)
Hemolysis	60 (45%)	10 (43%)	17 (33%)	53* (51%)	40 (41%)	27 (47%)	46 (46%)	24 (43%)	42 (43%)	28 (49)	42 (44%)	28 (47%)
CSH	43 (33%)	5 (22%)	13 (25%)	30 (29%)	34 (35%)	14 (24%)	33 (34%)	15 (25%)	33 (34%)	15 (25%)	33 (34%)	15 (25%)
SBA	124*** (94%)	8 (35%)	44 (86%)	88 (85%)	85 (88%)	47 (81%)	87 (88%)	45 (80%)	84 (86%)	48 (84%)	80 (83%)	52 (88%)
MRHA	36* (27%)	1 (4%)	8 (16%)	29 (28%)	30*** (31%)	7 (12%)	29* (30%)	8(14%)	27 (28%)	10 (17%)	27 (28%)	10 (17%)
MSHA	3 (2%)	0	0	3 (3%)	2 (2%)	1 (2%)	2 (2%)	1 (2%)	2 (%)	1 (1%)	2 (2%)	1 (1.6%)

P value <0.05 ***P<0.001, calculated by Chi square test.

4.5.2   Genotypic profiling of virulence factors and their correlation to resistance

4.5.2.1   Frequency of virulence genotypes

After confirming virulence phenotypes, all 155 UPEC isolates were subjected genetic screening of virulence factors. A total of 18 virulence factors grouped into adhesins (*fimH, papA, papC, papEF, papGI, papGII, papGIII, sfa, afa, bmaE*), iron acquisition system (*fyuA, iutA, feoB*), capsular proteins (*kpsMTII* & *kpsMTIII*) and uropathogenic-specific protein (*usp*) were scrutinized among 155 strains through PCR. Overall percentages of VF genes were as follows: *fim*H 155 (100%), *iut*A 86 (55%), *feoB* 76 (49%), *papC* 75 (48%), *papGII* 70 (45%), *kpsMTII* 40 (26%), *papEF 37* (24%), *fyuA* 37 (24%), *usp* 22 (14%), *papA* 20 (13%), *sfa/foc* 20 (13%), *hlyA* 18 (12%), *afa* 15 (10%), *cdtB* 11 (7%), *papGI* 6 (4%), *papGIII* 6 (4%), *kpsMTIII* 4 (3%) and *bmaE* 2 (1%).
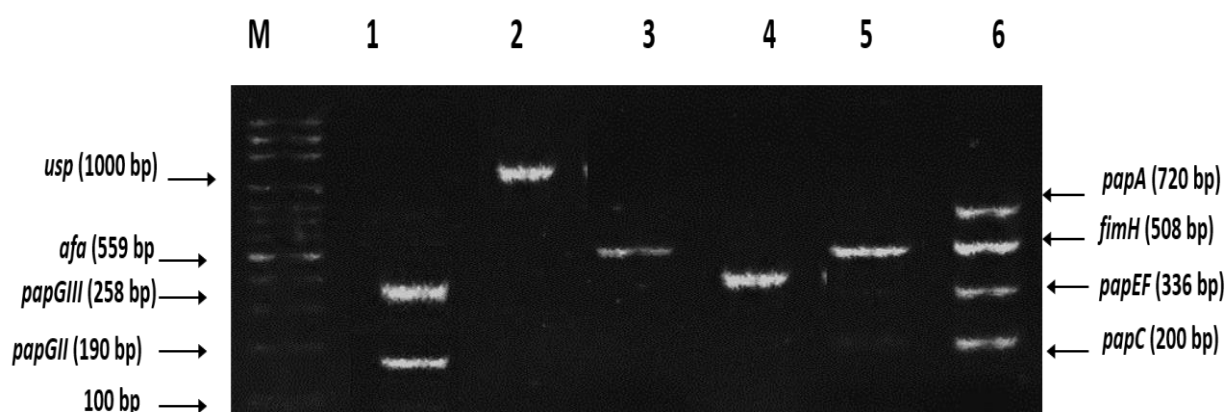
Figure 4.13. Molecular screening of VF encoding adhesins.

Agarose gel picture shows Thermofisher Scientific ™, 100 bp ladder (M), followed by 190 bp and 258 bp gene fragments of *papGII* and *papGIII* respectively (lane 1), 1000 bp gene fragment of *usp* (lane 2), 559 bp gene fragment of *afa* (lane 3), 410 bp gene fragment of *sfa/foc* (lane 4), 507 bp gene fragment of *bmaE* (lane 5) and 200 bp, 336 bp, 508 bp, 720 bp gene fragment of *papC, papEF, fimH* and *papA* (lane 6).
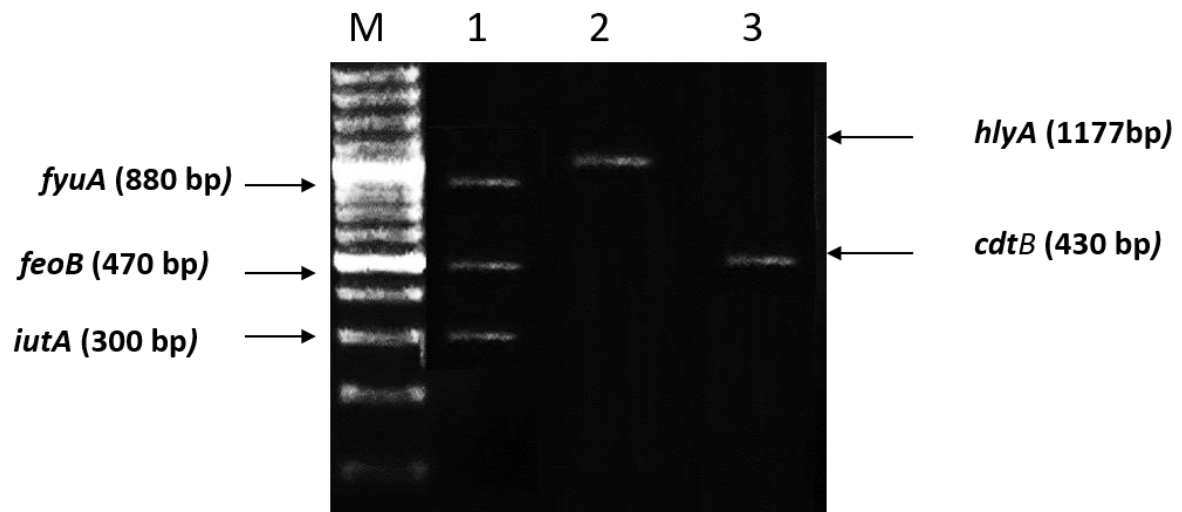
Figure 4.14 .Molecular screening of VF encoding iron acquisition systems and toxins.

Agarose gel picture shows Thermofisher Scientific ^{TM}, 100 bp ladder (M), followed by 300 bp, 470 bp and 880 bp gene fragments of *iutA, feoB* and *fyuA* respectively (lane 1), 1177 bp gene fragment of *hlyA* (lane 2) and 430 bp gene fragment of *cdtB* (lane 3).
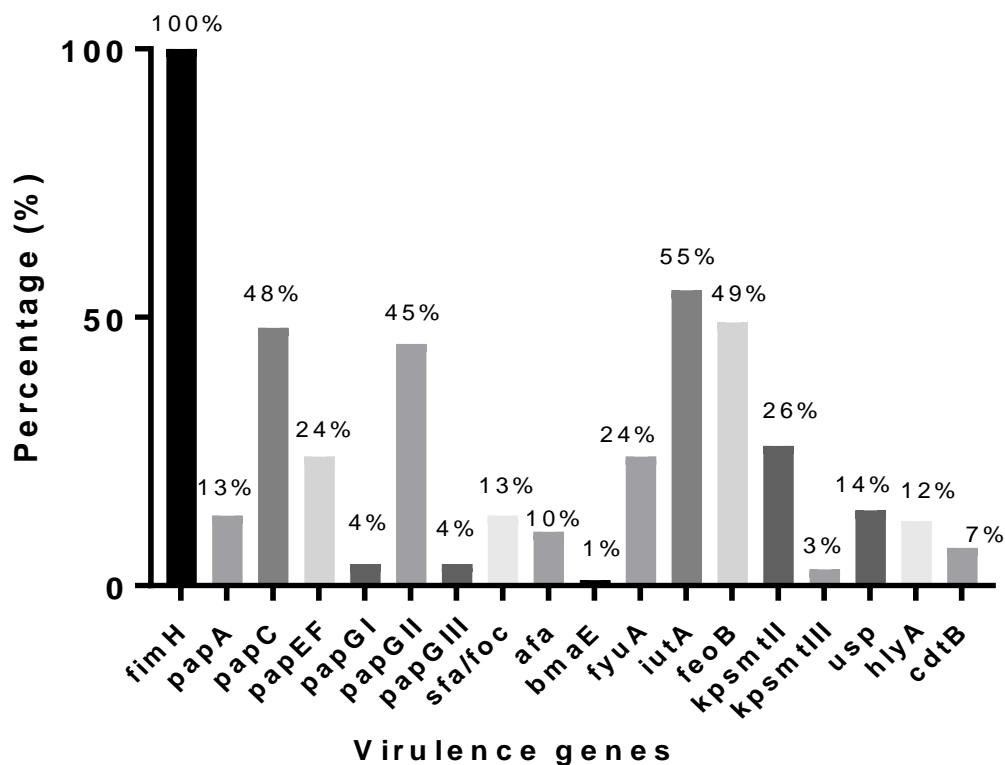
Figure 4.15 Virulence attributes of UPEC.

Bar graph shows frequency of genotypic attributes of UPEC. *fimH* is the major virulence factor present in all isolates, followed by aerobactin (*iutA,* 55%), *feoB* (49%), *papC* (48%). *bmaE* was found to be least frequent, only 2% of UPEC isolates were found positive for it.

4.5.2.2   Virulence genotype and their association with antimicrobial resistance

In order to determine the correlation between virulence factors (VF) and resistance phenotypes, VF were analyzed and compared to ESBL, MDR and individual antibiotic resistance phenotype (Table 4.8-4.9).

When compared with ESBL vs non-ESBL phenotype, VF such as *fimH, papA, papC, sfa/focA, bmAE, fyuA* and *kpsMTIII* were found uniformly distributed among both phenotypes. Other virulence factors such as *papEF, feoB, kpstMTII, usp,* and *hlyA* were seen more frequent in ESBL-producers, although no significant association was found. However, genes like *papGII*

and *iutA* were significantly (*P*<0.05) associated with ESBL producers (57% and 66% respectively) as compared to non-ESBL producers (37% and 48% respectively).

VF when compared with MDR phenotypes (Table 4.8) almost similar trend was observed, as in case of ESBL. VF such as *papGII* and *iutA* were more prevalent in MDR isolates (50% and 56% respectively), as compared to non-MDR isolates (26% and 39%). A significant association (*P*<0.05) was found between these factors. Similarly, *sfa* gene was found strongly associated with MDR isolates (15%), while it was totally absent in non-MDR isolates. In addition, VF such as *feoB* and *hlyA* were more frequent in MDR isolates, albeit no statistically significant association was found. Certain VF were also found associated with individual antibiotic resistance phenotypes such as *papC* was found more frequent (*P*<0.05) in gentamicin resistant isolates. Moreover, *papGII* and *sfa/foc* were found more common in FQR (levofloxacin and ciprofloxacin) and ceftazidime resistant isolates. A statistically significant association was found for these factors.

Table 4.8 Percentage distribution of VF among ESBL and non-ESBL, MDR and non-MDR phenotypes

Virulence trait	ESBL+ (n=65)	Non-ESBL (n=90)	MDR (n=124)	Non-MDR (n=31)
fimH	65 (100%)	90 (100%)	124 (100%)	31 (100%)
papA	8 (12%)	12 (13%)	14 (11%)	6 (19%)
papC	33 (51%)	42 (47%)	60 (48%)	15 (48%)
papEF	19 (29%)	18 (20%)	29 (23%)	8 (26%)
papGI	3 (5%)	3 (3%)	4 (3%)	2 (6%)
papGII	37*(57%)	33 (37%)	62*(50%)	8 (26%)
papGIII	2 (3%)	4 (4%)	4 (3%)	2 (6%)
sfa/foc	9 (14%)	11 (12%)	20* (15%)	0
Afa	8 (12%)	7 (8%)	11 (8%)	4 (13%)
bmaE	1 (2%)	1 (1%)	2 (2%)	0
fyuA	17 (26%)	20 (22%)	31 (24%)	6 (19%)
iutA	43*(66%)	43 (48%)	74* (56%)	12 (39%)
feoB	36 (55%)	40 (44%)	65 (50%)	11 (35%)
kpsmtII	21 (32%)	19 (21%)	32 (24%)	8 (33%)
kpsmtIII	2 (3%)	2 (2%)	2 (2%)	2 (6%)
usp	12 (18%)	10 (9%)	19 (15%)	3 (10%)
hlyA	11(17%)	7 (8%)	17 (13%)	1 (3%)
cdtB	5 (8%)	6 (7%)	10 (8%)	1 (3%)

*P value <0.05 ***P<0.001, calculated by Chi square test.

Table 4.9 Percentage distribution of VF among antibiotics resistant phenotypes

Virulence trait	TMP-SXT-R (n=132)	TMP-SXT-S (n=23)	CN-R (n=51)	CN-S (n=104)	CAZ-R (n=97)	CAZ-S (n=58)	CRO-R (n=99)	CRO-S (n=56)	LEV-R (n=98)	LEV-S (n=57)	CIP-R (n=96)	CIP-S (n=59)
fimH	132 (100%)	23 (100%)	51 (100%)	104 (100%)	97 (100%)	58 (100%)	99 (100%)	56 (100%)	98 (100%)	57 (100%)	96 (100%)	59 (100%)
papA	17 (13%)	3 (13%)	6 (12%)	14 (13%)	8 (8%)	12* (21%)	9 (9%)	11 (20%)	12 (12%)	8 (14%)	12 (13%)	8 (14%)
papC	66 (50%)	9 (39%)	31* (61%)	44 (42%)	46 (47%)	29 (50%)	48 (48%)	27 (48%)	48 (49%)	27 (47%)	47 (49%)	29 (49%)
papEF	33 (25%)	4 (17%)	14 (27%)	23 (22%)	18 (19%)	19* (33%)	22 (22%)	15 (27%)	24 (24%)	13 (23%)	24 (25%)	13 (22%)
papGI	5 (4%)	1 (4%)	2 (4%)	4 (4%)	3 (3%)	3 (5%)	0	6** (11%)	2 (2%)	4 (7%)	2 (2%)	4 (7%)
papGII	61 (46%)	9 (39%)	25 (49%)	45 (43%)	45 (46%)	25 (43%)	44 (44%)	26 (46%)	49* (50%)	21 (37%)	49* (51%)	21 (35%)
papGIII	4 (3%)	2 (9%)	1 (2%)	5 (5%)	3 (3%)	3 (5%)	3 (3%)	3 (5%)	4 (4%)	2 (4%)	3 (3%)	3 (5%)
sfa/foc	19 (14%)	1 (4%)	7 (14%)	13 (13%)	17* (18%)	3 (5%)	14 (14%)	6 (11%)	15 (15%)	5 (9%)	15 (16%)	5 (8%)
afa	14 (11%)	1 (4%)	6 (12%)	9 (9%)	12 (12%)	3 (5%)	11 (11%)	4 (7%)	11 (11%)	4 (7%)	11 (11%)	4 (7%)
bmaE	2 (2%)	0	0	2 (2%)	1 (1%)	1 (2%)	1 (1%)	1 (2%)	0	2 (4%)	0	2 (3%)
fyuA	31 (23%)	6 (26%)	12 (24%)	25 (24%)	23 (24%)	14 (24%)	25 (25%)	12 (21%)	23 (24%)	14 (25%)	23 (24%)	14 (24%)
iutA	75 (57%)	11 (48%)	30 (59%)	56 (54%)	53 (55%)	33 (57%)	55 (55%)	31 (55%)	56 (57%)	30 (52%)	55 (57%)	31 (56%)
feoB	66 (50%)	10 (43%)	27 (53%)	49 (47%)	48 (49%)	28 (48%)	45 (45%)	31 (55%)	49 (50%)	27 (47%)	49 (51%)	27 (46%)
kpsmtII	33 (25%)	7 (30%)	10 (20%)	30 (29%)	24 (25%)	16 (28%)	29 (29%)	11 (20%)	26 (27%)	14 (25%)	25 (26%)	15 (25%)
kpsmtIII	3 (2%)	1 (4%)	0	3 (3%)	2 (2%)	2 (3%)	3 (3%)	1 (2%)	2 (2%)	2 (4%)	2 (2%)	2 (34%)
usp	20 (15%)	2 (9%)	6 (12%)	16 (15%)	15 (15%)	7 (12%)	14 (14%)	8 (14%)	15 (15%)	7 (12%)	14 (15%)	8 (14%)
hlyA	17 (13%)	1 (4%)	4 (8%)	14 (13%)	12 (12%)	6 (10%)	13 (13%)	5 (9%)	14 (14%)	4 (7%)	13 (14%)	5 (8%)
cdtB	11 (8%)	0	2 (4%)	9 (9%)	8 (8%)	3 (5%)	8 (8%)	3 (5%)	9 (9%)	2 (4%)	8 (8%)	3 (5%)

*P value <0.05 ***P<0.001, calculated by Chi square test.

4.5.2.3   Virulence genotype and their association with different sequence types (STs)

Sequence typing of all the 155 UPEC isolates was previously determined by (Ali et al., 2016c).

A total of 18 different STs were confirmed in 152 (99%) isolates, while the 3 isolates (1%)

remained were un-typeable, in his study. Among all the STs, clonal group ST131 remained

predominant with 71(46%) of all the isolates, followed by ST405 28(18%) and ST168

16(10%). CH-typing confirmed that 35(49%) belonged to subclone ST131-*H*30, out of which

22(31%) isolates belonged to the serogroup O25b (Ali et al., 2016c).

VF factors were correlated with all the STs (Table 4.10). Most of the VF were found uniformly

distributed across all the STs. However, some VF such as *sfa/foc, fyu*A and *feo*B were

significantly ($P < 0.05$) associated with ST131 isolates, also VF such as *pap*EF, *sfa/foc* and

*hly*A were found in significantly strong association ($P < 0.05$) with ST131 *H30* sub-clone.

Likewise, aerobactin receptor *iutA* was found strongly associated ($P \leq 0.01$) with ST131-non-

H30 sub clone.

Table 4.10. Distribution of virulence traits of uropathogenic *E. coli* (n=155) among different sequence types.

Number of the isolates with traits n(%)

Traits	Total n=155	ST-131 n=71	Non H30 n=35	H30 n=36	ST-05 n=28	ST-168 n=16	ST-29 n=13	ST-69 n=5	ST-95 n=2	ST-31 n=2	ST-10 n=2	ST-448 n=2	ST-89 n=2	ST-703 n=2	ST-910 n=1	ST-545 n=1	ST-971 n=1	ST-153 n=1	ST-152 n=1	ST-12 n=1
fimH	155 (100)	71 (100)	35 (100)	36 (100)	28 (100)	16 (100)	13 (100)	5 (100)	2 (100)	2 (100)	2 (100)	2 (100)	2 (100)	2 (100)	1 (100)	1 (100)	1 (100)	1 (100)	1 (100)	1 (100)
papA	20 (13)	12 (17)	5 (14)	7 (19)	4 (14)	1 (6)	0	0	0	0	0	1 (50)	0	0	0	0	0	1 (100)	0	0
papC	75 (48)	33 (46)	17 (49)	16 (44)	15 (54)	9 (56)	5 (38)	3 (60)	1 (50)	1 (50)	0	0	1 (50)	1 (50)	1 (100)	0	1 (100)	1 (100)	0	0
papEF	37 (24)	20 (28)	7 (20)	13* (36)	7 (25)	3 (19)	3 (23)	1 (20)	0	0	0	1 (50)	0	0	0	1 (100)	1 (100)	0	0	0
papGI	6 (4)	2 (3)	0	2 (6)	1 (4)	1 (6)	0	1 (20)	0	0	0	0	0	0	0	0	0	0	0	0
papGII	70 (45)	32 (45)	17 (49)	15 (42)	12 (43)	6 (38)	4 (31)	4 (80)	2 (100)	0	2 (100)	1 (50)	2 (100)	1 (50)	0	1 (100)	0	0	0	1 (100)
papGIII	6 (4)	4 (6)	1 (3)	3 (8)	1 (4)	1 (6)	0	0	0	0	0	0	0	0	0	0	0	0	0	0
sfa/foc	20 (13)	13* (18)	4 (11)	9* (25)	2 (7)	1 (6)	1 (8)	0	1 (50)	0	1 (50)	0	0	0	1 (100)	0	0	0	0	0
afa	15 (10)	7 (10)	4 (11)	3 (8)	6* (21)	1 (6)	1 (8)	0	0	0	0	0	0	2 (100)	1 (100)	0	1 (100)	0	1 (100)	1 (100)
bmaE	2 (1)	1 (1)	1 (3)	0	0	1 (6)	0	0	0	0	0	0	0	0	0	0	0	0	0	0
fyuA	37 (24)	12* (17)	7 (20)	5 (14)	10 (36)	6 (38)	2 (15)	2 (40)	0	0	2 (100)	1 (50)	2 (100)	1 (50)	0	0	0	0	1 (100)	1 (100)
iutA	86 (55)	41 (58)	22*** (63)	19 (53)	14 (50)	10 (63)	5 (38)	3 (60)	2 (100)	1 (50)	2 (100)	1 (50)	1 (50)	1 (50)	1 (100)	1 (100)	1 (100)	0	1 (100)	0
feoB	76 (49)	28* (39)	13 (37)	15 (42)	12 (43)	10 (63)	6 (46)	4 (80)	2 (100)	1 (50)	2 (100)	1 (50)	2 (100)	2 (100)	1 (100)	0	1 (100)	0	1 (100)	1 (100)
kpsmtII	40 (26)	20 (28)	9 (26)	11 (31)	8 (29)	2 (13)	2 (15)	2 (40)	0	0	0	1 (50)	0	0	0	0	0	0	1 (100)	1 (100)
kpsmtIII	4 (3)	2 (3)	0	2 (6)	0	0	0	1 (20)	0	0	0	0	0	0	0	1 (100)	0	0	0	0
usp	22 (14)	13 (18)	5 (14)	8 (22)	2 (7)	3 (19)	1 (8)	0	0	0	1 (50)	0	0	0	0	1 (100)	0	0	0	0
hlyA	18 (12)	8 (11)	1 (3)	7* (32)	5 (18)	1 (6)	1 (8)	0	1 (50)	1 (50)	0	0	0	0	0	0	0	0	0	1 (100)
cdtB	11 (7)	4 (6)	1 (3)	3 (8)	4 (14)	1 (6)	0	0	1 (50)	0	0	0	0	0	0	0	0	0	0	0

The *P* values were calculated by comparing individual STs with each other. The table correlate different traits in vertical columns among different sequence types. The percentages were calculated with reference to total number of sequence types. $*P < 0.05$, $** \, P \le 0.01$, $*** \, P \le 0.001$.

113

4.6   *In-vitro* **virulence potential of selected MDR-virulent UPEC isolates**

In order to determine the *in-vitro* virulence potential of UPEC isolates, invasion assays based on gentamicin protection assays were performed. A total of ten selected MDR-virulent isolates belonging to six different STs (ST131, ST405, ST10, ST38 and 648) were selected. Results showed that out of 10 isolates 7 (70%) isolates were able to significantly ($P<0.05$) invade the bladder epithelial cell lines as compared to the commensal K-12 strains (Figure 4.16). Among all the isolates, UEC59 (ST38) was found to invade relatively higher as compared to other STs, although the invasion rate was not found significantly higher when tested against other STs.
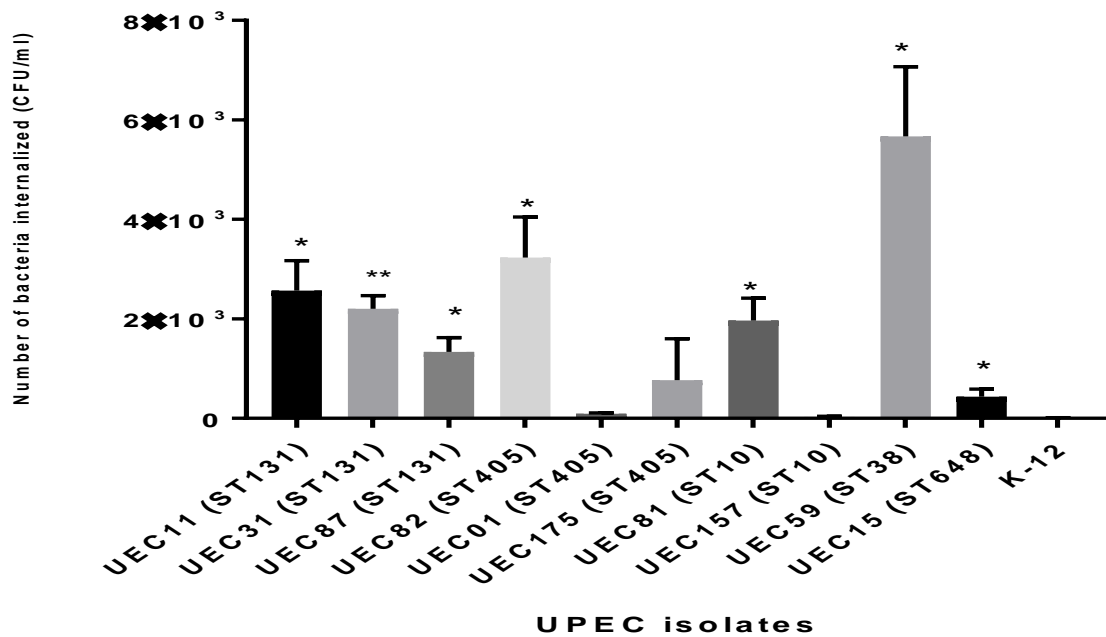
Figure 4.16. *In vitro* **invasion assays performed on 10 MDR-virulent UPEC isolates belonging to different STs.**

Invasion assays were performed using gentamicin protection assay. K-12 was used as a control strain. *P* values were calculated using paired t- test. *P= < 0.05, **P= <0.01.

CHAPTER 5:   Investigation of biofilm formation among UPEC isolates

5.1   Biofilm screening

In order to assess the biofilm formation (BF) capability, all of 155 UPEC isolates were scrutinized for BF production. Biofilm estimation was performed by two qualitative (Congo red agar and test tube) methods and one quantitative method (TCP). Of 155 isolates scrutinized for biofilm production, 145 (94%) were found positive for BF by CRA, however 10(6%) isolates were found negative for BF (Figure 5.1A).

Estimation of BF by TM method revealed that out of 155 isolates, 154 (99%) were biofilm producers, including 35(23%) strong positive, 81(52%) moderate positive and 38(25%) weak positive biofilm producer. Only one strain was found negative. Biofilm was observed as the ring on the bottom of the test tube. Strong biofilm producer (S), moderate biofilm producer (M), weak biofilm producer (W) and negative control (NC) is shown in figure (Figure 5.1B).

Interpretation of TCP results was based on optical density (OD_{540} nm). Isolates were categorized as strong (S), moderate (M), weak (W) and non-producers (NP) based on cutoff OD (OD_c) of control (crystal violet dye) at 540 nm. Investigation of BF using standard TCP method, revealed all the UPEC isolates positive for biofilm formation (Figure 5.1C). Among these isolates, 108 (70%) were categorized as strong biofilm producers (S), 37 (24%) were moderate biofilm producer (M), 10 (6%) were weak biofilm producer (W).

.
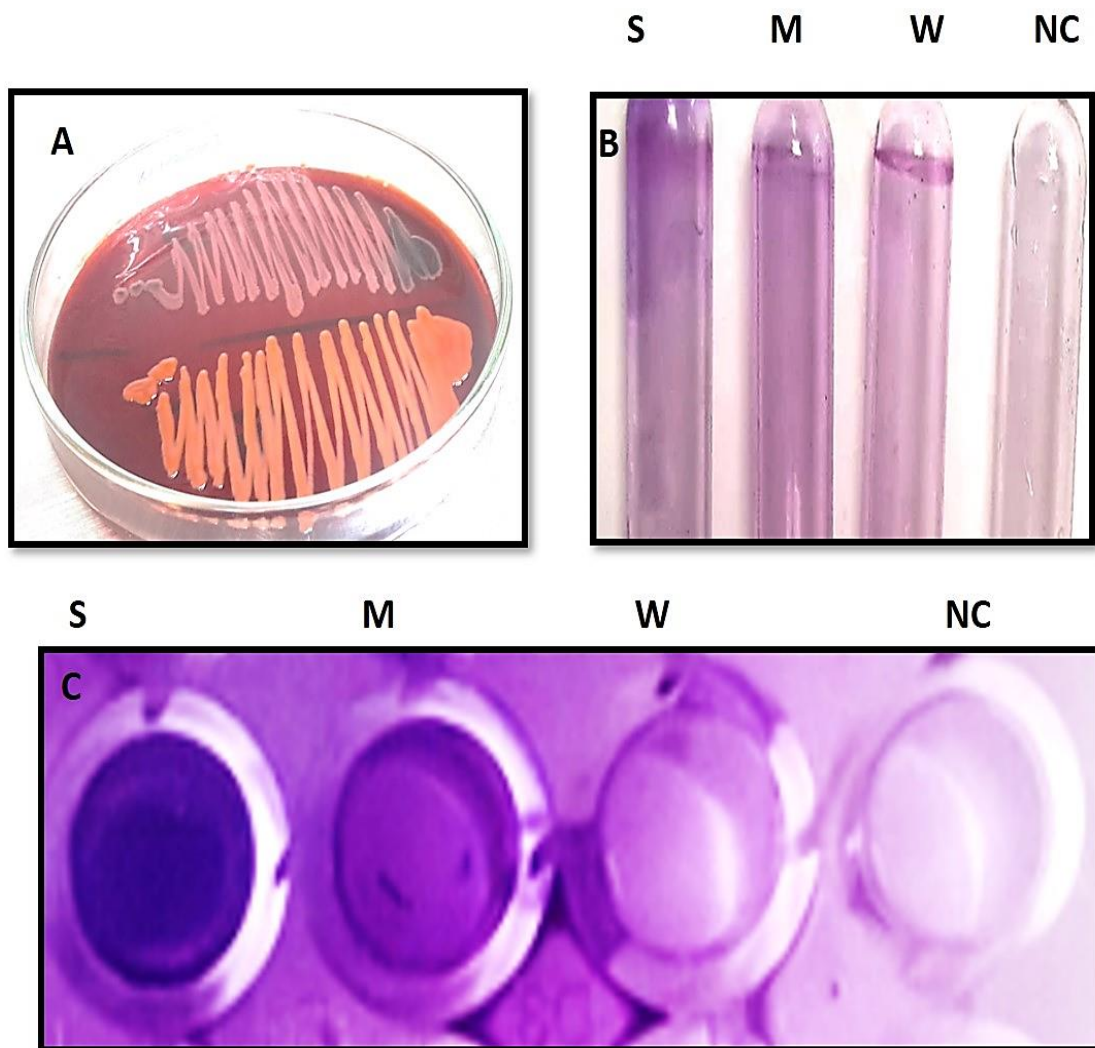
Figure 5.1 Estimation of biofilm by three methods.

(A) Congo red agar method, greyish-black growth shows biofilm producer whereas orange growth is an indication of non-biofilm producer. **(B)** Test tube method, A dark violet test tube on left is a strong biofilm producer (S), M is moderate biofilm producer, W is weak biofilm producer, whereas NC is negative control (no staining of CV on walls). **(C)** Tissue culture plate method, S is a (strong biofilm producer), M (moderate biofilm producer), W (weak biofilm producer), and NC (is a negative control).

Figure 5.2 Relative comparison of three methods used for biofilm estimation
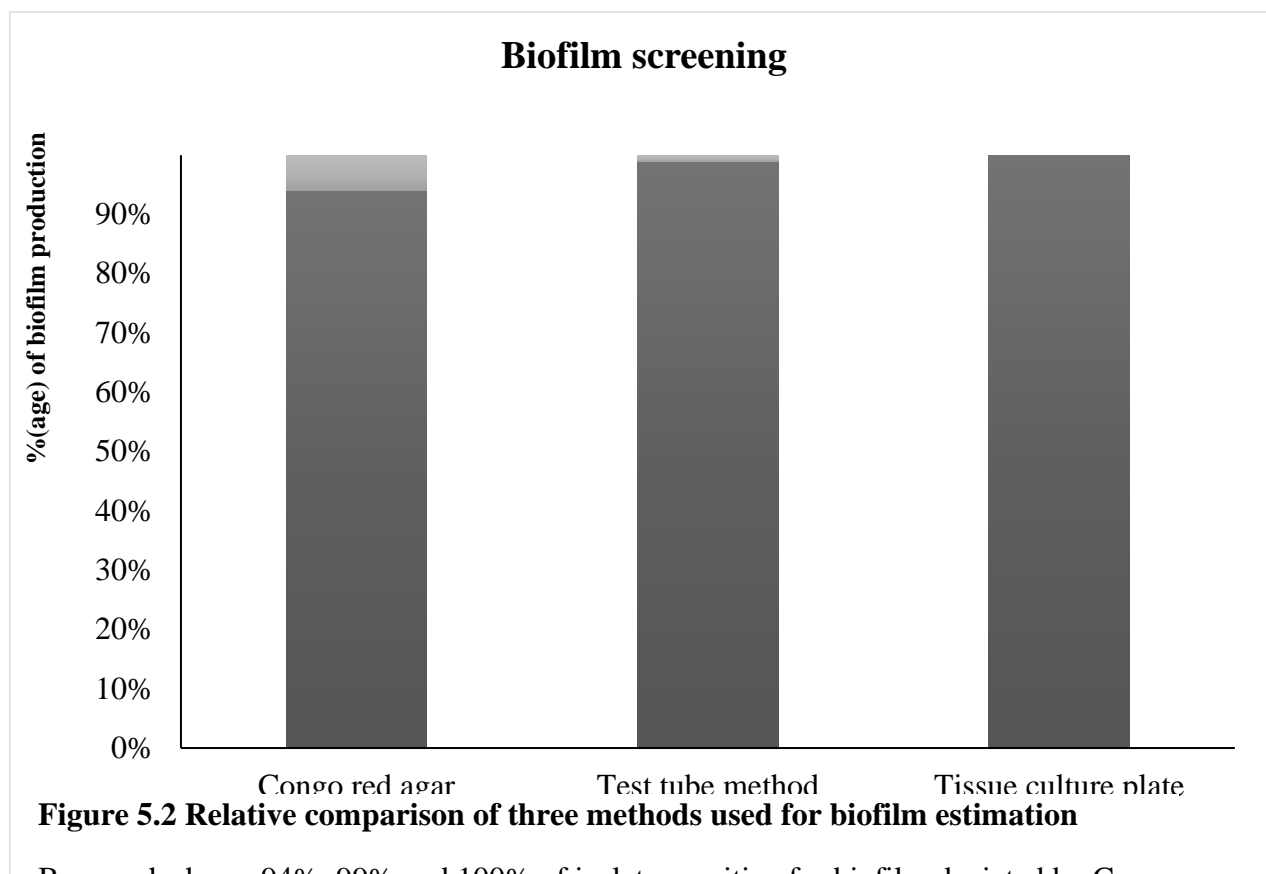
Bar graph shows 94%, 99% and 100% of isolates positive for biofilm depicted by Congo red agar method, test tube method and tissue culture plate method respectively.

5.2   Correlation of biofilm production with resistance and virulence factors

UPEC biofilm forming ability plays an important role in infection persistence. Biofilm structures not only provides protection against high concentrations of antibiotics but also shields them against phagocytosis (Trautner and Darouiche, 2004). Therefore, detection of biofilm producing strains is important for the recommendations of appropriate control measures for UPEC infections. After successful detection of biofilm producing strains, they were categorized into strong, moderate and weak producers based on their OD_{540}. Since strong and moderate biofilm producers comprised of significant population, they were compared with

virulence and resistance traits, to determine any possible correlation between biofilm production, virulence and resistance.

There was no correlation found between strong biofilm producers and virulence traits such as ESBL, MDR and antibiotic resistance phenotypes (Table 5.2 and 5.3). Although moderate biofilm producing isolates were found to have higher frequency of trimethoprim resistance (92%) as compared to other isolates (76%), the statistical difference was ($P= 0.0572$). Similarly, they had higher percentage of MDR (95%) resistant isolates as compared to other isolates (82%), albeit the difference was not statistically significant.

When compared with virulence phenotypes and genotypes, (Table 5.3) a strong correlation ($P<0.05$) was observed between strong biofilm production and both MRHA and MSHA. Other phenotypes such as hemolysin, CSH and SBR did not have any correlation with either strong biofilm or moderate biofilm producing isolates. In addition, pili encoding virulence factors such as *papA* and *papC* (<0.01) had a highly significant correlation with strong biofilm production. Another significant association of capsule protein (KpsmtII) and uropathogen specific protein (Usp) with moderate biofilm production was noted.

Table 5.1 Distribution of resistance phenotypes among strong and moderate biofilm producers.

Resistance trait	Strong (n=108)	Other (n=47)	*P value	Moderate (n=37)	Other (n=118)	*P value
ESBL	45 (42%)	20 (43%)	>0.9999	18 (49%)	47 (40%)	0.3481
MDR	86 (80%)	38 (81%)	>0.9999	34 (92%)	90 (76%)	0.0572
TMP-R	92 (85%)	30 (85%)	>0.9999	35 (95%)	97 (82%)	0.0691
CN-R	38 (35%)	13 (28%)	0.4574	8 (22%)	43 (36%)	0.1109
CAZ-R	67 (62%)	30 (64%)	0.8588	25 (68%)	72 (61%)	0.5609
CRO-R	71 (66%)	28 (60%)	0.4726	25 (68%)	74 (63%)	0.6961
LEV-R	70 (65%)	28 (60%)	0.5883	24 (65%)	74 (62%)	0.8477
CIP-R	69 (64%)	27 (57%)	0.4754	23 (62%)	73 (62%)	>0.9999

* *P* value was calculated using Fisher-exact test

Table 5.2 Distribution of virulence factors among strong and moderate biofilm producers

Virulence trait	Strong (n=108)	Other (n=47)	*P value	Moderate (n=37)	Other (n=118)	*P value
Hemolysis	43 (40%)	27 (57%)	0.0536	21 (57%)	49 (42%)	0.1304
CSH	33 (31%)	15 (32%)	0.8527	13 (35%)	35 (30%)	0.5458
SBA	90 (83%)	42 (89%)	0.4620	32 (86%)	100 (88%)	>0.9999
MRHA	31 (29%)	6 (13%)	0.0400	6 (16%)	31 (26%)	0.2713
MSHA	0	3 (6%)	0.0266	2 (5%)	1 (1%)	0.1419
fimH	108 (100%)	47 (100%)	>0.999	37 (100%)	118 (100%)	>0.9999
papA	20 (19%)	0	0.0005	0	20 (17%)	0.0041
papC	61 (56%)	14 (28%)	0.0028	13 (35%)	62 (53%)	0.0892
papEF	31 (29%)	6 (15%)	0.0713	6 (16%)	31 (26%)	0.2713
papGI	4 (4%)	2 (4%)	>0.9999	2 (5%)	4 (4%)	0.6293
papGII	50 (46%)	20 (43%)	0.7271	17 (46%)	53 (45%)	>0.9999
papGIII	4 (4%)	2 (4%)	>0.9999	2 (5%)	4 (3%)	0.6293
sfa/foc	15 (14%)	5 (10%)	0.7949	3 (8%)	17 (14%)	0.4085
afa	13 (12%)	2 (4%)	0.2349	2 (5%)	13 (11%)	0.5240
bmaE	1 (1%)	1 (2%)	0.5159	1 (3%)	1 (1%)	0.4216
fyuA	29 (25%)	8 (17%)	0.4082	8 (22%)	29 (25%)	0.8268
iutA	59 (55%)	27 (57%)	0.8607	24 (65%)	62 (53%)	0.2553
feoB	54 (50%)	22 (47%)	0.7302	19 (51%)	57 (48%)	0.8509
kpsmtII	25 (23%)	15 (32%)	0.3180	15 (41%)	26 (21%)	0.0300
kpsmtIII	4 (4%)	0	0.3151	0	4 (3%)	0.5730
usp	13 (12%)	7 (19%)	0.3161	9 (24%)	11 (9%)	0.0250
hlyA	13(12%)	5 (11%)	>0.9999	4 (11%)	14 (12%)	>0.9999
cdtB	7 (7%)	4 (9%)	0.7359	4 (11%)	7 (6%)	0.2948

* *P* value was calculated using Fisher-exact test.

Further 21 strains were selected, based on their sensitivity to all the frontline antibiotics such as trimethoprim, ceftazidime, ceftriaxone, levofloxacin, ciprofloxacin and gentamicin. These strains were further scrutinized for biofilm formation at different time intervals and *in-vitro* efficacy of trimethoprim, ceftazidime, levofloxacin and gentamicin for biofilm treatment.

5.3   *In-vitro* investigation of biofilm formation at different time points

Biofilm formation of 21 strains was monitored at different time intervals (2 h, 4 h, 10 h, 24 h) and measured by taking OD_{540} followed by crystal violet staining (Figure 5.3). Topological estimation of different biofilm stages was estimated by scanning electron microscopy (SEM) with the help of centralized resource lab (CRL), University of Peshawar. Average OD values revealed that biofilm formation started between 2 to 4 hours (initial adhesive stage) of incubation. During initial adhesive stage UPEC represented a weak biofilm formation (OD~ 0.08 to 0.11). By 10 h biofilm reached its exponential stage, almost completely covering the polystyrene surface and an average OD of ~0.157 was achieved. By 24 h it was in its plateau phase, entirely covering the polystyrene surface and an average OD of ≥0.2 was attained depending upon whether the strain is moderate or strong biofilm producer.
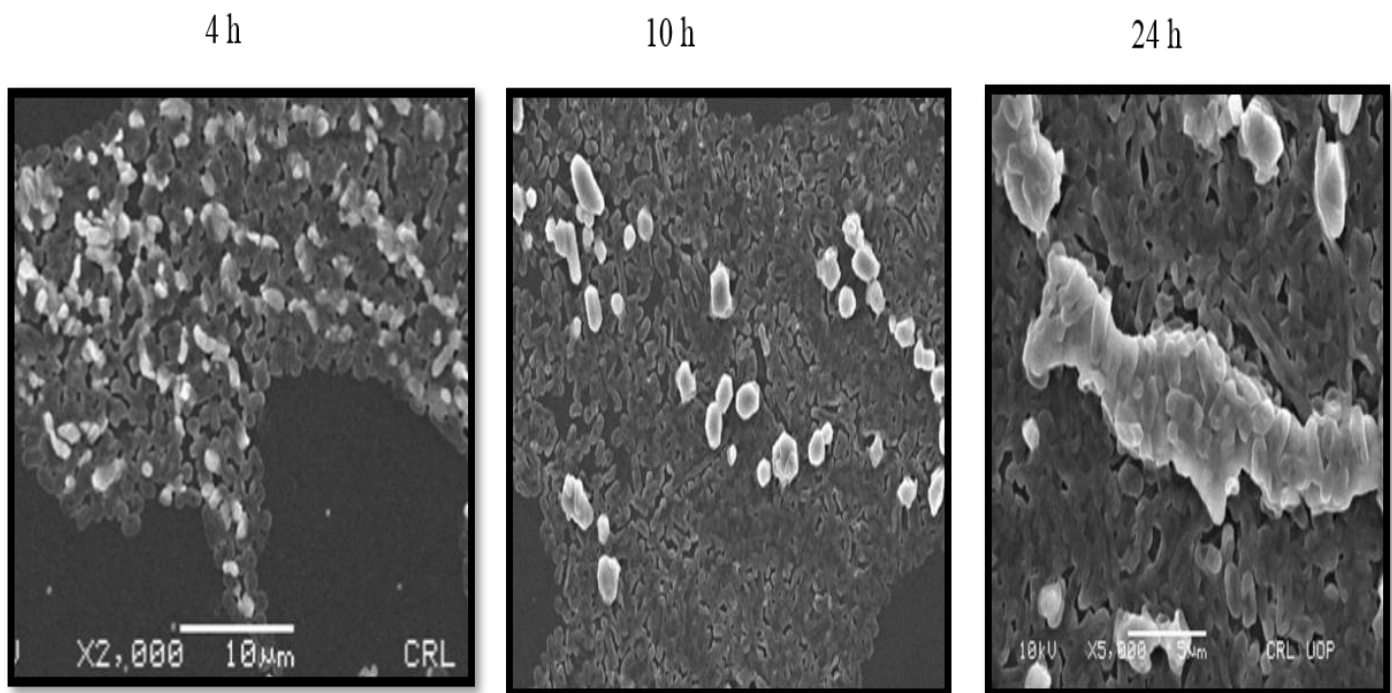
Figure 5.3 Development of biofilm at different time intervals as shown by SEM

SEM micrograph shows early development of biofilm at 4 h, the biofilm is patchy and extracellular matrix can be seen (gray) **(left)**, biofilm at 10 h almost covered the entire surface **(middle)**, at 24 h biofilm is seen entirely covering the surface and extracellular matrix (gray) can be seen coating the bacterial cells **(right)**.
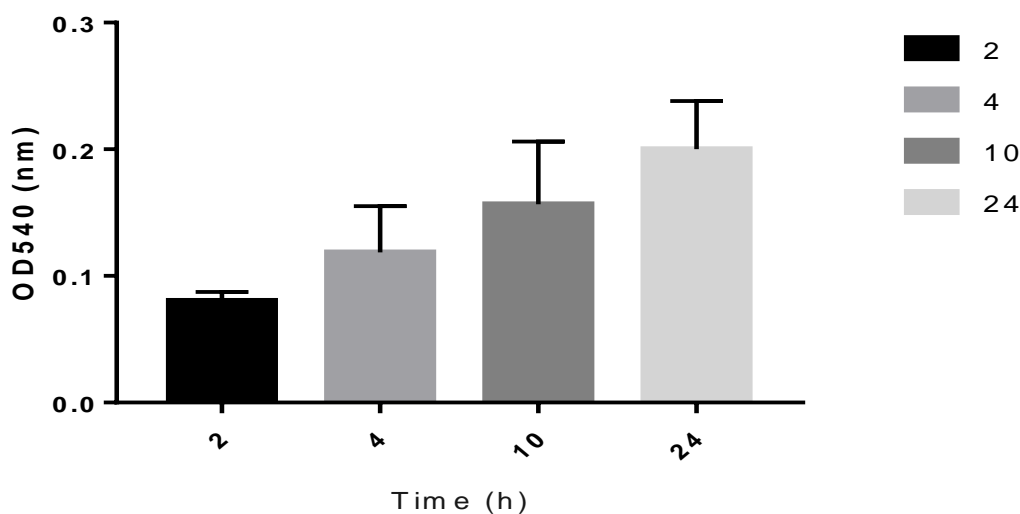
Figure 5.4 Average ODs of 21 UPEC strains as estimated by OD540 at different time points.

Bar graph shows weak biofilm formation at 2 and 4 h (OD~ 0.08 to 0.11), moderate biofilm formation at 10 h (OD~0.157) and mature biofilm at 24 h (OD~0.20). Error bars show SD from the mean value of all 21 strains.

5.4   Difference in MIC of planktonic (MIC-p) and biofilm (MIC-b) forms of UPEC isolates

All the 21 strains were subjected to MIC-p and MIC-b to determine the efficacy of antibiotics against the planktonic and biofilm forms of UPEC (Table 5.4 and 5.5). In case of ceftazidime the isolates had MIC-p ≤ 0.125 to 16 µg/ml, indicating the effectiveness of ceftazidime against the selected susceptible strains. Similarly, levofloxacin had the MIC-p in range of 0.125 to 8 µg/ml and gentamicin, trimethoprim each in the range of 0.125 to 16 µg/ml. When compared to MIC-b, the values were much higher as compared MIC-p for all the strains. Ceftazidime was observed to undergo a ~100 to 1000 times increase in values (MIC-b; 128 to >1024 µg/ml) as compared to MIC-p. Similarly, gentamicin and trimethoprim observed 8 to 1000 times increase in their MIC-b values (64-1024 µg/ml). Levofloxacin had relatively better efficacy against biofilm inhibition with MIC-b 32 to 64 µg/ml. Our results indicate levofloxacin has the

potential of inhibiting biofilm formation. In addition, our results suggest that ceftazidime failed

to inhibit biofilm formation even at higher concentrations 2048 µg/ml, while gentamicin (MIC-

b, 64 to 1024 µg/ml) and trimethoprim (MIC-b, 256 to 1024 µg/ml) are shown to have modest

effect on biofilm inhibition.

Table 5.3 Minimum inhibitory concentration of planktonic (MIC-p) and minimum inhibitory concentration of biofilm (MIC-b) of ceftazidime, levofloxacin and gentamicin against UPEC strains. Values represent means of at least two independent experiments.

Sample ID.	MIC-p			MIC-b		
	Ceftazidime	**Levofloxacin µg/ml**	**Gentamicin µg/ml**	**Ceftazidime**	**Levofloxacin µg/ml**	**Gentamicin µg/ml**
2	16	1	16	>2048	32	1024
3	0.125	0.125	8	>2048	32	1024
9	0.125	0.125	1	>2048	32	512
22	0.125	0.125	1	512	32	1024
33	16	4	16	>2048	32	1024
34	0.125	4	0.25	>2048	32	128
47	0.125	0.125	0.125	128	32	512
49	16	8	4	>2048	32	256
63	0.125	8	8	>2048	32	256
68	0.125	0.25	0.5	128	32	64
69	16	8	1	256	32	512
72	4	8	4	128	32	64
74	0.125	0.125	16	>2048	32	128
81	16	2	16	128	64	256
105	4	0.125	16	512	32	256
107	8	0.125	16	>2048	64	1024
117	<0.125	0.125	16	1024	64	128
120	<0.125	0.125	1	1024	32	128
161	16	2	8	2048	32	256
168	4	4	16	1024	32	256
176	<0.125	0.25	0.5	1024	32	256

Table 5.4 Minimum inhibitory concentration of planktonic (MIC-p) and minimum inhibitory concentration of biofilm (MIC-b) of trimethoprim against UPEC strains.

Sample ID	MIC-p (µg/ml)	MIC-b (µg/ml)
2	0.125	1024
3	2	256
49	1	1024
63	16	1024
68	16	1024
69	1	1024
105	1	1024

MIC-p; Minimum inhibitory concentration of planktonic cells, MIC-b; Minimum inhibitory concentration of biofilm, µg/ml; Microgram per milliliter

CHAPTER 6:   **Impact of iron and iron acquisition systems on the pathogenesis of UPEC**

6.1   Effect of iron on growth capacity

Altogether, a total of twenty UPEC strains were selected based upon their high virulence score and multidrug resistance. In order to check their growth efficacy under different iron conditions, they were subjected to growth in iron-deficient (without any addition of iron) and iron-sufficient (10 µM and 20 µM) solid and liquid M9 minimal medium.

6.1.1   Growth on solid medium

There was a significant difference in growth of the isolates in iron deficient and sufficient (10 µM) medium. After 24 and 48 h of incubation, it was observed that strains under iron restricted conditions had relatively weak growth. Their colony size was much smaller as compared to their counterparts grown in iron-sufficient medium.

6.1.2   Growth in liquid medium

In a similar fashion, these strains were grown in M9 liquid medium. The optical density (OD_{600}) of the strains at 0 h was ~0.01, which gradually increased after with time of incubation. The strains grown under iron restricted conditions were noted to have significantly lower growth as compared to iron-sufficient conditions. Statistical analysis of the average rate of growth of all the 20 strains showed that the presence of iron had significant effect ($P<0.01$) on the growth of these strains (Figure 6.1).
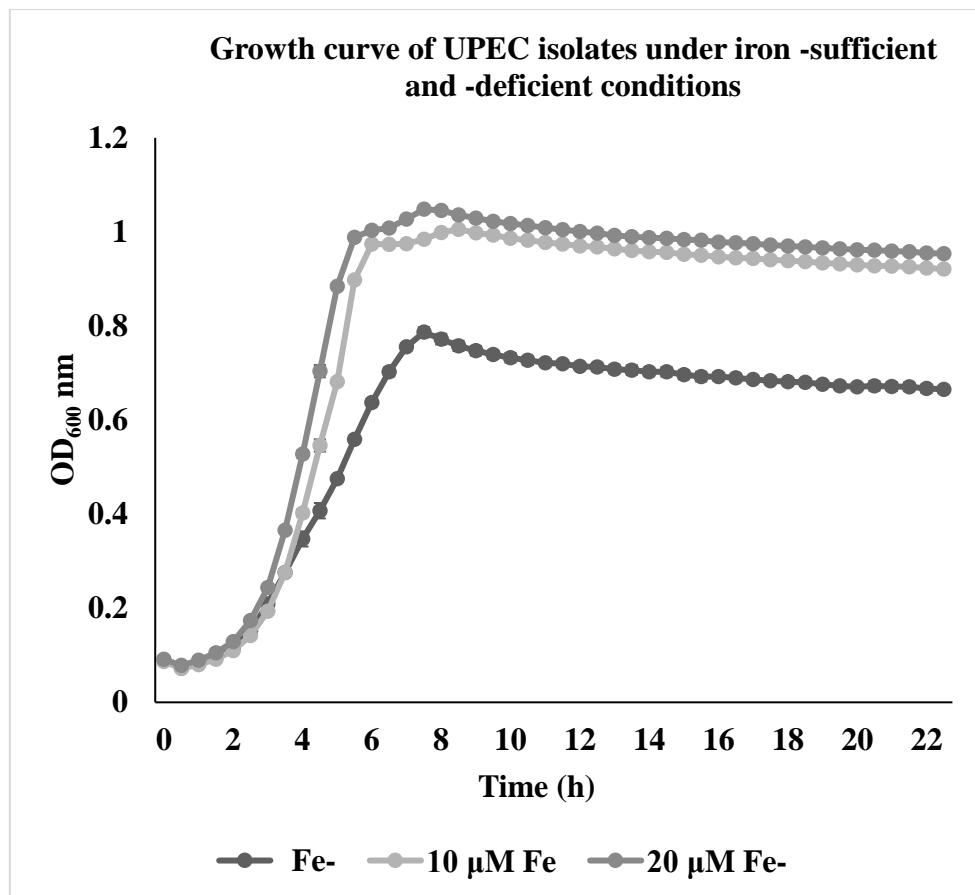
Figure 6.1. Growth curve showing an overall growth trend for all the selected 20 UPEC strains.

Strains show significantly better growth with iron-sufficient conditions in comparison to iron-deficient conditions. Values represented here are average of at least two experiments performed in duplicates. Error bars represent SD deviation of repeats.

6.1.3   Siderophore detection assay

The CAS agar assay showed that most of UPEC isolates produce siderophores under iron restricted conditions. No evidence of siderophore production was found in the strains grown under iron-sufficient M9 liquid medium. Moreover, it was observed that siderophore production starts at mid-log phase (after 5 h of incubation), no evidence of siderophore was found in primary-log phase (1-3 h). Based on size of zone, it was found that maximum siderophore production was during stationary phase (9-15 h), with a slight decrease in size after 24 h of incubation.

Out of the 20 strains tested for siderophore production, 19 (95%) produced siderophores, whereas 1 (5%) strain did not show any evidence of siderophore production. Amongst the 19 siderophore-producing strains, 17 were found to be strong siderophore producers with a maximum zone size between 15-20 mm while two were found to be moderate siderophore producers with a maximum zone size between 10-14 mm (Table 6.1).
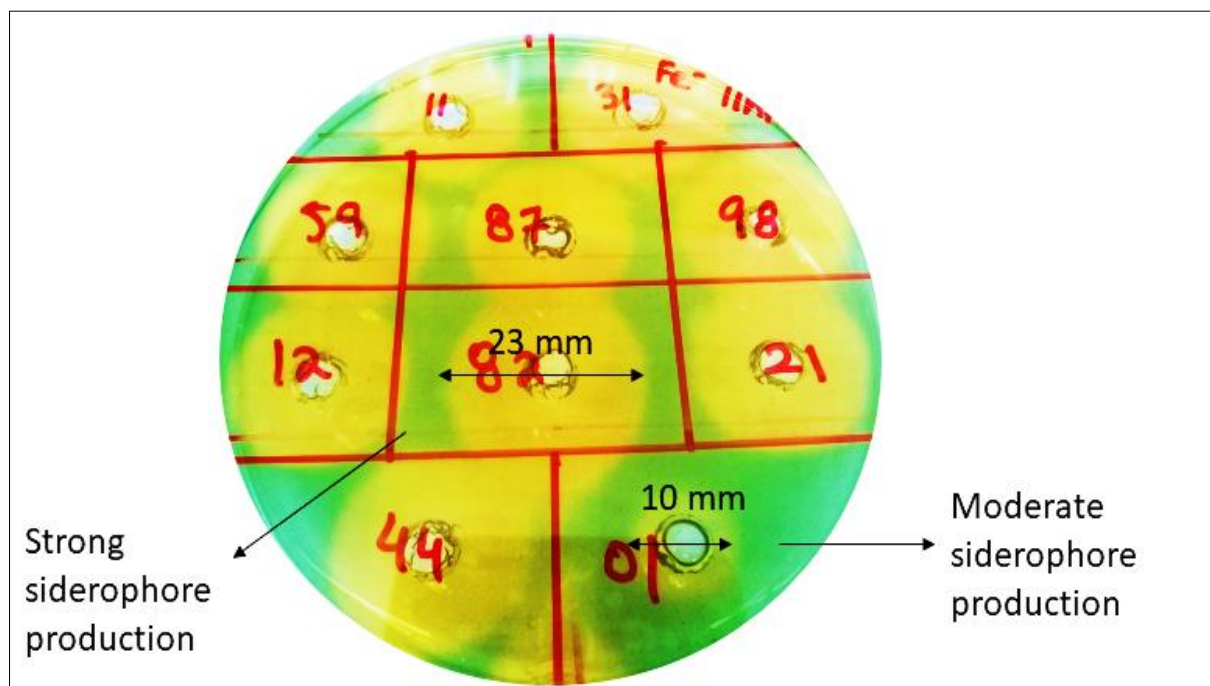
Figure 6.2 Siderophore production on CAS plates

Figure shows siderophore production and zone size among UPEC isolates. Arrows represent strain UEC82 (23mm) and UEC 01 (10mm) with the strong and moderate siderophore production.

Table 6.1 Pattern of siderophore production and zone diameter (mm) among 20 UPEC isolates

Sample ID	1hr	3hr	5hr	7hr	9hr	11hr	13hr	24hr
UEC11	0	0	13.5	15.00	17.00	17.50	17.50	18.50
UEC31	0	0	14.5	16.00	18.50	19.50	17.50	17.50
UEC59***	0	0	12.5	13.50	16.00	19.00	16.00	19.00
UEC87	0	0	13	13.50	16.00	18.50	16.50	18.50
UEC98	0	0	12	12.50	15.50	17.00	16.00	14.50
UEC12	0	0	12	14.00	15.00	18.00	17.00	17.00
UEC82***	0	0	16	17.50	19.50	20.50	20.00	20.50
UEC21	0	0	12.5	14.50	19.00	19.00	18.00	17.00
UEC44	0	0	13.5	12.00	15.00	16.50	14.00	16.00
UEC01**	0	0	7.50	8.5	10.00	9.00	6.50	0.00
UEC06	0	0	9.5	15.00	17.50	17.00	17.00	16.50
UEC15	0	0	11.5	17.00	19.00	18.00	17.50	15.50
UEC51	0	0	11.5	17.50	18.50	19.00	18.00	15.50
UEC14	0	0	12.5	18.00	20.50	19.00	18.00	16.00
UEC81	0	0	6	13.50	16.50	11.50	10.50	6.00
UEC38	0	0	12.5	17.50	19.50	19.00	17.50	15.50
UEC175**	0	0	0	8.00	14.00	11.00	9.50	0.00
UEC16	0	0	12	18.00	20.50	19.50	19.00	17.50
UEC85	0	0	10	16.00	17.50	18.00	8.00	16.50
UEC157*	0	0	0	0.00	0.00	0.00	0.00	0.00

Note: *** Strong, **moderate, *no/weak siderophore production.

Once it was confirmed that most of the isolates produced a siderophore, the next step was to determine the chemical type of the siderophore produced by UPEC isolates.

6.1.4   Arnow's assay for the detection of catecholates

Arnow's assay was used to detect catecholates type siderophores. Supernatants obtained without iron and with higher iron conditions together with uninoculated controls were tested. The supernatant obtained under higher iron condition and uninoculated media control showed no change in colour (Figure 6.3). While the supernatant obtained under iron deprived conditions turned out to be pink/red in color, that was measured at OD 500 nm, confirming presence of catechol-type siderophore. The intensity of color was measured at 500 nm using SpectraMax® Plus 384 Microplate Reader (Figure 6.4). All the siderophore-positive 19 isolates were also positive for catecholates, while the one strain that showed weak/no siderophore activity remained colorless and hence negative for catecholates.
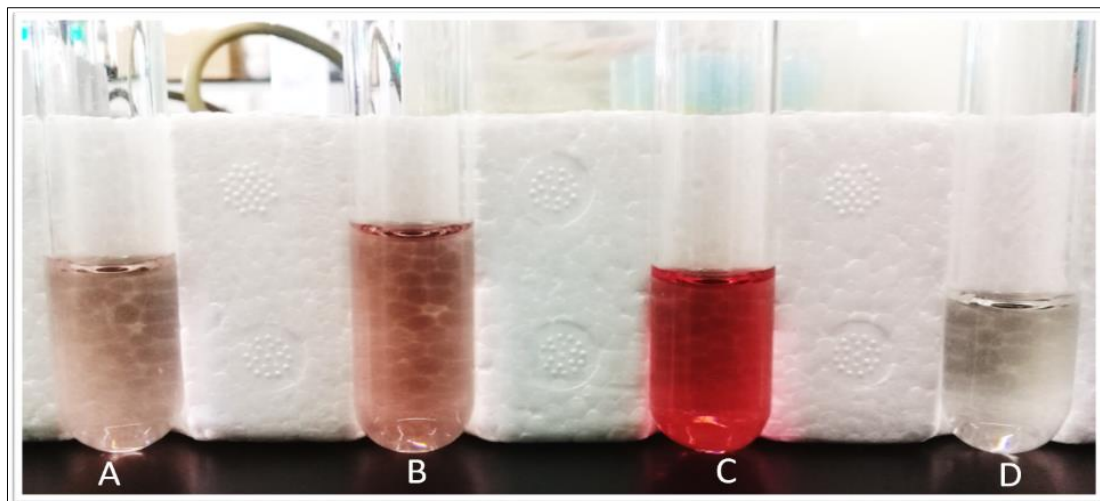
Figure 6.3 Catecholate detection by Arnow's assay.

Figure shows Arnow's assay for catecholates production over time **A**: After 7 h; **B**: 9 h; **C** 11h; **D** media control. An increase in color intensity (catecholates production) can be seen with time.
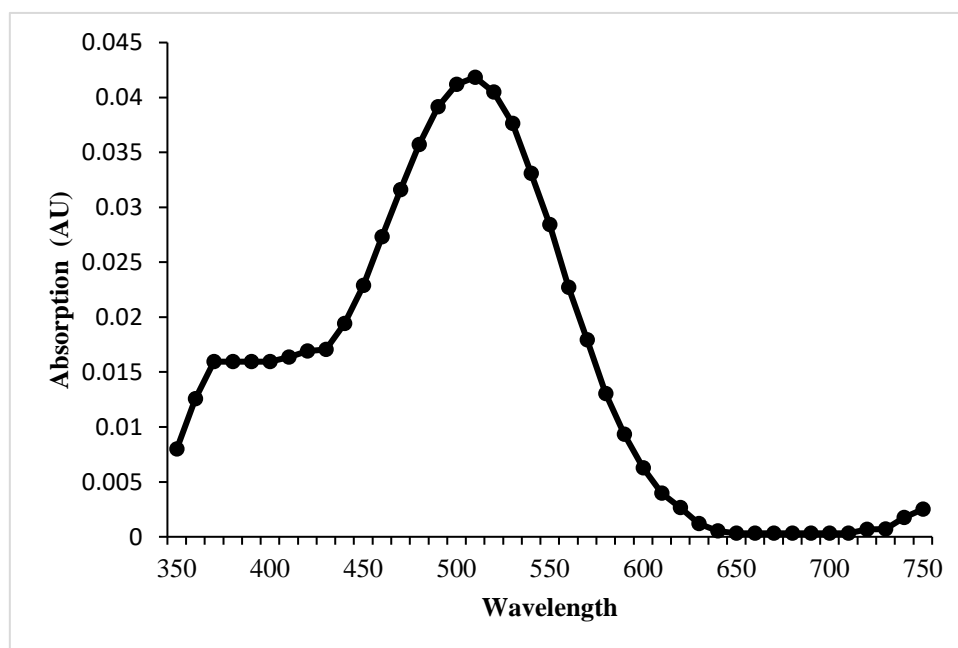
Figure 6.4 Absorption spectrum for catecholates detection.

Graph shows maximum absorption at 510 nm.

6.1.5   Atkin's assay for the detection of hydroxamates

Hydroxamate-type siderophores were detected using Atkin's assay. Of the 19 siderophore-positive strains, 17 strains were hydroxamate positive indicating hydroxamate production,

whilst 2 strains showed no sign of hydroxamates. A color change from colorless to orange-pink was considered positive for hydroxamates production (Figure 6.5). The intensity of color was measured at 480 nm using SpectraMax® Plus 384 Microplate Reader (6.6). Interestingly the strains which were found negative for hydroxamates production had the moderate zone size by CAS assay. The one strain that showed weak/no siderophore activity remained colorless and hence negative for hydroxamates as well.
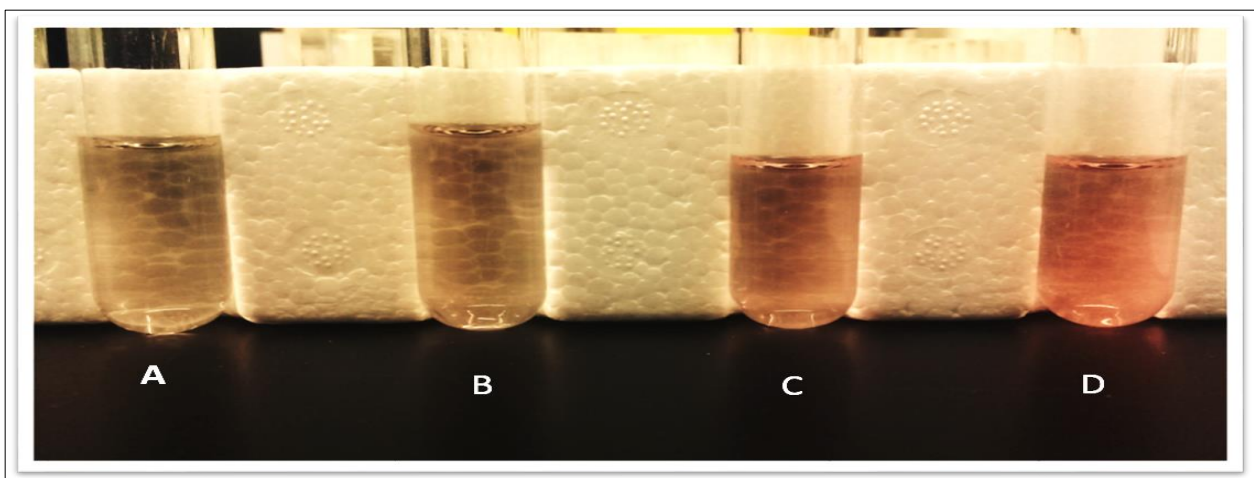
Figure 6.5 Hydroxamates detection by Atkin's assay.

Figure shows Atkin's assay for hydroxamates production over time **A**: media control; **B**: 3 h; **C** 5 h; **D** 7 h. An increase in color intensity (hydroxamate production) can be seen with time.
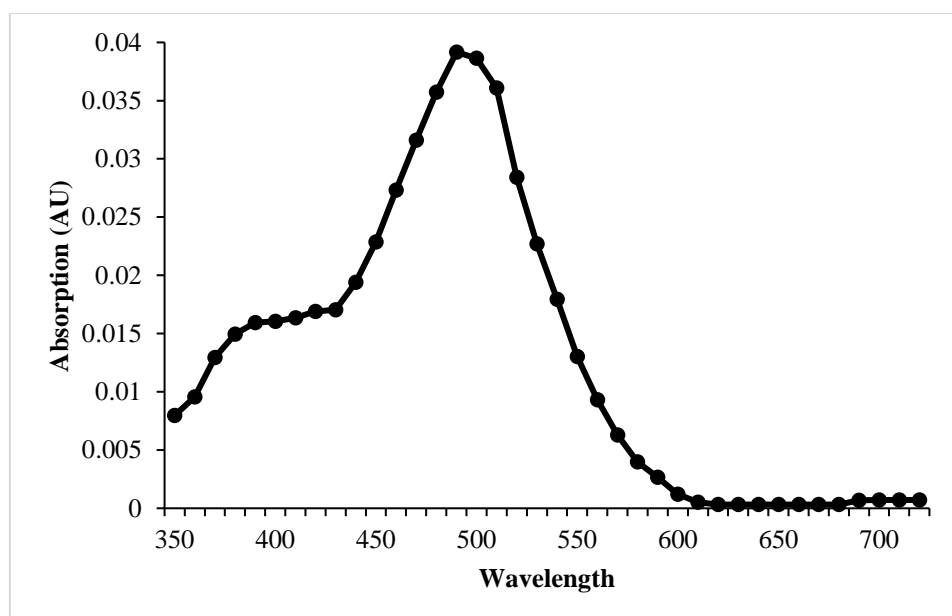
Figure 6.6 Absorption spectrum for hydroxamates detection.

Graph shows maximum absorption at 480 nm.

6.1.6   Correlation between siderophore production and type of siderophores

There was a direct correlation seen between zone size and siderophore production (strong, moderate and weak/non-siderophore producers). Strains UEC01 and UEC175 being moderate producers (zone size < 15mm) were found positive only for one kind of siderophore i.e., catecholates. There was no evidence found for hydroxamate production when detected by Atkin's assay. In addition, UEC157 was found negative for both catecholates and hydroxamates (Table 6.2). Whole genome analysis also confirmed our results, strains UEC59, UEC82 the strong siderophore producers encoded all the three siderophores (enterobactin, aerobactin and yersiniabactin), while the strains UEC01, UEC175 the moderate siderophore producers were found to encode two siderophores (enterobactin and yersiniabactin), while the strain UEC157 which showed a very weak or no zone on CAS plate was found to encode only enterobactin (Table 6.3).

Table 6.2 Siderophore production and the respective types as determined by Arnow's and Atkin's assays.

Sample ID	Zone size (mm)	Catecholate production	Hydroxamate production
UEC11	18.50	+ive	+ive
UEC31	19.50	+ive	+ive
UEC59	19.00	+ive	+ive
UEC87	18.50	+ive	+ive
UEC98	17.00	+ive	+ive
UEC12	18.00	+ive	+ive
UEC82	20.50	+ive	+ive
UEC21	19.00	+ive	+ive
UEC44	16.50	+ive	+ive
UEC01*	10.00	+ive	-ive
UEC06	17.50	+ive	+ive
UEC15	19.00	+ive	+ive
UEC51	19.00	+ive	+ive
UEC14	20.50	+ive	+ive
UEC81	16.50	+ive	+ive
UEC38	19.50	+ive	+ive
UEC175*	14.00	+ive	-ive
UEC16	20.50	+ive	+ive
UEC85	18.00	+ive	+ive
UEC157**	0	-ive	-ive

Table 6.3 Genome annotation indicates presence of the iron acquisition systems encoded by the five UPEC strains.

Sample ID	Siderophore production	Enterobactin	Yersiniabactin	Aerobactin	Heme uptake system	Other iron uptake systems
UEC59	Strong	Yes	Yes	Yes	Yes	Efe, Feo
UEC82	Strong	Yes	Yes	Yes	Yes	Efe, Feo
UEC01	Moderate	Yes	Yes	No	Yes	Efe, Feo
UEC175	Moderate	Yes	Yes	No	Yes	Efe, Feo
UEC157	Weak/No	Yes	No	No	No	Efe, Feo

6.2   Infection of urothelial cell lines

This experiment aims to infect urothelial cell lines under a range of iron regimes, to determine the any differences in infection capacity. The effect of bacterial growth under high and low iron conditions was tested, as well as the impact of siderophore production capacity.

Five strains were selected for invasion assays (as highlighted in Table 6.2 and 6.3), exhibiting strong, moderate and no siderophore production, to determine if there is any difference in their capacity to adhere to and invade host cells. A range of iron conditions were given to each of the five strains.

6.2.1   Low-Low iron

In this condition all the 5 strains were grown in iron deficient M9 minimal media and the invasion assays were executed on cell lines grown in iron deficient RPMI 1640. UEC59 and UEC82 (strong siderophore producers) were able to affectively invade the host cell lines (Figure 6.7). While in case of UEC01 and UEC175 (moderate siderophore producers) only a

small number of bacteria were able to invade the cells. UEC157 (apparently a weak/non-siderophore producer) seemed unable to invade the cell lines.

6.2.2 High-low iron

Under high-low condition strains were grown in iron-sufficient conditions (10 µM Fe) and the invasion assays were assays were executed on cell lines grown in iron deficient RPMI 1640. UEC59 and UEC82 (strong siderophore producers) were able to affectively invade the host cell line and there was significant increase in bacterial count under high-low condition as compared to their counter parts grown under low-low iron conditions ($P \leq 0.001$ and $P \leq 0.05$, for UEC59 and UEC82 respectively). In case of UEC01 and UEC175 only a small number of bacteria were able to invade, without any significant impact of increased iron concentration on them. UEC157 was found unable to invade the cell lines.

6.2.3 Low-high iron

In low-high concentration all the 5 strains were grown in iron deficient M9 minimal media and the invasion assays were executed on cell lines grown in iron-sufficient (10 µM Fe) RPMI 1640. UEC59 had an increase bacterial count in comparison to low-low and high-iron conditions ($P \leq 0.05$) as evident from Figure 6.7. Bacterial uptake of UEC82 also increased under low-high conditions as compared to low-low iron condition ($P \leq 0.05$), however there was no significant increase found between high-low and low-high iron concentrations. Increase in iron concentration seemed to have no effect on invasion potential of UEC01, UEC175 and UEC157.

6.2.4   High-high iron

Under high-high condition strains were grown in iron-sufficient conditions (10 µM Fe) and the invasion assays were assays were executed on cell lines grown in iron sufficient (10 µM Fe) RPMI 1640. UEC59 appeared to have an increase in the bacterial load with increasing iron concentration and was able to invade more effectively with an increase of 10-fold as compared to low-low iron concentration ($P \leq 0.01$) and 5-fold as compared to high-low iron concentration ($P \leq 0.05$). In a similar fashion UEC82 observed a 8-fold ($P \leq 0.05$) increase in bacterial count as compared to low-low iron concentration. Although there was a plausible increase in bacterial count in UEC01, UEC175 and UEC157 strains under high-high iron but none of the strains had statistically significant value ($P > 0.05$).
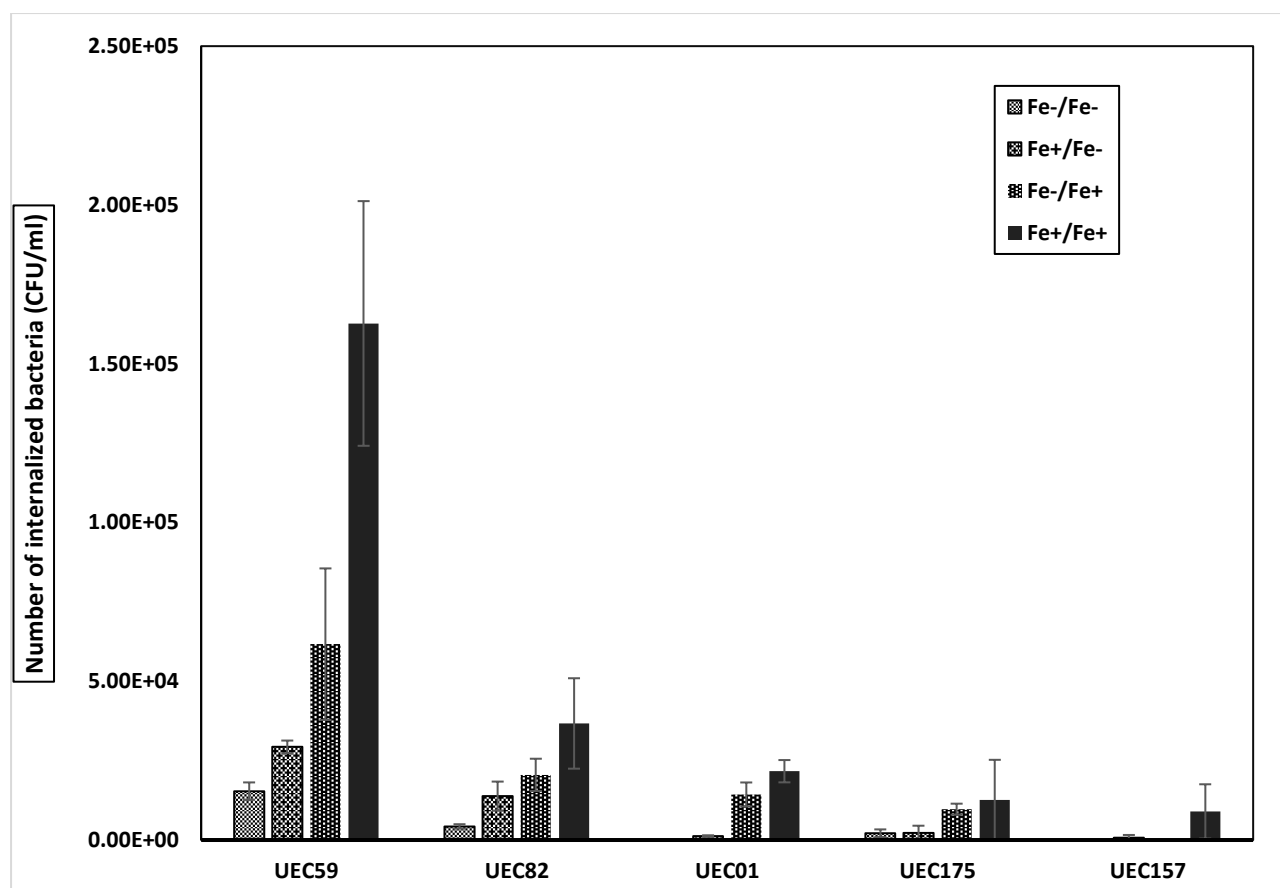
Figure 6.7 Invasion rate of UPEC strains under low-low (Fe-/Fe-), high-low (Fe+/Fe-), low-high (Fe-/Fe+), high-high (Fe+/Fe+) iron regimes, inside bladder epithelial cell lines ATCC HTB-9 (5736).

UEC59 and UEC82 (strong siderophore producers) are seen effectively invading bladder cell lines with a significant increase (5-10 folds) in bacterial count under "iron sufficient conditions" as compared to "low-low iron conditions". Whereas UEC01, UEC175 (moderate siderophore producers) and UEC157 (weak/non-siderophore producer) were found unable to invade the cell lines in low-low iron conditions, however a plausible increase in bacterial count could be seen in them when grown under iron sufficient conditions. UEC157 (a non-siderophore producer) seems to have 10 times lower intracellular bacterial count as compared to the strong siderophore producing strains even under high-high iron concentration.

6.3   Construction of *ΔentBEC, ΔhemRT, Δirp1_2* and *ΔiucABCD* mutants in UEC59

As described in methodology prior to gene KO, *cat* cassette carrying almost 60 bp homologous sequence of the targeted genes were amplified using PCR. After successful amplification of PCR, the PCR products were run in 0.8% agarose gel. Expected amplicon size of *cat* cassette for each of the above genes was 1193bp (~ 1.2 kb) as shown in Figure 6.8. PCR products were then purified using Thermo Scientific™ GeneJET PCR Purification Kit. The concentration of DNA was measured using NanoDrop®ND-1000 spectrophotometer and recorded (Table 6.4). The results show high quality and quantity of these PCR products which is the prerequisite of successful KO.

After successful amplification of *cat* cassette UEC59 was transformed with pACBSR-*hyg* as described previously (section 3.13.4), selected transformant was then inoculated in 10ml of low salt L-broth supplemented with 200 µg/ml of hygromycin and incubated at 37 °C in a shaker incubated at 180 RPM. Following day culture pellet was harvested and plasmid mini-prep was performed to ensure the transformation of UEC59 with pACBSR-*hyg*. Wild type UEC59 was used as control. Plasmid was visualized on 0.8% agarose gel. Transformants were found to have an extra plasmid (7660 bp) as compared to the wild type as evident in Figure 6.9. This confirms successful transformation of UEC59 with pACBSR-*hyg* a plasmid required for recombination event to generate mutants. Following successful transformation of UE59 (with pACBSR-*hyg* plasmid), *cat* cassette was electroporated as described in section 3.13.5.

6.3.1   Genotypic confirmation of *ΔentBEC, ΔhemRT, Δirp1_2* and *ΔiucABCD* mutants

All the four mutants were confirmed genotypically by using confirmation PCR. Mutants with correct insertion of *cat* cassette were expected to have PCR product of ~1.5kb this being the *cat* cassette plus the gene fragments adjacent to the gene of interest amplified by confirmation

140

primers. Whilst the WT of these genes were expected to have a 4009 bp, 3909 bp, 16015 bp and 6035 bp for *entBEC, hemRT, irp1_2* and *iucABCD*, the size being the gene of interest plus the gene fragments adjacent to the gene of interest amplified by confirmation primers. The amplicons were visualized on 0.8% agarose gel. All the WT amplicons, as expected were much larger in size as compared to the mutants (Figure 6.10), confirming the correct insertion of the *cat* cassette and deletion of gene of interest (s).
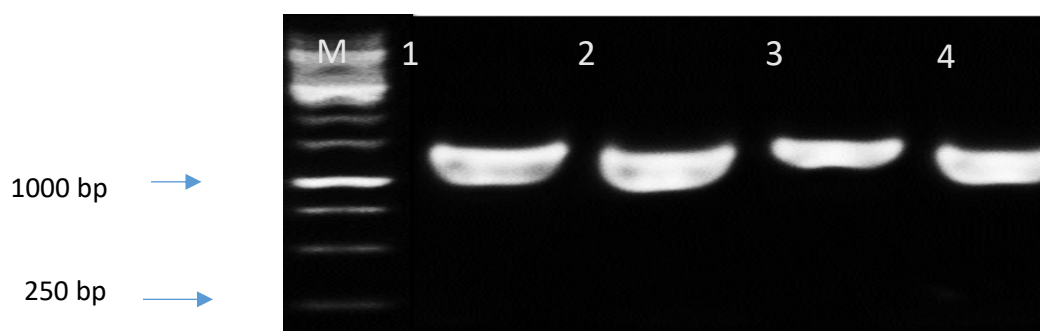
Figure 6.8 PCR amplification of *entBEC, hemRT, irp1_2* and *iucABCD* and their visualization on 0.8% agarose by gel electrophoresis.

M, GeneRulerTM 1kb ladder; lanes 1-4, *entBEC, hemRT, irp1_2* and *iucABCD* respectively each giving a product size of ~1.2kb.

Table 6.4 Concentration of amplicons' DNA using NanoDrop®ND-1000 spectrophotometer at 230 nm.

Amplicon	Concentration ng/ μl
entBEC	64.5
hemRT	73.7
irp1_2	53.7
iucABCD	102.6
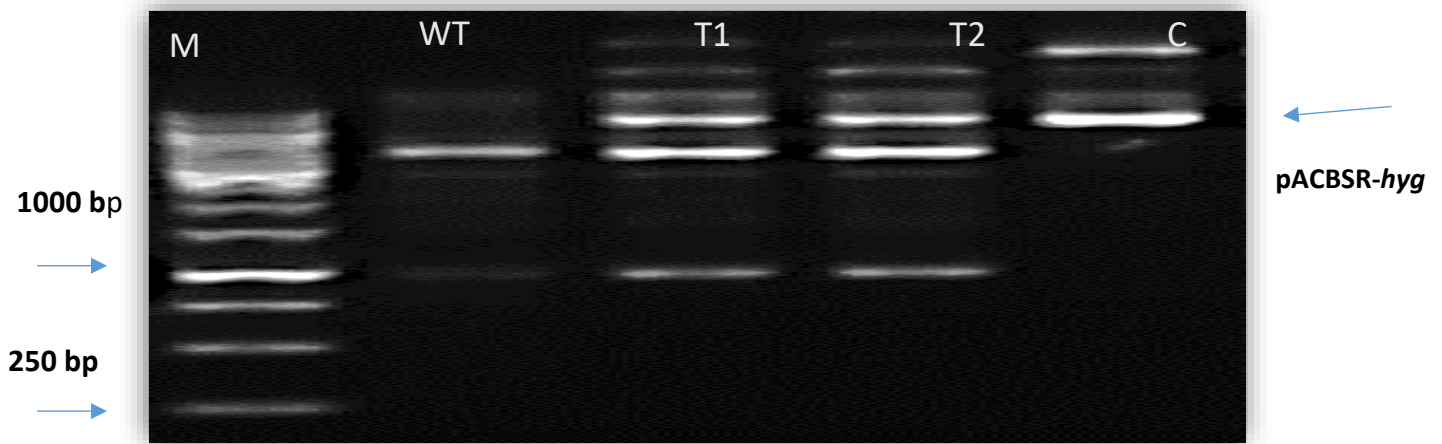
Figure 6.9 Agarose gel (0.8%) electrophoresis of plasmids extracted from WT UEC59 and UEC59 transformants with pACBSR-*hyg*.

Shows (L-R) M: GeneRuler^{TM} 1kb ladder, WT: WT UEC59 carrying intrinsic plasmids but not pACBSR-*hyg*, T1 and T2: transformants 1 and 2 with additional plasmids other than the intrinsic plasmids carried by UEC59, C: pACBSR-*hyg* plasmid run as a control
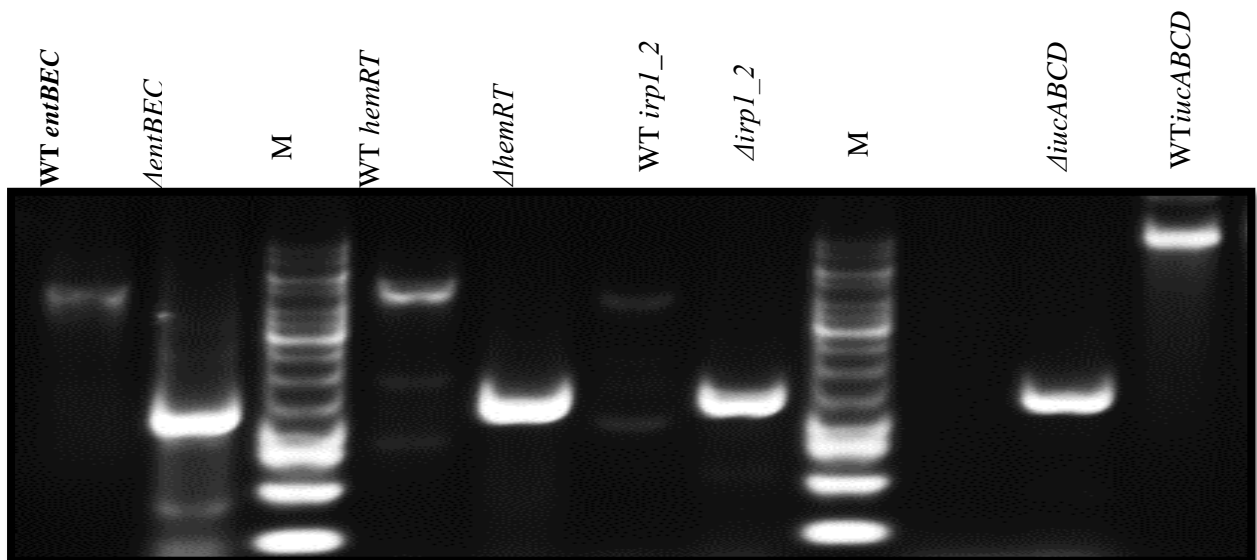
Figure 6.10 PCR amplification of *ΔentBEC, ΔhemRT, Δirp1_2, ΔiucABCD* and their WT counterparts.

PCR amplification of Δ*entBEC,* Δ*hemRT,* Δ*irp1_2,* Δ*iucABCD* and their WT counterparts; visualization on 0.8% agarose by gel electrophoresis. One can clearly see the size in gene fragment of mutants (~1.5kb) and the WT genes, whereas M is GeneRuler^{TM} 1kb ladder.

6.3.2   Phenotypic confirmation of mutants

In order to phenotypically confirm gene knock out and the relative effect of each mutation on siderophore production, all the four mutants Δ*entBEC*::*cat,* Δ*hemRT*::*cat,* Δ*irp1_2*::*cat* and Δ*iucABCD*::*cat* were subjected to CAS plate assay. Mutants were grown in 50 ml of iron deficient and iron sufficient (10 µM) M9 medium. Optical density was measured after every 2 hours and ~ 2 ml of supernatant was collected for CAS plate assay for siderophores detection, followed by downstream assays for catecholate (Arnow's) and hydroxamate (Atkin's) detection. While growth curves (Figure 6.11 and 6.12) showed that there is no significant difference between WT and the respective mutants, under both "iron-deficient and -sufficient" conditions, possibly because the multiple iron-acquisition systems are redundant such that absence of one type can be compensated by other type. Thus, it can be presumed that since each of the strains were mutated for one type of iron-acquisition systems out of four, the three remaining systems are sufficient enough to overcome this inability under the conditions tested. However, it should be noted that the medium used lacks a source of heme such that the effect of the *hemRT* mutation was not really tested.

In addition, in the CAS assay, siderophore production was enhanced after the late log phase (after 6 h) and continued to increase up to a plateau phase at 24 h Moreover, WT UEC59 was found having maximum zone size about an average of ~17 mm, followed by *Δirp1_2 and ΔhemRT* each having a zone size of ~15 mm, followed by *ΔentBEC* with a zone size of ~14 mm as compared to WT ($P<0.01$). However, *ΔiucABCD* was found to have least zone size of ~12 mm as compared to WT ($P<0.001$), suggesting that enterobactin and aerobactin hold key role in iron-acquisition in case of UPEC (Figure 6.14).
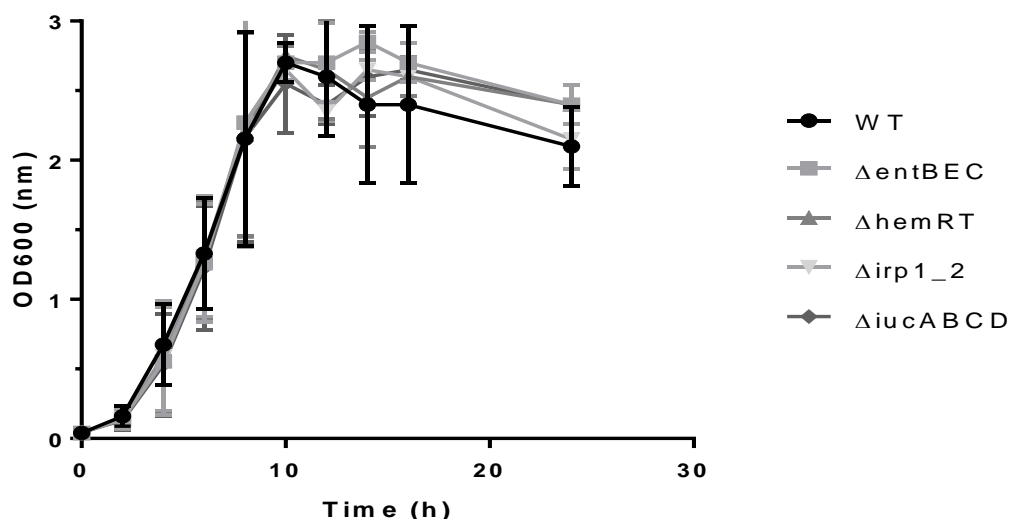
Figure 6.11 Effect of *ΔentBEC, ΔhemRT, Δirp1_2* and *ΔiucABCD* on UEC59 growth in minimal medium without iron.

Strains were grown aerobically in MM containing 0.4%-glucose, using 50-ml medium in 250-ml flasks (37°C, 180 RPM). Values presented are average of at least two independent growth experiments. Growth was measured after every 2 hours. Error bars represent standard deviation from mean value.
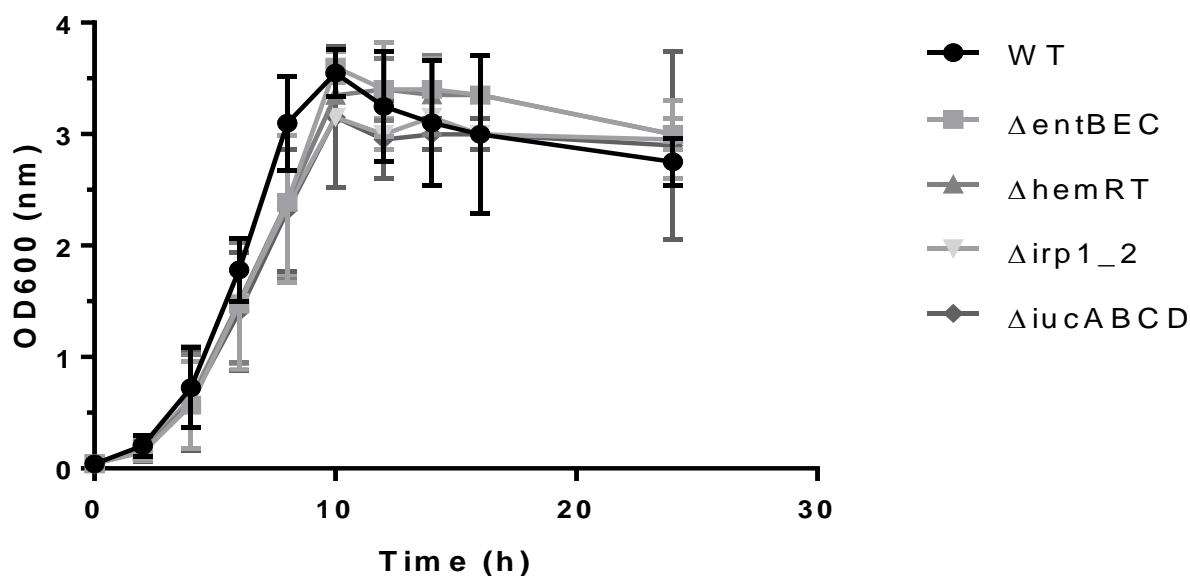
Figure 6.12 Effect of *ΔentBEC, ΔhemRT, Δirp1_2* and *ΔiucABCD* on UEC59 growth in minimal medium with iron.

Strains were grown aerobically in MM containing 0.4%-glucose with 10 µM ferric citrate, using 50-ml medium in 250-ml flasks (37°C, 180 RPM). Values presented are average of at least two independent growth experiments. Growth was measured after every 2 hours. Error bars represent standard deviation from mean value.

144
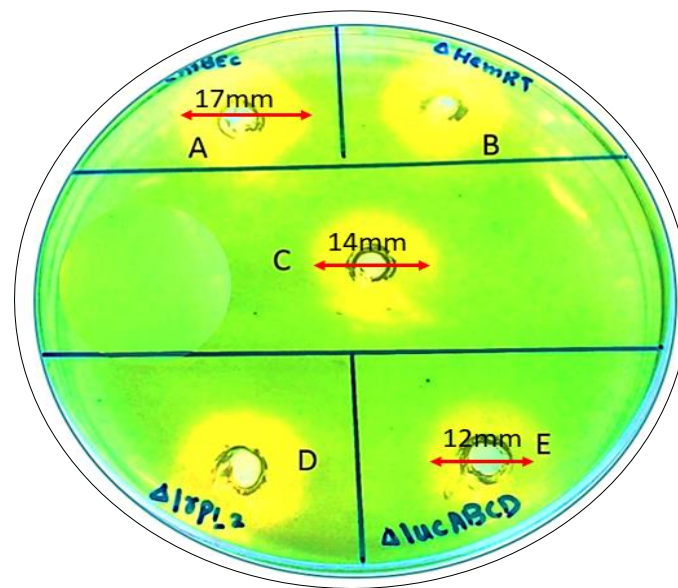
Figure 6.13 CAS assay shows siderophore production on a CAS plate.

The plate shown is after 14 hours of growth. Golden halo around the wells shows the binding of iron by siderophores. *ΔentBEC* (C) and *ΔiucABCD* (E) have lower zone sizes as compared to WT (A), *ΔhemRT* (B) and *Δirp1_2* (D)
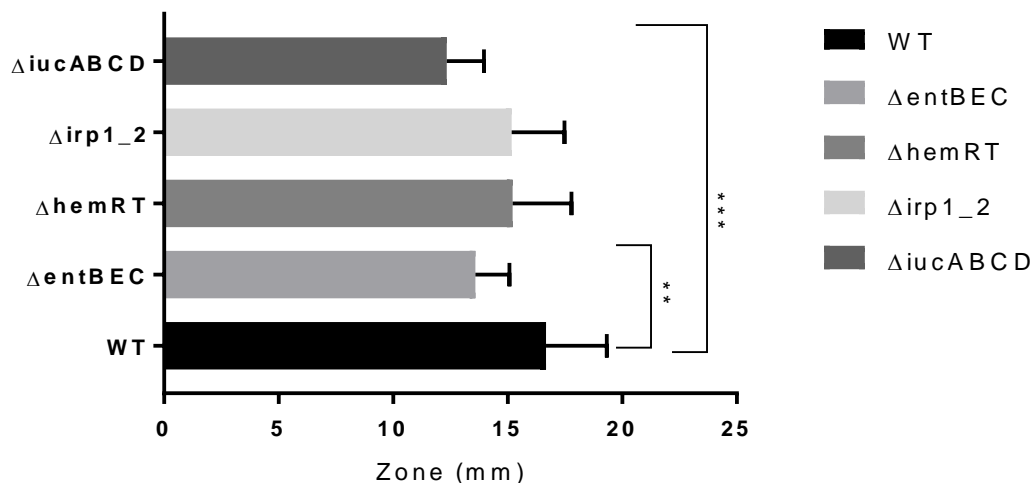
Figure 6.14 : Differences in zone sizes of WT, *ΔentBEC, ΔhemRT, Δirp1_2* and *ΔiucABCD* on CAS agar plate.

Graph shows WT with maximum siderophore production with a mean zone size of 17mm, *ΔentBEC* and *ΔiucABCD* with least siderophore activity (mean zone size, 13.5mm and 12.3 mm respectively). Error bars represent standard deviation from mean value. *P* values were calculated by t- test (non-parametric), using GraphPad Prism version 7©.

Arnow's assay was performed to ensure deletion of enterobactin synthesis genes (*entBEC*). *ΔentBEC* was found negative for catecholates production, as compared to its WT (Figure 6.15). As expected, other mutants *ΔhemRT, Δirp1_2* and *ΔiucABCD* were also positive for catecholates production validating the fact that all the targeted siderophore biosynthesis pathways are independent of each other. The phenotypic negative result for enterobactin for *ΔentBEC* further endorses the correct mutant production. Atkin's assay was performed to confirm deletion of aerobactin synthesis genes (*iucABCD*). As expected, *ΔiucABCD* was the only phenotype negative for hydroxamate (aerobactin production) test (Figure 6.16).
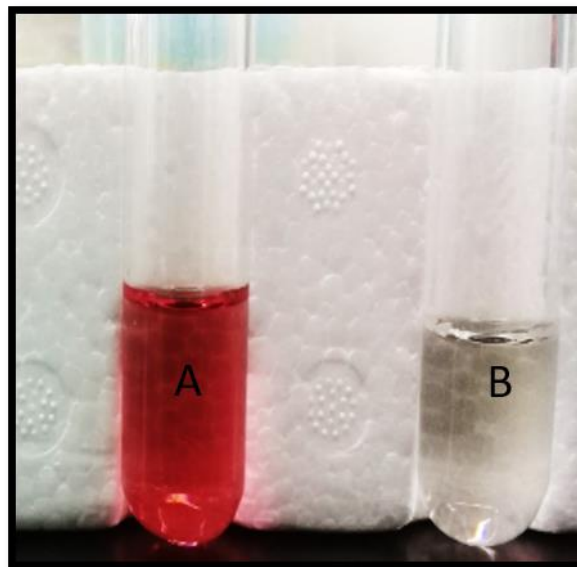
Figure 6.15 Arnow's assay for detection of catecholate production in *ΔentBEC*.

A is WT UEC59 showing positive indication (red-pink color) for catecholate test while B is *ΔentBEC* negative for catecholate test.
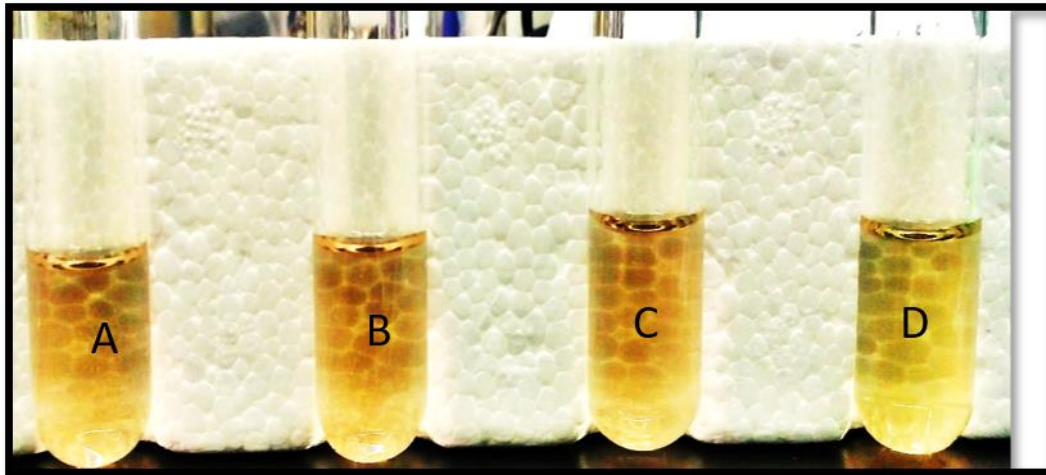
Figure 6.16 Atkin's assay for hydroxamate (aerobactin) detection in ΔiucABCD.

A-C are WT, *ΔentBEC, Δirp1_2* giving orange color, a positive indication for hydroxamate test, while D is *ΔiucABCD* giving yellow color a negative indication for hydroxamate test.

6.3.3   Effect of iron concentration on growth of *ΔentBEC, ΔhemRT, Δirp1_2* and *ΔiucABCD* using Bioscreen-C

6.3.3.1   Effect of iron on growth capacity of mutants: under iron-reduced and iron - restricted conditions

In order to determine whether the absence of either of the siderophore causes a growth deficit, all the four mutants were grown under different iron concentrations. Hence, mutants were allowed to grow in minimal medium without iron (0 µM) and with 2µM DTPA, using Bioscreen-C. WT UEC59 was used as a control.

Both mutants and WT were found to exhibit reduced growth under iron-deficient condition and maximum OD of ~0.7 was achieved (Figure 6.17). There was no significant difference among growth of mutants and WT, except *ΔentBEC*. When compared to WT, *ΔentBEC*, seemed to have a clear growth deficit ($P<0.01$) during log phase from 1 to 8 hours of growth. However, after reaching its plateau phase, it attained similar growth as WT and other three mutants.

In order to confirm the results whether *ΔentBEC* actually effects the iron acquisition and growth characteristic of UEC59, growth experiments were replicated further with the addition of 2 µM DTPA in M9 medium to enhance the iron restriction. Strains were found to exhibit very reduced growth in the presence of 2 µM DTPA (OD~ 0.4) (Figure 6.18). Mutants such as *ΔentBEC* and *Δirp1_2* showed extremely significantly reduced growth ($P<0.0001$) as compared to WT, under iron restricted conditions. Thus, the findings validated our previous results, where *ΔentBEC* faced a growth deficit under iron deficient conditions. Moreover, the results showed that under iron restricted conditions, yersiniabactin mutant (*Δirp1_2*) also faced a growth deficit as compared to its WT. Similarly, *ΔhemRT* faced a significant growth deficit ($P<0.05$) as compared to WT.
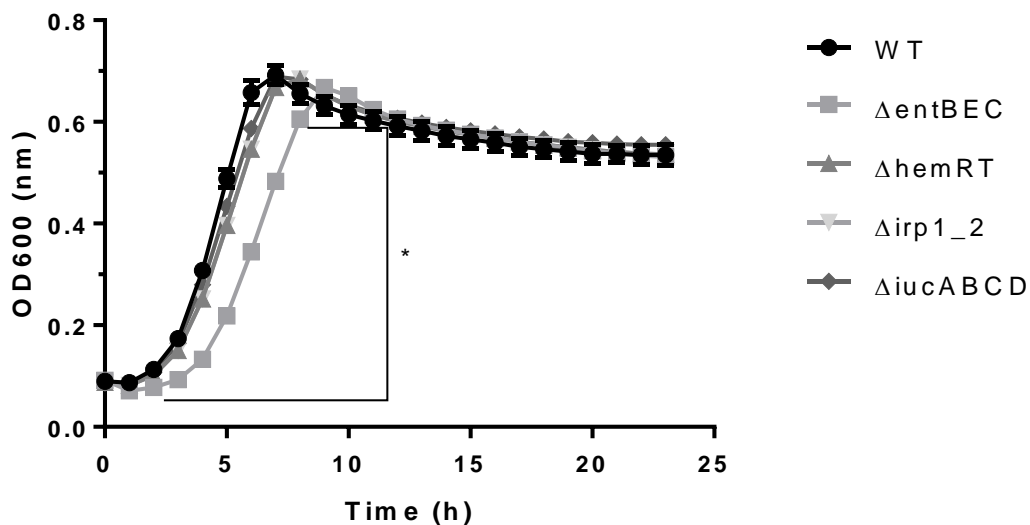
Figure 6.17 Effect of *ΔentBEC, ΔhemRT, Δirp1_2* and *ΔiucABCD* on UEC59 growth in minimal medium without iron.

Effect of *ΔentBEC, ΔhemRT, Δirp1_2* and *ΔiucABCD* on UEC59 growth in minimal medium without iron. Strains were grown aerobically in MM containing 0.4%-glucose, in Bioscreen-C (250 µl, 37°C, continuous shaking). *P* values were calculated by paired t- tests, using GraphPad Prism version 7©.
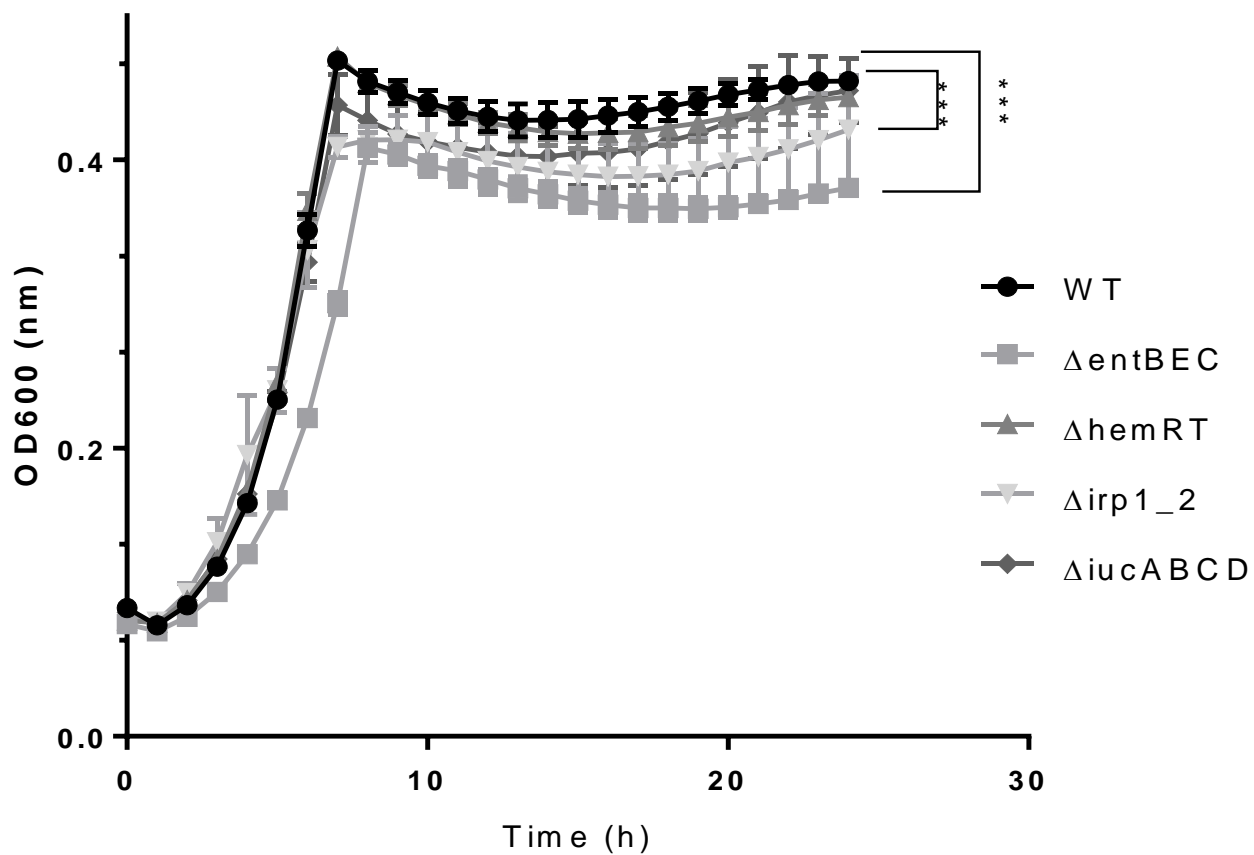
Figure 6.18 Effect of *ΔentBEC, ΔhemRT, Δirp1_2* and *ΔiucABCD* on UEC59 growth in minimal medium with 2 μM DTPA.

Strains were grown aerobically in MM containing 0.4%-glucose and 2 μM DTPA, in Bioscreen-C (250 μl, 37°C, continuous shaking). Error bars represent standard deviation from mean value. *P* values were calculated by paired t- tests, using GraphPad Prism version 7©.

6.3.3.2   Effect of iron on growth capacity of mutants: under iron-sufficient conditions

Results were further elaborated by studying the mutants under iron-sufficient conditions with the addition of 10 and 20 µM ferric citrate in M9 medium (Figure 6.19).

Addition of iron increased overall growth of strains and an average OD600 of ~ 0.8 was attained. All the strains seemed to grow at same rate as that of WT, except enterobactin mutant (*ΔentBEC*) which appeared to have significant growth deficit (*P<0.05*) in log phase (1 to 8 hours), as compared to the WT. However, after its stationary phase it was growing at similar rate as its WT and other mutants. All the other three mutants were observed to have a similar growth rate as the WT.
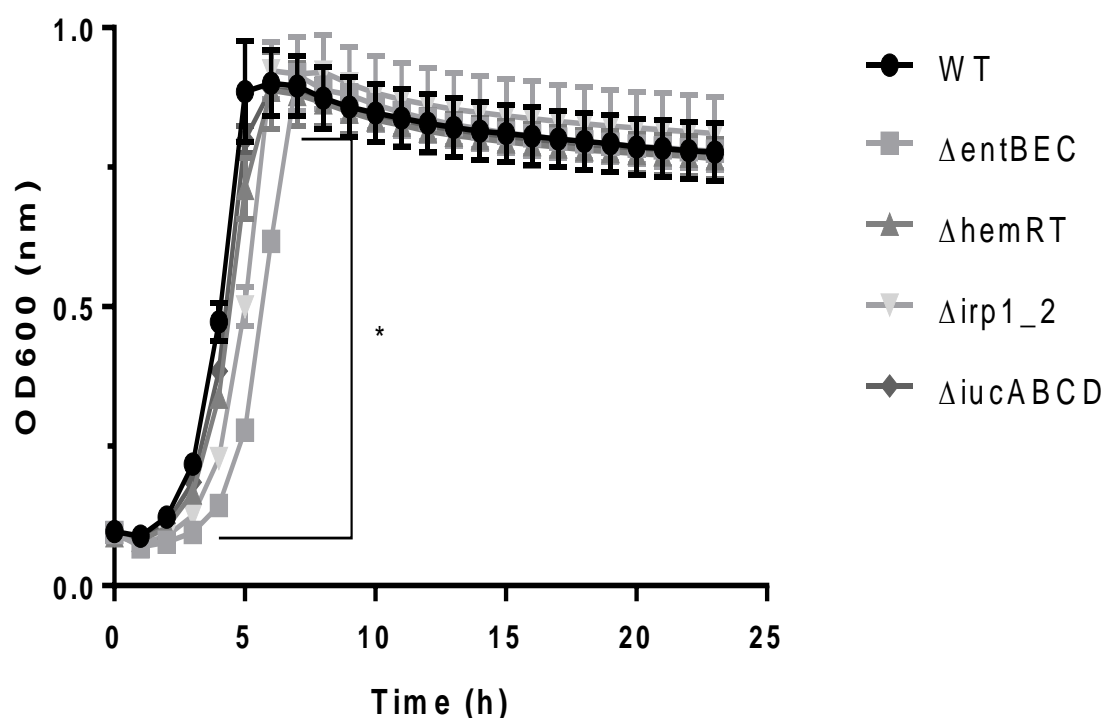
Figure 6.19 : Effect *of ΔentBEC,   ΔhemRT, Δirp1_2* and *ΔiucABCD* on UEC59 growth in minimal medium with 10 μM iron.

 Strains were aerobically grown in M9 medium (MM) containing 0.4%-glucose and 10 µM ferric citrate, in Bioscreen-C (250 µl, 37°C, continuous shaking). Error bars represent standard deviation from mean value. *P* values were calculated by paired t- tests, using GraphPad Prism version 7[©].

6.3.3.3   Effect of heme concentration on growth of *ΔentBEC, ΔhemRT, Δirp1_2* and *ΔiucABCD* usin*g* Bioscreen-C

Heme is the most abundant iron source *in-vivo* and is utilized by certain pathogenic bacteria like *Brucella, Pseudomonas* and pathogenic *E. coli* (Choby and Skaar, 2016). In order to determine the effect of heme on growth of WT and mutants, and relative contribution of each of the four iron-acquisition systems in heme uptake, the four mutants and WT UEC59 were grown under different heme concentrations. The five strains were grown in Bioscreen-C system with 0.5 µM and 5 µM heme. Experiments were run in triplicates and repeated at least twice to validate the results.

All the strains were observed to have a relatively better growth under heme-enriched conditions, with OD_{600} approaching ~0.8 as compared to heme-deficient conditions with OD OD_{600} approaching ~0.6. Under heme-deficient conditions, mutants and WT were found to have same growth level, however under heme-enriched conditions *ΔhemRT* was found at a compromised state as compared to WT and other mutants. Its OD_{600} was observed to be around ~0.5 and ~0.7 under 0.5 µM heme and 5 µM heme concentrations respectively, as compared to the WT and *ΔentBEC, Δirp1_2* and *ΔiucABCD* each of them having an average OD_{600} 0.6 to ~0.8 (Figure 6.20 and 6.21). The difference in growth was calculated to be significant ($P < 0.0001$). Our results suggest that since *ΔhemRT* is deficient in heme acquisition system it faces a growth deficit as compared to other strains. Thus, it validates the role of *hemRT* in heme acquisition and its effect on successful growth of UPEC in the presence of heme as an iron source. Other than *ΔhemRT,* again *ΔentBEC* observed a significant growth deficit ($P < 0.0001$) in the presence of heme, pertaining to increased oxidative stress in the absence of enterobactin.
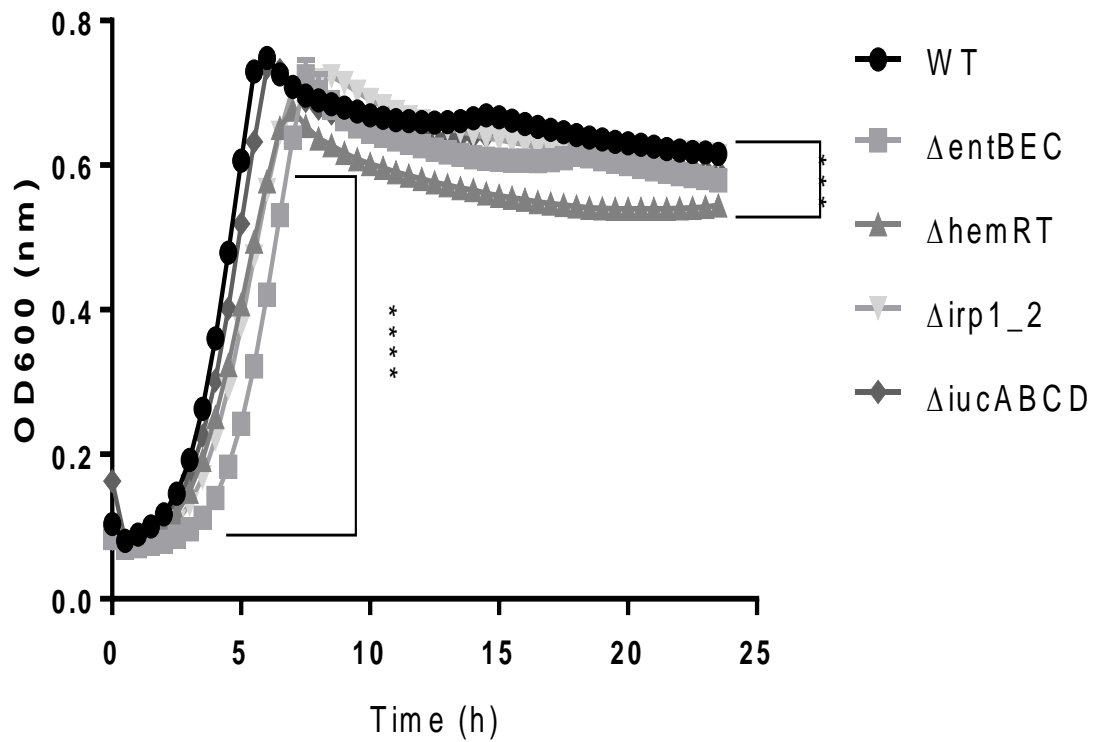
Figure 6.20 Effect of *ΔentBEC, ΔhemRT, Δirp1_2* and *ΔiucABCD* on UEC59 growth in minimal medium with 0.5 μM heme.

Strains were grown aerobically in MM containing 0.4%- glucose and 0.5 µM hematin, in Bioscreen-C (250 µl, 37°C, continuous shaking). Error bars represent standard deviation from mean value. *P* values were calculated by paired t- tests, using GraphPad Prism version 7[©].
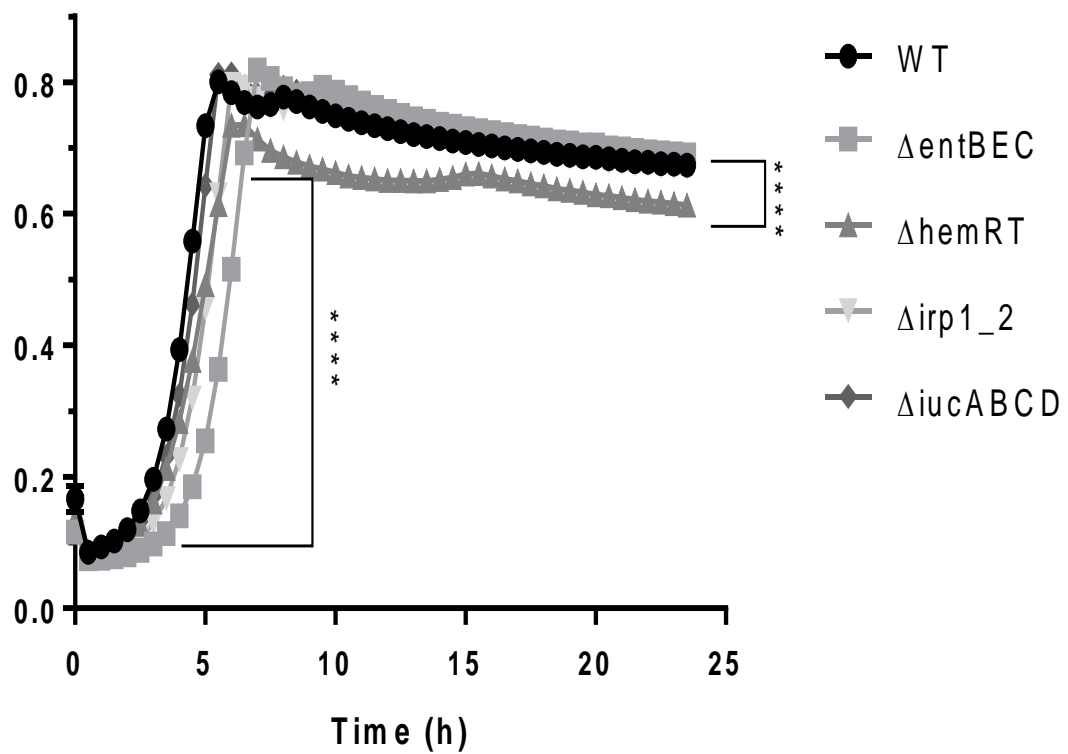
Figure 6.21 Effect of *ΔentBEC, ΔhemRT, Δirp1_2* and *ΔiucABCD* on UEC59 growth in minimal medium with 5 μM heme

Strains were grown aerobically in MM containing 0.4%-glucose and 5 µM hematin, in Bioscreen-C (250 µl, 37°C, continuous shaking). Error bars represent standard deviation from mean value. *P* values were calculated by paired t- tests, using GraphPad Prism version 7[©].

6.3.3.4   Effect of heme concentration under iron restricted conditions, on growth of *ΔentBEC, ΔhemRT, Δirp1_2* and *ΔiucABCD* using Bioscreen-C

As observed in previous experiment under heme-enriched conditions, *ΔhemRT* faced a growth deficit. In order to validate the results, all the four mutants were grown in iron restricted medium (supplemented with 1 µM DTPA and 2 µM DTPA) with 5 µM heme (Figure 6.22 and 6.23). In the presence of 1 µM DTPA it was observed that WT had significant advantage over its mutants and achieved the maximum growth (OD=1.20) after 8 h and maintained the plateau till 24 h. Next *ΔiucABCD* was found undergoing a growth deficit and took 13 h before it could reach the stationary phase and attained the maximum growth (OD=1.20). A highly significant difference ($P<0.0001$) was observed between WT and *ΔiucABCD* during first 10 h of growth. Similar trend was observed in case of *Δirp1_2*. Although there was no significant growth difference between *ΔiucABCD* and *Δirp1_2,* it happened to have a substantial growth deficit as compared to WT in its exponential phase and attained the maximum growth (OD=1.20) after 14 h. However, *ΔentBEC* were found to have a huge growth constraint ($P<0.0001$) under iron restricted and heme sufficient conditions. It attained a maximum growth of 1.14 after 24 h and growth seemed incomplete. On the other hand, *ΔhemRT* reached its stationary phase after 18 h and could attain a maximum growth of 0.97. An overall highly significant growth ($P<0.0001$) was observed growth between WT and *ΔhemRT.*

In the presence of 2 µM DTPA a severe growth constraint was observed by *ΔentBEC* and *ΔhemRT* each reaching a maximum OD of 0.79 and 0.85 respectively after 24 hours as compared to WT with maximum growth of 1.20 (Figure 6.23). Although *ΔiucABCD* and *Δirp1_2* seemed to undergo a growth deficit, their growth was better as compared *ΔentBEC* and *ΔhemRT,* reaching a maximum OD of 1.17 and 1.02 respectively. These results explain the definite role of *hemRT* in heme acquisition.
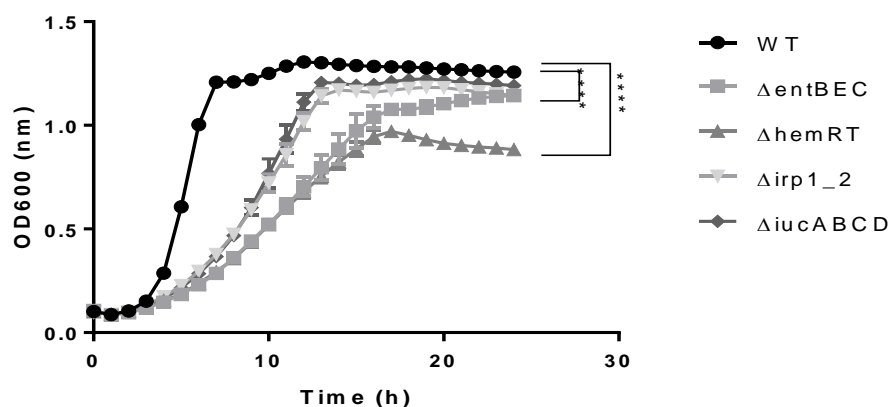
Figure 6.22 Effect of *ΔentBEC, ΔhemRT, Δirp1_2* and *ΔiucABCD* on UEC59 growth in minimal medium with 5 μM heme and 1 μM DTPA.

Strains were aerobically grown in M9 medium (MM) containing 0.4%-glucose,1 μM DTPA and 5 μM hematin, in Bioscreen-C (250 μl, 37°C, continuous shaking). Error bars represent standard deviation from mean value. *P* values were calculated by paired t- tests, using GraphPad Prism version 7©.
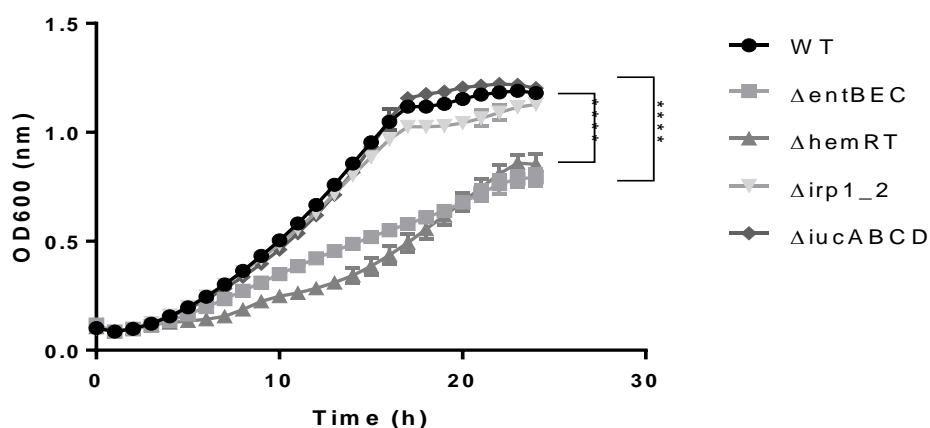
Figure 6.23 : Effect of *ΔentBEC, ΔhemRT, Δirp1_2* and *ΔiucABCD* on UEC59 growth in minimal medium with 5 μM heme and 2 μM DTPA.

Strains were aerobically grown in M9 medium containing 0.4% glucose,2 μM DTPA and 5 μM hematin, in Bioscreen-C (250 μl, 37°C, continuous shaking). Error bars represent standard deviation from mean value. *P* values were calculated by paired t- tests, using GraphPad Prism version 7©.

6.4   Construction of double mutants

The loss of *cat* cassette was confirmed by using confirmation primers as described above (Section 6.3.1) After loss of cat cassette the confirmation primers are expected to give PCR product of ~200bp (see Figure 6.24). After successful removal of resistance gene cassette (*cat* cassette) using pFLP-*hyg,* single mutants were again transformed with pACBSR-*hyg* to execute double knock out. As a result, six possible double mutants were generated from the single mutants. The six possible combination of double KO are: *ΔentBEChemRT::cat* (EH)*, ΔentBECirp1_2::cat* (EY)*, ΔentBECiucABCD::cat* (EA), *ΔhemRTirp1_2::cat* (HY)*, ΔhemRTiucABCD::cat* (HA)*,*   and *Δirp1_2iucABCD::cat* (YA).

All the six double mutants were confirmed both genotypically and phenotypically as described under section (6.3.1 and 6.3.2)

6.4.1   Genotypic confirmation of double mutants

A successful mutant was confirmed by using confirmation primers for each of the genes. The mutants are expected to give PCR product of ~1.5kb this being the *cat* cassette plus the gene fragments adjacent to the gene of interest amplified by confirmation primers (see Figure 6.25).
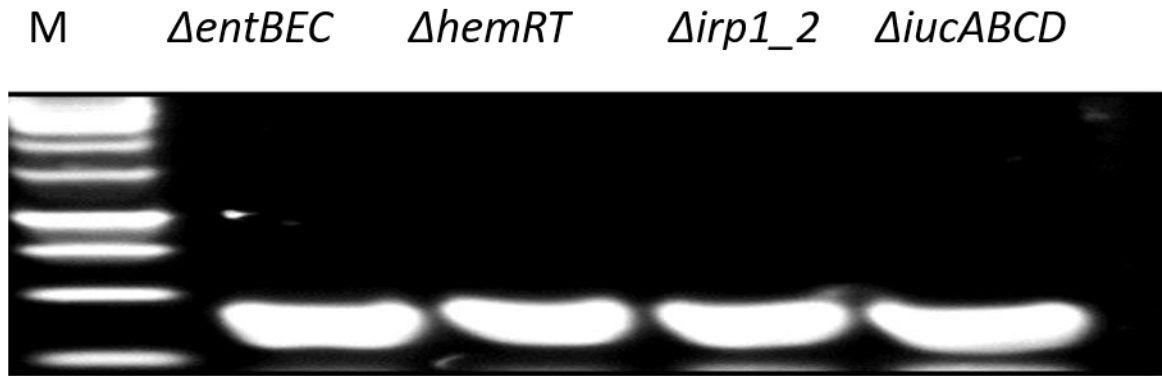
Figure 6.24 PCR amplification of *ΔentBEC, ΔhemRT, Δirp1_2* and *ΔiucABCD* after cat gene removal.

PCR amplification of Δ*entBEC,* Δ*hemRT,* Δ*irp1_2* and Δ*iucABCD* after *cat* gene removal; visualization on 0.8% agarose by gel electrophoresis. One can clearly see the size in gene fragment of mutants (~200 bp) indicating removal of ~1.5 kb *cat* cassette and amplification of adjoining gene locus, whereas M is GeneRuler™ 1kb ladder.
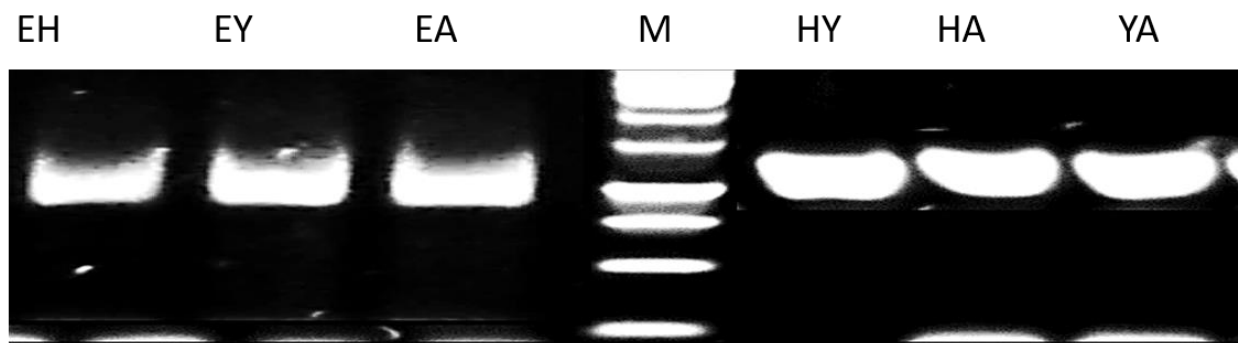
Figure 6.25 PCR amplification of double mutants

PCR amplification of double mutants *ΔentBEChemRT::cat* (EH)*, ΔentBECirp1_2::cat* (EY)*, ΔentBECiucABCD::cat* (EA)*, ΔhemRTirp1_2::cat* (HY)*, ΔhemRTiucABCD::cat* (HA) and *Δirp1_2iucABCD::cat* (YA) visualization on 0.8% agarose by gel electrophoresis. One can clearly see the integration of *cat* cassette and adjoining gene fragments in mutants (~1.5kb), whereas M is GeneRuler™ 1kb ladder.

6.4.2   Phenotypic confirmation of double mutants

CAS plate assay was performed to observe the difference in growth curve and zone size after double deletions. In case of iron deficient conditions, mutants EH ($P<0.05$) and EA ($P<0.01$) seemed to have compromised growth as compared to their WT, while HY ($P>0.05$)) had roughly the same growth trend as that of WT. However, mutants like EY ($P<0.05$), HA ($P<0.01$) and YA ($P<0.01$) had a significant growth advantage as compared to their WT strain. Among the three mutants HA had the highest growth rate and attained a maximum growth of 1.40 as compared to the WT which had the maximum growth of 1.30. Similarly, YA and EY had attained a maximum growth of 1.38 and 1.33 respectively as compared to their WT strain (Figure   6.26).
As expected under iron enriched conditions there was no growth difference observed; WT and mutants seemed to grow at an equal rate (Figure 6.27).

CAS plate assay was performed to measure the difference in zone sizes. The production of zone size started after 8 hours and strains were found increasing the production in stationary phase. As expected, WT was found having maximum zone size of ~18mm, HY with a zone size of 16mm, followed by HA ~14mm and finally EH was found to have a zone size of 13mm. On the other hand, mutants EY, EA and YA were found to have low level of siderophore production to be measured on detected on plate as evident in Figure 6.28.
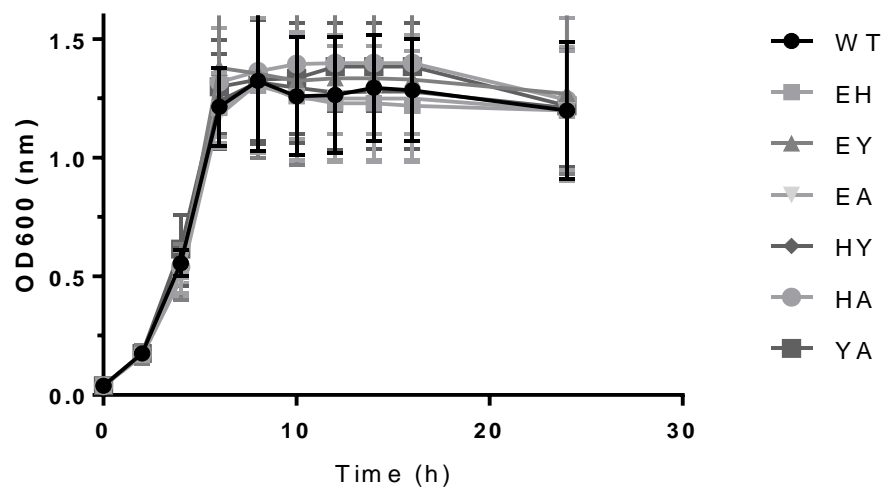
Figure 6.26 Effect of double mutations on growth capacity of UEC59 in minimal media without iron.

Effect of *ΔentBEChemRT::cat* (EH)*, ΔentBECirp1_2::cat* (EY)*, ΔentBECiucABCD::cat* (EA), *ΔhemRTirp1_2::cat* (HY)*, ΔhemRTiucABCD::cat* (HA) and *Δirp1_2iucABCD::cat* (YA), mutations on growth capacity of UEC59 in minimal media without iron. Strains were grown aerobically in MM containing 0.4%-glucose, using 50-ml medium in 250- ml flasks (37ºC, 180 RPM). Error bars represent standard deviation from mean value. *P* values were calculated by paired t- tests, using GraphPad Prism version 7©.
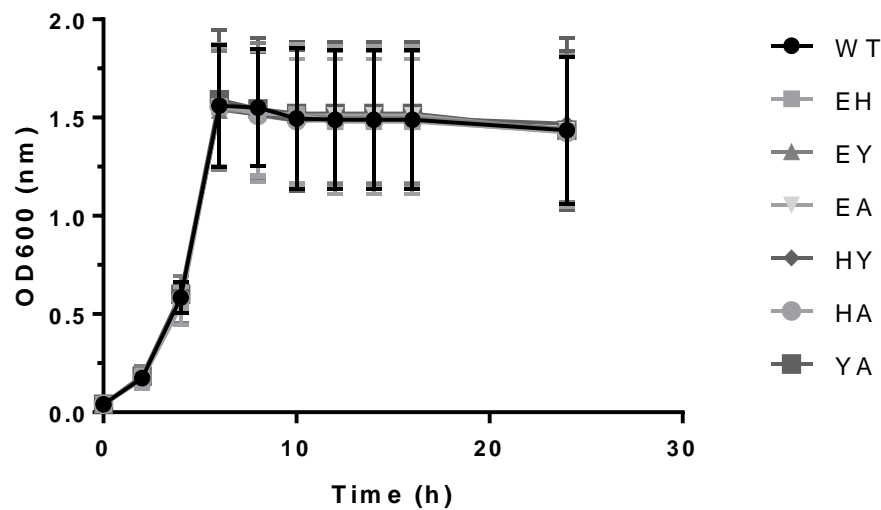
Figure 6.27 Effect of double mutations on growth capacity of UEC59 in minimal media with iron.

Effect of *ΔentBEChemRT::cat* (EH)*, ΔentBECirp1_2::cat* (EY)*, ΔentBECiucABCD::cat* (EA), *ΔhemRTirp1_2::cat* (HY)*, ΔhemRTiucABCD::cat* (HA) and *Δirp1_2iucABCD::cat* (YA), mutations on growth capacity of UEC59 in minimal media with iron. Strains were grown aerobically in MM containing 0.4%-glucose and 10 µM ferric citrate, using 50-ml medium in 250-ml flasks (37ºC, 180 RPM). Error bars represent standard deviation from mean value. *P* values were calculated by paired t- tests, using GraphPad Prism version 7[©].
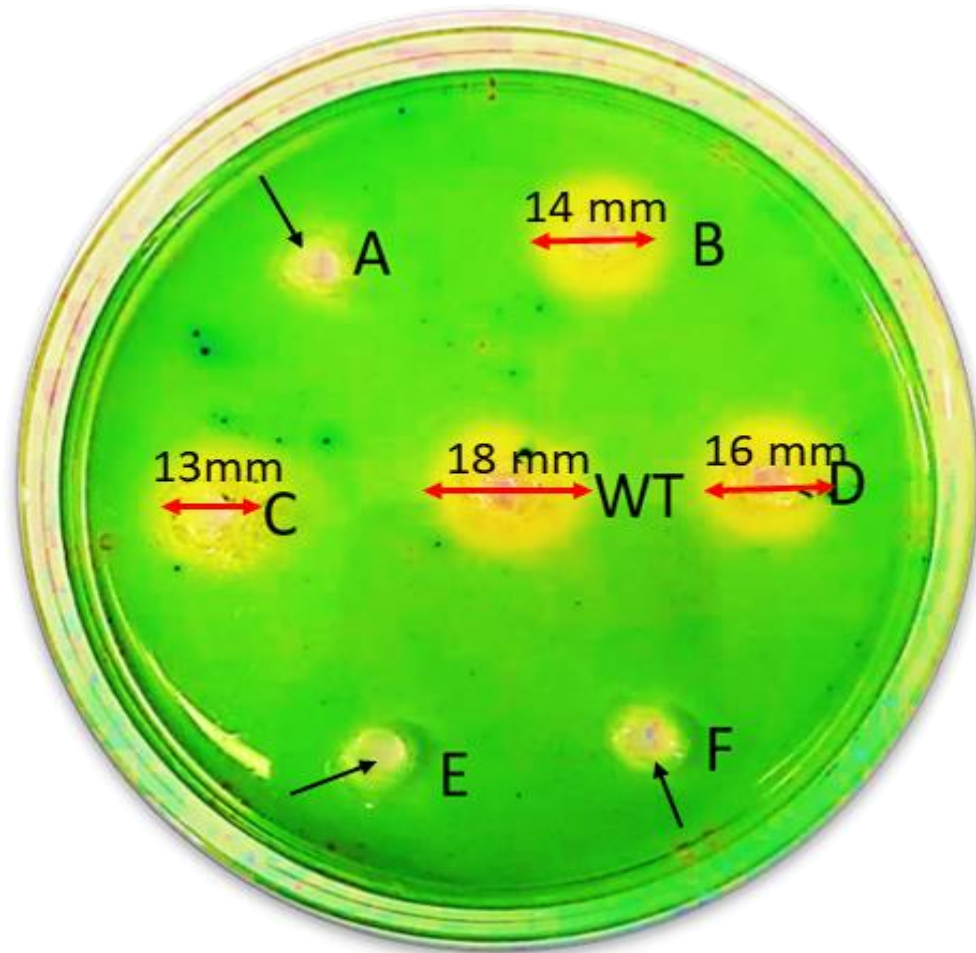
Figure 6.28 CAS assay shows siderophore production on a CAS plate.

CAS assay shows siderophore production on a CAS plate. The plate shown is after 14 hours of growth. Golden halo around the wells shows the binding of iron by siderophores. Black arrows indicate double mutants EY (A) , EA (E) and YA (F) show either very weak or no sign of siderophore production. Whereas, HA (B), EH (C) and HY (D) have moderate siderophore production.

Arnow's assay was performed to confirm catecholate production among the *ΔentBEC* mutants. As expected, double mutants such as EH, EY and EA were found negative for catecholate production as evident from the Figure 6.29. However, the other three mutants were found positive for catecholate production. This further validates the correct gene deletion.

Atkin's assay was executed for the confirmation of aerobactin (hydroxamate) gene deletion. Mutants such as EA, HA and YA were found negative for hydroxamate production as compared to non *iucABCD* mutants confirming the correct deletion of gene. (Figure 6.30).
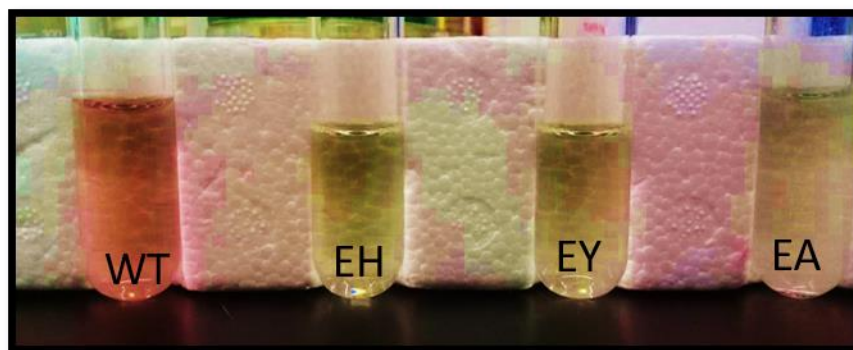
Figure 6.29 Arnow's assay for detection of catecholate production in *ΔentBEC* double mutants.

WT UEC59 showing positive indication (red-pink color) for catecholate test while double mutants such as EH, EY and EA are negative for catecholate test (white-yellow coloration).
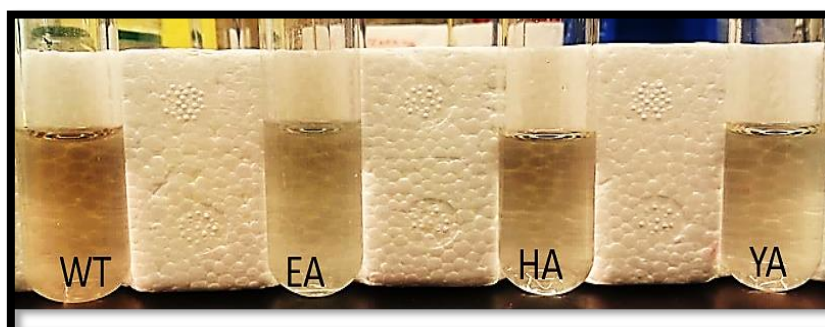
Figure 6.30 Atkin's assay for detection of hydroxamate production in ΔiucABCD double mutants.

WT UEC59 showing positive indication (orange color) for hydroxamate test while double mutants such as EA, HA and YA are negative for hydroxamate test (white-yellow coloration).

6.4.3   Growth phenotypes for iron acquisition system (siderophore) double mutants

In order to see the effect of double mutations on growth phenotype of strain, further growth experiments were conducted. The experiments were conducted in Bioscreen-C system to ensure better quantification, replication and standardization of growth data.

A series of conditions were replicated to determine the effect of double mutations.

6.4.3.1   Effect of iron concentration: under reduced and iron restricted conditions on growth of double mutants using Bioscreen-C

The six double mutants were allowed to grow in minimal medium without iron (0 µM) and with iron (10 µM, 20 µM), using Bioscreen-C. WT UEC59 was used as a control.

Both mutants and WT were found to exhibit reduced growth under iron-deficient condition and maximum OD of ~0.8 was achieved (Figure 6.31). An unusual trend was observed in growth of double mutants where double mutants such as HA ($P<0.001$) and YA ($P<0.001$) were seen growing faster and better than WT. Each of the three mutants had a maximum cell density of ~ 0.8 as compared to the WT which attained a maximum growth of ~0.7. Other than that, double mutant EH ($P<0.01$), EY ($P<0.0001$), EA ($P<0.0001$) was observed to face a statistically significant growth deficit as compared to WT. Mutants such as HY and HA were observed   growing   at   the   same   rate   as   that   of   WT. As expected strains were found to have better growth under iron-sufficient (10 µM, 20 µM) conditions, with OD approaching ~1 (Figure 6.32). However, no significant growth difference ($P>0.05$) was noted between WT and mutants.

Growth experiments were replicated further with the addition of 2 µM DTPA in M9 medium to enhance the iron restriction and ensure the reliability of above results. Strains were found to

exhibit very reduced growth in the presence of DTPA with WT strain able to attain a maximum OD~ 0.5. Results were in accordance with the previous experiment when conducted in M9 without iron. Mutants such as HA, YA were again seen at a growth advantage as compared to the WT. HA attained its maximum growth (~0.54) after 14 h as compared to WT which was found to reach its stationary phase after 16 h (~0.52), while HA was seen having a continuous increase in growth up to ~ 0.57 up to 24 h. On the other hand, YA attained its stationary phase after 15 h as compared to WT (after 16 h) and attained a maximum growth of ~ 0.55. EY faced a significant growth deficit ($P<0.01$) during log phase and attained its stationary phase after 18 h as compared to WT. At stationary phase its growth was a similar rate as that of WT. Mutants such as EA ($P<0.001$) and EH ($P<0.01$) faced a significant growth constraint in log as well as stationary phase, when compared to WT. Both mutants attained the stationary growth after 17 and 19 h respectively and a maximum OD of ~0.45 was achieved by each of them (Figure 6.33). Overall, it suggests that enterobactin mutants (EH, EY and EA) as well as yersiniabactin mutant (HY) face growth constraints in comparison to other mutants.
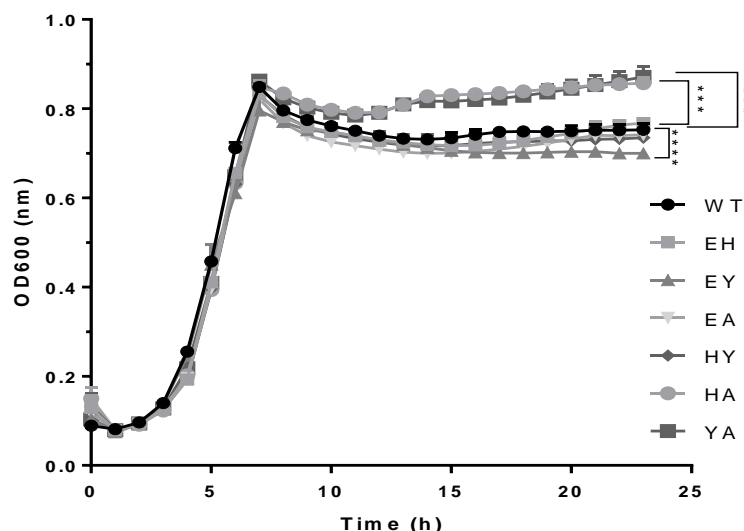
Figure 6.31 Effect of double mutations on UEC59 growth in minimal medium without iron.

Strains were aerobically grown in M9 medium (MM) containing 0.4%- glucose, in Bioscreen-C (250 µl, 37°C, continuous shaking). Error bars represent standard deviation from mean value. *P* values were calculated by paired t- tests, using GraphPad Prism version 7[©].
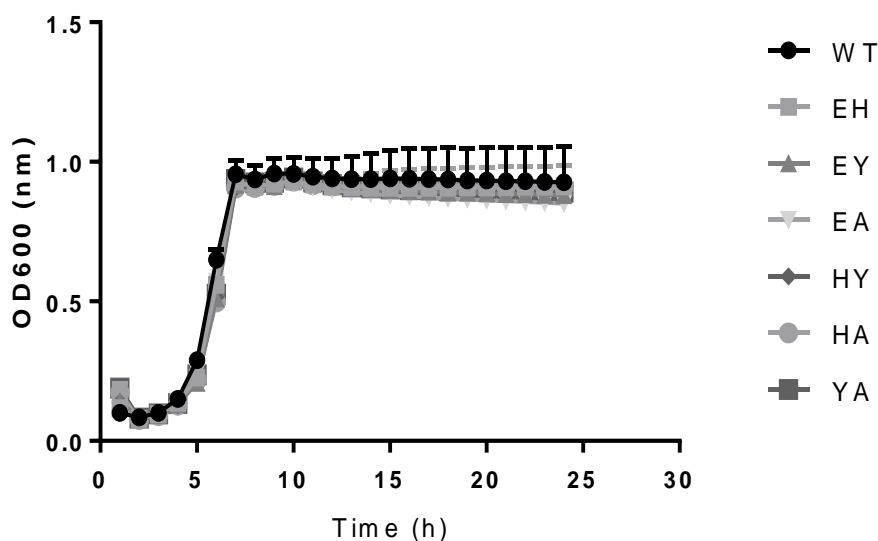
Figure 6.32 Effect of double mutations on UEC59 growth in minimal medium with iron.

Strains were aerobically grown in M9 medium (MM) containing 0.4%-glucose and 10 µM ferric citrate, in Bioscreen-C (250 µl, 37°C, continuous shaking). Error bars represent standard deviation from mean value. *P* values were calculated by paired t- tests, using GraphPad Prism version 7[©].
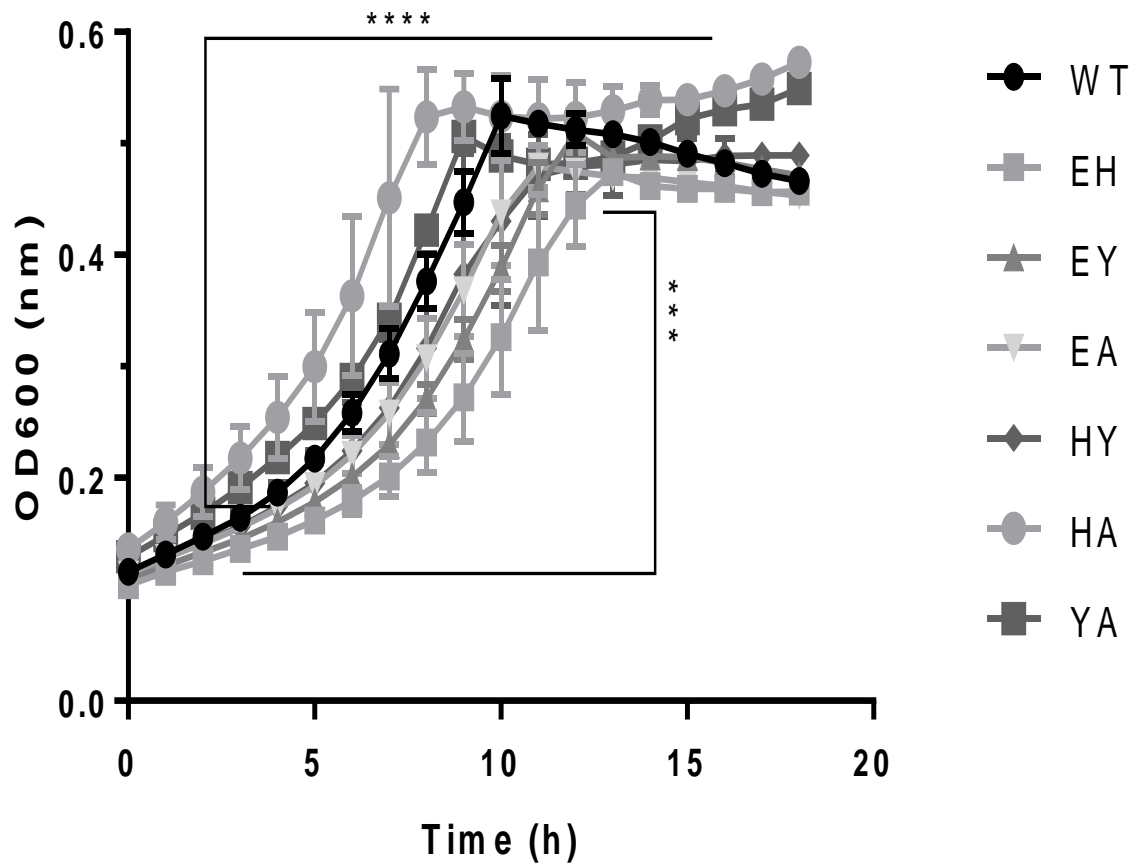
Figure 6.33 Effect of double mutations on UEC59 growth in minimal medium under iron-restricted conditions.

Strains were aerobically grown in M9 medium (MM) containing 0.4%-glucose and 2 µM DTPA, in Bioscreen-C (250 µl, 37°C, continuous shaking). Error bars represent standard deviation from mean value. *P* values were calculated by paired t- tests, using GraphPad Prism version 7[©].

6.4.3.2   Effect of heme concentration: iron restricted growth of double mutants

In order to check the effect of double mutations on heme uptake and relative effect of each of the mutations, mutants were tested in M9 medium supplemented with 0.5 µM. Addition of 2 µM DTPA was made to ensure iron restriction and mutants sole dependence on heme as an iron source. Presence of heme in media improved the overall growth of mutants as compared to previous experiment (in total absence of iron). WT observed an increase in growth from ~ 0.52 to ~0.63 and stationary phase was attained at 14 h as compared to previous experiment where it had attained stationary phase at 16 h. Similarly, YA observed an increase from ~0.55 to ~0.64 (Figure 6.34).

Comparing the growth of mutants among themselves, it was observed that YA had highest growth rate as compared to the WT and other mutants. This result comes in agreement with the previous two experiments (under iron deficient and iron restricted), where it had a higher growth as compared to WT and other mutants. However, HA faced a growth constraint unlike the previous two experiments. It was observed to reach the stationary phase at 17 h and its growth was significantly slower ($P<0.0001$ than that of WT. At stationary phase (after17 h) it had similar growth as that of WT. This slow grow rate could be attributed to absence of heme uptake system and its inability to utilize heme as an alternative iron source. Mutants such as EA, EH and EY had significantly lower growth rates ($P<0.0001$) as compared to WT and these strains were found growing at same rate and a maximum growth of ~0.5 was achieved by each of them. Mutant HY had the slowest growth of all ($P<0.0001$), it could reach the stationary phase after 19h and had a maximum growth of ~0.47. Slow growth rate of mutants of heme uptake system authenticate the correct mutations. Moreover, it validates the role of heme uptake system in growth of UPEC.

Our results are in accordance with our previous experiment with single mutants (section 6.3.3.3) where *ΔentBEC* was unable to grow actively even in the presence of heme.

It was found growing at same rate as *ΔhemRT*. Another experiment was replicated with 5 µM heme and 2 µM DTPA to validate the results (Figure 6.35). As expected, increase in heme oncentration helped in growth of WT and a maximum growth of ~ 0.67 was achieved. Again, YA was seen to have significantly higher growth as compared to WT reaching a maximum growth of ~0.74. Heme uptake mutants such as EH, HA and HY were significantly behind WT in terms of growth rate, other than that enterobactin biosynthesis mutants EY, EA and EH were seen at a growth disadvantage as compared to WT. HY was amongst the slow growing mutant again.
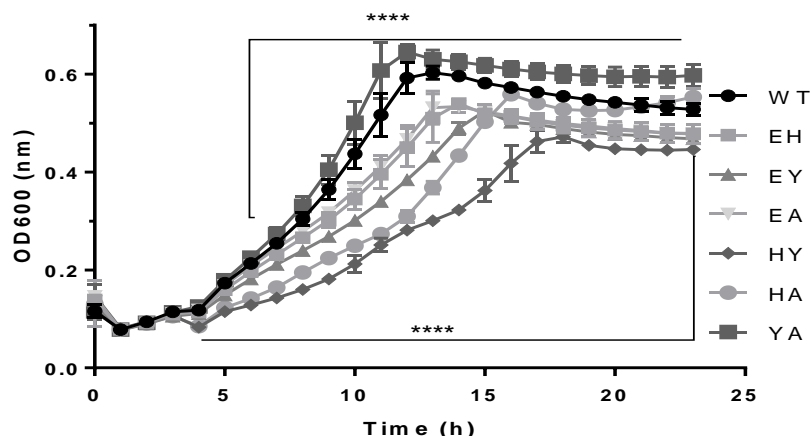
Figure 6.34 Effect of double mutations on UEC59 growth in minimal medium under iron-restricted conditions in the presence of heme.

Strains were aerobically grown in M9 medium (MM) containing 0.4%-glucose, 0.5 µM hematin and 2 µM DTPA, in Bioscreen-C (250 µl, 37ºC, continuous shaking). Error bars represent standard deviation from mean value. *P* values were calculated by paired t- tests, using GraphPad Prism version 7©
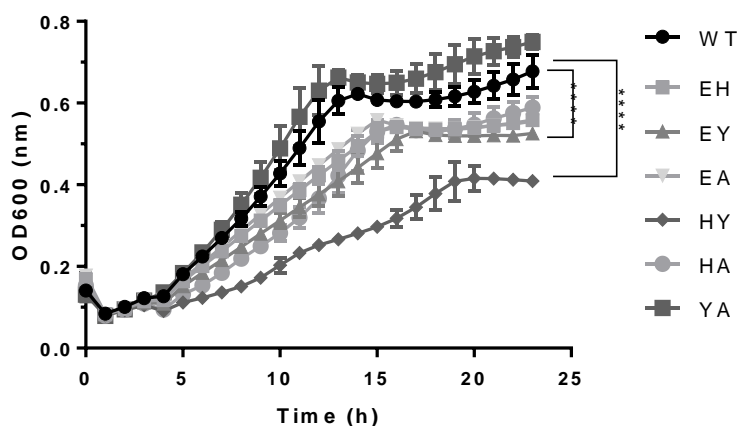

Figure 6.35 Effect of double mutations on UEC59 growth in minimal medium under iron-restricted conditions in the presence of heme.

Strains were aerobically grown in M9 medium (MM) containing 0.4%-glucose, 5 µM hematin and 2 µM DTPA, in Bioscreen-C (250 µl, 37ºC, continuous shaking). Error bars represent standard deviation from mean value. *P* values were calculated by paired t- tests, using GraphPad Prism version 7©.

6.4.3.3 Effect of pH: iron-deficient growth of double mutants under acidic or alkaline conditions

In order to determine relative contribution of siderophores in growth under different pH conditions, growth assays were performed in M9 medium and adjusted to a range of pH; pH 5.5, 7 and 8.5. The medium pH were maintained using mixture of TAPS,MES and HEPES buffer.

It was observed that at pH 7.0 double mutants such as HA ($P<0.05$) and YA ($P<0.001$) were found growing at significantly rapid rate as compared to WT. The trend is similar as seen in previous growth assays under iron deficient conditions (section 6.4.3.1). EY, EH and EA were found an extremely significant ($P< 0.0001$) growth differences were observed., whereas HY was found to have no signifiacnt growth difference ($P> 0.05$) (Figure 6.36). At pH 5.5 again mutants such as HA and YA were found growing at significantly ($P< 0.001$) rapid rate as compared to WT, while other four mutants were found growing at same rate as WT and no signifiacnt differences were observed (Figure 6.36). Under alkalkine conditions (pH 8.5) rate of growth was rapid as compared to pH 7.0 and 5.5. As evident from Figure 6.36 mutants HA ($P<0.0001$) and YA ($P<0.001$) were at significant growth advantage as compared to WT and other mutants. Other than EY which was at siginificant growth deficit ($P<0.0001$) all other mutants were found growing at same rate as WT.

In order to further clarify the above results strains were once again grown under iron restricted conditions with the addition of 2 µM DTPA in M9 medium and adjusted to a range of pH; pH 5.5, 7 and 8.5. The medium pH were maintained using mixture of TAPS,MES and HEPES buffer. At pH 7.0 under iron restricted conditions HA had significant growth advantage as compared to the WT, while enterobactin mutanst such as EY and EA seemed to have significant ($P< 0.05$) growth deficit as compared to their WT counterpart. Other than that HA along with

HY had significantly slower growth as compared to WT. While mutants YA had no significant disdavantage under iron restricted neutral pH conditions.

In iron restricted acidic conditions (pH 5.5) mutants such as HA and EA had almost similar growth as that of WT. On the other hand mutants such has EH, EY, HY and YA had significantly ($P<0.05$) low growth as compared to that of WT. The common feature the three mutants was absence of enterobactin and yersiniabactin, which makes these results quiet interesting to discuss. Under iron restricted alkaline conditions (pH 8.5) contrarily enterobactin deficient muatnts such as EH, EY and EA were significantly growth defected as compared to their WT however mutants such as YA and HY (both yersiniabactin mutant) had better growth as compared to their WT. While HA as usual had better growth as compared to WT.

Our results indicate that at pH 7.0, under iron deficient as well as iron resricted conditions, mutants such as EY, EH and EA were observed to have slow growith suggesting that enterobactin plays a pivotal role in iron-acquition at neutral pH. At pH 5.5 , under both iron-deficient and- restricted conditions again strains EH, EY, HY, had slow growth rates, while at pH 8.5 EH, EY and EA were significantly growth defected as compared to their WT however mutants such as YA and HY (both yersiniabactin mutant) had better growth as compared to their WT. This can again be attributed to absence of enterobactin in (EH, EY and EA) , that showed poor growth at pH 8.5 and presence of enterobactin in YA and HY muants, leading to their better growth at alkaline pH.

Figure 6.36 Effect of double mutations on UEC59 growth in minimal medium at a range of pH under iron-restricted conditions.

Strains were grown aerobically in MM containing 0.4%-glucose, with and without 2 µM DTPA, in Bioscreen-C (250 µl, 37ºC, continuous shaking). Error bars represent standard deviation from mean value. *P* values were calculated by paired t- tests, using GraphPad Prism version 7$^{©}$.

6.4.3.4   Effect of competing metals on the growth of double mutants

Transition metals such as iron, manganese, copper and zinc play key roles in the matabolism of prokaryotes as well as eukaryotes. However, host inhibits their availibility to bacteria by sequestering them (Hood and Skaar, 2012, Skaar, 2010). Bacteria release siderophores (iron

squestering molecules) and zincophores (zinc squestering molecules) to uptake these transition elements in order to fulfill their metabolic needs (Johnstone and Nolan, 2015b). While siderophores are mainly required for iron uptake, recently siderophores such as yersiniabactin have been shown to be involved in zinc and copper uptake as well, although its direct role in zinc uptake has not been fully elucidated yet (Chaturvedi et al., 2012, Bobrov et al., 2014). This experiment aimed at determining the role of siderophores in uptake of transtion metals such as manganese (Mn^{2+}) and zinc (Zn^{2+}) at different pH (Figure 6.37 and 6.38).

(i) Growth at pH (7.0), under iron restricted conditions, with competing metals

In order to determine role of relative mutations on growth under iron restricted conditions in the prsence of competing metals and to suggest whether there is any possible effect on other metals uptake in the absence of respective siderophores. Strains were grown in M9 medium supplemented with 10 µM $MnCl_2$ and $ZnSO_4$ (each in a separate set of experiments) under iron restricted conditions (with addition of 2 µM DTPA).

At pH 7.0 in the presence of 10 µM $MnCl_2$ no growth differences were observed between wildtype and its mutants. However in the presence of 10 µM $ZnSO_4$ a plausible increase (*P*<0.05) in growth of HA and YA mutants was observed. The competing metals overall had a positive effect on the growth of strains helping them to attain a maximum growth of ~ 0.7 to 0.9 as compared to their growth when allowed to grow under iron restricted conditions (see experiment 6.4.3.1) where a maximum growth of ~0.4 to 0.5 was observed, thus increasing upto 2 two fold growth.

(ii) Growth at pH (5.5), under iron restricted conditions, with competing metals

Under acidic conditions (pH 5.5) in the presence of 10 µM $MnCl_2$ mutants such as HY, EH, EA and EY had significantly (*P*<0.001) lesser growth as compared to their WT, while the

mutants such as HA and YA (P>0.05) had similar growth rate as that of WT. Among HY, EH, EA and EY (having decreased growth rate) enterobactin mutants (EH, EA and EY) were the one with the slowest growth rate (~0.5) as compared to WT with a growth rateOD$_{600}$ ~0.6 at sttionary phase. In the presence of 10 µM ZnSO$_4$ however mutants such as HA and YA had highest growth rate with a maximum growth rate ~ 0.8 while the mutants were at growth deficit. While all other mutants (EH, EY, EA, HY,) were found with lowest growth rate ((P<0.0001) with an average growth of ~0.5, as compared to their WT (~0.7).

(iii) Growth at pH (8.5), under iron restricted conditions, with competing metals

Under alkaline conditions (pH 8.5), in the presence of 10 µM MnCl$_2$ mutants HA and YA were seen with a better growth rate as compared to WT and other mutants except EA which was observed to have a slight growth difference. However in the presence of 10 µM ZnSO$_4$ mutants all the mutants except (EH) were observed to have a better growth as compared to WT
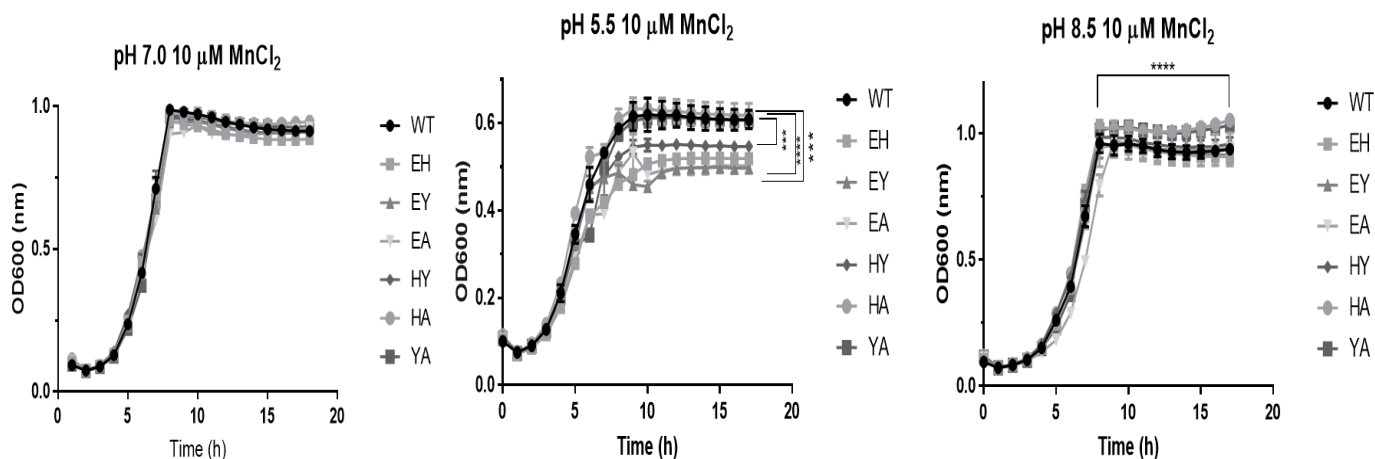
Figure 6.37 Effect of double mutations on UEC59 growth in minimal medium at a range of pH under iron-restricted conditions with the addition of MnCl₂.

Strains were grown aerobically in MM containing 0.4% glucose, with 2 µM DTPA and 10 µM MnCl₂, in Bioscreen-C (250 µl, 37°C, continuous shaking). pH was adjusted using using mixture of TAPS,MES and HEPES buffer. Error bars represent standard deviation from mean value. *P* values were calculated by paired t- tests, using GraphPad Prism version 7©.
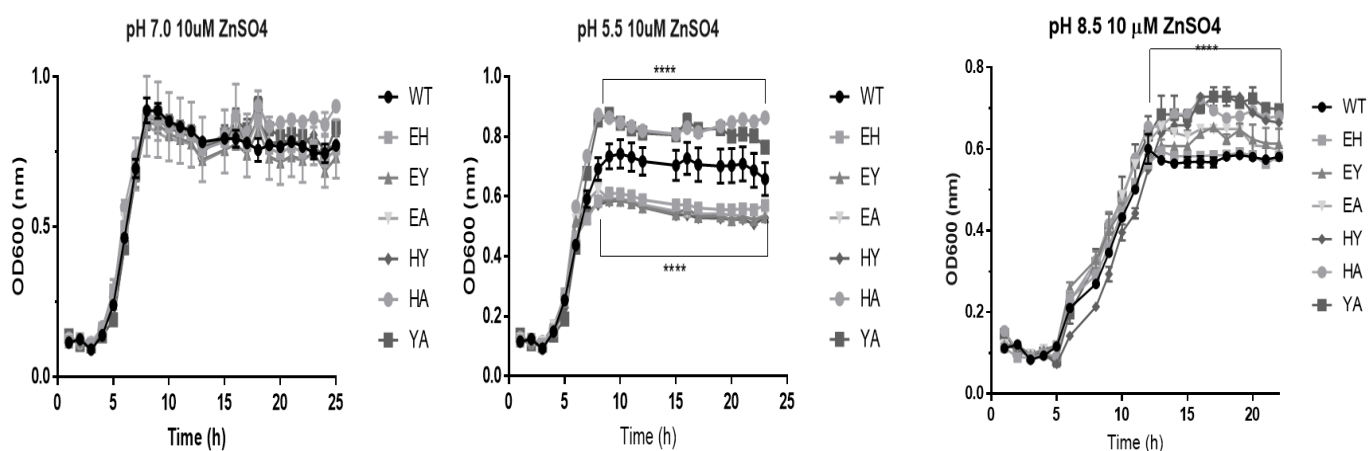
Figure 6.38 Effect of double mutations on UEC59 growth in minimal medium at a range of pH under iron-restricted conditions with the addition of ZnSO₄.

Strains were grown aerobically in MM containing 0.4% glucose, with 2 µM DTPA and ZnSO₄, in Bioscreen-C (250 µl, 37°C, continuous shaking). pH was adjusted using using mixture of TAPS,MES and HEPES buffer. Error bars represent standard deviation from mean value. *P* values were calculated by paired t- tests, using GraphPad Prism version 7©.

## 6.5   Effect of human lipocalin on the growth of double mutants

Enterobactin (Ent) is known to have highest affinity for ferric iron and poses huge challenge for host cells (Holden and Bachman, 2015). Lipocalin 2 (Lcn2) is an innate immunity protein that sequesters iron for host and starves bacteria of iron (Bachman et al., 2009). It is secreted by host neutrophils and epithelial cells to oppose the acquisition of iron by bacterial siderophore (enterobactin). However, human Lcn2 is found to have similar affinity for Ent as its receptor FepA and gives bacteria a tough competition in race for iron. The protective effect of lipocalin was documented in a sepsis model of *Escherichia coli* (Flo et al., 2004). The experiment aimed at determining the effects of double mutation on the survival of UPEC strains in the presence of human lipocalin (HLcn-2). The protein was generously provided by my lab colleague Louis Julien, who is determining HLcn-2 effect on another pathogen.

In order to determine the effect of HLcn-2 on double mutants, strains were allowed to grow under i) M9 medium (without iron and HLcn-2) ii) M9 medium (without iron) supplemented with 8 µM HLcn-2 and iii) M9 medium (supplemented with 10 µM ferric citrate and 8 µM HLcn-2).

Under iron deficient conditions mutants such as HA and YA were growing significantly better as compared to the WT and other competitors. Mutants such as EY, EH and HY had reasonably low growth rate as compared to WT (Figure 6.39). The results are in accordance with previous experiment (section 6.4.3.1), when mutants were grown under iron reduced conditions. However, under iron deficient conditions (no added iron) with the addition of 8 µM HLcn-2 all the enterobactin mutants (EH, EY and EA) were found to have highly significant ($P<0.0001$) growth difference as compared to the WT (Figure 7.40). EY and EH were observed to have similar growth pattern and both showed increase in growth as compared to WT. Similarly, mutants EA, HA and YA (aerobactin deficient) were also observed to have increased

growth as compared to WT and these three seemed to follow similar growth trend. However mutant HY (encoding both enterobactin and aerobactin) had a significantly ($P<0.0001$) reduced growth a compared to other mutants and followed almost similar growth rate as WT.

Under iron-enriched (10 µM Fe) with the addition of 8 µM HLcn-2, as expected no growth differences were observed (Figure 6.41)
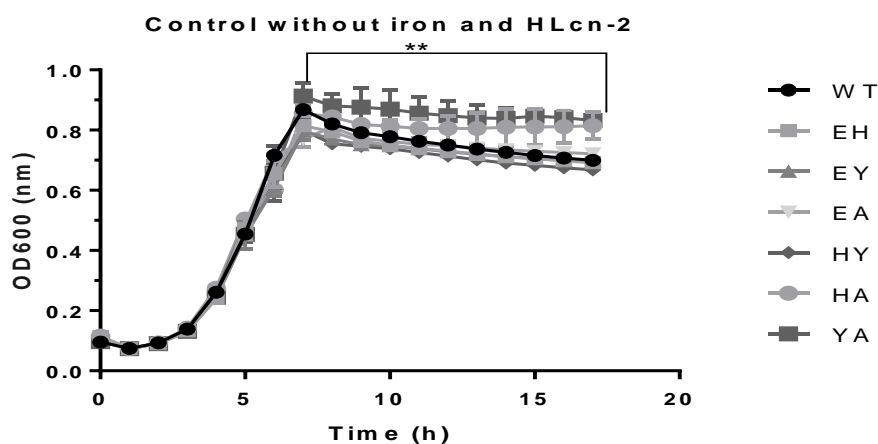
Figure 6.39 Effect of double mutations on UEC59 growth in minimal medium under iron-deficient conditions.

Strains were grown aerobically in MM containing 0.4%-glucose, without added ferric citrate, in Bioscreen-C (250 µl, 37°C, continuous shaking). Error bars represent standard deviation from mean value. *P* values were calculated by paired t- tests, using GraphPad Prism version 7©.
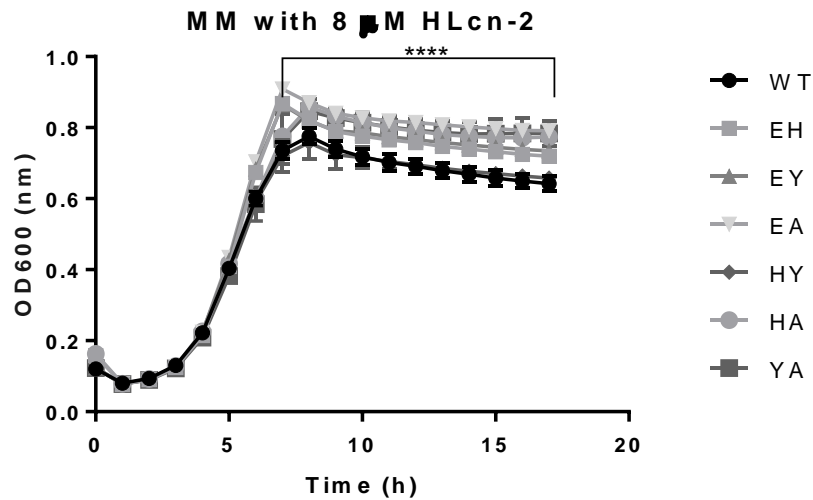
Figure 6.40 Effect of double mutations on UEC59 growth in minimal medium under iron-deficient conditions with 8 μM HLcn-2.

Strains were grown aerobically in MM containing 0.4%-glucose, with 8 µM HLcn-2, in Bioscreen-C (250 µl, 37ºC, continuous shaking). Error bars represent standard deviation from mean value. *P* values were calculated by paired t- test, using GraphPad Prism version 7©.

M M w ith Fe iron and 8 μM H Lcn-2
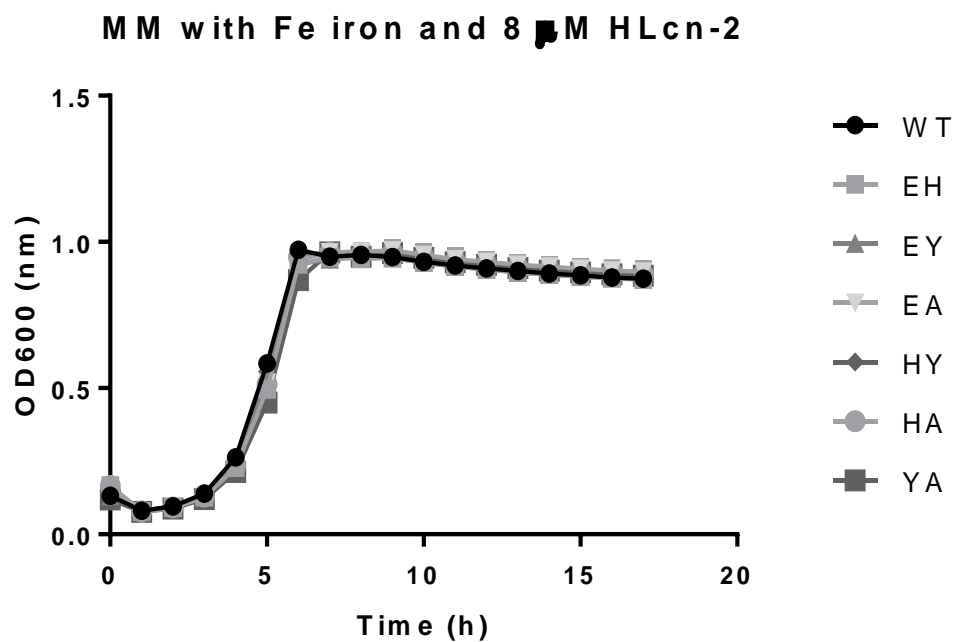
Figure 6.41 Effect of double mutations on UEC59 growth in minimal medium under iron-sufficient conditions with 8 μM HLcn-2.

Strains were grown aerobically in MM containing 0.4%-glucose, with 10 μM ferric citrate and 8 μM HLcn-2, in Bioscreen-C (250 µl, 37°C, continuous shaking). Error bars represent standard deviation from mean value. *P* values were calculated by paired t- tests, using GraphPad Prism version 7©.

6.6   Impact of iron on pathogenesis and virulence of UPEC

All the mutants (single, double and triple) were initially screened for their invasion potential using invasion assays based on gentamicin protection assays (section 6.6.1). Later all the mutants were grown under a regime of iron conditions; i) Low-Low iron (Fe-/Fe-) ii) High-Low iron (Fe+/Fe-) iii) Low-High iron (Fe-/Fe+) and iv) High-High (Fe+/Fe+), to determine the impact of iron availability on UPEC invasion capability (section 6.6.2).

6.6.1   Outcome of relative mutations on virulence potential of UPEC

 All the single, double and triple mutants were scrutinized to determine the relative effect of each of mutations on virulence potential of UPEC. All the mutants had significantly decreased invasion rate as compared to their wild types. Among single mutants, mutants with yersiniabactin (Y) and aerobactin (A) mutants had highly significant decreased in invasion (see Figure 6.42). Enterobactin biosynthesis (E) and heme uptake system (H) both had almost similar level of decrease in invasion with 54.26% and 56.5% respectively, while Y and A each had about 68% and 77 % lesser invasion respectively as compared to their WT.

Among double and triple mutants, each one had clearly decreased virulence as compared to their single mutants. The relative decrease in virulence was found as; EH (64.57%), EY (64.13%), EA (77.58%), HY (84.75%), HA (83.86%), YA (81.61%) (Figure 6.43). Among double mutants, mutants lacking heme uptake system with any other siderophores (particularly Y and A) appeared to have a drastic effect on loss of virulence as compared to enterobactin defected mutants. In accordance with single mutant results double mutant (YA) had also a decreased virulence as compared to WT. As expected, triple mutant (EYA) had the most significant (89.69%) effect on loss of virulence and the intracellular load was very low as compared to the WT. Although our *in-vitro* results revealed importance of each of the iron uptake systems in invasion of UPEC, heme, yersiniabactin and aerobactin seem to be the major

contributors. These results also correlate with our results with WT strains UEC59, UEC11, UEC82, UEC01 and UEC157. Where the UEC59 and UEC82 (encoding all the three siderophores and heme acquisition system) were the one with increased virulence as compared to UEC82 and UEC01 (encoding enterobactin, yersiniabactin and heme, no aerobactin) had lesser invasion, while UEC157 (encoding only enterobactin) was the least virulent.
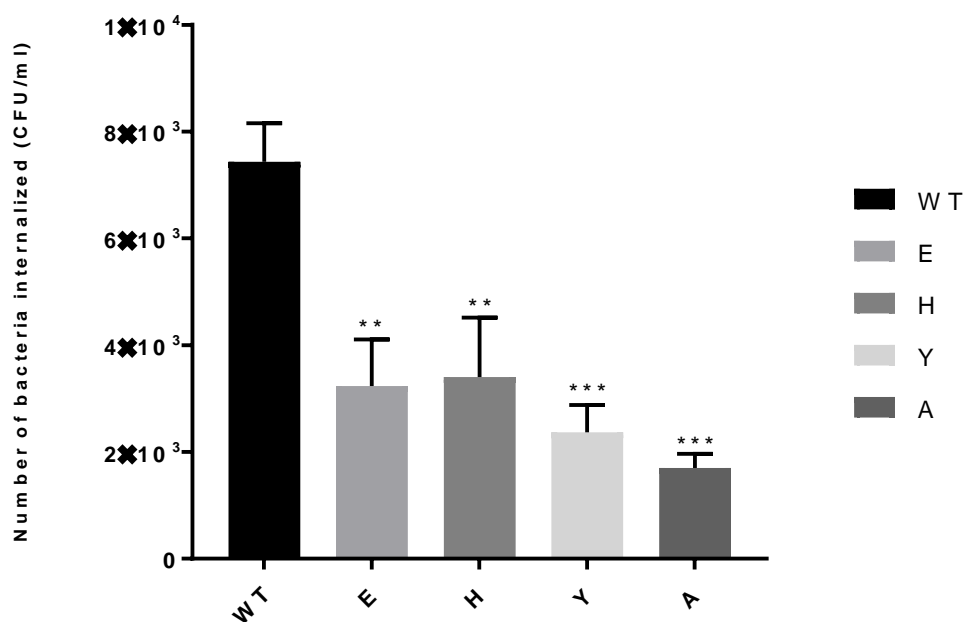
Figure 6.42 Relative invasion of UEC59 single mutants and its WT in bladder urothelial cell lines.

Each of the four mutants show reduced invasion, however yersiniabactin mutant (Y) and aerobactin mutant (A) indicate more pronounced effect as compared to WT.
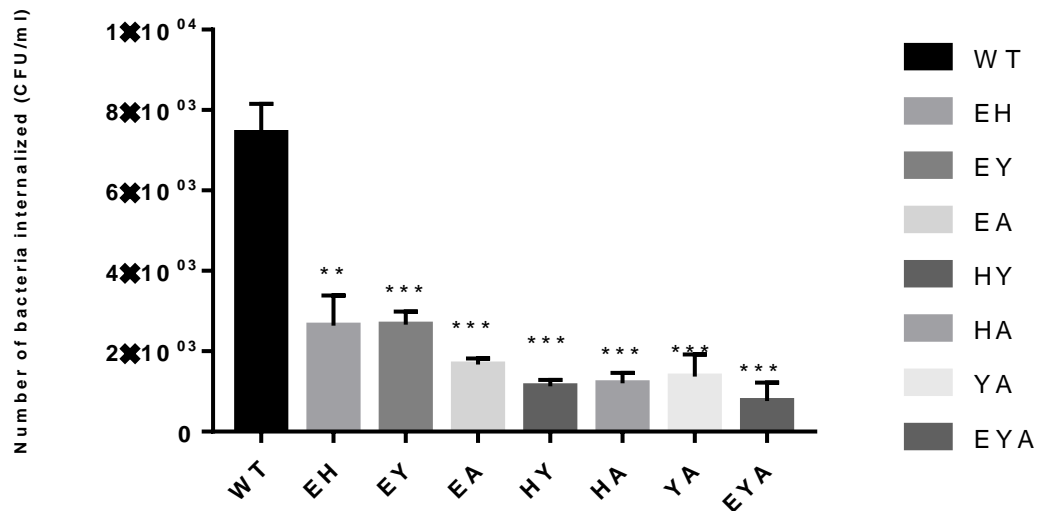
Figure 6.43 Relative invasion of UEC59 double and triple mutants and its WT in bladder urothelial cell lines.

Triple mutant EYA shows impaired invasion as compared to WT

6.6.2   Impact of iron on virulence potential of UPEC

In the previous experiment (section 6.2) it was found that increase in iron availibity had a significant effect on pathogenesis of WT strains such as UEC59 and UEC82. In order to further investigate the role of iron on pathogenesis of UPEC. All the mutants were subjected to a regime of iron conditions and their viruelnce potential was re-evaluated.

WT was observed undergoing a 3 fold ($P < 0.05$) increase when pre-culture (O/N) was grown in iron sufficient (high-low, Fe+/Fe-) conditions as compared to the condition when strain was grown in iron-deficient conditions (low-low, Fe-/Fe-) -see Figure 6.44 and 6.45. Similarly a 22 fold ($P < 0.0001$) increase in bacterial load was observed when iron was supplemented extracellularly (low-high, Fe-/Fe+) in cell culture medium and a 30 fold ($P < 0.0001$) increase was observed when pre-culture and cell culture medium both were supplemented with 10 µM ferric citrate (high-high, Fe+/Fe+). Similarly enterobactin mutant (E) observed a 2 fold increase ($P < 0.05$) when grown under high-low iron conditions as compared to low-low iron conditions.

Under high-low conditions an increase in 25 fold ($P<0.01$) was determined, following high-high iron conditions with a 28 fold ($P<0.0001$) increase in bacterial invasion. Single mutant such as heme uptake mutantst (H) obseved a 17 fold ($P<0.001$) increase in intracellular bacateriaa load under high-high iron conditiions as compared to low-low iron conditions. Yersinabactin mutant (Y) and aerobactin mutant (A) also showed a sginificant increase in intracellular load under increased iron conditions as compared to the low-low conditions. Although there was a significant increase in bacterial invasion potential with incareasing iron conditions, yet there was a clear difference in their ability to invade cell lines when comapared to WT and none of the single mutants could restore their WT virulence potential in the presence of iron.

In case of double mutants (EH, EY, EA, HY, HA and YA), a significant increase ($P<0.05$) in bacterial invasion was observed only under high-high conditions. Similarly triple mutant showed increase in invasion under high-high iron conditions,as compared to low-low, high-low and low-high conditions. These observations clearly define role of iron in pathogenesis of UPEC, moreover they identify the importance of extracellular iron in increasing the invasion poential, by providing excessive bio available iron for their cellular needs.
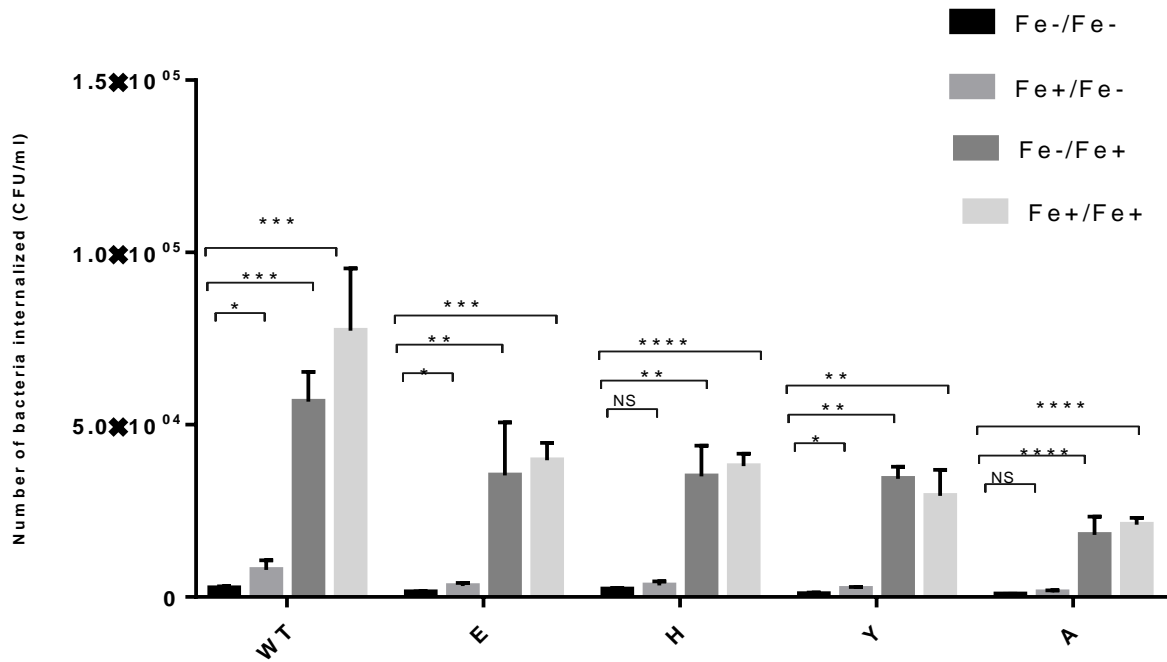
Figure 6.44 Effect of iron concentrations on invasion of UEC59 and its single mutants.

Figure shows an increase in rate of invasion with increasing iron concentration. WT had the most apparent increase in invasion.
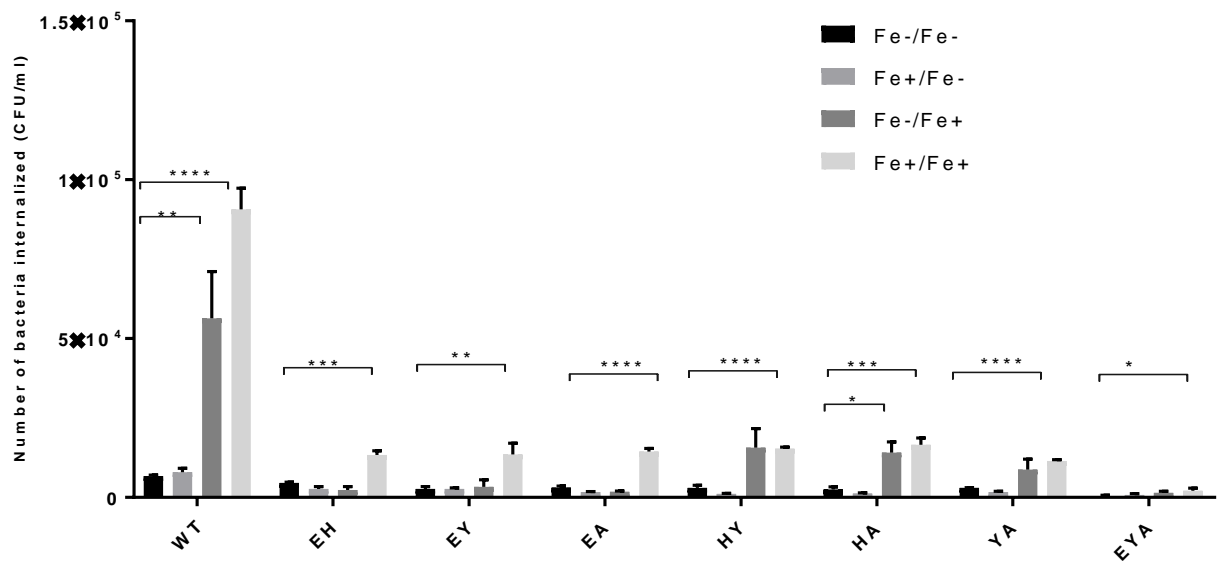
Figure 6.45 Effect of iron on invasion of UEC59 double and triple mutants.

Figure shows an increase in invasion potential of double and triple mutants, only under high-high (Fe+/Fe+). WT has the most significant effect on it invasion potential under all the iron regimes

CHAPTER 7:   **Whole genome sequencing and comparative genomic analysis of UPEC isolates demonstrating multidrug resistance and high virulence profile**

7.1   Next generation sequence (NGS) analysis of Uropathogenic *E. coli* strain UEC11

7.1.1   Background

UPEC is the major etiological agent of UTI and is increasingly becoming resistant to all the frontline antibiotics recommended against it (Tandogdu and Wagenlehner, 2016a). ST131 is an intriguing sequence type of extra-intestinal pathogenic *E. coli* (EXPEC) that is not only multi drug resistant but also possess an arsenal of virulence factors (Nicolas-Chanoine et al., 2014). This deleterious combination is making its treatment extremely difficult. Whole genome sequencing of UPEC strains can give a comprehensive insight about its resistance markers, virulence factors, plasmid types and other epidemiological markers. Till now, none of UPEC strains from Pakistan has been sequenced. The present study focuses on whole genome sequencing of twenty MDR strains isolated from patients of community acquired UTIs. Present study focuses on detailed description of one isolate (UEC11, section 7.1) while later section 7.2 describes the comparative genomic analysis of these twenty isolates (including UEC11) to give comprehensive picture of genetic attributes of MDR UPEC isolates.

7.1.2   Genome sequencing of UEC11

UEC11 is a ST131 UPEC strain collected from a 23-year-old female patient (Islamabad, Pakistan) suffering from a CA-UTI. Sequencing was performed by MicrobesNG (IMI- School of Biological Sciences, University of Birmingham) on MiSeq and HiSeq 2500 platforms (Illumina, UK) and a sequence coverage of 30X was obtained. The reads were trimmed using

Trimmomatic by identification of adapter sequences and quality filtering (Bolger et al., 2014b). The quality of trimmed reads was assessed using in-house scripts combined with the SAMTools (Sequence Alignment/Map) tools, BEDTools (Browser Extensible Data) and BWA-MEM (Burrows-Wheeler Alignment , software (Li and Durbin, 2009). Kraken taxonomic sequence classification system (https://ccb.jhu.edu/software/kraken/) was used to assign taxonomic labels to the short DNA reads using exact alignment of *k-mers*. Table 7.1 shows the top hits obtained for the genome sequence data obtained for UEC11 confirming that the genome is from a *E. coli* strain.

Table 7.1 Taxonomic distribution of UEC11 isolate using Kraken software.

		Percentage (%)
Unclassified	Unclassified	0.34
Most frequent family	Enterobacteriaceae	98.22
2nd most frequent family	Myoviridae	0.03
Most frequent genus	*Escherichia*	88.12
2nd most frequent species	*Shigella*	0.10
Most frequent species	***Escherichia coli***	87.46
Escherichia coli	*Escherichia coli*	87.46

7.1.3   Genome assembly

De novo assembly of the reads was performed using SPAdes (v 3.11.) genome assembler based on de Bruijn graph assembler (Bankevich et al., 2012). The assembly was done by merging overlapping sequence reads into contiguous sequences (contigs). The genome assemblies were evaluated, and the metrics were calculated using Quality Assessment Tool for Genome Assemblies (QUAST) (Gurevich et al., 2013). QUAST report indicated UEC11 has a total genome size of 5310985 bp (5.31Mb) and a GC content of 50.73%. A total of 144 contigs were obtained after assembly (Table 7.2).

Table 7.2 Quality metrics for Uropathogenic *E. coli* UEC11 assembly using QUAST (Quality Assessment Tool for Genomic Assemblies).

# contigs	144
Largest contig	667628 bp
Total length	5310985 bp
N50[a]	191062 bp
GC (%)	50.55
Mismatches	
# N's per 100 kb[b]	0

[a] N50 is the shortest sequence length at the 50% of genome. [b] #N's per 100 kb is the total number of uncalled bases per 100000 assembly bases.

7.1.4   Finding closest reference genome

In order to find the closest match for mapping, the nucleotide sequence of seven housekeeping genes of UEC11 were concatenated in the order *adk, fumC, gyrB, icd, mdh, purA* and *recA* using CLC Main workbench 7. The resulting 9015 bp fragment was then blasted using NCBI BLAST to find the closest reference genomes using the same software the results of alignment were used to construct maximum likelihood phylogenetic tree. Figure 7.1 shows closet genomes found with NCBI BLAST tool.
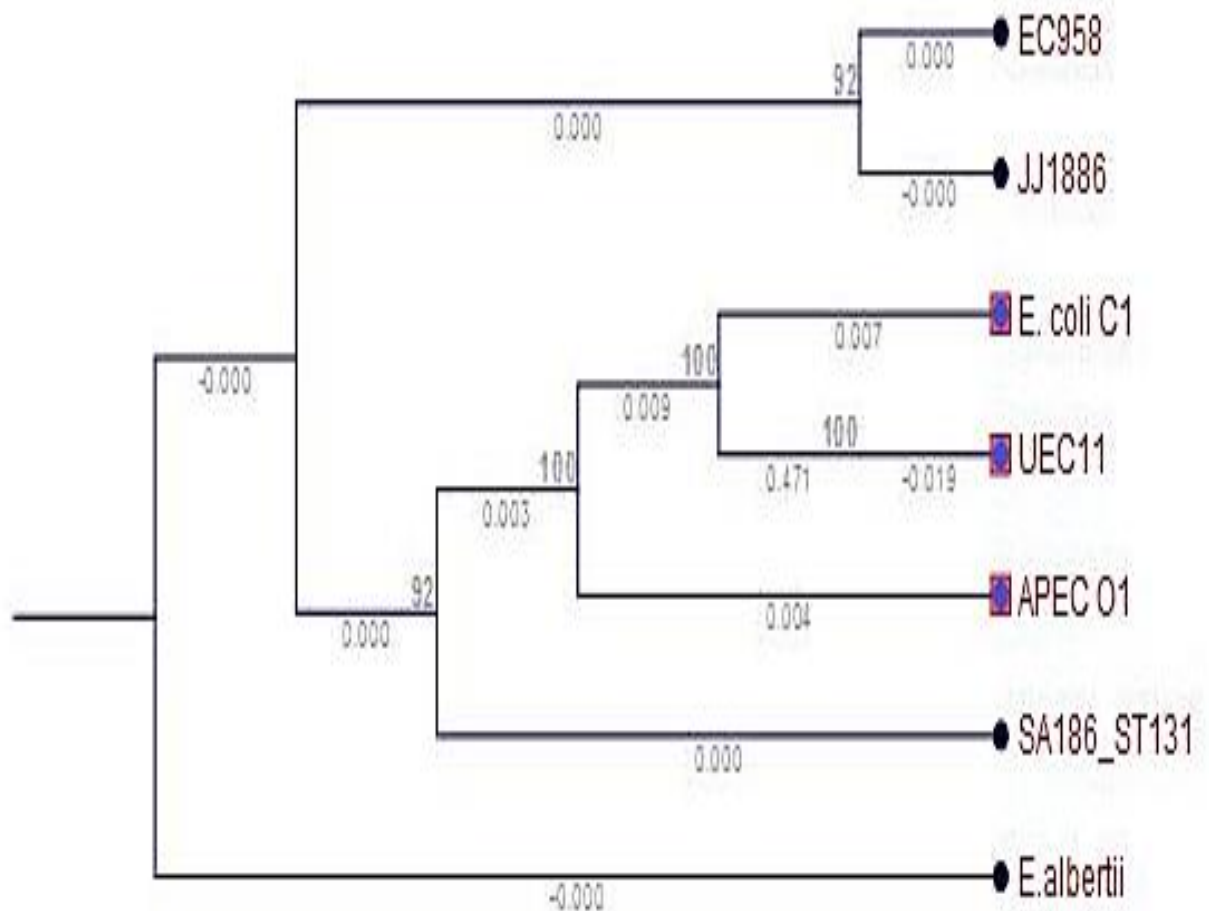
Figure 7.1 Maximum likelihood phylogenetic tree of UEC11.

Phylogenetic tree was constructed using concatenated nucleotide sequences of the seven MLST housekeeping gene fragments in the order *adk, fumC, gyrB, icd, mdh, purA and recA* using the CLC main workbench v 7.0. A bootstrap value and branch length are attached to each node, the value indicates measure of the confidence in the subtree rooted at the node. *E. albertii* was used as an outgroup strain.

7.1.5   Mapping against reference genome

Mapping of the contigs against the reference genome was carried out using an online tool

CONTIGuator (http://combo.dbe.unifi.it/contiguator). This tool combines the routines of one

of the most commonly used tool ABACAS (BLAST and MUMmer) and allows the

visualization of a map of contigs with Artemis comparison tool (ACT) (Galardini et al., 2011).

While mapping our strain with the closely matched genomes, the strain which showed maximum number of contigs mapped against our strain was further used as a reference genome. The strain with maximum mapping was JJ1886, which is highly virulent CTX-M-15 producing UPEC strain isolated from a patient with urosepsis in 2007. Genome size of the strain is 5,129,938-bp (chromosome) with a GC content of 50.8% (accession number: CP006784), and also harbors five plasmids (Andersen et al., 2013). The output files were viewable in ACT, with the reference genome on top and query UEC11 on bottom (Fig 7.2 and 7.3).

A total of 46 contigs of 5010033 bp (94% of the genome) were mapped with chromosomes, while 8 contigs of size 112503 bp (2% of the genome) were mapped against its plasmids. Whereas 40 contigs of 188449 bp remained unmapped (3.5% of the genome) and 50 contigs of size <500 bp (0.5% of the genome) were eliminated by the software due their small size.
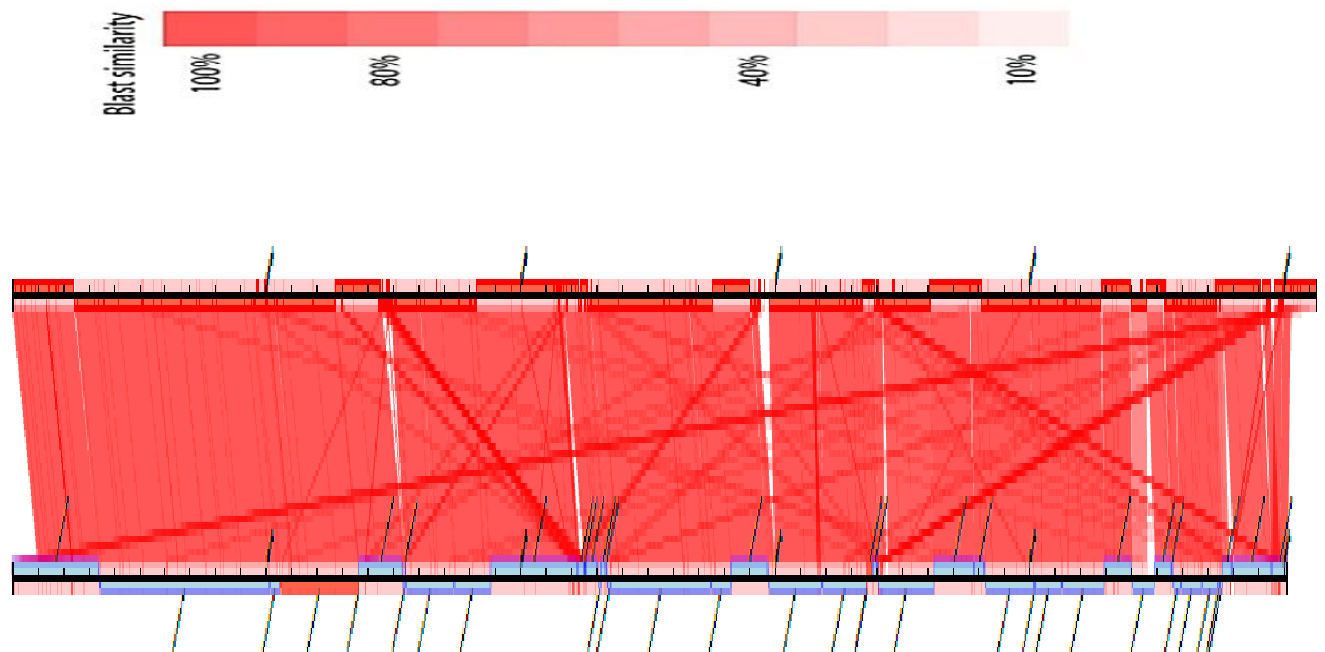
Figure 7.2 Mapping of UEC11 (on bottom) against reference genome of JJ1886 (on top) using CONTIGuator software

Figure shows 46 contigs of size 5010033 bp mapped against chromosome (replicon I) of strain JJ1886. The map view was generated using ACT.
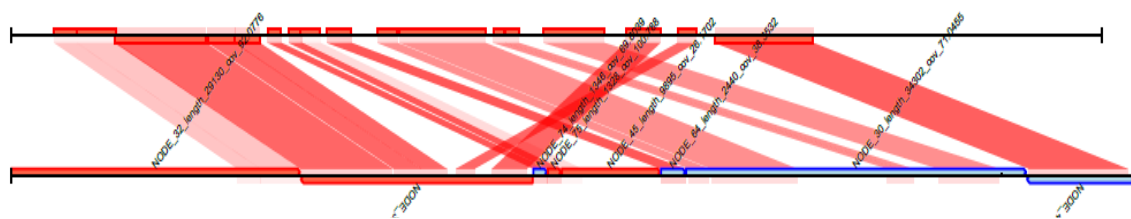
Figure 7.3 Mapping of UEC11 (on bottom) against reference genome of JJ1886 (on top) using CONTIGuator software.

Figure shows 8 contigs of size 112503 bp mapped against plasmid (replicon II) of strain JJ1886. The map view was generated using ACT.

7.1.6   Sequence typing and serogrouping

Sequence type of UEC11 was determined using Achtman pubmlst database

(https://pubmlst.org), based on seven housekeeping genes (*adk, fumC, gyrB, icd, mdh, purA,*

recA). According to the allelic profile of each of these seven loci, UEC11 was assigned as sequence type (ST) ST131 and clonal group ST131 complex (Table 7.3).

Serotyping and FimH typing was performed using SerotypeFinder (https://cge.cbs.dtu.dk/services/SerotypeFinder/) and FimTyper webtool (https://cge.cbs.dtu.dk/services/FimTyper/) respectively, which identified UEC11 as H4-O25b sub-clone H-30, indicating that it is an epidemiologically virulent and MDR strain. Overall, UEC11 was indicated as ST131-O25b-H30.

Table 7.3 . Allelic profile of seven housekeeping genes of UEC11 according to Atchtman's PubMLSTdatabase.

Locus	Allele	Length	Contig	Start position	End position
adk	53	536	NODE_1	389225	389760
fumC	40	469	NODE_16	70145	70613
gyrB	47	460	NODE_12	62043	62502
icd	13	518	NODE_5	11661	12178
mdh	36	452	NODE_13	110874	111325
purA	28	478	NODE_14	50895	51372
recA	29	510	NODE_7	147768	148277

7.1.7   Genome annotation

Genome annotation was performed using "The Pathosystems Resource Integration Center (PATRIC)" database (**https://www.patricbrc.org**) and NCBI Prokaryotic Genome Annotation Pipeline (PGAP)   (Wattam et al., 2016, Wattam et al., 2014) **.** PATRIC derives information from two basic annotation tools RAST tool kit (RASTtk) and BLAST. RASTtk offers users a standard software pipeline for identifying genomic features (i.e., protein-encoding genes and RNA) and annotating their functions (Brettin et al., 2015). While BLAST performs comparison with several externally curated 'Specialty Genes' databases such as

virulence factors databases like Virulence Factor Database (VFDB) and Victors (Chen et al., 2005, Mao et al., 2014). It also derives information from databases for antimicrobial resistance such as; National Database of Antibiotic Resistant Organisms (NDARO)**,** the Comprehensive Antibiotic Resistance Database (CARD) and Antibiotic Resistance Database (ARDB) (Antonopoulos et al., 2017)**.**

Genome annotation using PGAP revealed total 5600 coding sequences (CDS) with 106 genes specific for RNA. Out of 106 RNA genes, 7, 9, 4 (5S, 16S, 23S) encoded rRNA, 81 (tRNA) and 8 encoded ncRNA. Moreover, 289 pseudogenes were also part of UEC11 draft genome.

7.1.8   Virulence repertoire encoded by UEC11

PATRIC revealed UEC11 also encodes a wide array of virulence genes that explains its virulent and invasive nature. Such virulence genes include those encoding adhesins and invasins (*fimH, papGI, papGII, papGIII, papC*, *papH*), toxins (*cnf1*, RTX, *espC*) and a hypothetical enterotoxin similar to *senB* of *Shigella flexneri* 2a str. 30. UEC11 also encodes various iron-acquisition systems: uptake and synthesis of enterobactin, aerobactin and yersiniabactin; uptake of heme; and uptake of ferrous iron (Feo and Efe). The serum-resistance gene (*traT*) and *csgB* (encoding curlin) required for biofilm formation were also identified. Phenotypic detection of virulence factors correlated well with whole genome results.

7.1.9   Antimicrobial resistome encoded by UEC11

Genome annotation performed using PATRIC and CARD (https://card.mcmaster.ca/analyze/rgi), indicated three β-lactamases: CTXM-15 (class A); OXA-1 (class D); and AmpC (class C). Additionally, genes conferring resistance to tetracycline (*tetA*), chloramphenicol (*catB*), fluoroquinolones (*gyrA* mutations; S83L, D87N), aminoglycosides (*aac(3')-IIc,   aac(6')-Ib/aac(6')-II,   aph(3'')-Ia*), sulfonamide (*sul2*),

trimethoprim (*dfrA17*) and macrolides (*mph(A)*) were identified, explaining the observed ESBL and MDR status. A Tn*3* transposon (carrying a tetracycline resistance gene) and a class 1 integron (carrying a trimethoprim resistance gene), were also identified.

7.1.10 Insertion sequence elements and Integrated and conjugative elements

Insertion elements (IS) and integrated and conjugative elements (ICE) were determined with IS finder (https://isfinder.biotoul.fr/) (Varani et al., 2011) and ICEberg (http://db-mml.sjtu.edu.cn/ICEberg/) (Bi et al., 2012).A yersiniabactin synthesis-associated ICE (highly similar to ICEEcoUMN026-1 of UPEC UMN026) of 65,732 bp was also identified. A total of 77 IS elements (belonging to 18 families) were identified. IS3, ISL3, IS200 and IS66 families were those predominantly present.

7.1.11 Plasmid identification

Four plasmids incompatibility (Inc) groups were identified using PLASMIDFinder (https://cge.cbs.dtu.dk//services/PlasmidFinder/) (Carattoli et al., 2014) corresponding to incompatibility groups IncFII, IncFIA, IncFIB and Col156.

Table 7.4 Plasmid incompatibility groups in UEC11 as identified by Plasmid MLST.

Locus	Allele	Length	Contig	Start position	End position
FIA	2	384	NODE_32_length_29130_cov_92.0776	25221	25604
FIA	6	329	NODE_32_length_29130_cov_92.0776	25276	25604
FIB	20	373	NODE_32_length_29130_cov_92.0776	8860	9232
FII	2	157	NODE_30_length_34302_cov_71.0455	2052	2208

7.1.12 CRISPR-CAS detection

In order to detect CRISPR-cas sequences in draft genome, CRISPRcasfinder database (http://crispr.i2bc.paris-saclay.fr/) was used (Grissa et al., 2007). CRISPRs are Clustered Regularly Interspaced Short Palindromic Repeats, found in the DNA of many archaea and bacteria. These direct repeats (DR) vary in size from 23 to 47 bp and are usually separated by spacer sequences of simililar length. While the spacers are conserved sequences, direct repeats are not totally conserved and may be called as degenerate repeats. Spacers are unique in genome and are thought to be derived from phages nad protect bacteria from infection (Grissa et al., 2007).

UEC11 was found to have three CRISPR sequences of 292, 324 and 283 bp respectively were found but no Cas locus was found (Figure 7.4 and 7.5).
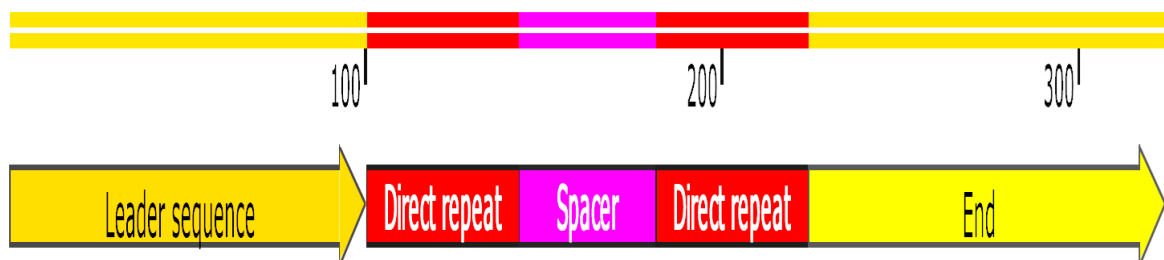
Figure 7.4 CRISPR sequence of 324 bp identified by CRISPR-Cas in UEC11

CRISPR sequence of 324 bp identified by CRISPR-Cas finder shows, a leader sequence of 100 bp, followed by two DR of 43 bp (conservation DR 100 %) and a spacer sequence of 38 bp (Conservation Spacer100 %). No Cas sequence was detected. Figure was generated for Contig 16, using SnapGene® software (from GSL Biotech; available at snapgene.com).
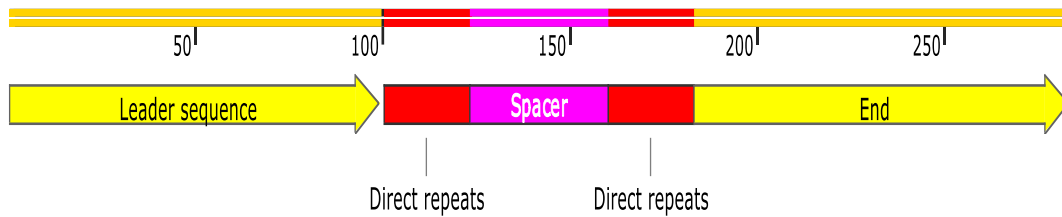
Figure 7.5 CRISPR sequence of 283 bp identified by CRISPR-Cas finder in UEC11

 CRISPR sequence of 283 bp identified by CRISPR-Cas finder shows, a leader sequence of 99 bp, followed by two DR of 23 bp (cconservation DR 95.65 %) and a spacer sequence of 37 bp (Conservation Spacer100.00 %). No Cas sequence was detected. Figure was generated for Contig 28, using SnapGene® software (from GSL Biotech; available at snapgene.com).

7.1.13 Prophage identification

Prophage sequences in UEC11 genome were detected using PHASTER (http://phaster.ca/) (Arndt et al., 2016). Seven intact (PHAGE_Gordon_Kita, 27.1Kb; PHAGE_Entero_BP, 29.4Kb;   PHAGE_Burkho_phiE255,   36.8Kb;   PHAGE_Entero_P88,   41.2Kb; PHAGE_Entero_lambda, 28.4Kb; PHAGE_Yersin_L_413C, 33.9Kb; PHAGE_Entero_BP, 25.7kb) and one incomplete (PHAGE_Entero_BP_4795, 26.5kb) prophage regions were detected.. In addition, two questionable prophage regions were also identified (Figure 7.6). Altogether, they comprised ~5% of the whole genome of UEC11.

PHASTER identified a genomic island of 26642 bp encoding multiple resistance genes incorporated at position 5256883 to 5283524 (See Figure 7.7).
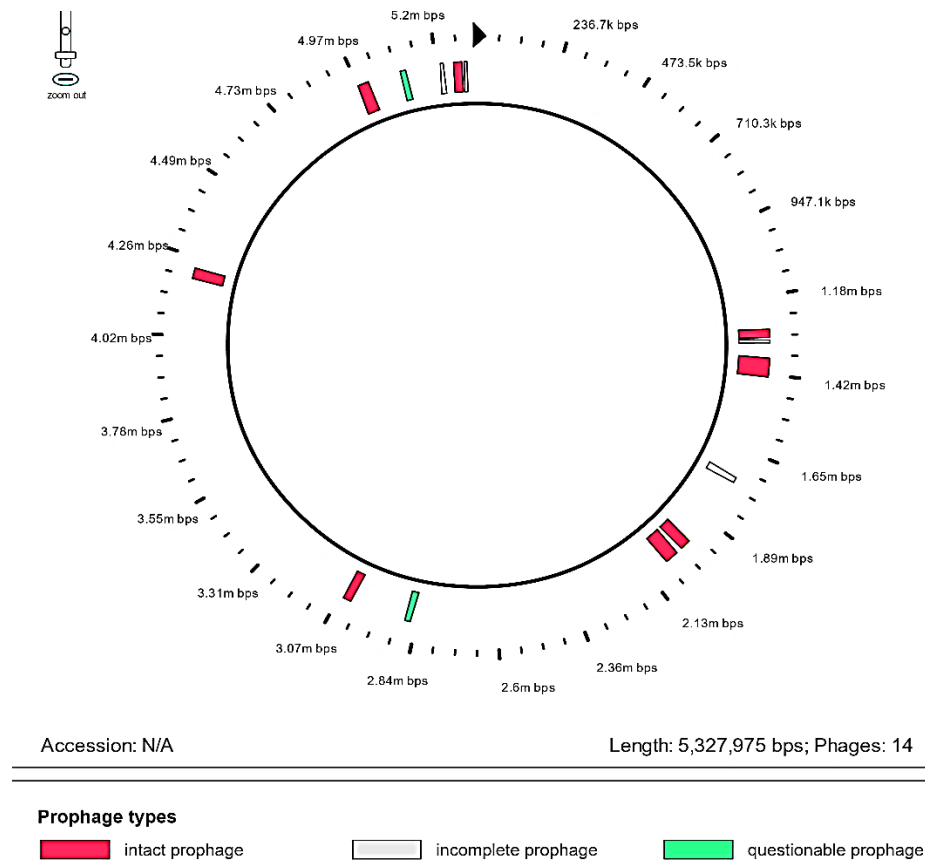
Figure 7.6 Circular map of UEC11 shows prophage sequences detected by PHASTER

Circular map of UEC11 shows prophage sequences detected by PHASTER, eight intact prophages (in red), four incomplete (in white) and two questionable (in teal) prophages are indicated at different positions on draft genome.

Figure 7.7 Prophage region 13 encoding antimicrobial resistance genes.

Prophage region (5256883 to 5283524) is shown encoding (left-right) insertion sequences, transposases, *catB*, *bla*$_{OXA-1}$, ANT (3'')-Ia-AadA5 and *sul-1*.

7.1.14 GeneBank accession number

This Whole Genome Shotgun project has been deposited at GenBank under the accession QICE00000000. The version described here is version QICE01000000.

7.2   Comparative genomic analysis of twenty (20) UPEC isolates

Comparative genomic analysis based on WGS was performed on twenty UPEC isolates. Previous phenotypic and genotypic profiling of these isolates confirmed them as MDR-virulent isolates.

7.2.1   Strains information

The assembly of the twenty UPEC isolates used in this analysis were comprised of 79 to 161 contigs (Table 7.5). Average GC content was ~50% and the average coding sequences (CDS) of all the twenty strains were found to be ~5360 and on average 84 sequences per isolate encoded tRNA.

Table 7.5 Twenty MDR-virulent UPEC isolates assembly and genomic information

Strain ID	Genome size (bp)	GC content (%)	CDS	Contigs (n)	tRNAs
UEC11	5310985	50.7	5433	126	82
UEC59	5324938	50.5	5386	116	86
UEC31	5326740	50.6	5475	95	80
UEC87	5141326	50.6	5174	79	79
UEC98	5371191	50.5	5452	126	89
UEC12	5477810	50.5	5574	109	88
UEC82	5274347	50.6	5297	123	87
UEC21	4979563	50.6	4990	95	82
UEC44	5389426	50.7	5539	118	86
UEC01	5198112	50.6	5174	95	87
UEC06	5351018	50.6	5459	108	86
UEC15	5246326	50.48	5313	121	86
UEC51	5475873	50.5	5691	110	80
UEC14	5275521	50.7	5399	121	84
UEC81	5271745	50.5	5447	161	87
UEC38	5478680	50.5	5701	111	80
UEC175	5194620	50.6	5175	102	87
UEC16	4980015	50.6	4994	95	83
UEC85	5354420	50.6	5517	95	79
UEC157	4927090	50.51	5008	113	87
JJ1886 (Ref)*	5308284	50.7	5349	Complete genome	89
NA114 (Ref)*	5246175	50.7	5319	126	81
EAEC 266917 (Ref)*	5887450	50.3	6014	Complete genome	102

- UPEC reference genomes

7.2.2   Phylogenomic analysis

Phylogenomic analysis was performed using GeGeenes V 3.10. GeGeenes clustered the isolates along with three reference strains into 6 clusters based on their similarity index (Figure 7.8 and 7.9). MLST of these isolates confirmed that the isolates belong to six (6) distinct sequence types.

7.2.3   Sequence typing and serogrouping

Out of 20, nine isolates (UEC06, UEC11, UEC 14, UEC31, UEC38, UEC44, UEC51, UEC85, UEC87) belong to ST131 (Table 7.6). These nine isolates were found closely related to reference strains JJ1886 and NA114, both belonged to ST131. Similarly, 5 isolates (UEC01, 12, UEC82, UEC12, UEC175) belonged to ST405 and were clustered together in one group. 2 isolates (UEC16 and UEC21) belonged to ST162 and other two isolates (UEC81 and UEC57) belonged to ST10. One isolate (UEC59) belonged to ST38 and was found closely related to reference strain EAEC266917(ST38).

Serogrouping and FimH typing revealed that all the nine isolates of ST131 clonal group belonged to serogroup O25b:H4/H30. Likewise, all five isolates of ST405 clonal group were found in serogroup O102:H6/H27. Interestingly one isolate, UEC15 (ST648) was found to have a unknown serotype (On:H6/Hn).
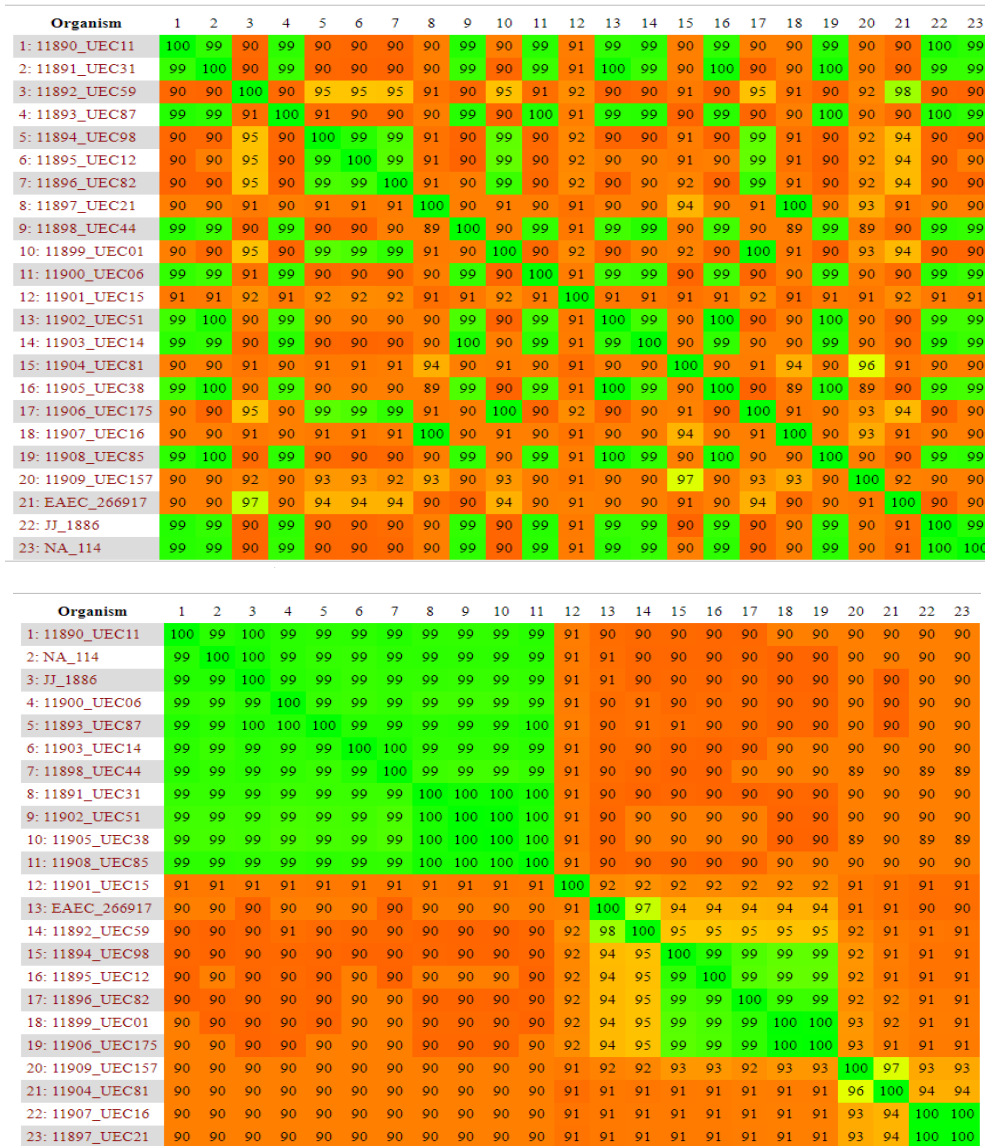
Figure 7.8. Heat-plots of the similarity matrices of 23 UPEC isolates including three reference genomes (JJ1886, NA114 and EAEC266917).

The heat-plot is based on a fragmented alignment using BLASTN made with settings 500/500 at threshold 30. Heat maps were generated using Gegenees V 3.10. The numbers in heatmap represent the similarity index (in percentages) between twenty-three (23) genomes. The colors vary from high (green) to low (orange) similarity.
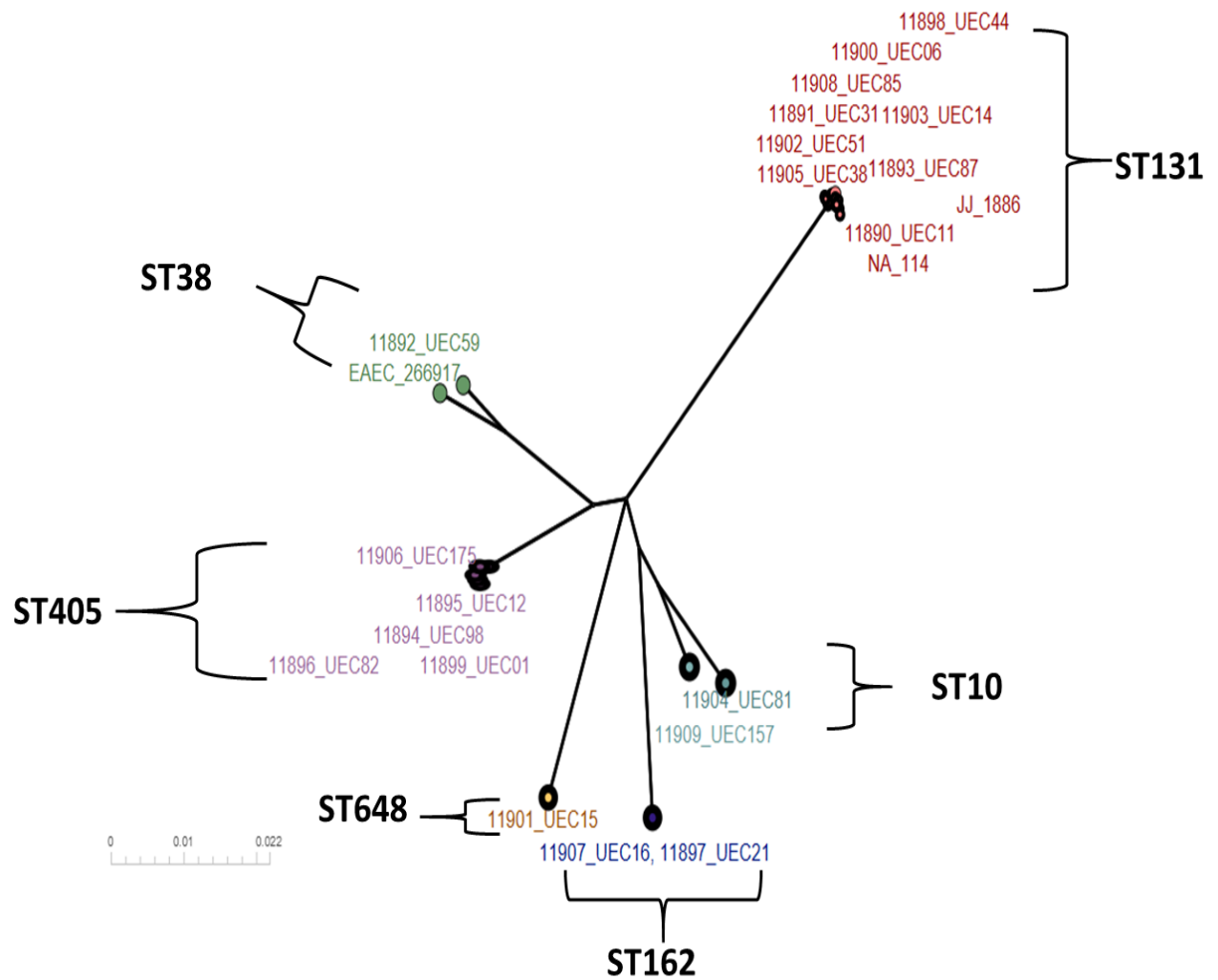
Figure 7.9. A dendrogram constructed in SplitsTree 4 (using neighbor joining method).

Phylogenetic tree was constructed in SplitsTree based on distance matrix obtained from Gegenees. The tree shows 23 UPEC isolates belong to six different clusters. MLST analysis confirmed the clusters as 6 distinct STs (ST131. ST405, ST38, ST648, ST10, ST162).

Table 7.6 Sequence typing and serogrouping of UPEC isolates.

Strain ID	ST	Serotype/FimHtype
UEC11	131	O25:H4/H30
UEC59	38	O1:H15/H65
UEC31	131	O25:H4/H30
UEC87	131	O25:H4/H30
UEC98	405	O102:H6/H27
UEC12	405	O102:H6/H27
UEC82	405	O102:H6/H27
UEC21	162	O88:H10/H32
UEC44	131	O25:H4/H30
UEC01	405	O102:H6/H27
UEC06	131	O25:H4/H30
UEC15	648	On:H6/Hn
UEC51	131	O25:H4/ H30
UEC14	131	O25:H4/H30
UEC81	10	O15:H4/H28
UEC38	131	O25:H4/H30
UEC175	405	O102:H6/H27
UEC16	162	O88:H10/H32
UEC85	131	O25:H4/H30
UEC157	10	O89:H9/Hn

7.2.4   Virulence repertoire of UPEC isolates

Virulence attributes of the twenty isolates were detected using PATRIC and VFDB. VF such as *fimH, papGII, papGII, csgB, fepA* and *traT* were found uniformly distributed among all the STs. However, certain VF such as *papI, papC, papEF* (adhesins) and toxins such as RTX and *cnf1* were significantly associated with ST131 (Table 7.7). Iron acquisition genes (*iutA, fyuA* and *chuA)* were also more frequent among ST131, although the association was not statistically significant. These results suggest that ST131 has relatively robust virulence profile which could be a driving force for their better adaptability and successful dissemination.

7.2.5   Antibiotic resistome and plasmid typing

Presence of antibiotic resistance genes were confirmed by blasting the WGS against CARD database. All the isolates carried resistance genes conferring resistance to multiple antibiotics. A A wide range of resistance genes such as extended spectrum beta lactamases *(bla*CTXM-15, *bla*TEM, *bla*OXA, *bla*SHV, *bla*CMY), sulfonamide resistance genes (*sul-1, sul-2*) chloramphenicol resistance gene [*cat(B)*], [*tet(A/B)*], macrolide resistance genes *mph(A),* trimethoprim resistance genes (*dfrA17*) and genes conferring resistance to aminoglycosides [*(aph(3″)-I, aph(3″)-Ia*] were also detected. In addition, *gyrA, gyrB, parA, parE* mutations conferring resistance against fluroquinolones were also detected among all STs.

However, resistance genes such as *bla*CTXM-15, *bla*OXA, *cat(B)*, *dfrA17* were significantly (*P<0.05*) associated with ST131. Likewise, plasmid typing confirmed that plasmid type IncF1A and IncI1 were significantly more prevalent among ST131. Plasmid type Col156 was also found more frequent (78%) among ST131 isolates as compared to non-ST131 isolates (45%), although the association was not statistically significant (Table 7.8).
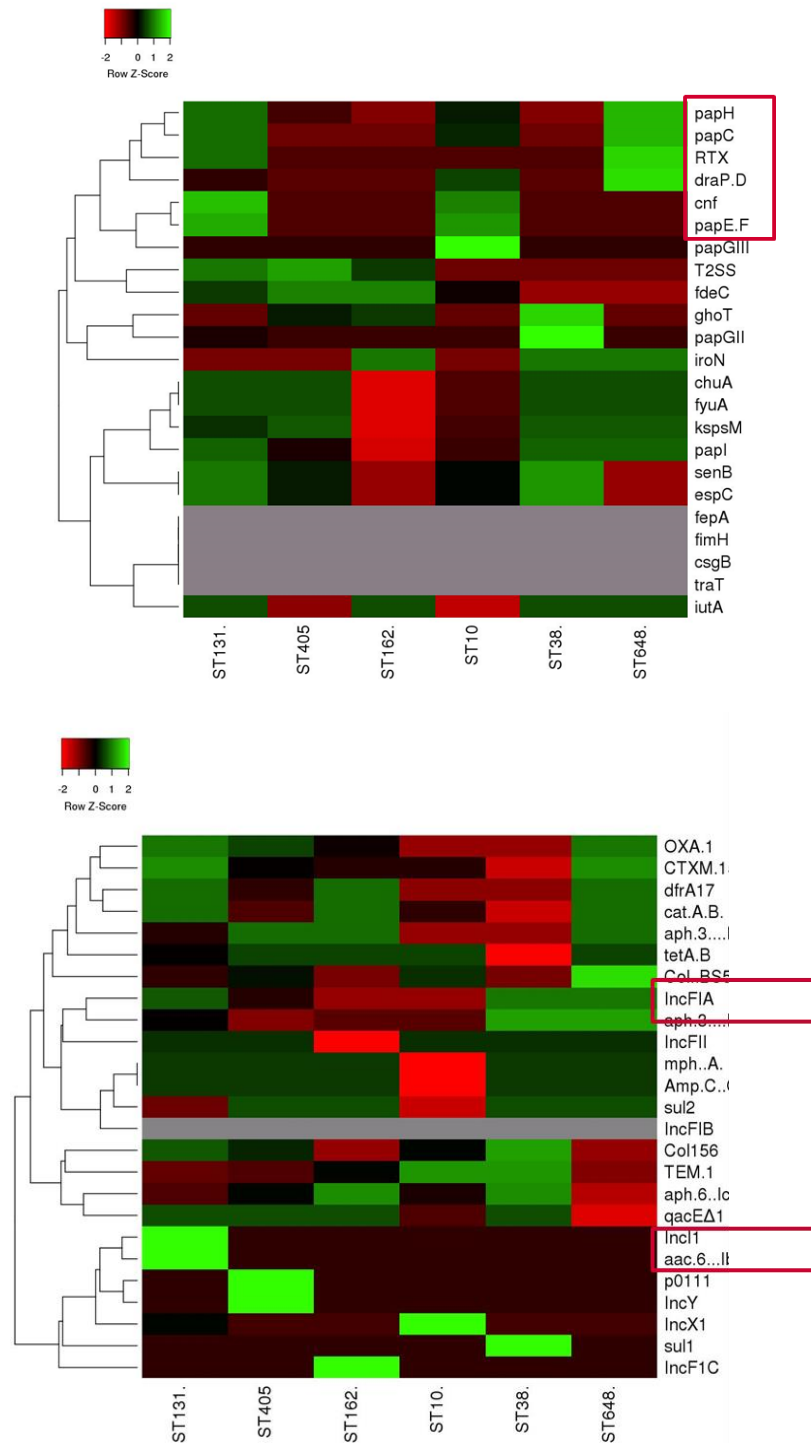
Figure 7.10. Heat map shows distribution of virulence factors, resistance markers among different STs.

VF such as *papC, papEF, papH, RTX, cnf* seem significantly more distributed among ST131. Similarly, resistance markers such as CTXM-15, OXA-1 and plasmids types IncFIA and IncI1 are observed more in ST 131. Gray areas mark traits with uniform distribution among all STs.

Table 7.7 Distribution of virulence factors among different STs

Traits	ST131 (n=9)	Other STs (n=11)	*P value
fimH	9 (100%)	11 (100%)	>0.9999
papI	9 (100%)	6 (54.5%)	0.0379
papGII	1 (11.11%)	1 (9%)	>0.9999
papGIII	0	1 (9%)	>0.9999
papC	7 (77.77%)	2 (18.18%)	0.0216
papE/F	5 (55.56%)	1 (9%)	0.0498
papH	7 (77.77%)	3 (27.27%)	0.0698
draP/D	1 (11.11%)	2 (18.18%)	>0.9999
fdeC	7 (77.77%)	8 (72.73%)	>0.9999
kspsM	8 (88.89%)	8 (72.73%)	0.5913
RTX	6 (66.69%)	1 (9%)	0.0166
cnf	6 (66.69%)	1 (9%)	0.0166
espC	8 (88.89%)	5 (45%)	0.0703
senB	8 (88.89%)	5 (45%)	0.0703
T2SS	6 (66.67%)	6 (54.55%)	0.6699
ghoT	0	4 (36.36%)	0.0941
iutA	9 (100%)	8 (72.73%)	0.2184
fepA	9 (100%)	11 (100%)	>0.9999
iroN	0	4 (36.36%)	0.0941
fyuA	9 (100%)	8 (72.73%)	0.2184
chuA	9 (100%)	8 (72.73%)	0.2184
csgB	9 (100%)	11 (100%)	>0.9999
traT	9 (100%)	11 (100%)	>0.9999

* *P* value was calculated using Fisher-exact test.

Table 7.8 Distribution of resistance markers and plasmid types among different STs

Traits	ST131 (n=9)	Other STs (11)	*P value
CTXM-15	9 (100%)	6 (54.5%)	0.0379
TEM-1	1 (11.11%)	5 (45%)	0.1571
OXA-1	9 (100%)	6 (54.5%)	0.0379
Amp(C)/CMY-2	9 (100%)	10 (91%)	>0.9999
cat(A/B)	9 (100%)	6 (54.5%)	0.0379
tetA/B	7 (77.8%)	10 (91%)	0.5658
sul1	0	1 (9%)	>0.9999
sul2	6(66.6%)	10 (91%)	0.2848
dfrA17	9 (100%)	5 (45%)	0.0141
mph (A)	9 (100%)	10 (91%)	>0.9999
qacEΔ1	9 (100%)	9 (82%)	0.4789
aph(3")-I	6 (66.67%)	6 (54.55%)	0.6699
aph(3")-Ia	4 (44.44%)	8 (72.73%)	0.3618
aph(6)-Ic/aph(6)-Id	3 (33.33%)	7 (63.64%)	0.1775
aac(6')-Ib-cr	3 (33.33%)	0	0.0737
IncFII	9 (100%)	9 (82%)	0.4789
IncFIA	8 (88.89%)	4 (36.36%)	0.0281
IncFIB	9 (100%)	11 (100%)	>0.9999
IncF1C	0	2 (18.18%)	0.4789
IncI1	5 (55.56%)	0	0.0081
IncX1	1 (11.11%)	1 (9%)	>0.9999
IncY	0	1 (9%)	>0.9999
p0111	0	2 (18.18%)	0.4789
Col (BS512)	2 (22.22%)	4 (36.36%)	0.6424
Col156	7 (77.8%)	5 (45%)	0.1968

* *P* value was calculated using Fisher-exact test.

7.2.6   Prophage and CRISPR-cas identification

Prophage identification using PHASTER showed that ST131 isolates on average encode 6 intact prophage regions per isolate of about ~200 kb of whole genome as compared to non-ST131 isolates hat on average were comprised of ~3 intact region per isolate comprising of about ~98 kb of whole genome. These findings suggest that a significant chunk of these ST131 isolates is comprised of prophage regions, with high probability of carrying resistance and virulence determinants.

CRISPR-cas identification showed that none of the ST-131 isolates showed a strong evidence of CRISPR sequences and none of the isolates carried CAS genes.   On the other hand, all of the non-ST131 isolates showed a strong evidence of CRISPR sequences along with the presence of   CAS-genes (CAS-typeIE).

CHAPTER 8: DISCUSSION

Pakistan is the sixth most populous country with population size of 207.8 million individuals constituting 2.65% of the world population. The data from the World Bank 2018 confirms an average annual income per capita of 1641 USD. Although the organizational infrastructure of the country is fairly well developed, health indicators are relatively poor and show higher mortality rates for both communicable and noncommunicable diseases (Khalil et al., 2017). There is a deep deficit in compliance and understanding the biosafety issues in health care institutions (Hussain, 2015). The rampant use of antibiotics has further compromised the health care system by giving rise to antibiotic resistance. Over the past 15 years (2000-2015) Pakistan has witnessed a 65% increase in antibiotic consumption. The increase in defined daily doses (DDD) has risen from 0.8 to 1.3 billion DDDs in Pakistan (Klein et al., 2018). The consumption of antibiotics recorded in lower-middle income countries (LMICs) is among the highest in Pakistan with only exception of India and China. Among antibiotics the consumption rate of macrolides, quinolone and cephalosporins increased up to 119, 125 and 399% respectively in LMICs (Klein et al., 2018). This hike in the use of antibiotics has led to the emergence of MDR pathogens worldwide causing 700,000 deaths every year across the globe. Recent reports suggests that with the current rate of resistance against antibiotics it may surpass 10 million cases per year by the year 2050 hence problem needs urgent intervention (de Kraker et al., 2016). Moreover, World Bank suggests an estimated loss of $100 trillion by 2050 in combating such infections (Brown et al., 2017, O'Neill, 2014). UTIs are a highly prevalent group of infectious diseases affecting 150 million individuals each year across the globe. (Tandogdu and Wagenlehner, 2016a). These are the second most common infections for which prescription of antibiotics are made globally, besides otitis media (Foxman, 2010).

The treatment costs \$3.5 billion each year in terms of economic losses in the U.S alone. In Pakistan UTI are responsible for 11.6-23.5% of all the reported infections and cause huge economic losses (Farooqui et al., 1989, Ullah et al., 2018). The most common microorganism responsible for the UTI is *E. coli* which accounts for up to 85% of the community acquired urinary tract infections, (Tandogdu and Wagenlehner, 2016a, Foxman, 2014a, Flores-Mireles et al., 2015c). UPEC is responsible for 65% of the complicated and 80-90% of uncomplicated UTIs (Flores-Mireles et al., 2015a, Foxman, 2014a). UPECs are increasingly becoming resistant to antibiotics and cause significant morbidity and health care costs. European continent spends €1.5billion every year because of the drug resistant *E. coli* causing UTI infections (Smelov et al., 2016b, World Health Organization %J World Health Organization, 2016).

According to our previous study 155 confirmed *E. coli* MDR isolates were tested for antibiotic resistance. Among these isolates (80%) were MDR with highest level of resistance against sulfonamide-trimethoprim (84%), cephalothin (81%), amoxicillin-calvulanic acid (72%), cefixime (65%), cefotaxime (65%), ceftriaxone (64%), levofloxacin (63%), ceftazidime (62%), ciprofloxacin (61%), sparfloxacin (61%), norfloxacin (59%), aztreonam (54%) and gentamicin (32%) (Ali et al., 2016a). Similar percentage of resistance against antibiotics was also observed by other studies in Pakistan. For example, a study conducted in Pakistan in year 2015 reported cephradine resistance (95%), cephalexin (95%) both are first generation β-lactam drugs. Same study reported higher resistance against fluoroquinolones (82%) while prevalence of ESBLs producer UPEC remained 66.8%. Resistance against ceftriaxone, ceftazidime and cefixime was 71-80% and 78% of UPEC were resistant to sulfonamide-trimethoprim (Sohail et al., 2015). A study conducted in year 2011 in Pakistan reports higher resistance to sulfamethoxazole-trimethoprim 86.14%   that was followed by ceftazidime 84.16% nalidixic acid 84.16% ampicillin 78.22% cefotaxime 76.24% and ciprofloxacin 34.65% (Muhammad et al., 2011).

Studies during the last decade by different authors in Pakistan endorse prevalence of MDR isolates and higher antibiotic resistance to the above mentioned antibiotics (Fatima et al., 2018, Ullah et al., 2009, Tanvir et al., 2012). A recent meta-analysis conducted in Pakistan reports a 40% pooled proportion of ESBL (Abrar et al., 2018). In neighboring countries such as China, 46% of the *E. coli* strains were ESBL producers from 30 different hospitals (Zhang et al., 2014). These observations suggest that antibiotic options recommended for the treatment of complicated and uncomplicated UTI by IDSA and ESCMID may not be very effective in this region hence there is a need for the development of national surveillance systems to assess local susceptibility profiles. However, the lower antibiotic resistance observed against fosfomycin (10%) minocycline (8%) sulbactam (6%) nitrofurantoin (6%) tazobactam (5%) amikacin (5%) meropenem (1%) cefepime (1%) and tigecycline (1%) indicates that these antibiotics may serve alternative treatment options when appropriate (Ali et al., 2016a).

In this study ESBL genes were scrutinized and their occurrence remains as follows $bla_{\text{TEM-1}}$ (36%), bla_{SHV} (7%), $bla_{\text{OXA-1}}$ (15%) and $bla_{\text{PSE-1}}$ (1%). Earlier we screened *bla*CTX-M-15 (88%) in the context of fluoroquinolone resistance (Ali et al., 2016c). Similar findings have also been previously reported by studies in Pakistan, Spain and Lebanon (Rahman et al., 2018, del Castillo et al., 2013, Sana et al., 2011). Extended spectrum β- lactamases (ESBL) are bacterial enzymes that lyse the β-lactam antibiotics and make bacteria resistant to them. ESBL-producing *Enterobacteriaceae* (EPE) is an increasing challenge associated with members of *Enterobacteriaceae.* EPE are a source of increased burden on health care costs due to, high morbidity, mortality and prolonged hospital stays associated with them (Brolund, 2013). ESBL determinants are often carried on plasmids, transposons and other genetically mobile elements. *E. coli* carries a range of plasmids that confer antibiotic resistance to multitude of antibiotics. Among them plasmid incompatibility (Inc) groups IncFIA, IncFIIA, IncI, Col-V, Col-156 are the characteristic plasmids of *E. coli* pathotypes such as UPEC. IncF group of plasmids is the

most prevalent group of plasmids and are reported worldwide for their association with antibiotic resistance (Carattoli, 2009). Recent studies have demonstrated that they act as a rapid vehicle system for transfer of multiple antibiotic resistance genes conferring resistance to all the major classes of antibiotics including β-lactams, aminoglycosides, chloramphenicol, quinolones and tetracyclines (Liao et al., 2013; Liu et al., 2013). Our results also indicated a significant co-prevalence of ESBL genes $bla_{CTXM}, bla_{OXA}, bla_{TEM}, bla_{SHV}$. Plasmid type IncFIA, and IncI1 often carry bla_{CTXM}, bla_{OXA} and bla_{TEM} concurrently and help them in rapid dissemination (Nicolas-Chanoine et al., 2014). Spread of such MDR plasmids aggravates problem of antibiotic resistance, thus the knowledge of their prevalence and association with antibiotic resistance genes can be useful aid for devising antiplasmid based treatment strategies IncF and Col plasmids are also better known for their association with virulence (Johnson and Nolan, 2009). The successful dissemination of ESBL producing, pathogenic phylogenetic group B2 and clonal lineage ST131 is noteworthy (Nicolas-Chanoine et al., 2014, Peirano and Pitout, 2010). ST-131 clone is often associated with the carriage of virulence plasmids such as IncFIA, IncFIIA, Col-156 (Calhau et al., 2013, Slater et al., 2016). UPEC encodes a repertoire of VF that enables this bacterium to survive the otherwise unfavorable environment of UTI. UPEC is categorized into four phylogroups (A, B1, B2 and D) on the basis of genetically mobile pathogenicity associated islands (PAI) and the occurrence of virulence factors (VF) such as adhesins, invasins, surface polysaccharides (LPS, capsular antigens), toxins and iron-acquisition systems (Bien et al., 2012c).

UPEC requires multiple VF which helps these bacteria at various stages of infection such as entry (flagella, pili) adhesion (fimbriae, pili) invasion (cytotoxins) formation of intracellular bacterial communities (iron-acquisition systems, cytokines, pili, curli) and immune evasion (serum resistance, capsular proteins). In this study a repertoire of 18 different virulence factors were scrutinized among 155 isolates. Genetic screening of 18 different virulence factors

confirmed presence of fimbriae, pili and iron acquisition systems as major factors. Among scrutinized isolates *fimH* was detected in 100% of the isolates confirming its role in pathogenesis and virulence of these strains. Similar finding was reported from USA (Johnson and Stell, 2000b, Yun et al., 2014). Role of type 1 fimbriae (*fimH*) in pathogenesis is difficult to elaborate since they are equally expressed in commensal and pathogenic bacteria (Bien et al., 2012c). However, in murine UTI model they have been shown to aid UPEC attachment and colonization stimulate mucosal inflammation, promote biofilm formation intracellularly (IBCs) and enhance bacterial survival. They have also been shown to promote bacterial invasion and translocation of ExPEC through intestinal barriers (Poole et al., 2017). Because of its role in UPEC pathogenesis therapeutic strategies such as mannosides and vaccines have been used to inhibit *fimH* mediated binding of UPEC to bladder epithelial cells. Presence of fimbrial adhesins like *pap* (pyelonephritis associated pili) are frequently associated with pyelonephritis causing UPEC (Spurbeck and Mobley, 2013). Our results showed a notable presence of *pap* genes; *papC* (48%), *papGII* (45%), *papEF* (24%) and *papA* (13%). Occurrence of these variety of virulence factors among multidrug resistant clinical strains of UPEC suggest that these strains are equipped with variety of adhesins required for the infection process and persistence. In this context it is important to note the role of *pap* genes in mediating adherence to uroepithelial cells *in-vivo*. Genes such as *papGII* are responsible for renal damage by inducing inflammatory response during kidney infection. Mutants lacking P-fimbriae are outcompeted by wildtype UPEC during kidney infection (Lane and Mobley, 2007). UPEC secretes several toxic proteins which play central role in the pathogenesis of uropathogenic *E. coli* (Finlay and Falkow, 1997). Toxins modulate the host cell signaling cascade and elicit inflammatory responses causing damage to host tissues (Grabe et al., 2008). UPEC are reported to encode α-hemolysin (*hlyA*), cytolethal distending toxin (*cdtB*), cytotoxic necrotizing factor (*cnf*), vacuolating autotransporter toxin (*vat*), arginine succinyl-transferase (*ast*) and secreted

autotransporter toxin (*sat*). We scrutinized α-hemolysin (*hlyA*) and cytolethal distending toxin (*cdtB*) detected in 12% and 8% of the 155 UPEC trains. Similar frequencies have been reported by other studies from Tunisia, South Korea and US (Tarchouna et al., 2013, Yun et al., 2014, Luna-Pineda et al., 2018). Epidemiological data suggests that although these toxins have low prevalence among UPEC however they have been clinically associated with highly virulent strains of urosepsis and pyelonephritis (Johnson et al., 2005a). While deletion of *hlyA* did not attenuate UPEC in UTI mouse model it appeared to result in lesser bladder hemorrhage when compared to WT (Smith et al., 2008). At higher concentration hemolysin-A lysis erythrocytes and nucleated host cells by eliciting inflammatory response, causing cell death. The lysed cells are used as a source of iron and other nutrients. It also has an increased role in production of IL-6 and IL-8 in renal epithelial cells through Ca^{2+}induced oscillations (Garcia et al., 2013). Similarly, cytolysin (CDT) although less frequent, has DNAse like activity and attacks DNA, resulting in cell distending and eventually cell death (Lara-Tejero and Galán, 2001).

Capsular polysaccharides genes (*kpsMTII, kpsMTIII)* and bacteriocin (*usp*) were also detected among scrutinized strains. Our results showed a plausible presence of *kpsMTII* (26%) and *usp* (14%), however *kpsMTIII* was detected only in 3% of the isolates. Capsular proteins act as protectins and protect UPEC from host immune response. Group II capsule (K1 capsule, *kpsMTII*) helps UPEC evade immune response against complement-mediated engulfment and bactericidal effect. K1 polysaccharides also has an important role in IBC development (Anderson et al., 2010). Urine is a nutrient limited milieu, thus more challenging for bacterial survival as compared to the intestinal environment. It is particularly scarce in iron- which is vital for bacterial survival. UPEC has well developed metabolic capacity to thrive in this hostile niche. It expresses a variety of iron acquisition and transport systems such as siderophores and hemophores. Transcriptomic studies of UTI mouse model have indicated the significant upregulation of siderophores mediated genes *in-vivo* (Conover et al., 2016). In addition, high

prevalence of salmochelin, yersiniabactin and aerobactin among UPEC isolates suggest their possible role in progression of UTI (Henderson et al., 2009). These findings highlight the importance of iron uptake and transport systems in UPEC pathogenesis. In this regard three iron acquisition genes such as aerobactin receptor (*iutA*), ferrous iron transport protein (*feoB*) and yersiniabactin uptake receptor (*fyuA*) were screened in present study. Our results showed 55%, 49% and 24% presence of *iut*A, *feo*B and *fyu*A respectively. Our findings are in alignment with the studies reported by Korea, Mexico and Iran (Yun et al., 2014, López-Banda et al., 2014, Momtaz et al., 2013). All the screened UPEC isolates in our study had a consistent presence of at least one of the three iron uptake systems, highlighting the importance of iron uptake in survival of UPEC. The results also confirm previous findings that UPEC have more than one kind of iron uptake mechanism.

Iron is a ubiquitous micronutrient required by virtually all organisms. It plays an essential role as a co-factor in numerous biological processes such as respiration, DNA biosynthesis, tricarboxylic acid cycle and gene regulation. However, under aerobic conditions it can be toxic, as it may serve as a source for highly reactive hydroxyl radicals, generating oxidative stress. In addition, the predominant, ferric form has very poor solubility at physiological pH resulting in major problems of bioavailability (lack of iron is the commonest form of nutritional restriction in biology). Therefore, effective iron homeostasis is crucial for all living organisms, including bacteria (Andrews et al., 2003b, Cassat et al., 2013). In the harmless model organism *E. coli* K-12, iron uptake and homeostasis are well understood while little is known about the manner in which urinary tract (UT) pathogens respond to iron restriction and how iron regime might influence their colonization potential/pathogenicity. While few studies have demonstrated the role of iron-acquisition systems such as *iutA, iroN, fyuA* and *chuA* in the pathogenesis of UPEC, very little is known about the role of iron in pathogenesis of UPEC (Hagan, 2009, Watts et al., 2012, Gao et al., 2012a). Particularly the role of siderophores in invasion process of UPEC has

not been elucidated yet, except the role of *iroN* receptor, where loss of *iroN* has showed impaired invasion when compared with WT UPEC (Feldmann et al., 2007).

The impact of iron on growth capacity of selected MDR-virulent 20 UPEC isolates indicated that iron is vital for UPEC successful growth. UPEC had a significant growth deficit under iron-deficient and iron-restricted conditions as compared to iron-sufficient conditions. Siderophore production assay confirmed the presence of at least one of three types of siderophores. Overall, out of 20 UPEC isolates, 17 showed strong siderophore production, 2 showed moderate to weak siderophore production, while 1 showed v weak to no siderophore production on CAS plate assay. The strong siderophore producers were found positive for both catecholates and hydroxamates, while moderate siderophore producer was positive only for catecholates, suggesting that the zone size is directly proportional to types of siderophores produced. Our results also correlated well with the whole genome sequencing results, which confirmed the presence of enterobactin (catecholates), aerobactin (hydroxamates), yersiniabactin and heme uptake systems in strong siderophore producers. It also confirmed that moderate siderophore producers encoded enterobactin, yersiniabactin and heme uptake systems, with no aerobactin. Similarly, weak/no siderophore producer had only enterobactin operon present in their genome. On the basis of zone size and type of siderophores produced, five strains were further selected to study the role of iron on invasion and pathogenesis of UPEC. UPEC isolates with strong siderophore producers (UEC59 and UEC82) which had all the three siderophore along with heme uptake system, were observed to have ~ 5 fold more intracellular bacterial load as compared to moderate siderophore producers (UEC175 and UEC01) which encoded two out of three siderophores (lacked aerobactin) along with heme uptake. The weak siderophore producer (UEC157) which encoded only one siderophore (enterobactin) had negligible intracellular bacterial load when compared to strong and moderate siderophore producers. Increase in iron concentration was observed to increase the

invasion cacpcity of UPEC. Strong siderophore producing isolates showed 8-10 fold increase in intracellular bacterial load under iron-enriched conditions as compared to iron-deficient conditions. Likwise, they showed an ~12 to 18 fold increase in invasion capacity when compared to moderate siderophore producers (UEC175 and UEC01) and weak/no siderophore producer (UEC157). These findings suggest that siderophore production enhances invasion rate of UPEC in the presence of iron. In order to further investigate the role of iron and iron acquistion systems in the invasionsof UPEC, UEC59 (a strong siderophore producer and hypervirulent isolate) was mutated to generate four single mutants (*ΔentBEC, ΔhemRT, Δirp1_2* and *ΔiucABCD*), six double mutants *ΔentBEChemRT* (EH)*, ΔentBECirp1_2* (EY)*, ΔentBECiucABCD* (EA), *ΔhemRTirp1_2* (HY)*, ΔhemRTiucABCD* (HA) and *Δirp1_2iucABCD* (YA)) and one triple mutant (*ΔentBECirp1_2iucABCD)* (EYA), for siderophores and heme uptake system.

Growth assays performed on each of single, double and triple mutants showed that enterobactin mutants (E, EH, EY and EA), yersiniabactin mutants (Y, HY) had significant growth constraints as compared to WT under both iron-deficient and iron-restricted condition. Likewise, heme uptake mutant (H) had significant growth deficit when compared to WT, under iron restricted conditions. On the other hand, aerobactin mutants (A, HA and YA) had unexpectedly higher growth trend as compared to WT and other mutants. These results suggest significant role of enterobactins in iron acquisition as compared to the aerobactin and yersiniabactin. This significance can be attributed to higher binding affinity of enterobactin for iron, with a log $\beta 110$ of 49 (Loomis and Raymond, 1991). $\beta 110$ represents the stability constant and is calculated based on the ratio of siderophore-bound iron to unbound iron in mixed solutions (Boukhalfa and Crumbliss, 2002). Higher values for log $\beta 110$ indicate that the siderophore-iron complex has a higher association rate (Boukhalfa and Crumbliss, 2002) (Boukhalfa & Crumbliss, 2002). In a study conducted by Watts and colleagues (Watts et al.,

2012) the UPEC strain ABU 83972with enterobactin biosynthesis genes mutations were shown to have significantly slower cell densities and growth rates after 10 h as compared to the WT ABU 83972. On the other hand, higher rate of growth of A, HA and YA could be associated with a fact that aerobactin is encoded on large plasmids. Aerobactin is borne on ColV plasmid, which, typically ranges in size from 80 to 180 kb (Johnson and Nolan, 2009, Johnson et al., 2006). Similarly, yersiniabactin is encoded on pathogenicity island of 30 kb, referred as high-pathogenicity island (HPI) (Jürgen et al., 1993, Welch et al., 2002, Schubert et al., 2000b). Such plasmids confer higher metabolic costs and put constrain on active bacterial growth. Watt et al., 2012 reports a 63% and 71% increase in cell density of yersiniabactin (Y) and salmochelin yersiniabactin (SY) double mutants respectively. Similar results were reported by previously (Jones et al., 2007), in case of *Pseudomonas syringae* where an increase in growth of yersiniabactin mutant was observed and this increase was attributed to high metabolic cost of yersiniabactin. However, none of the studies above have observed an increase in growth of aerobactin mutants, which in our case is evident and its speculated to be related to high metabolic cost associated with plasmid mediated aerobactin production.

In order to determine the effect of heme on UPEC growth WT, single and double mutants were grown in M9 medium supplemented with 0.5 µM heme. Addition of 2 µM DTPA was made to ensure iron restriction and mutants sole dependence on heme as an iron source. Presence of heme in media improved the overall growth of mutants as compared to previous experiment (in total absence of iron). Under heme-enriched conditions heme mutants (H, EH and HY) were found at a significantly compromised state as compared to WT. Other than heme mutants, enterobactin mutants (E, EA and EY) observed a significant growth deficit (P <0.0001) in the presence of heme, as compared to WT. Mutant HY had the slowest growth of all (P<0.0001), Slow growth rate of mutants of heme uptake system authenticate the correct mutations. Moreover, it validates the role of heme uptake system in growth of UPEC. Slower growth rates

of enterobactin biosynthesis system may be attributed to heme toxicity in the absence of enterobactin, or increased ROS production as described in previous studies (Adler et al., 2014; Adler et al., 2012; Peralta et al., 2016). Enterobactin is reported to have role of protective agent against ROS, H_2O_2 and paraquat, other than its fundamental role in iron uptake. An increased level of ROS in e*ntE* mutant of *E. coli* and poor colony growth minimal media has also been reported (Adler et al., 2014). Its further demonstrated that while presence of iron represses enterobactin production, H_2O_2 and paraquat favor its production even iron is present (Peralta et al., 2016), which is very much according to our results where even in the presence of heme as an iron source, *entBEC* mutant couldn't compete well with WT and other mutants and faced a growth constraint inability to produce enterobactin. Our results also explain the definite role of *hemRT* in heme acquisition. The heme uptake cluster (*chu*) of *E. coli* CFT073 is comprised of eight genes, *chuS, chuA, chuT, chuW, chuY, chuX*, and *chuU,* involved in transport as well as subsequent processing (Hagan, 2009, Hagan et al., 2010) Genetic arrangement of *chu* cluster is homologous to the *shu* cluster of *Shigella dysenteriae*, which is reported to be involved in heme acquisition and homeostasis (Wyckoff et al., 1998). While some of the genes of this cluster are characterized, e.g., *chuS* and *chuX* are characterized as heme oxygenase and heme binding/ trafficking, while other remain poorly elucidated e.g., *chuA* (*hemR*), *chuT* (*hemT*) are putatively characterized as heme uptake receptor and transporter respectively. Very few studies have elucidated the role of *chuA* and *chuT* together. A study conducted by Thompson et al., 1999, in *Yersinia pestis* reported *hmuR* mutant was unable to utilize hemin or any other hemoprotein for growth, and complementation of *hmuP9R* clone restored its ability to utilize hemin. Similarly, *hmuT* mutant grew poorly in the presence of hemin, whereas it showed equally good growth as WT, when grown with hemoglobin, suggesting that *hmuTUV* does not have any role in hemoglobin utilization and uptake (Thompson et al., 1999). These results are

in collaboration with our findings, since our mutant *hemRT* showed poor growth as compared to its WT and other mutants.

For longest time researchers have been arguing, why pathogenic *E. coli* would produce multiple siderophores. However, as we look closer each system appears to have specificity and has optimum condition in different environment. For instance, enterobactin is a non-glycosylated catecholate and has high affinity for iron at neutral to alkaline pH. However, it is readily recognized by human lipocalin (HLcn-2) protein. On the other hand, salmochelin is glycosylated enterobactin and is not recognized by HLcn-2, thus readily evades host immune response. Yersiniabactin also possesses maximum binding affinity at neutral-alkaline pH and is not recognized by HLcn-2. While aerobactin works best under acidic pH 5.5, it correlates with higher stability of Fe^{3+}-aerobactin in acidic environments. Our results showed that enterobactin mutants at pH 7.0, under iron deficient as well as iron restricted conditions, mutants such as EY, EH and EA were observed to have slow growth suggesting that enterobactin plays a pivotal role in iron-acquisition at neutral pH. Previous study by Valdebenito et al., 2006 on *E. coli* probiotic strain Nissle 1917 have demonstrated that catecholates and yersiniabactin have maximum production at neutral to slightly alkaline pH (Valdebenito, Crumbliss, Winkelmann, & Hantke, 2006). At pH 5.5, under both iron-deficient and- restricted conditions again strains EH, EY, HY, had slow growth rates, while at pH 8.5 EH, EY and EA were significantly growth defected as compared to their WT however mutants such as YA and HY (both yersiniabactin mutant) had better growth as compared to their WT. This can again be attributed to absence of enterobactin in (EH, EY and EA), that showed poor growth at pH 8.5 and presence of enterobactin in YA and HY mutants, leading to their better growth at alkaline pH. Thus, enterobactin play a crucial role at neutral and alkaline pH, while aerobactin plays an important role at acidic pH 5.5 (Valdebenito et al., 2006). Another study reports similar results, where enterobactin mutants E, ES, EAS and EASY had shown growth

at pH 7.0 and 5.5 as compared to WT. While yersiniabactin mutant Y and SY had rapid growth as compared to WT and other mutants (Watts et al., 2012).

Enterobactin (Ent) is known to have highest affinity for ferric iron and poses huge challenge for host cells (Holden and Bachman, 2015). Lipocalin 2 (Lcn2) is an innate immunity protein that sequesters iron for host and starves bacteria of iron (Bachman et al., 2009). It is secreted by host neutrophils and epithelial cells to oppose the acquisition of iron by bacterial siderophore (enterobactin). However, human Lcn2 is found to have similar affinity for Ent as its receptor FepA and gives bacteria a tough competition in race for iron. Its protective effect was first illustrated in *Escherichia coli* sepsis model where wild type mice survived infection with enterobactin producing *E. coli*, in contrast to Lcn2-deficient mice (Flo et al., 2004).

Under iron deficient conditions mutants such as HA and YA were growing significantly better as compared to the WT and other competitors. Mutants such as EY, EH and HY had reasonably low growth rate as compared to WT. The results are in accordance with previous experiment when mutants were grown under iron reduced conditions. However, under iron deficient conditions (no added iron) with the addition of 8 µM HLcn-2 all the enterobactin mutants (EH, EY and EA) were found to have highly significant ($P<0.0001$) growth difference as compared to the WT. EY and EH were observed to have similar growth pattern and both showed increase in growth as compared to WT. Similarly, mutants EA, HA and YA (aerobactin deficient) were also observed to have increased growth as compared to WT and these three seemed to follow similar growth trend. However mutant HY (encoding both enterobactin and aerobactin) had a significantly ($P<0.0001$) reduced growth as compared to other mutants and followed almost similar growth rate as WT. These results come as unexpected since several *in vivo* studies (Flo et al., 2004, Steigedal et al., 2014) conducted on enterobactin mutants suggest that *ent* UPEC mutants are out competed in the presence HLcn-2, while our results show the opposite. One reason is may be because we have performed the experiment *in-vitro,* and conditions are not

what they happen to be inside the host cells. Similar results were obtained by colleagues Louis et al., (personal communication) where they found increases growth of *entB* mutants of *Salmonella enteridis*, in the presence of 8 µM HLcn-2 (Julien et al., 2019). One hypothesis could be that "The lack of enterobactin production results in favourable growth with Lcn2- presumably because the Ent binds the Fe, and then Lcn2 binds the Fe-Ent such that the culture becomes Fe restricted. However, the *ent-* strain is still able to obtain iron as the Lcn2 has no influence, and thus has the advantage". to the wild type (paired T-test *P*-value < 0.001) when exposed to Lcn2 under low iron conditions. The enhanced growth of the *entB* mutant likely relates to its ability to escape competition with Lcn2 for iron due to its lack of enterobactin production. However, it confirms that although Lcn2 is able to bind enterobactin (Goetz et al., 2002) it cannot bind salmochelin, yersiniabactin and aerobactin (Valdebenito et al., 2006). Similarly (HY) can encode enterobactin likewise of WT and has a growth disadvantage as compared to other mutants. Decreased growth of HY itself validates our hypothesis of increased chances of getting sequestered by Lcn2 in the presence of Fe-Ent complex since HY encodes enterobactin. On the other hand, aerobactin mutants (HA and YA) has been consistently showing a growth advantage as compared to WT and other mutants presumably because of loss of aerobactin, hence their increase in growth comes as no surprise.

While investigating the role of each iron-acquistion systems in invasion , it was observed that each of four systems when knocked out had a significant impact on invasion . However, single mutants of yersiniabactin (Y) and aerobactin (A) had the most significant decrease in virulence , each with 68% and 77 % lesser invasion respectively as compared to their WT. Similarly, among double mutants, mutants lacking heme uptake system with any other siderophores (particularly Y and A) appeared to have a pronounced effect on loss of virulence as compared to enterobactin defected mutants. In accordance with single mutant results double mutant (YA) had also a decreased virulence as compared to WT. As expected, triple mutant (EYA) had the

most significant (89.69%) effect on loss of virulence and the intracellular bacterial load was very low as compared to the WT. Similar results have been reported by Gao et al., 2012 where aerobactin mutant (*iucD*) was found to have 10–100 times reduced colonization as compared to WT (Gao et al., 2012b). However, this study didn't observe significance differences invasion ability of WT and siderophore mutants, probably because the invasion assays were performed on macrophages rather than bladder epithelial cells. Yersiniabactin (*irp2*) mutant of ExPEC strain ST69 was outcompeted in UTI and sepsis model (Johnson et al., 2018). Complementation with *irp2* was reported to fully restore parental virulence. Gao et al., 2012 also reports greatest impact of triple mutation (*ΔchuTΔiroDΔiucD*) in reduction of UPEC and APEC pathogenesis (Gao et al., 2012b, Hagan et al., 2010). While this study (Gao *et al.,* 2012) reports insignificant effect of heme uptake (*ΔchuT*) in UPEC strain, a study by Erin *et al.*, 2010 prominent roles for aerobactin and heme uptake during UPEC colonization of the bladder and kidneys, respectively (Hagan et al., 2010). However, none of these studies have determined the role of siderophores in invasion process, except one study where the precise role of *iroN* (salmochelin receptor) was elucidated. The study reports impaired invasion of UPEC isolates in bladder cell lines after loss of *iroN* receptor (Feldmann et al., 2007). Invasion is a crucial process for UPEC infection, within UT niche UPEC faces many challenges including scarcity of nutrients, shear flow of urine, antibacterial molecules such as lipocalins and macrophages. In order to circumvent these challenges, UPEC invades the host cell and not only gains asses to host nutrients but also gains protection against antibiotic treatments and host defenses. Translocation through host cells helps UPEC to disseminate through UT and establishment of IBCs. These IBCs are bacterial compartments, where UPEC restricts its growth and enters a latent/quiescent state. Just after few hour of inoculation, the number of IBCs can range 3 to 700 in mice (Schwartz et al., 2011). IBCs are the most organized reservoirs for chronic and recurrent UTIs.

In order to investigate the the role of extracellular iron on the pathogenesis of mutants and WT, they were grown under a regime of iron concentrations (Fe-/Fe-, Fe+/Fe-, Fe-/Fe+, Fe+/Fe+) and the potential virulence was re –evaluated. Results showed that single mutants such as E,H, Y and A each had a continuous increase (reaching utpo 2-28 fold) in invasion under all the four iron concentrations. Whereas double mutants showed a signficant increase in invasion only under (high-high, Fe+/Fe+ iron concentrations). Similarly, triple mutant showed only a plausible increase under high-high iron conditions, owing to loss of all the three iron-acquisition systems. Despite that there was a signficant increase in invasion potential of single, double and triple mutants *in-vitro* when compared to iron-deficient (low-low iron) conditions , yet there was clear difference in their invasion potential when compared to WT. None of the mutants could reach their WT virulence potential, even in the presence of extracellular iron sources. These results suggest that iron plays an important role in increasing the invasion capability of UPEC, and the strains with all the three iron-acquisition systems are at significant advantage compared to those lacking one or more iron-acquisition systems. These observations clearly define role of iron in pathogenesis of UPEC, moreover they identify the importance of extracellular iron in increasing the invasion potential, by providing excessive bio available iron for their cellular needs. The present results can be further explained by the fact that normal level of serum iron in healthy adults is less than 31mM, whereas patients with liver damage or severe hemochromatosis, this level reaches far greater than 31 mM (Bauckman and Mysorekar, 2016). Patients with iron dysfunction are more likely to have increased bacterial burden resulting in damage to urothelium cell lines of bladder. Infants with higher basal level serum iron are at more risk of developing infections (Christopher, 1985). Similarly a study conducted by Collard *et al.,* 2009 reports increased incidence of UTI in infants with increased iron supplementation (Collard, 2009). Similarly studies have reported higher level of iron in urine of post-menopausal women suffering from recurrent UTI (Matsumoto, 2001). Study conducted

by (Dikshit et al., 2015). Bauckman *et al*., 2016 report increase in virulence of UPEC CFT073 in bladder epithelial cell lines (BEC), when BEC were treated with high iron concentrations. They have demonstrated the role of iron as ferritinophagy which leads to iron colocalizing in autophagosomes and autolysosomes (Bauckman and Mysorekar, 2016). UPEC infection under high iron conditions leads to host damage as a result of lysosomal damage. Another study by Dikshit *et al*., 2015 reports a significant increase in intracellular bacterial count in BECs after supplementation of iron in the form of holotransferrin. The study also reported reduced intracellular survival in the presence of deferoxamine, an iron chelator. It reports role of small GTPase Rab35 in UPEC survival in UPEC-containing vacuoles (UCV) within BECs. Rab35 facilitates endosomal recycling of transferrin receptor (TfR), the key protein involved in transferrin-mediated iron uptake (Dikshit et al., 2015). Although previous studies have reported the induction of iron acquisition-associated genes in UPEC during IBC formation (Reigstad et al., 2007b, Berry et al., 2009), none of the studies have so far reported on role of iron in intracellular survival and the relative effect of iron on mutants. Our study reports a critical role of iron in invasion and intracellular survival and coincides well with the studies reported previously. It gives a new insight about the modulation of iron in UT milieu to prevent UTI and opens new avenues for therapeutic intervention.

UPEC biofilm forming ability plays an important role in infection persistence and recurrence. It not only forms biofilms on abiotic surfaces such as catheter but also forms intracellular biofilms in the form of IBCs (Kostakioti et al., 2013a). Biofilm production helps protect bacteria from innate immune responses such as phagocytosis, opsonization and antibiotic treatments (Trautner and Darouiche, 2004, Kostakioti et al., 2013a). It also helps bacteria in dissemination of drug resistance and virulence markers, as a result biofilm producing pathogens cause recalcitrant and chronic infections such as recurrent UTI (UPEC), upper respiratory tract (*Pseudomonas aeruginosa*) infections, catheter and device induced infections (*Klebsiella*

pneumoniae, UPEC, *Enterococcus faecalis*) (Kostakioti et al., 2013a, Foxman, 2014a). Therefore, detection of biofilm producing strains is important for the recommendations of appropriate control measures for UPEC infections. Our study showed that all the tested 155 UPEC isolates were capable of biofilm formation. Among these isolates, 108 (70%) were categorized as strong biofilm producers (S), 37 (24%) were moderate biofilm producer (M), 10 (6%) were weak biofilm producer (W). Overall, no correlation was found between biofilm production (strong/moderate) and resistance traits such as ESBL, MDR and antibiotic resistance phenotypes, which is similarly reported in other studies by (Rijavec et al., 2008, Pompilio et al., 2018). Rijavec *et al.,* (2008) reports no correlation between where no correlation between biofilm production, MDR and resistance to ampicillin and trimethoprim was observed (Rijavec et al., 2008). Our results also significantly relate with the findings of Pompilio et al., 2018 where they found no correlation between prevalence of biofilm producers and their resistance/sensitivity pattern (Pompilio et al., 2018). In our study a strong correlation was observed between mannose resistant hemagglutination (MRHA) and mannose sensitive hemagglutination (MSHA). MRHA is associated with type P- pili and other surface associated adhesins while MSHA is associated with type 1 fimbriae (Johnson, 1991b). Both factors are involved in adhesion and colonization of host urothelial cells, hence promote biofilm formation. Other phenotypes such as hemolysin, cell surface hydrophobicity (CSH) and serum bactericidal resistance (SBR) were observed to have no correlation with either strong biofilm or moderate biofilm producing isolates. Likewise, a significant association between pili genes (*papA* and *papC*) and strong biofilm production was found. Capsule protein (KpsmtII) and uropathogen specific protein (Usp) were found strongly associated with moderate biofilm production. Pap genes are pyelonephritis-associated pili and code P-pili. P-pili bind to $\text{Gal}(\alpha 1-4)\text{Gal}\beta$ motifs of renal epithelial cells and play a key role in pyelonephritis pathogenesis (Mobley et al., 2009, Mobley et al., 1993). In another study *papC, papG,*

sfa/foc DE, *focG*, *hlyA* and *cnf1* were found more frequent among strong biofilm producers (Naves et al., 2008). Likewise a strong association between biofilm formation and *pap* genes has been reported in a recent study (González et al., 2017b). Capsule protein are one of the characteristic features of UPEC and play an important role in capsule synthesis, they were found differentially upregulated in chicken infection model, suggesting a possible role in invasion (Zhao et al., 2009). Similarly Usp is reported to be involved in bacteremia of UT origin (Rijavec et al., 2008). The plethora of adhesins, fimbrial structures and other non-fimbrial adhesins possibly can determine the tropism of the pathogen to host tissues, bacterial–bacterial interactions, formation of IBC and biofilms. The prevention of the first step in adhesion is an interesting strategy that could lead to the reduction of the impact of this type of infection.

In present study, optical density values at different time points and SEM analysis showed initial adhesive stage within 4 hours. In 10 hours biofilm, extracellular polysaccharide matrix can be clearly seen with entire polystyrene surface occupied with uropathogenic *E. coli* cells while this biofilm become more intense after 18 hours of incubation. Generally, the biofilm formation takes place in five stages, although variation may exist between species. In first stage, there is reversible attachment of planktonic bacteria to the surface, through flagella role(Toutain et al., 2007). In second stage, an important change in gene expression takes place and bacteria start producing adhesins such as type 1 pili, curli fibers and antigen 43, that lead to irreversible bacterial attachment (Lemon et al., 2007). In third stage, bacteria start producing extracellular polysaccharides (EPS) matrix, which in case of *E. coli* is comprised of colanic acid, cellulose and polyglucosamine. After this stage the biofilm starts to grow and forms a three-dimensional structure called macrocolony. By the end of fourth stage biofilm acquires its mature form and in last stage it shed planktonic bacteria and start biofilm at another surface (Soto, 2014, González et al., 2017a).

In-vitro efficacy of antibiotics (trimethoprim, ceftazidime, levofloxacin and gentamicin) was determined to treat biofilms. The MIC-b is defined as the lowest concentration of antibiotics which inhibits the growth of planktonic bacteria after being shed from biofilm. MIC-b when compared with MIC-p (MIC of planktonic forms), were found significantly higher than their MIC-p values. Ceftazidime was observed to undergo a ~100 to 1000 times increase in values (MIC-p; 128 to >1024 µg/ml) as compared to MIC-b. Similarly, gentamicin and trimethoprim observed 8 to 1000 times increase in their MIC-b values (64-1024 µg/ml). Levofloxacin had relatively better efficacy against biofilm inhibition with MIC-b 32 to 64 µg/ml. Previous study on biofilm inhibition of *E. coli* reports similar results, where highest degree MIC-b was seen against gentamicin and ciprofloxacin, followed by cefotaxime (Naves et al., 2010). Our results indicate levofloxacin has the potential of inhibiting biofilm formation, which is in agreement with another study where levofloxacin and ulifloxacin were able to prevent biofilm formation but failed to eradicate the biofilm (Minardi et al., 2008). Bacterial biofilms are protected from host immune response and phagocytic activity of macrophages. Biofilm form are generally more resistant to antibiotic treatments than their planktonic forms. The higher level of antibiotic resistance in biofilm forms is attributed to limited diffusion of antibiotic through EPS matrix, HGT of resistance genes, inactivation of antibiotics by changing pH and metal ions and metabolically inactive state of bacteria. It is also proposed that it is an adaptive and reversible situation and bacteria has been shown to achieve the susceptibility after bacteria returns to its planktonic form (Keren et al., 2004). The level of resistance also depends upon the stage of biofilm formation, and the initial reversible stage is proposed to be more susceptible (González et al., 2017a, Soto, 2014). Thus, appropriate antibiotic therapy and at right stage of biofilm formation can help in better treatment of biofilm mediated infections.

Until recently, antibiotic resistance has been associated with high fitness cost. The scientific notion that, as high fitness cost is associated with antibiotic resistance, susceptible strains

would overtake the resistant strains , was widely accepted (Melnyk et al., 2015). The relationship between resistance and virulence is complex phenomenon and none of the dogma could be entirely accepted. Several studies have reported loss of virulence with the acquisition of fluoroquinolone resistance in *E. coli* (Velasco et al., 2001, Blázquez et al., 1999). However, the increasing resistance and emergence of multi-resistant and virulent clones such as ST131 (*E. coli*) and ST23 (*Klebsiella pneumoniae*) reflect on contrary observations (Nicolas-Chanoine et al., 2014, Shon et al., 2013). Hence the evolutionary dimensions of resistance and virulence have become an interesting area of research (Schroeder et al., 2017b).

Several animal infection models showed the increased fitness of MDR strains *in-vivo* (Roux et al., 2015). Similarly, studies have shown an increases association between P- fimbriae and amoxicillin, carbenicillin and tetracycline resistance than P-fimbriated strains (Vranes et al., 1994). Therefore, in an attempt to determine a correlation between resistance and virulence in our UPEC strains, phenotypic and genotypic virulence characteristics were analyzed in the presence and absence of ESBLs, MDR and resistance to individual antibiotics. VF factors were also further correlated with the sequence types to elucidate the correlation between VF and STs.

Our results showed that VF such as *papGII* and *iutA* are significantly ($P<0.05$) associated with ESBL producing and MDR isolates. Additionally, afimbrial adhesin *sfa* was found strongly associated with MDR isolates and was found totally absent from non-MDR isolates. Although VF such as *feoB* and *hlyA* were more frequent in MDR isolates, the association was not statistically significant. Our results are in alignment with numerous studies reported in recent years, where an increasing correlation between of resistance and virulence attributes has been reported in UPEC, *K. pneumoniae* and *P. aeruginosa* (Malekzadegan et al., 2018, Gharrah and Mostafa El-Mahdy, 2017). Our study also found a correlation between certain VF and with

individual antibiotic resistance phenotype, such as genes like *papC* was found significantly associated ($P<0.05$) in gentamicin resistant isolates, which has also been previously reported by Alabsi *et al.*, 2014 (Alabsi et al., 2014). Other genes like, *papGII* and *sfa/foc* were found more frequent in FQR (levofloxacin and ciprofloxacin) and ceftazidime resistant isolates. A statistically significant association ($P<0.05$) was found for these factors. These results are against the findings of Johnson et al., 2003 (Johnson et al., 2003), where these genes were found significantly associated with FQ susceptible isolates. Our results together with other studies suggest that unlike previous observation, increase in resistance is associated with enhanced virulence and better adaptation under stress conditions. In a recent study acquisition of ESBL plasmid in pandemic lineages (ST131 and ST648) of *E. coli* did not cause any fitness cost. Infact it increased the virulence potential of *E. coli* by enhancing chromosomal expression of certain genes (Giraud et al., 2017). In this context it is important to note that certain VF such as aerobactins (i*utA)* are encoded on large virulence plasmids that acquired via HGT and may also carry resistance determinants. Similarly, *pap* operon is encoded high pathogenicity island (HPI) and reportedly encodes integron, transposons and tetracycline resistance genes in avian pathogenic *E. coli* (Kariyawasam and Nolan, 2011). Acquisition of such mobile genetic elements favor co-selection of both resistance and virulence traits. Likewise, acquisition of plasmids such as IncFIA, IncFIB and IncI1 which carry ESBL genes; *bla*CTXM, *bla*OXA and *bla*TEM and is also reported to carry VF such as sit*tABCD*, *iucABCD-iutA*, *iroCDEN*, *etsABC*, *hlyF*, *iss*, *ompT*, and *vagCD* (Johnson and Nolan, 2009, Zong, 2013).

In current study, the sequence typing data suggested that overall majority of VF were uniformly distributed across all the STs. However, certain VF such as *sfa/foc, fyu*A and *feo*B were significantly ($P < 0.05$) associated with ST131 isolates, also VF such as *pap*EF*, sfa/foc* and *hly*A were found in strong association significantly ($P < 0.05$) with ST131 *H30* sub-clone. Likewise, aerobactin receptor *iutA* was found strongly associated ($P \leq 0.01$) with ST131-non-

H30 sub clone. ST131 is a pandemic clonal lineage and is associated with multidrug resistance and high virulence profile (Nicolas-Chanoine et al., 2014). Its dissemination across all the five continents is reported. It's the predominant clonal lineage involved in extraintestinal infections particularly UTI. However, there is no data from Pakistan regarding its prevalence and association with VF. Current study reports significance presence (45%) prevalence of ST131 isolates among UPEC. The data further suggests that co-occurrence of MDR and VF such as adhesins (P-pili and toxins) could be a driving factor in its better adaptability in hostile niche of UT. Our results corroborate with other studies which have also reported higher incidence of VF such as *papC*, *papEF* and *fyuA* among ST131 isolates (AL-hetar and Lakshmidevi, 2016).

In-vitro invasion assays based on gentamicin protection further confirmed that tested MDR-virulent strains of UPEC isolates were capable of invasion without any fitness cost. These results are in lines with previous study where MDR strain of *P. aeruginosa* was able to successfully cause lung infection *in-vivo*. Several other animal infection models showed the increased fitness of MDR strains *in-vivo* (Roux et al., 2015). These results indicate that acquisition of resistance genes enhances the virulence and antibiotic pressure leads to the selection of MDR-virulent strains without losing or compromising their virulence backbone. Increasing evidences suggest that the earlier paradigm of increased resistance associated with reduced fitness cost may not be as solid as previously thought (Guillard et al., 2016). Invasion assays also showed that UPEC strains possess pathogenic properties such as invasion and adherence irrespective of their sequence types. These findings are in line with the findings of Shaik et al., 2017, where all the STs were able to invade the bladder cell lines without any significant difference with each other (Shaik et al., 2017).

Taken together it can be stated that *E. coli* is a highly adaptable microorganisms, having evolved multiple mechanisms of antibiotic resistance. It carries multiple plasmid mediated resistant mechanism and these conjugative plasmids may also carry virulence factors which

can be co-selected. As a result, these factors might get selected by antibiotic pressure. Despite the evidence of correlation between resistance and virulence, most of them are clonal, there are contradictory evidences of inverse relationship between resistance and virulence traits, such as FQR and loss of virulence have been documented in UPEC isolates. Under such circumstances research need to be undertaken to determine whether chromosomal mutations interfere with the transcriptional events that curb expression of specific VFs.

Although phenotypic and molecular methods offer rapid and cost-effective typing of isolates and screening of gene functions, they often fail to distinguish closely related strains. For example, during outbreak analysis of antimicrobial resistant organisms, conventional genotypic methods are employed which will detect only AMR genes and not virulence genes. However, if we employ techniques like WGS, we will get concurrent information about resistance, virulence as well as phylogenetic relatedness which will significantly improve outbreak analysis (Quainoo et al., 2017). With the recent advancement in genomic technology and user-friendly analysis tools has not only increased the analysis speed but also reduced the cost of sequencing. WGS can discriminate highly related clones and provides an important tool for understanding transmission of such pathogens by comparing them with available databases.

Comparative genomic analysis of twenty MDR-virulent UPEC revealed that all the 20 UPEC isolates are equipped with a plethora of VF along with series of resistance genes. Virulence potential of isolates was confirmed by *in-vitro* cell lines assays using uroepithelial cell line ATCC HTB5637. Sequence typing and serogrouping confirmed that 9 isolates (45%) belong to ST131-O25b-H30, confirming their pandemic nature. ST131-O25b-H30 strains are reported to ESBL producers and fluoroquinolone resistant (Hefzy and Hassuna, 2017, Johnson et al., 2010, Nicolas-Chanoine et al., 2014, Peirano and Pitout, 2010). While 5 (25%) belonged to ST405, along with other STs such as ST10, ST38, ST648. Virulence profiling showed that ST131 isolates have significantly higher incidence certain of VF such as P-pili genes (*pap1,*

papC, papEF) and toxins such as RTX and *cnf*. Likewise, antibiotic resistome revealed that all UPEC isolates encode an arsenal of resistance genes conferring resistance to cephalosporins, fluroquinolones, sulfonamide-trimethoprim, tetracycline, aminoglycosides, chloramphenicol, macrolides and quaternary ammonium compounds. However, resistance genes such as $bla_{CTXM-15}$, bla_{OXA-1}, *catB, tetA, dfrA17* were significantly more prevalent among ST131 isolates. Plasmids IncF1A and IncI1 were more frequent among ST-131 isolates. Both these plasmids are reported to carry resistance as well as virulence genes. Similarly, higher incidence of Col156 (virulent plasmid) among ST131 isolates suggest that this clonal lineage can successfully retain the resistance and virulence backbone simultaneously without any fitness cost. This striking combination helps ST131 clone adapt more quickly as compared to its non-ST131 counterparts. Presence of huge chunks of foreign DNA in the form of prophages and absence of CRISPR-cas sequences further supports our finding. Apparently, these characteristics seem help ST131 to readily uptake foreign DNA and successfully flourish under different environmental conditions.

Conclusively it could be said that it is highly likely that multiresistant-virulent high-risk clones will continue to emerge and disseminate in coming years. It may be because of increasing exposure of pathogenic strains to antibiotic treatments, as a result these pathogenic strains acquire resistance determinants at minimal fitness cost. Despite the increasing evidence of high-risk clones, resistance and virulence are studied separately. It is high time that integrative research should be incorporated to understand the co-evolution of both these traits, so that we may be better armed against such infectious threats.

Conclusion

Overall this study concludes that virulent UPEC strains have relatively uniform distribution of variety of VF. The invasion ability of UPEC strains is directly dependent upon iron availability and siderophores production. At least three different kinds of siderophores were witnessed among these strains. Diminishing siderophore production by gene KO impairs their invasion ability. Additionally, UPEC strains vary regarding their invasion ability which is proven to be independent of their ST types. Entire genome sequence of virulent MDR UPEC strains revealed their diverse virulence profile along with robust MDR profile that indicates a successful acquisition of MDR factors at minimal fitness cost. The predominant ST131 lineage is simultaneously equipped with diverse virulence factors and MDR genes that might contribute towards its better adaptation as a pathogenic strain.

 With the rapid increase in antibiotic resistance and emerging virulent bacterial strains in the current world, it is necessary to understand the genetic link between resistance and virulence. Large scale epidemiological studies addressing both virulence and resistance attributes of such isolates should be conducted. Research should be focused on anti-virulent target and in this context siderophore-mediated drugs and vaccine seem a promising candidate. Based on this study, *in-vivo* effect of siderophore loss should be determined in UTI mouse model. In addition, the role of other putative VF such as ferrous iron uptake systems in UPEC should be further elucidated. Future studies should also be focused on high-risk emerging global clones and their genetic attributes. Antibiotic resistance is a global issue and global issues can be better solved when addressed in collaboration with global teams. In this regard collaborations and alliances should be strengthened to wage war against rising threats.

Abrar, S., Hussain, S., Khan, R. A., Ul Ain, N., Haider, H. & Riaz, S. 2018. Prevalence of extended-spectrum-β-lactamase-producing Enterobacteriaceae: first systematic meta-analysis report from Pakistan. *Antimicrobial resistance and infection control,* 7**,** 26-26.

Ahmed, I., Sajed, M., Sultan, A., Murtaza, I., Yousaf, S., Maqsood, B., Vanhara, P. & Anees, M. 2015. The erratic antibiotic susceptibility patterns of bacterial pathogens causing urinary tract infections. *EXCLI journal,* 14**,** 916.

Ahmed, K. & Imran 2008. Prevalence and antibiogram of uncomplicated lower urinary tract infections in human population of Gilgit, Northern Areas of Pakistan. *PAKISTAN Journal of Zoology,* 40**,** 295-301.

Al-Badr, A. & Al-Shaikh, G. 2013. Recurrent Urinary Tract Infections Management in Women: A review. *Sultan Qaboos University Medical Journal,* 13**,** 359-367.

Al-Hetar, K. Y. A. & Lakshmidevi, N. 2016. Virulence Factors of *E. coli* ST131 and Its H30 and H30Rx Subclones Among Extended-Spectrum Beta-Lactamase Producing Isolates. *International Journal of Genetics and Genomics,* 4**,** 36.

Alabsi, M. S., Ghazal, A., Sabry, S. A. & Alasaly, M. M. 2014. Association of some virulence genes with antibiotic resistance among uropathogenic *Escherichia coli* isolated from urinary tract infection patients in Alexandria, Egypt: A hospital-based study. *Journal of Global Antimicrobial Resistance,* 2**,** 83-86.

Ali, I., Kumar, N., Ahmed, S. & Dasti, J. I. 2014. Antibiotic Resistance in Uropathogenic *E. coli* Strains Isolated from Non-Hospitalized Patients in Pakistan. *Journal of Clinical and Diagnostic Research : JCDR,* 8**,** DC01-DC04.

Ali, I., Rafaque, Z., Ahmed, S., Malik, S. & Dasti, J. I. 2016a. Prevalence of multi-drug resistant uropathogenic *Escherichia coli* in Potohar region of Pakistan. *Asian Pacific Journal of Tropical Biomedicine,* 6**,** 60-66.

Ali, I., Rafaque, Z., Dasti, J. I., Graham, S. E., Salzman, E. & Foxman, B. Uropathogenic *E. coli* from Pakistan have high prevalence of multidrug resistance, ESBL, and O25b-ST131. *Open Forum Infectious Diseases,* 2016b. Oxford University Press.

Ali, I., Rafaque, Z., Dasti, J. I., Graham, S. E., Salzman, E. & Foxman, B. 2016c. Uropathogenic *E. coli* from Pakistan Have High Prevalence of Multidrug Resistance, ESBL, and O25b-ST131. *Open Forum Infectious Diseases,* 3**,** 2008-2008.

Allsopp, L. P., Totsika, M., Tree, J. J., Ulett, G. C., Mabbett, A. N., Wells, T. J., Kobe, B., Beatson, S. A. & Schembri, M. A. 2010. UpaH is a newly identified autotransporter

protein that contributes to biofilm formation and bladder colonization by uropathogenic *Escherichia coli* CFT073. *Infection and immunity,* 78**,** 1659-1669.

Alteri, C. J., Hagan, E. C., Sivick, K. E., Smith, S. N. & Mobley, H. L. 2009. Mucosal immunization with iron receptor antigens protects against urinary tract infection. *PLoS Pathog,* 5**,** e1000586.

Amna, M. A., Chazan, B., Raz, R., Edelstein, H. & Colodner, R. 2013. Risk factors for non-*Escherichia coli* community-acquired bacteriuria. *Infection,* 41**,** 473-477.

Andersen, P. S., Stegger, M., Aziz, M., Contente-Cuomo, T., Gibbons, H. S., Keim, P., Sokurenko, E. V., Johnson, J. R. & Price, L. B. 2013. Complete genome sequence of the epidemic and highly virulent CTX-M-15-producing H30-Rx subclone of *Escherichia coli* ST131. *Genome announcements,* 1**,** e00988-13.

Anderson, G. G., Goller, C. C., Justice, S., Hultgren, S. J. & Seed, P. C. 2010. Polysaccharide capsule and sialic acid-mediated regulation promote biofilm-like intracellular bacterial communities during cystitis. *Infection and immunity,* 78**,** 963-975.

Anderson, G. G., Palermo, J. J., Schilling, J. D., Roth, R., Heuser, J. & Hultgren, S. J. 2003a. Intracellular bacterial biofilm-like pods in urinary tract infections. *Science,* 301**,** 105-7.

Anderson, G. G., Palermo, J. J., Schilling, J. D., Roth, R., Heuser, J. & Hultgren, S. J. 2003b. Intracellular bacterial biofilm-like pods in urinary tract infections. *Science,* 301**,** 105-107.

Andrews, S. C., Robinson, A. K. & Rodríguez-Quiñones, F. 2003a. Bacterial iron homeostasis. *FEMS microbiology reviews,* 27**,** 215-237.

Andrews, S. C., Robinson, A. K. & Rodríguez-Quiñones, F. J. F. M. R. 2003b. Bacterial iron homeostasis. 27**,** 215-237.

Anis-Ur-Rehman, M. J., Siddiqui, T. S. & Idris, M. 2008. Frequency And Clinical Presentation Of Uti Among Children Of Hazara Division, Pakistan. *J Ayub Med Coll Abbottabad,* 20.

Antonopoulos, D. A., Assaf, R., Aziz, R. K., Brettin, T., Bun, C., Conrad, N., Davis, J. J., Dietrich, E. M., Disz, T. & Gerdes, S. 2017. PATRIC as a unique resource for studying antimicrobial resistance. *Briefings in bioinformatics*.

Arndt, D., Grant, J. R., Marcu, A., Sajed, T., Pon, A., Liang, Y. & Wishart, D. S. 2016. PHASTER: a better, faster version of the PHAST phage search tool. *Nucleic acids research,* 44**,** W16-W21.

Arnow, L. E. J. J. B. C. 1937. Colorimetric determination of the components of 3, 4-dihydroxyphenylalanine-tyrosine mixtures. 118**,** 531-537.

Arpin, C., Quentin, C., Grobost, F., Cambau, E., Robert, J., Dubois, V., Coulange, L. & Andre, C. 2009. Nationwide survey of extended-spectrum {beta}-lactamase-producing Enterobacteriaceae in the French community setting. *J Antimicrob Chemother,* 63**,** 1205-14.

Atkin, C., Neilands, J. & Phaff, H. J. J. O. B. 1970. Rhodotorulic acid from species of Leucosporidium, Rhodosporidium, Rhodotorula, Sporidiobolus, and Sporobolomyces, and a new alanine-containing ferrichrome from Cryptococcus melibiosum. 103**,** 722-733.

Bachman, M. A., Miller, V. L. & Weiser, J. N. 2009. Mucosal Lipocalin 2 Has Pro-Inflammatory and Iron-Sequestering Effects in Response to Bacterial Enterobactin. *PLOS Pathogens,* 5**,** e1000622.

Bankevich, A., Nurk, S., Antipov, D., Gurevich, A. A., Dvorkin, M., Kulikov, A. S., Lesin, V. M., Nikolenko, S. I., Pham, S. & Prjibelski, A. D. 2012. SPAdes: a new genome assembly algorithm and its applications to single-cell sequencing. *Journal of computational biology,* 19**,** 455-477.

Barber, A. E., Norton, J. P., Spivak, A. M. & Mulvey, M. A. 2013. Urinary tract infections: current and emerging management strategies. *Clinical infectious diseases : an official publication of the Infectious Diseases Society of America,* 57**,** 719-724.

Bartoletti, R., Cai, T., Wagenlehner, F. M., Naber, K. & Bjerklund Johansen, T. E. 2016. Treatment of Urinary Tract Infections and Antibiotic Stewardship. *European Urology Supplements,* 15**,** 81-87.

Bates Jr, J. M., Raffi, H. M., Prasadan, K., Mascarenhas, R., Laszik, Z., Maeda, N., Hultgren, S. J. & Kumar, S. J. K. I. 2004. Tamm-Horsfall protein knockout mice are more prone to urinary tract infection Rapid Communication. 65**,** 791-797.

Bauckman, K. A. & Mysorekar, I. U. 2016. Ferritinophagy drives uropathogenic *Escherichia coli* persistence in bladder epithelial cells. *Autophagy,* 12**,** 850-863.

Bäumler, A. J., Norris, T. L., Lasco, T., Voigt, W., Reissbrodt, R., Rabsch, W. & Heffron, F. 1998. IroN, a novel outer membrane siderophore receptor characteristic of Salmonella enterica. *Journal of Bacteriology,* 180**,** 1446-1453.

Beahm, N. P., Nicolle, L. E., Bursey, A., Smyth, D. J. & Tsuyuki, R. T. 2017. The assessment and management of urinary tract infections in adults: Guidelines for

pharmacists. *Canadian pharmacists journal : CPJ = Revue des pharmaciens du Canada : RPC,* 150**,** 298-305.

Beceiro, A., Tomás, M. & Bou, G. 2013. Antimicrobial resistance and virulence: a successful or deleterious association in the bacterial world? *Clinical microbiology reviews,* 26**,** 185-230.

Bennett, J. E., Dolin, R. & Blaser, M. J. 2014. *Principles and practice of infectious diseases*, Elsevier Health Sciences.

Bens, M., Vimont, S., Ben Mkaddem, S., Chassin, C., Goujon, J. M., Balloy, V., Chignard, M., Werts, C. & Vandewalle, A. 2014. Flagellin/TLR5 signalling activates renal collecting duct cells and facilitates invasion and cellular translocation of uropathogenic *Escherichia coli*. *Cell Microbiol,* 16**,** 1503-17.

Bergsten, G., Wullt, B., Schembri, M. A., Leijonhufvud, I. & Svanborg, C. 2007. Do type 1 fimbriae promote inflammation in the human urinary tract? *Cellular microbiology,* 9**,** 1766-1781.

Bergsten, G., Wullt, B. & Svanborg, C. 2005. < i> *Escherichia coli*</i>, fimbriae, bacterial persistence and host response induction in the human urinary tract. *International journal of medical microbiology,* 295**,** 487-502.

Bergstrom, C. T., Mcelhany, P. & Real, L. A. 1999. Transmission bottlenecks as determinants of virulence in rapidly evolving pathogens. 96**,** 5095-5100.

Berry, R. E., Klumpp, D. J., Schaeffer, A. J. I. 2009. Urothelial cultures support intracellular bacterial community formation by uropathogenic *Escherichia coli*. *Immunity,*77**,** 2762-2772.

Bi, D., Xu, Z., Harrison, E. M., Tai, C., Wei, Y., He, X., Jia, S., Deng, Z., Rajakumar, K. & Ou, H.-Y. 2012. ICEberg: a web-based resource for integrative and conjugative elements found in Bacteria. *Nucleic Acids Research,* 40**,** D621-D626.

Bien, J., Sokolova, O. & Bozko, P. 2012a. Role of uropathogenic *Escherichia coli* virulence factors in development of urinary tract infection and kidney damage. *International journal of nephrology,* 2012.

Bien, J., Sokolova, O. & Bozko, P. 2012b. Role of Uropathogenic *Escherichia coli* Virulence Factors in Development of Urinary Tract Infection and Kidney Damage. *International Journal of Nephrology,* 2012**,** 15.

Bien, J., Sokolova, O. & Bozko, P. 2012c. Role of Uropathogenic *Escherichia coli* Virulence Factors in Development of Urinary Tract Infection and Kidney Damage %J International Journal of Nephrology. 2012**,** 15.

Billström, H., Lund, B., Sullivan, Å. & Nord, C. E. J. I. J. O. A. A. 2008. Virulence and antimicrobial resistance in clinical Enterococcus faecium. 32**,** 374-377.

Blanco, M., Blanco, J. E., Alonso, M. P. & Blanco, J. 1996. Virulence factors and O groups of *Escherichia coli* isolates from patients with acute pyelonephritis, cystitis and asymptomatic bacteriuria. *European journal of epidemiology,* 12**,** 191-198.

Blango, M. G. & Mulvey, M. A. 2010. Persistence of uropathogenic *Escherichia coli* in the face of multiple antibiotics. *Antimicrobial agents and chemotherapy,* 54**,** 1855-1863.

Blázquez, R., Menasalvas, A., Carpena, I., Ramírez, C., Guerrero, C. & Moreno, S. 1999. Invasive Disease Caused by Ciprofloxacin-Resistant Uropathogenic *Escherichia coli*. *European Journal of Clinical Microbiology and Infectious Diseases,* 18**,** 503-505.

B**obrov, A. G., Kirillina, O., Fetherston, J. D., Miller, M. C., Burlison, J. A. & Perry, R. D.** 2014. The Yersinia pestis siderophore, yersiniabactin, and the ZnuABC system both contribute to zinc acquisition and the development of lethal septicaemic plague in mice. *Mol Microbiol,* 93**,** 759-75.

Bolger, A. M., Lohse, M. & Usadel, B. 2014a. Trimmomatic: a flexible trimmer for Illumina sequence data. *Bioinformatics,* 30**,** 2114-20.

Bolger, A. M., Lohse, M. & Usadel, B. 2014b. Trimmomatic: a flexible trimmer for Illumina sequence data. *Bioinformatics,* 30**,** 2114-2120.

Boukhalfa, H. & Crumbliss, A. L. 2002. Chemical aspects of siderophore mediated iron transport. *Biometals,* 15**,** 325-339.

Bray, J. 1945. Isolation of antigenically homogeneous strains of Bact. coli neapolitanum from summer diarrhoea of infants. *The Journal of Pathology,* 57**,** 239-247.

Brettin, T., Davis, J. J., Disz, T., Edwards, R. A., Gerdes, S., Olsen, G. J., Olson, R., Overbeek, R., Parrello, B. & Pusch, G. D. 2015. RASTtk: a modular and extensible implementation of the RAST algorithm for building custom annotation pipelines and annotating batches of genomes. *Scientific reports,* 5**,** 8365.

Brolund, A. 2013. *Plasmid mediated antibiotic resistance: with focus on extended spectrum β-lactamases (ESBL)*, Inst för mikrobiologi, tumör-och cellbiologi/Dept of Microbiology, Tumor and ….

Brolund, A., Edquist, P. J., Makitalo, B., Olsson-Liljequist, B., Soderblom, T., Wisell, K. T. & Giske, C. G. 2014. Epidemiology of extended-spectrum beta-lactamase-producing *Escherichia coli* in Sweden 2007-2011. *Clin Microbiol Infect,* 20**,** O344-52.

Brown, L., Langelier, C., Reid, M. J. A., Rutishauser, R. L. & Strnad, L. 2017. Antimicrobial Resistance: A Call to Action! *Clinical infectious diseases : an official publication of the Infectious Diseases Society of America,* 64**,** 106-107.

Brumbaugh, A. R., Smith, S. N., Subashchandrabose, S., Himpsl, S. D., Hazen, T. H., Rasko, D. A. & Mobley, H. L. T. 2015. Blocking Yersiniabactin Import Attenuates Extraintestinal Pathogenic *Escherichia coli* in Cystitis and Pyelonephritis and Represents a Novel Target To Prevent Urinary Tract Infection. *Infection and Immunity,* 83**,** 1443-1450.

Burkhard, K. A. & Wilks, A. J. B. 2008. Functional characterization of the Shigella dysenteriae heme ABC transporter. 47**,** 7977-7979.

Calhau, V., Ribeiro, G., Mendonça, N. & Da Silva, G. J. 2013. Prevalent combination of virulence and plasmidic-encoded resistance in ST 131 *Escherichia coli* strains. *Virulence,* 4**,** 726-729.

Carattoli, A. 2009. Resistance Plasmid Families in Enterobacteriaceae. *Antimicrobial Agents and Chemotherapy,* 53**,** 2227-2238.

Carattoli, A., Zankari, E., Garcia-Fernandez, A., Voldby Larsen, M., Lund, O., Villa, L., Moller Aarestrup, F. & Hasman, H. 2014. In silico detection and typing of plasmids using PlasmidFinder and plasmid multilocus sequence typing. *Antimicrob Agents Chemother,* 58**,** 3895-903.

Cassat, J. E., Skaar, E. P. J. C. H. 2013. Iron in infection and immunity. *Microbe,* 13**,** 509-519.

Caza, M., Lépine, F., Milot, S. & Dozois, C. M. 2008. Specific Roles of the iroBCDEN Genes in Virulence of an Avian Pathogenic *Escherichia coli* O78 Strain and in Production of Salmochelins. *Infection and Immunity,* 76**,** 3539-3549.

Chaturvedi, K. S., Hung, C. S., Crowley, J. R., Stapleton, A. E. & Henderson, J. P. 2012. The siderophore yersiniabactin binds copper to protect pathogens during infection. *Nat Chem Biol,* 8**,** 731-6.

Chen, L., Yang, J., Yu, J., Yao, Z., Sun, L., Shen, Y. & Jin, Q. 2005. VFDB: a reference database for bacterial virulence factors. *Nucleic acids research,* 33**,** D325-D328.

Choby, J. E. & Skaar, E. P. J. J. O. M. B. 2016. Heme synthesis and acquisition in bacterial pathogens. 428**,** 3408-3428.

Chorell, E., Pinkner, J. S., Bengtsson, C., Banchelin, T. S.-L., Edvinsson, S., Linusson, A., Hultgren, S. J. & Almqvist, F. 2012a. Mapping pilicide anti-virulence effect in

Escherichia coli, a comprehensive structure-activity study. *Bioorganic & medicinal chemistry,* 20**,** 3128-3142.

Chorell, E., Pinkner, J. S., Bengtsson, C., Banchelin, T. S., Edvinsson, S., Linusson, A., Hultgren, S. J. & Almqvist, F. 2012b. Mapping pilicide anti-virulence effect in *Escherichia coli*, a comprehensive structure-activity study. *Bioorg Med Chem,* 20**,** 3128-42.

Christensen, G. D., Simpson, W., Younger, J., Baddour, L., Barrett, F., Melton, D. & Beachey, E. 1985. Adherence of coagulase-negative staphylococci to plastic tissue culture plates: a quantitative model for the adherence of staphylococci to medical devices. *Journal of clinical microbiology,* 22**,** 996-1006.

Christopher, G. W. 1985. *Escherichia coli* bacteremia, meningitis, and hemochromatosis. 145**,** 1908-1908.

Chu, B. C., Garcia-Herrero, A., Johanson, T. H., Krewulak, K. D., Lau, C. K., Peacock, R. S., Slavinskaya, Z. & Vogel, H. J. 2010. Siderophore uptake in bacteria and the battle for iron with the host; a bird's eye view. *Biometals,* 23**,** 601-611.

Clermont, O., Bonacorsi, S. & Bingen, E. 2000. Rapid and simple determination of the *Escherichia coli* phylogenetic group. *Applied and environmental microbiology,* 66**,** 4555-4558.

Collard, K. J. 2009. Iron homeostasis in the neonate. 123**,** 1208-1216.

Connell, I., Agace, W., Klemm, P., Schembri, M., Mărild, S. & Svanborg, C. 1996. Type 1 fimbrial expression enhances *Escherichia coli* virulence for the urinary tract. *Proceedings of the National Academy of Sciences,* 93**,** 9827-9832.

Conover, M. S., Hadjifrangiskou, M., Palermo, J. J., Hibbing, M. E., Dodson, K. W. & Hultgren, S. J. 2016. Metabolic Requirements of *Escherichia coli* in Intracellular Bacterial Communities during Urinary Tract Infection Pathogenesis. *MBio,* 7**,** e00104-16.

Cornelissen, C. N. J. F. B. 2003. Transferrin-iron uptake by Gram-negative bacteria. 8**,** 836-847.

Crosa, J. H. & Walsh, C. T. 2002. Genetics and Assembly Line Enzymology of Siderophore Biosynthesis in Bacteria. *Microbiology and Molecular Biology Reviews,* 66**,** 223-249.

Da Silva, G. J. & Mendonca, N. 2012. Association between antimicrobial resistance and virulence in *Escherichia coli*. *Virulence,* 3**,** 18-28.

Da Silva, G. J. & Mendonça, N. J. V. 2012. Association between antimicrobial resistance and virulence in *Escherichia coli*. 3**,** 18-28.

Darling, A. C. E., Mau, B., Blattner, F. R. & Perna, N. T. 2004. Mauve: multiple alignment of conserved genomic sequence with rearrangements. *Genome research,* 14**,** 1394-1403.

De Kraker, M. E. A., Stewardson, A. J. & Harbarth, S. 2016. Will 10 Million People Die a Year due to Antimicrobial Resistance by 2050? *PLoS medicine,* 13**,** e1002184-e1002184.

De Lorenzo, V., Bindereif, A., Paw, B. H. & Neilands, J. B. 1986. Aerobactin biosynthesis and transport genes of plasmid ColV-K30 in *Escherichia coli* K-12. *Journal of Bacteriology,* 165**,** 570-578.

De Ree, J. & Van Den Bosch, J. 1987. Serological response to the P fimbriae of uropathogenic *Escherichia coli* in pyelonephritis. *Infection and immunity,* 55**,** 2204-2207.

De Rossi, B. P., García, C., Calenda, M., Vay, C. & Franco, M. 2009. Activity of levofloxacin and ciprofloxacin on biofilms and planktonic cells of Stenotrophomonas maltophilia isolates from patients with device-associated infections. *International journal of antimicrobial agents,* 34**,** 260-264.

Deborah Chen, H. & Frankel, G. 2005. Enteropathogenic *Escherichia coli*: unravelling pathogenesis. *FEMS microbiology reviews,* 29**,** 83-98.

Del Castillo, B. R., Vinué, L., Román, E. J., Guerra, B., Carattoli, A., Torres, C. & Martínez-Martínez, L. 2013. Molecular characterization of multiresistant *Escherichia coli* producing or not extended-spectrum β-lactamases. *BMC microbiology,* 13**,** 84.

Denève, C., Bouttier, S., Dupuy, B., Barbut, F., Collignon, A., Janoir, C. J. A. A. & CHEMOTHERAPY 2009. Effects of subinhibitory concentrations of antibiotics on colonization factor expression by moxifloxacin-susceptible and moxifloxacin-resistant Clostridium difficile strains. 53**,** 5155-5162.

Dhakal, B., Kulesus, R. & Mulvey, M. J. E. J. O. C. I. 2008. Mechanisms and consequences of bladder cell invasion by uropathogenic *Escherichia coli*. 38**,** 2-11.

Dikshit, N., Bist, P., Fenlon, S. N., Pulloor, N. K., Chua, C. E. L., Scidmore, M. A., Carlyon, J. A., Tang, B. L., Chen, S. L. & Sukumaran, B. 2015. Intracellular Uropathogenic *E. coli* Exploits Host Rab35 for Iron Acquisition and Survival within Urinary Bladder Cells. *PLOS Pathogens,* 11**,** e1005083.

Dobrindt, U., Agerer, F., Michaelis, K., Janka, A., Buchrieser, C., Samuelson, M., Svanborg, C., Gottschalk, G., Karch, H. & Hacker, J. 2003. Analysis of genome plasticity in pathogenic and commensal *Escherichia coli* isolates by use of DNA arrays. *Journal of bacteriology,* 185**,** 1831-1840.

Donnenberg, M. 2013. *Escherichia coli: Pathotypes and Principles of Pathogenesis*, Academic Press.

Donnenberg, M. S., Newman, B., Utsalo, S. J., Trifillis, A. L., Hebel, J. R. & Warren, J. W. 1994. Internalization of *Escherichia coli* into human kidney epithelial cells: comparison of fecal and pyelonephritis-associated strains. *J Infect Dis,* 169**,** 831-8.

Dozois, C. M., Daigle, F. & Curtiss, R. 2003. Identification of pathogen-specific and conserved genes expressed in vivo by an avian pathogenic Escherichia coli strain. *Proceedings of the National Academy of Sciences,* 100**,** 247-252.

Edwards, A. M. & Massey, R. C. 2011. Invasion of human cells by a bacterial pathogen. *Journal of visualized experiments: JoVE.*

Falzano, L., Fiorentini, C., Donelli, G., Michel, E., Kocks, C., Cossart, P., Cabanié, L., Oswald, E. & Boquet, P. 1993. Induction of phagocytic behaviour in human epithelial cells by *Escherichia coli* cytotoxic necrotizing factor type1. *Molecular microbiology,* 9**,** 1247-1254.

Farooqui, B. J., Alam, M. & Khurshid, M. 1989. Urinary tract infection. *Journal of Pakistan Medical Association,* 39**,** 129.

Fatima, S., Muhammad, I. N., Usman, S., Jamil, S., Khan, M. N. & Khan, S. I. 2018. Incidence of multidrug resistance and extended-spectrum beta-lactamase expression in community-acquired urinary tract infection among different age groups of patients. *Indian journal of pharmacology,* 50**,** 69-74.

Feldmann, F., Sorsa, L. J., Hildinger, K. & Schubert, S. 2007. The salmochelin siderophore receptor IroN contributes to invasion of urothelial cells by extraintestinal pathogenic *Escherichia coli* in vitro. *Infection and immunity,* 75**,** 3183-3187.

Finlay, B. B. & Falkow, S. 1997. Common themes in microbial pathogenicity revisited. *Microbiology and Molecular Biology Reviews,* 61**,** 136-169.

Fischbach, M. A., Lin, H., Liu, D. R. & Walsh, C. T. 2005. In vitro characterization of IroB, a pathogen-associated C-glycosyltransferase. *Proceedings of the National Academy of Sciences of the United States of America,* 102**,** 571-576.

Fischbach, M. A., Lin, H., Zhou, L., Yu, Y., Abergel, R. J., Liu, D. R., Raymond, K. N., Wanner, B. L., Strong, R. K., Walsh, C. T., Aderem, A. & Smith, K. D. 2006. The pathogen-associated iroA gene cluster mediates bacterial evasion of lipocalin 2. *Proceedings of the National Academy of Sciences,* 103**,** 16502-16507.

Flo, T. H., Smith, K. D., Sato, S., Rodriguez, D. J., Holmes, M. A., Strong, R. K., Akira, S. & Aderem, A. 2004. Lipocalin 2 mediates an innate immune response to bacterial infection by sequestrating iron. *Nature,* 432**,** 917-21.

Flores-Mireles, A. L., Walker, J. N., Caparon, M. & Hultgren, S. J. 2015a. Urinary tract infections: epidemiology, mechanisms of infection and treatment options. *Nat Rev Microbiol,* 13**,** 269-84.

Flores-Mireles, A. L., Walker, J. N., Caparon, M. & Hultgren, S. J. 2015b. Urinary tract infections: epidemiology, mechanisms of infection and treatment options. *Nature reviews microbiology,* 13**,** 269-284.

Flores-Mireles, A. L., Walker, J. N., Caparon, M. & Hultgren, S. J. 2015c. Urinary tract infections: epidemiology, mechanisms of infection and treatment options. *Nature reviews. Microbiology,* 13**,** 269-284.

Foxman, B. 2010. The epidemiology of urinary tract infection. *Nature Reviews Urology,* 7**,** 653.

Foxman, B. 2014a. Urinary Tract Infection Syndromes: Occurrence, Recurrence, Bacteriology, Risk Factors, and Disease Burden. *Infectious Disease Clinics of North America,* 28**,** 1-13.

Foxman, B. 2014b. Urinary tract infection syndromes: occurrence, recurrence, bacteriology, risk factors, and disease burden. *Infectious Disease Clinics,* 28**,** 1-13.

Foxman, B., Barlow, R., D'arcy, H., Gillespie, B. & Sobel, J. D. 2000a. Urinary tract infection: self-reported incidence and associated costs. *Annals of epidemiology,* 10**,** 509-515.

Foxman, B., Barlow, R., D'arcy, H., Gillespie, B. & Sobel, J. D. 2000b. Urinary tract infection: self-reported incidence and associated costs. 10**,** 509-515.

Fukushi, Y., Orikasa, S. & Kagayama, M. 1979. An electron microscopic study of the interaction between vesical epitherlium and *E. coli*. *Invest Urol,* 17**,** 61-8.

Galardini, M., Biondi, E. G., Bazzicalupo, M. & Mengoni, A. 2011. CONTIGuator: a bacterial genomes finishing tool for structural insights on draft genomes. *Source code for biology and medicine,* 6**,** 11.

Galloway-Peña, J. R., Nallapareddy, S. R., Arias, C. A., Eliopoulos, G. M. & Murray, B. 2009. Analysis of clonality and antibiotic resistance among early clinical isolates of Enterococcus faecium in the United States. 200**,** 1566-1573.

Gao, Q., Wang, X., Xu, H., Xu, Y., Ling, J., Zhang, D., Gao, S. & Liu, X. 2012a. Roles of iron acquisition systems in virulence of extraintestinal pathogenic *Escherichia coli*:

salmochelin and aerobactin contribute more to virulence than heme in a chicken infection model. *BMC Microbiology,* 12**,** 143.

Gao, Q., Wang, X., Xu, H., Xu, Y., Ling, J., Zhang, D., Gao, S. & Liu, X. J. B. M. 2012b. Roles of iron acquisition systems in virulence of extraintestinal pathogenic *Escherichia coli*: salmochelin and aerobactin contribute more to virulence than heme in a chicken infection model. 12**,** 143.

Garcia, E. C., Brumbaugh, A. R. & Mobley, H. L. 2011. Redundancy and specificity of *Escherichia coli* iron acquisition systems during urinary tract infection. *Infection and immunity,* 79**,** 1225-1235.

Garcia, T. A., Ventura, C. L., Smith, M. A., Merrell, D. S. & O'brien, A. D. 2013. Cytotoxic necrotizing factor 1 and hemolysin from uropathogenic *Escherichia coli* elicit different host responses in the murine bladder. *Infect Immun,* 81**,** 99-109.

Garénaux, A., Caza, M. & Dozois, C. M. 2011. The Ins and Outs of siderophore mediated iron uptake by extra-intestinal pathogenic *Escherichia coli*. *Veterinary Microbiology,* 153**,** 89-98.

Gharrah, M. M. & Mostafa El-Mahdy, A. 2017. Association between Virulence Factors and Extended Spectrum Beta-Lactamase Producing Klebsiella pneumoniae Compared to Nonproducing Isolates. 2017**,** 7279830.

Gibson, F. & Magrath, D. I. 1969. The isolation and characterization of a hydroxamic acid (aerobactin) formed by Aerobacter aerogenes 62-1. *BBA - General Subjects,* 192**,** 175-184.

Giraud, E., Rychlik, I. & Cloeckaert, A. 2017. Editorial: Antimicrobial Resistance and Virulence Common Mechanisms. *Frontiers in Microbiology,* 8.

Gleckman, R., Esposito, A., Crowley, M. & Natsios, G. A. 1979. Reliability of a single urine culture in establishing diagnosis of asymptomatic bacteriuria in adult males. *Journal of Clinical Microbiology,* 9**,** 596-597.

Goetz, D. H., Holmes, M. A., Borregaard, N., Bluhm, M. E., Raymond, K. N. & Strong, R. K. 2002. The neutrophil lipocalin NGAL is a bacteriostatic agent that interferes with siderophore-mediated iron acquisition. *Mol Cell,* 10**,** 1033-43.

González, M. J., Robino, L., Iribarnegaray, V., Zunino, P. & Scavone, P. 2017a. Effect of different antibiotics on biofilm produced by uropathogenic *Escherichia coli* isolated from children with urinary tract infection. *Pathogens and Disease,* 75**,** ftx053-ftx053.

González, M. J., Zunino, P., Iribarnegaray, V., Scavone, P. & Robino, L. 2017b. Effect of different antibiotics on biofilm produced by uropathogenic *Escherichia coli* isolated from children with urinary tract infection. *Pathogens and Disease,* 75.

Grabe, M., Bishop, M., Bjerklund-Johansen, T., Botto, H., Çek, M., Lobel, B., Naber, K., Palou, J. & Tenke, P. 2008. Management of urinary and male genital tract infections. *Update*.

Grissa, I., Vergnaud, G. & Pourcel, C. 2007. CRISPRFinder: a web tool to identify clustered regularly interspaced short palindromic repeats. *Nucleic acids research,* 35**,** W52-W57.

Guglietta, A. 2017. Recurrent urinary tract infections in women: risk factors, etiology, pathogenesis and prophylaxis. *Future Microbiology,* 12**,** 239-246.

Guillard, T., Pons, S., Roux, D., Pier, G. B. & Skurnik, D. 2016. Antibiotic resistance and virulence: Understanding the link and its consequences for prophylaxis and therapy. *Bioessays,* 38**,** 682-93.

Gupta, K., Hooton, T. M., Naber, K. G., Wullt, B., Colgan, R., Miller, L. G., Moran, G. J., Nicolle, L. E., Raz, R. & Schaeffer, A. J. 2011a. International clinical practice guidelines for the treatment of acute uncomplicated cystitis and pyelonephritis in women: a 2010 update by the Infectious Diseases Society of America and the European Society for Microbiology and Infectious Diseases. *Clinical infectious diseases,* 52**,** e103-e120.

Gupta, K., Hooton, T. M., Naber, K. G., Wullt, B., Colgan, R., Miller, L. G., Moran, G. J., Nicolle, L. E., Raz, R., Schaeffer, A. J. & Soper, D. E. 2011b. International clinical practice guidelines for the treatment of acute uncomplicated cystitis and pyelonephritis in women: A 2010 update by the Infectious Diseases Society of America and the European Society for Microbiology and Infectious Diseases. *Clin Infect Dis,* 52**,** e103-20.

Gurevich, A., Saveliev, V., Vyahhi, N. & Tesler, G. 2013. QUAST: quality assessment tool for genome assemblies. *Bioinformatics,* 29**,** 1072-1075.

Habeeb, M. A., Haque, A., Iversen, A. & Giske, C. G. 2014. Occurrence of virulence genes, 16S rRNA methylases, and plasmid-mediated quinolone resistance genes in CTX-M-producing *Escherichia coli* from Pakistan. *European Journal of Clinical Microbiology & Infectious Diseases,* 33**,** 399-409.

Hagan, E. C. 2009. Iron Acquisition by Uropathogenic *Escherichia coli*: ChuA and Hma Heme Receptors as Virulence Determinants and Vaccine Targets.

Hagan, E. C., Lloyd, A. L., Rasko, D. A., Faerber, G. J. & Mobley, H. L. J. P. P. 2010. *Escherichia coli* global gene expression in urine from women with urinary tract infection. 6**,** e1001187.

Hagberg, L., Engberg, I., Freter, R., Lam, J., Olling, S. & Eden, C. S. 1983. Ascending, unobstructed urinary tract infection in mice caused by pyelonephritogenic *Escherichia coli* of human origin. *Infection and immunity,* 40**,** 273-283.

Hagberg, L., Jodal, U., Korhonen, T. K., Lidin-Janson, G., Lindberg, U. & Eden, C. S. 1981. Adhesion, hemagglutination, and virulence of *Escherichia coli* causing urinary tract infections. *Infection and immunity,* 31**,** 564-570.

Han, Z., Pinkner, J. S., Ford, B., Obermann, R., Nolan, W., Wildman, S. A., Hobbs, D., Ellenberger, T., Cusumano, C. K., Hultgren, S. J. & Janetka, J. W. 2010. Structure-based drug design and optimization of mannoside bacterial FimH antagonists. *Journal of medicinal chemistry,* 53**,** 4779-4792.

Hancock, V., Ferrières, L. & Klemm, P. 2008. The ferric yersiniabactin uptake receptor FyuA is required for efficient biofilm formation by urinary tract infectious *Escherichia coli* in human urine. *Microbiology,* 154**,** 167-175.

Harvey, R. A. 2007. *Microbiology*, Lippincott Williams & Wilkins.

Hasan, A. S., Nair, D., Kaur, J., Baweja, G., Deb, M. & Aggarwal, P. 2007. Resistance patterns of urinary isolates in a tertiary Indian hospital. *J Ayub Med Coll Abbottabad,* 19**,** 39-41.

He, X. L., Wang, Q., Peng, L., Qu, Y. R., Puthiyakunnon, S., Liu, X. L., Hui, C. Y., Boddu, S., Cao, H. & Huang, S. H. 2015. Role of uropathogenic *Escherichia coli* outer membrane protein T in pathogenesis of urinary tract infection. *Pathog Dis,* 73.

Hefzy, E. M. & Hassuna, N. A. 2017. Fluoroquinolone-Resistant Sequence Type 131 Subgroups O25b and O16 Among Extraintestinal *Escherichia coli* Isolates from Community-Acquired Urinary Tract Infections. *Microbial Drug Resistance,* 23**,** 224-229.

Helen S. Lee, J. L. 2018. *Urinary Tract Infections*, PSAP 2018 BOOK 1

Henderson, I. R., Cappello, R. & Nataro, J. P. 2000. Autotransporter proteins, evolution and redefining protein secretion. *Trends in microbiology,* 8**,** 529-532.

Henderson, J. P., Crowley, J. R., Pinkner, J. S., Walker, J. N., Tsukayama, P., Stamm, W. E., Hooton, T. M. & Hultgren, S. J. 2009. Quantitative Metabolomics Reveals an Epigenetic Blueprint for Iron Acquisition in Uropathogenic *Escherichia coli*. *PLOS Pathogens,* 5**,** e1000305.

Herzer, P. J., Inouye, S., Inouye, M. & Whittam, T. S. 1990. Phylogenetic distribution of branched RNA-linked multicopy single-stranded DNA among natural isolates of *Escherichia coli*. *J Bacteriol,* 172**,** 6175-81.

Hilbert, D. W., Paulish-Miller, T. E., Tan, C. K., Carey, A. J., Ulett, G. C., Mordechai, E., Adelson, M. E., Gygax, S. E. & Trama, J. P. 2012. Clinical< i> *Escherichia coli*</i> isolates utilize alpha-hemolysin to inhibit< i> in vitro</i> epithelial cytokine production. *Microbes and Infection,* 14**,** 628-638.

Hoban, D. J., Lascols, C., Nicolle, L. E., Badal, R., Bouchillon, S., Hackel, M. & Hawser, S. 2012. Antimicrobial susceptibility of Enterobacteriaceae, including molecular characterization of extended-spectrum beta-lactamase-producing species, in urinary tract isolates from hospitalized patients in North America and Europe: results from the SMART study 2009-2010. *Diagn Microbiol Infect Dis,* 74**,** 62-7.

Hof, H. 2017. [Candiduria! What now? : Therapy of urinary tract infections with Candida]. *Urologe A,* 56**,** 172-179.

Hofman, P., Le Negrate, G., Mograbi, B., Hofman, V., Brest, P., Alliana-Schmid, A., Flatau, G., Boquet, P. & Rossi, B. 2000. *Escherichia coli* cytotoxic necrotizing factor-1 (CNF-1) increases the adherence to epithelia and the oxidative burst of human polymorphonuclear leukocytes but decreases bacteria phagocytosis. *Journal of leukocyte biology,* 68**,** 522-528.

Holden, V. I. & Bachman, M. A. 2015. Diverging roles of bacterial siderophores during infection. *Metallomics,* 7**,** 986-995.

Hood, M. I. & Skaar, E. P. 2012. Nutritional immunity: transition metals at the pathogen-host interface. *Nat Rev Microbiol,* 10**,** 525-37.

Hooton, T. M. 2012. Uncomplicated urinary tract infection. *New England Journal of Medicine,* 366**,** 1028-1037.

Hopkins, W. J., Elkahwaji, J., Beierle, L. M., Leverson, G. E. & Uehling, D. T. 2007. Vaginal mucosal vaccine for recurrent urinary tract infections in women: results of a phase 2 clinical trial. *J Urol,* 177**,** 1349-53; quiz 1591.

Hull, R. A., Gill, R. E., Hsu, P., Minshew, B. H. & Falkow, S. 1981. Construction and expression of recombinant plasmids encoding type 1 or D-mannose-resistant pili from a urinary tract infection *Escherichia coli* isolate. *Infection and Immunity,* 33**,** 933-938.

Hultgren, S. J., Porter, T. N., Schaeffer, A. J. & Duncan, J. L. 1985. Role of type 1 pili and effects of phase variation on lower urinary tract infections produced by *Escherichia coli*. *Infection and immunity,* 50**,** 370-377.

Hussain, A., Ewers, C., Nandanwar, N., Guenther, S., Jadhav, S., Wieler, L. H. & Ahmed, N. 2012. Multiresistant uropathogenic *Escherichia coli* from a region in India where urinary tract infections are endemic: genotypic and phenotypic characteristics of sequence type 131 isolates of the CTX-M-15 extended-spectrum-β-lactamase-producing lineage. *Antimicrobial agents and chemotherapy,* 56**,** 6358-6365.

Hussain, T. 2015. Pakistan at the verge of potential epidemics by multi-drug resistant pathogenic bacteria. *Advancements in life sciences,* 2**,** 46-47.

JADHAV, S., HUSSAIN, A., DEVI, S., KUMAR, A., PARVEEN, S., GANDHAM, N., WIELER, L. H., EWERS, C. & AHMED, N. J. P. O. 2011. Virulence characteristics and genetic affinities of multiple drug resistant uropathogenic *Escherichia coli* from a semi urban locality in India. 6**,** e18063.

Jean, S.-S., Coombs, G., Ling, T., Balaji, V., Rodrigues, C., Mikamo, H., Kim, M.-J., Rajasekaram, D. G., Mendoza, M. & Tan, T. Y. J. I. J. O. A. A. 2016. Epidemiology and antimicrobial susceptibility profiles of pathogens causing urinary tract infections in the Asia-Pacific region: Results from the Study for Monitoring Antimicrobial Resistance Trends (SMART), 2010–2013. 47**,** 328-334.

Johanson, I.-M., Plos, K., Marklund, B.-I. & Svanborg, C. 1993. < i> Pap, papG</i> and< i> prsG</i> DNA sequences in< i> *Escherichia coli*</i> from the fecal flora and the urinary tract. *Microbial pathogenesis,* 15**,** 121-129.

Johnson, J. R. 1991a. Virulence factors in *Escherichia coli* urinary tract infection. *Clinical microbiology reviews,* 4**,** 80.

Johnson, J. R. 1991b. Virulence factors in *Escherichia coli* urinary tract infection. *Clinical microbiology reviews,* 4**,** 80-128.

Johnson, J. R., Brown, J. J. & Maslow, J. N. 1998. Clonal distribution of the three alleles of the Gal (α1–4) Gal-specific adhesin gene papG among *Escherichia coli* strains from patients with bacteremia. *Journal of Infectious Diseases,* 177**,** 651-661.

Johnson, J. R., Delavari, P., Kuskowski, M. & Stell, A. L. 2001. Phylogenetic distribution of extraintestinal virulence-associated traits in *Escherichia coli*. *J Infect Dis,* 183**,** 78-88.

Johnson, J. R., Johnston, B., Clabots, C., Kuskowski, M. A. & Castanheira, M. 2010. *Escherichia coli* sequence type ST131 as the major cause of serious multidrug-resistant *E. coli* infections in the United States. *Clinical infectious diseases,* 51**,** 286-294.

Johnson, J. R., Kuskowski, M. A., Owens, K., Gajewski, A. & Winokur, P. L. 2003. Phylogenetic Origin and Virulence Genotype in Relation to Resistance to

Fluoroquinolones and/or Extended-Spectrum Cephalosporins and Cephamycins among *Escherichia coli* Isolates from Animals and Humans. *The Journal of Infectious Diseases,* 188**,** 759-768.

Johnson, J. R., Magistro, G., Clabots, C., Porter, S., Manges, A., Thuras, P. & Schubert, S. J. M. P. 2018. Contribution of yersiniabactin to the virulence of an *Escherichia coli* sequence type 69 ("clonal group A") cystitis isolate in murine models of urinary tract infection and sepsis. 120**,** 128-131.

Johnson, J. R., Owens, K., Gajewski, A. & Kuskowski, M. A. 2005a. Bacterial Characteristics in Relation to Clinical Source of *Escherichia coli* Isolates from Women with Acute Cystitis or Pyelonephritis and Uninfected Women. *Journal of Clinical Microbiology,* 43**,** 6064-6072.

Johnson, J. R., Owens, K., Gajewski, A. & Kuskowski, M. A. 2005b. Bacterial characteristics in relation to clinical source of *Escherichia coli* isolates from women with acute cystitis or pyelonephritis and uninfected women. *Journal of clinical microbiology,* 43**,** 6064-6072.

Johnson, J. R., Russo, T. A., Tarr, P. I., Carlino, U., Bilge, S. S., Vary, J. C. & Stell, A. L. 2000. Molecular Epidemiological and Phylogenetic Associations of Two Novel Putative Virulence Genes, iha and iroN*E. coli* , among *Escherichia coli* Isolates from Patients with Urosepsis. *Infection and Immunity,* 68**,** 3040-3047.

Johnson, J. R. & Stell, A. L. 2000a. Extended virulence genotypes of *Escherichia coli* strains from patients with urosepsis in relation to phylogeny and host compromise. *The Journal of infectious diseases,* 181**,** 261-272.

Johnson, J. R. & Stell, A. L. 2000b. Extended virulence genotypes of *Escherichia coli* strains from patients with urosepsis in relation to phylogeny and host compromise. *Journal of Infectious Diseases,* 181**,** 261-272.

Johnson, T. J. & Nolan, L. K. 2009. Pathogenomics of the virulence plasmids of *Escherichia coli*. *Microbiol Mol Biol Rev,* 73**,** 750-74.

Johnson, T. J., Siek, K. E., Johnson, S. J. & Nolan, L. K. 2006. DNA Sequence of a ColV Plasmid and Prevalence of Selected Plasmid-Encoded Virulence Genes among Avian *Escherichia coli* Strains. *Journal of Bacteriology,* 188**,** 745-758.

Johnstone, T. C. & Nolan, E. M. 2015a. Beyond iron: non-classical biological functions of bacterial siderophores. *Dalton Trans,* 44**,** 6320-39.

Johnstone, T. C. & Nolan, E. M. 2015b. Beyond iron: non-classical biological functions of bacterial siderophores. *Dalton transactions (Cambridge, England : 2003),* 44**,** 6320-6339.

Jones, A. M., Lindow, S. E. & Wildermuth, M. C. 2007. Salicylic Acid, Yersiniabactin, and Pyoverdin Production by the Model Phytopathogen Pseudomonas syringae pv. tomato DC3000: Synthesis, Regulation, and Impact on Tomato and Arabidopsis Host Plants. *Journal of Bacteriology,* 189**,** 6773-6786.

Jose, J., Jähnig, F. & Meyer, T. F. 1995. Common structural features of IgA1 protease-like outer membrane protein autotransporters. *Molecular microbiology,* 18**,** 378-380.

Julien, L. A., Baron, F., Bonnassie, S., Nau, F., Guérin-Dubiard, C., Jan, S. & Andrews, S. C. 2019. The anti-bacterial iron-restriction defence mechanisms of egg white; the potential role of three lipocalin-like proteins in resistance against Salmonella. *BioMetals***,** np.

Jürgen, H., Klaus, H., Tilman, V., Elizabeth, S., Alexander, R., Igor, S. & Reinhard, B. 1993. Virulence of Yersinia enterocolitica is closely associated with siderophore production, expression of an iron-repressible outer membrane polypeptide of 65 000 Da and pesticin sensitivity. *Molecular Microbiology,* 8**,** 397-408.

Kakkanat, A., Totsika, M., Schaale, K., Duell, B. L., Lo, A. W., Phan, M.-D., Moriel, D. G., Beatson, S. A., Sweet, M. J. & Ulett, G. C. 2015a. The role of H4 flagella in *Escherichia coli* ST131 virulence. *Scientific reports,* 5**,** 16149.

Kakkanat, A., Totsika, M., Schaale, K., Duell, B. L., Lo, A. W., Phan, M.-D., Moriel, D. G., Beatson, S. A., Sweet, M. J., Ulett, G. C. & Schembri, M. A. 2015b. The role of H4 flagella in *Escherichia coli* ST131 virulence. *Scientific reports,* 5**,** 16149-16149.

Källenius, G., Svenson, S., Hultberg, H., Möllby, R., Helin, I., Cedergren, B. & Winberg, J. 1981. Occurrence of P-fimbriated *Escherichia coli* in urinary tract infections. *The Lancet,* 318**,** 1369-1372.

Kalsoom, B., Jafar, K., Begum, H., Munir, S., Ul Akbar, N., Ansari, J. A. & Anees, M. 2012. Patterns of antibiotic sensitivity of bacterial pathogens among urinary tract infections (UTI) patients in a Pakistani population. *African Journal of Microbiology Research,* 6**,** 414-420.

Kaper, J. B., Nataro, J. P. & Mobley, H. L. 2004. Pathogenic *Escherichia coli*. *Nature Reviews Microbiology,* 2**,** 123-140.

Kariyawasam, S. & Nolan, L. K. 2011. papA gene of avian pathogenic *Escherichia coli*. *Avian Dis,* 55**,** 532-8.

Kausar, A., Akram, M., Shoaib, M., Mehmood, R. T., Abbasi, M. N., Adnan, M., Aziz, D. & Asad, M. J. 2014. Isolation and identification of UTI causing agents and frequency of ESBL (Extended Spectrum Beta Lactamase) in Pakistan. *Am. J. Phytomed. Clin. Ther,* 2**,** 963-975.

Keren, I., Shah, D., Spoering, A., Kaldalu, N. & Lewis, K. 2004. Specialized persister cells and the mechanism of multidrug tolerance in *Escherichia coli*. *Journal of bacteriology,* 186**,** 8172-8180.

Khalil, A. T., Ali, M., Tanveer, F., Ovais, M., Idrees, M., Shinwari, Z. K. & Hollenbeck, J. E. 2017. Emerging Viral Infections in Pakistan: Issues, Concerns, and Future Prospects. *Health Security,* 15**,** 268-281.

Khan, B. A., Saeed, S., Akram, A., Khan, F. B. & Nasim, A. 2010. Nosocomial uropathogens and their antibiotic sensitivity patterns in a tertiary referral teaching hospital in Rawalpindi, Pakistan. *J. Ayub Med. Coll. Abbottabad,* 22**,** 11-2.

Khan, I. U., Gannon, V., Kent, R., Koning, W., Lapen, D. R., Miller, J., Neumann, N., Phillips, R., Robertson, W. & Topp, E. 2007. Development of a rapid quantitative PCR assay for direct detection and quantification of culturable and non-culturable< i> *Escherichia coli*</i> from agriculture watersheds. *Journal of microbiological methods,* 69**,** 480-488.

Klein, E. Y., Van Boeckel, T. P., Martinez, E. M., Pant, S., Gandra, S., Levin, S. A., Goossens, H. & Laxminarayan, R. 2018. Global increase and geographic convergence in antibiotic consumption between 2000 and 2015. *Proceedings of the National Academy of Sciences of the United States of America,* 115**,** E3463-E3470.

Klemm, P., Krogfelt, K., Hedegaard, L. & Christiansen, G. 1990. The major subunit of *Escherichia coli* type 1 fimbriae is not required for D-mannose-specific adhesion. *Molecular microbiology,* 4**,** 553-559.

Klemm, P., Roos, V., Ulett, G. C., Svanborg, C. & Schembri, M. A. 2006. Molecular characterization of the *Escherichia coli* asymptomatic bacteriuria strain 83972: the taming of a pathogen. *Infection and immunity,* 74**,** 781-785.

König, B. & König, W. 1993. Induction and suppression of cytokine release (tumour necrosis factor-alpha; interleukin-6, interleukin-1 beta) by *Escherichia coli* pathogenicity factors (adhesions, alpha-haemolysin). *Immunology,* 78**,** 526.

Kostakioti, M., Hadjifrangiskou, M. & Hultgren, S. J. 2013a. Bacterial Biofilms: Development, Dispersal, and Therapeutic Strategies in the Dawn of the Postantibiotic Era. 3.

Kostakioti, M., Hadjifrangiskou, M. & Hultgren, S. J. 2013b. Bacterial biofilms: development, dispersal, and therapeutic strategies in the dawn of the postantibiotic era. *Cold Spring Harb Perspect Med,* 3**,** a010306.

Krussel, E., Kishony, R., Balaban, N. & Leibler, S. 2005. Bacterial persistence: A model of survival in changing encironment. *Genetics,* 169**,** 1807-1814.

Kunin, C. M. 1997. *Urinary tract infections. Detection, prevention, and management*, Williams & Wilkins.

Lane, M. C. & Mobley, H. L. T. 2007. Role of P-fimbrial-mediated adherence in pyelonephritis and persistence of uropathogenic *Escherichia coli* (UPEC) in the mammalian kidney. *Kidney International,* 72**,** 19-25.

Langermann, S., Mollby, R., Burlein, J. E., Palaszynski, S. R., Auguste, C. G., Defusco, A., Strouse, R., Schenerman, M. A., Hultgren, S. J., Pinkner, J. S., Winberg, J., Guldevall, L., Soderhall, M., Ishikawa, K., Normark, S. & Koenig, S. 2000. Vaccination with FimH adhesin protects cynomolgus monkeys from colonization and infection by uropathogenic *Escherichia coli*. *J Infect Dis,* 181**,** 774-8.

Lara-Tejero, M. A. & Galán, J. E. 2001. CdtA, CdtB, and CdtC form a tripartite complex that is required for cytolethal distending toxin activity. *Infection and immunity,* 69**,** 4358-4365.

L**eavis, H. L., Willems, R. J., Top, J. & Bonten, M. J. J. J. O. C. M.** 2006. High-level ciprofloxacin resistance from point mutations in gyrA and parC confined to global hospital-adapted clonal lineage CC17 of Enterococcus faecium. 44**,** 1059-1064.

Lecointre, G., Rachdi, L., Darlu, P. & Denamur, E. 1998. *Escherichia coli* molecular phylogeny using the incongruence length difference test. *Mol Biol Evol,* 15**,** 1685-95.

Leffler, H. & Svanborg-Eden, C. 1981. Glycolipid receptors for uropathogenic *Escherichia coli* on human erythrocytes and uroepithelial cells. *Infection and immunity,* 34**,** 920-929.

Lemon, K. P., Higgins, D. E. & Kolter, R. 2007. Flagellar motility is critical for Listeria monocytogenes biofilm formation. *Journal of bacteriology,* 189**,** 4418-4424.

Lesage, A. 1897. Contribution a l'étude des entérites infantiles—sérodiagnostic des races de Bacterium coli. *CR Soc Biol (Paris),* 49**,** 900-1.

Lewis, A. J., Richards, A. C. & Mulvey, M. A. 2016. Invasion of Host Cells and Tissues by Uropathogenic Bacteria. *Microbiology spectrum,* 4**,** 10.1128/microbiolspec.UTI-0026-2016.

Li, H. & Durbin, R. 2009. Fast and accurate short read alignment with Burrows–Wheeler transform. *bioinformatics,* 25**,** 1754-1760.

Liu, J., Duncan, K. & Walsh, C. T. 1989. Nucleotide sequence of a cluster of *Escherichia coli* enterobactin biosynthesis genes: identification of entA and purification of its product 2,3-dihydro-2,3-dihydroxybenzoate dehydrogenase. *Journal of Bacteriology,* 171**,** 791-798.

Lloyd, A. L., Smith, S. N., Eaton, K. A. & Mobley, H. L. 2009. Uropathogenic *Escherichia coli* suppresses the host inflammatory response via pathogenicity island genes sisA and sisB. *Infection and immunity,* 77**,** 5322-5333.

Loomis, L. D. & Raymond, K. N. 1991. Solution equilibria of enterobactin and metal-enterobactin complexes. *Inorganic Chemistry,* 30**,** 906-911.

López-Banda, D. A., Carrillo-Casas, E. M., Leyva-Leyva, M., Orozco-Hoyuela, G., Manjarrez-Hernández, Á. H., Arroyo-Escalante, S., Moncada-Barrón, D., Villanueva-Recillas, S., Xicohtencatl-Cortes, J. & Hernández-Castro, R. 2014. Identification of virulence factors genes in *Escherichia coli* isolates from women with urinary tract infection in Mexico. *BioMed research international,* 2014.

Louden, B. C., Haarmann, D. & Lynne, A. M. 2011. Use of Blue Agar CAS Assay for Siderophore Detection. *Journal of microbiology & biology education,* 12**,** 51-53.

Luna-Pineda, V. M., Ochoa, S. A., Cruz-Córdova, A., Cázares-Domínguez, V., Reyes-Grajeda, J. P., Flores-Oropeza, M. A., Arellano-Galindo, J., Castro-Hernández, R., Flores-Encarnación, M., Ramírez-Vargas, A., Flores-García, H. J., Moreno-Fierros, L. & Xicohtencatl-Cortes, J. 2018. Features of urinary *Escherichia coli* isolated from children with complicated and uncomplicated urinary tract infections in Mexico. *PLOS ONE,* 13**,** e0204934.

Malekzadegan, Y., Khashei, R., Sedigh Ebrahim-Saraie, H. & Jahanabadi, Z. 2018. Distribution of virulence genes and their association with antimicrobial resistance among uropathogenic *Escherichia coli* isolates from Iranian patients. *BMC Infectious Diseases,* 18**,** 572.

Mao, C., Abraham, D., Wattam, A. R., Wilson, M. J., Shukla, M., Yoo, H. S. & Sobral, B. W. 2014. Curation, Integration And Visualization Of Bacterial Virulence Factors In Patric. *Bioinformatics,* 31**,** 252-258.

Martinez, J. J., Mulvey, M. A., Schilling, J. D., Pinkner, J. S. & Hultgren, S. J. 2000a. Type 1 pilus-mediated bacterial invasion of bladder epithelial cells. *The EMBO journal,* 19**,** 2803-2812.

Martinez, J. J., Mulvey, M. A., Schilling, J. D., Pinkner, J. S. & Hultgren, S. J. 2000b. Type 1 pilus-mediated bacterial invasion of bladder epithelial cells. *The EMBO journal,* 19**,** 2803-2812.

Martínez, J. L. & Baquero, F. J. C. M. R. 2002. Interactions among strategies associated with bacterial infection: pathogenicity, epidemicity, and antibiotic resistance. 15**,** 647-679.

Matsumoto, T. J. C. U. R. 2001. Urinary tract infections in the elderly. 2**,** 330-333.

Mclellan, L. K. & Hunstad, D. A. 2016. Urinary Tract Infection: Pathogenesis and Outlook. *Trends in Molecular Medicine,* 22**,** 946-957.

Melnyk, A. H., Wong, A. & Kassen, R. 2015. The fitness costs of antibiotic resistance mutations. *Evolutionary applications,* 8**,** 273-283.

Microbiology& Infection 2003. Determination of minimum inhibitory concentrations (MICs) of antibacterial agents by broth dilution. 9**,** ix-xv.

Miethke, M. & Marahiel, M. A. 2007. Siderophore-based iron acquisition and pathogen control. *Microbiology and Molecular Biology Reviews,* 71**,** 413-451.

Mignini, L., Carroli, G., Abalos, E., Widmer, M., Amigot, S., Nardin, J. M., Giordano, D., Merialdi, M., Arciero, G. & Del Carmen Hourquescos, M. 2009. Accuracy of diagnostic tests to detect asymptomatic bacteriuria during pregnancy. *Obstetrics & Gynecology,* 113**,** 346-352.

Miller, M. C., Fetherston, J. D., Pickett, C. L., Bobrov, A. G., Weaver, R. H., Demoll, E. & Perry, R. D. 2010. Reduced synthesis of the Ybt siderophore or production of aberrant Ybt-like molecules activates transcription of yersiniabactin genes in Yersinia pestis. *Microbiology,* 156**,** 2226-2238.

Mills, M. & Payne, S. M. J. J. O. B. 1995. Genetics and regulation of heme iron transport in Shigella dysenteriae and detection of an analogous system in *Escherichia coli* O157: H7. 177**,** 3004-3009.

Minardi, D., Montanari, M. P., Tili, E., Cochetti, I., Mingoia, M., Varaldo, P. E. & Muzzonigro, G. 2008. Effects of fluoroquinolones on bacterial adhesion and on preformed biofilm of strains isolated from urinary double J stents. *J Chemother,* 20**,** 195-201.

Mobley, H. L., Donnenberg, M. S. & Hagan, E. C. 2009. Uropathogenic *Escherichia coli.* *EcoSal Plus,* 3.

Mobley, H. L., Jarvis, K. G., Elwood, J. P., Whittle, D. I., Lockatell, C., Russell, R. G., Johnson, D. E., Donnenberg, M. S. & Warren, J. W. 1993. Isogenic P-fimbrial

deletion mutants of pyelonephritogenic *Escherichia coli*: the role of α Gal (1–4) β Gal binding in virulence of a wild-type strain. *Molecular microbiology,* 10**,** 143-155.

Momtaz, H., Karimian, A., Madani, M., Dehkordi, F. S., Ranjbar, R., Sarshar, M. & Souod, N. 2013. Uropathogenic *Escherichia coli* in Iran: serogroup distributions, virulence factors and antimicrobial resistance properties. *Annals of clinical microbiology and antimicrobials,* 12**,** 8.

Morrissey, I., Hackel, M., Badal, R., Bouchillon, S., Hawser, S. & Biedenbach, D. 2013. A Review of Ten Years of the Study for Monitoring Antimicrobial Resistance Trends (SMART) from 2002 to 2011. *Pharmaceuticals (Basel, Switzerland),* 6**,** 1335-1346.

Muhammad, I., Uzma, M., Yasmin, B., Mehmood, Q. & Habib, B.** 2011. Prevalence of antimicrobial resistance and integrons in *Escherichia coli* from Punjab, Pakistan. *Brazilian Journal of Microbiology,* 42**,** 462-466.

Mulvey, M. A. 2002. Adhesion and entry of uropathogenic *Escherichia coli*. *Cellular Microbiology,* 4**,** 257-271.

Mulvey, M. A., Lopez-Boado, Y. S., Wilson, C. L., Roth, R., Parks, W. C., Heuser, J. & Hultgren, S. J. J. S. 1998. Induction and evasion of host defenses by type 1-piliated uropathogenic *Escherichia coli*. 282**,** 1494-1497.

Mulvey, M. A., Schilling, J. D., Martinez, J. J. & Hultgren, S. J. J. P. O. T. N. A. O. S. 2000. Bad bugs and beleaguered bladders: interplay between uropathogenic *Escherichia coli* and innate host defenses. 97**,** 8829-8835.

Mysorekar, I. U. & Hultgren, S. J. 2006. Mechanisms of uropathogenic *Escherichia coli* persistence and eradication from the urinary tract. *Proceedings of the National Academy of Sciences of the United States of America,* 103**,** 14170-14175.

Mysorekar, I. U., Mulvey, M. A., Hultgren, S. J. & Gordon, J. I. 2002. Molecular regulation of urothelial renewal and host defenses during infection with uropathogenic *Escherichia coli*. *J Biol Chem,* 277**,** 7412-9.

Nagamatsu, K., Hannan, T. J., Guest, R. L., Kostakioti, M., Hadjifrangiskou, M., Binkley, J., Dodson, K., Raivio, T. L. & Hultgren, S. J. J. P. O. T. N. A. O. S. 2015. Dysregulation of *Escherichia coli* α-hemolysin expression alters the course of acute and persistent urinary tract infection. 201500374.

Najar, M. S., Saldanha, C. L. & Banday, K. A. 2009. Approach to urinary tract infections. *Indian Journal of Nephrology,* 19**,** 129-139.

Naves, P., Del Prado, G., Huelves, L., Gracia, M., Ruiz, V., Blanco, J., Dahbi, G., Blanco, M., Ponte Mdel, C. & Soriano, F. 2008. Correlation between virulence factors and in vitro biofilm formation by *Escherichia coli* strains. *Microb Pathog,* 45**,** 86-91.

Naves, P., Del Prado, G., Ponte, C. & Soriano, F. 2010. Differences in the in vitro susceptibility of planktonic and biofilm-associated *Escherichia coli* strains to antimicrobial agents. *Journal of Chemotherapy,* 22**,** 312-317.

Neilands, J. 1981a. Iron absorption and transport in microorganisms. *Annual review of nutrition,* 1**,** 27-46.

Neilands, J. B. 1981b. Microbial iron compounds. *Annual review of biochemistry,* 50**,** 715-731.

Nicolas-Chanoine, M.-H., Bertrand, X. & Madec, J.-Y. 2014. *Escherichia coli* ST131, an intriguing clonal group. *Clinical microbiology reviews,* 27**,** 543-574.

Nielubowicz, G. R. & Mobley, H. L. J. N. R. U. 2010. Host–pathogen interactions in urinary tract infection. 7**,** 430.

Nowicki, B., Labigne, A., Moseley, S., Hull, R., Hull, S. & Moulds, J. 1990. The Dr hemagglutinin, afimbrial adhesins AFA-I and AFA-III, and F1845 fimbriae of uropathogenic and diarrhea-associated *Escherichia coli* belong to a family of hemagglutinins with Dr receptor recognition. *Infection and immunity,* 58**,** 279-281.

O'brien, V. P., Hannan, T. J., Nielsen, H. V. & Hultgren, S. J. 2016. Drug and Vaccine Development for the Treatment and Prevention of Urinary Tract Infections. *Microbiol Spectr,* 4.

O'neill, J. 2014. AMR Review Paper–Tackling a crisis for the health and wealth of nations.

Oelschlaeger, T. A., Dobrindt, U. & Hacker, J. 2002. Virulence factors of uropathogens. *Current opinion in urology,* 12**,** 33-38.

Okhuysen, P. C. & Dupont, H. L. 2010. Enteroaggregative *Escherichia coli* (EAEC): a cause of acute and persistent diarrhea of worldwide importance. The University of Chicago Press.

Opal, S. M., Cross, A. S., Gemski, P. & Lyhte, L. W. 1990. Aerobactin and α-hemolysin as virulence determinants in *Escherichia coli* isolated from human blood, urine, and stool. *Journal of Infectious Diseases,* 161**,** 794-796.

Organization, W. H. O. J. G. W. H. 2017. Global priority list of antibiotic-resistant bacteria to guide research, discovery, and development of new antibiotics.

Ott, M., Hoschützky, H., Jann, K., Van Die, I. & Hacker, J. 1988. Gene clusters for S fimbrial adhesin (sfa) and F1C fimbriae (foc) of *Escherichia coli*: comparative aspects of structure and function. *Journal of bacteriology,* 170**,** 3983-3990.

Ozenberger, B. A., Brickman, T. J. & Mcintosh, M. A. 1989. Nucleotide sequence of *Escherichia coli* isochorismate synthetase gene entC and evolutionary relationship of isochorismate synthetase and other chorismate-utilizing enzymes. *Journal of bacteriology,* 171**,** 775-783.

Paauw, A., Leverstein-Van Hall, M. A., Van Kessel, K. P. M., Verhoef, J. & Fluit, A. C. 2010. Yersiniabactin Reduces the Respiratory Oxidative Stress Response of Innate Immune Cells. *PLOS ONE,* 4**,** e8240.

Parham, N. J., Srinivasan, U., Desvaux, M., Foxman, B., Marrs, C. F. & Henderson, I. R. 2004. PicU, a second serine protease autotransporter of uropathogenic *Escherichia coli*. *FEMS microbiology letters,* 230**,** 73-83.

Parish, A. & Holliday, K. 2012. Long-Term Care Acquired Urinary Tract Infections' Antibiotic Resistance Patterns and Empiric Therapy: A Pilot Study. *Geriatric Nursing,* 33**,** 473-478.

Paterson, D. L. 2004. "Collateral damage" from cephalosporin or quinolone antibiotic therapy. *Clin Infect Dis,* 38 Suppl 4**,** S341-5.

Peiffer, I., Servin, A. L., Bernet-Camard, M. 1998. Piracy of decay-accelerating factor (CD55) signal transduction by the diffusely adhering strain *Escherichia coli* C1845 promotes cytoskeletal F-actin rearrangements in cultured human intestinal INT407 cells. *Immunity,* 66**,** 4036-4042.

Peigne, C., Bidet, P., Mahjoub-Messai, F., Plainvert, C., Barbe, V., Médigue, C., Frapy, E., Nassif, X., Denamur, E., Bingen, E. & Bonacorsi, S. 2009. The Plasmid of *Escherichia coli* Strain S88 (O45:K1:H7) That Causes Neonatal Meningitis Is Closely Related to Avian Pathogenic *E. coli* Plasmids and Is Associated with High-Level Bacteremia in a Neonatal Rat Meningitis Model. *Infection and Immunity,* 77**,** 2272-2284.

Peirano, G. & Pitout, J. D. 2010. Molecular epidemiology of *Escherichia coli* producing CTX-M β-lactamases: the worldwide emergence of clone ST131 O25: H4. *International journal of antimicrobial agents,* 35**,** 316-321.

Peralta, D. R., Adler, C., Corbalán, N. S., Paz García, E. C., Pomares, M. F. & Vincent, P. A. 2016. Enterobactin as Part of the Oxidative Stress Response Repertoire. *PloS one,* 11**,** e0157799-e0157799.

Pinkner, J. S., Remaut, H., Buelens, F., Miller, E., Aberg, V., Pemberton, N., Hedenstrom, M., Larsson, A., Seed, P., Waksman, G., Hultgren, S. J. & Almqvist, F. 2006. Rationally designed small compounds inhibit pilus biogenesis in uropathogenic bacteria. *Proc Natl Acad Sci U S A,* 103**,** 17897-902.

Pitout, J. D. & Devinney, R. 2017. *Escherichia coli* ST131: a multidrug-resistant clone primed for global domination. *F1000Res,* 6.

Plançon, L., Du Merle, L., Le Friec, S., Gounon, P., Jouve, M., Guignot, J., Servin, A. & Le Bouguénec, C. J. C. M. 2003. Recognition of the cellular β1-chain integrin by the bacterial AfaD invasin is implicated in the internalization of afa-expressing pathogenic *Escherichia coli* strains. 5**,** 681-693.

Plos, K., Connell, H., Jodal, U., Marklund, B.-I., Mårild, S., Wettergren, B. & Svanborg, C. 1995. Intestinal carriage of P fimbriated *Escherichia coli* and the susceptibility to urinary tract infection in young children. *Journal of Infectious Diseases,* 171**,** 625-631.

Poggio, T. V., La Torre, J. L. & Scodeller, E. A. 2006. Intranasal immunization with a recombinant truncated FimH adhesin adjuvanted with CpG oligodeoxynucleotides protects mice against uropathogenic *Escherichia coli* challenge. *Can J Microbiol,* 52**,** 1093-102.

Pompilio, A., Crocetta, V., Savini, V., Petrelli, D., Di Nicola, M., Bucco, S., Amoroso, L., Bonomini, M. & Di Bonaventura, G. 2018. Phylogenetic relationships, biofilm formation, motility, antibiotic resistance and extended virulence genotypes among *Escherichia coli* strains from women with community-onset primitive acute pyelonephritis. *PLOS ONE,* 13**,** e0196260.

Poole, N. M., Green, S. I., Rajan, A., Vela, L. E., Zeng, X. L., Estes, M. K. & Maresso, A. W. 2017. Role for FimH in Extraintestinal Pathogenic *Escherichia coli* Invasion and Translocation through the Intestinal Epithelium. *Infect Immun,* 85.

Posey, J. E. & Gherardini, F. C. 2000. Lack of a Role for Iron in the Lyme Disease Pathogen. *Science,* 288**,** 1651-1653.

Quainoo, S., Coolen, J. P. M., Van Hijum, S. A. F. T., Huynen, M. A., Melchers, W. J. G., Van Schaik, W. & Wertheim, H. F. L. 2017. Whole-Genome Sequencing of Bacterial Pathogens: the Future of Nosocomial Outbreak Analysis. 30**,** 1015-1063.

Rahman, S. U., Ali, T., Muhammad, N., Umer, T., Saddique, Ahmad, S., Ayaz, S. & Han, B. Characterization and mechanism of dissemination of extended spectrum beta lactamase producers *Escherichia coli* in food producing animals in Pakistan and China.

2018 15th International Bhurban Conference on Applied Sciences and Technology (IBCAST), 9-13 Jan. 2018 2018. 203-214.

Rahn, D. D. 2008. Urinary tract infections: contemporary management. *Urol Nurs,* 28**,** 333-341.

Ramzan, M., Bakhsh, S., Salam, A., Khan, G. M. & Mustafa, G. 2004. Risk factors in urinary tract infection. *Gomal Journal of Medical Sciences,* 2.

Raz, R., Gennesin, Y., Wasser, J., Stoler, Z., Rosenfeld, S., Rottensterich, E. & Stamm, W. E. 2000a. Recurrent urinary tract infections in postmenopausal women. *Clinical Infectious Diseases,* 30**,** 152-156.

Raz, R., Gennesin, Y., Wasser, J., Stoler, Z., Rosenfeld, S., Rottensterich, E. & Stamm, W. E. J. C. I. D. 2000b. Recurrent urinary tract infections in postmenopausal women. 30**,** 152-156.

Reigstad, C. S., Hultgren, S. J. & Gordon, J. I. 2007a. Functional Genomic Studies of Uropathogenic *Escherichia coli* and Host Urothelial Cells when Intracellular Bacterial Communities Are Assembled. *Journal of Biological Chemistry,* 282**,** 21259-21267.

Reigstad, C. S., Hultgren, S. J. & Gordon, J. I. 2007b. Functional genomic studies of uropathogenic *Escherichia coli* and host urothelial cells when intracellular bacterial communities are assembled. 282**,** 21259-21267.

Reyna-Flores, F., Barrios, H., Garza-Ramos, U., Sánchez-Pérez, A., Rojas-Moreno, T., Uribe-Salas, F. J., Fagundo-Sierra, R. & Silva-Sanchez, J. 2013. Molecular epidemiology of *Escherichia coli* O25b-ST131 isolates causing community-acquired UTIs in Mexico. *Diagnostic Microbiology and Infectious Disease,* 76**,** 396-398.

Rijavec, M., Müller-Premru, M., Zakotnik, B. & Žgur-Bertok, D. 2008. Virulence factors and biofilm production among *Escherichia coli* strains causing bacteraemia of urinary tract origin. *Journal of medical microbiology,* 57**,** 1329-1334.

Rizvi, R. M. & Siddiqui, K. M. 2010. Recurrent urinary tract infections in females. *Journal of the Pakistan Medical Association,* 60**,** 55.

Roberts, J. A., Marklund, B.-I., Ilver, D., Haslam, D., Kaack, M. B., Baskin, G., Louis, M., Möllby, R., Winberg, J. & Normark, S. 1994. The Gal (alpha 1-4) Gal-specific tip adhesin of *Escherichia coli* P-fimbriae is needed for pyelonephritis to occur in the normal urinary tract. *Proceedings of the National Academy of Sciences,* 91**,** 11889-11893.

Robino, L., Scavone, P., Araujo, L., Algorta, G., Zunino, P. & Vignoli, R. 2013. Detection of intracellular bacterial communities in a child with *Escherichia coli* recurrent urinary tract infections. *Pathog Dis,* 68**,** 78-81.

Roche, E. D. & Walsh, C. T. 2003. Dissection of the EntF Condensation Domain Boundary and Active Site Residues in Nonribosomal Peptide Synthesis. *Biochemistry,* 42**,** 1334-1344.

Ronald, A. 2002. The etiology of urinary tract infection: traditional and emerging pathogens. *The American journal of medicine,* 113**,** 14-19.

Rosen, D. A., Hooton, T. M., Stamm, W. E., Humphrey, P. A. & Hultgren, S. J. 2007. Detection of intracellular bacterial communities in human urinary tract infection. *PLoS medicine,* 4**,** e329-e329.

Roux, D., Danilchanka, O., Guillard, T., Cattoir, V., Aschard, H., Fu, Y., Angoulvant, F., Messika, J., Ricard, J. D., Mekalanos, J. J., Lory, S., Pier, G. B. & Skurnik, D. 2015. Fitness cost of antibiotic susceptibility during bacterial infection. *Sci Transl Med,* 7**,** 297ra114.

Rubin, R. H., Shapiro, E. D., Andriole, V. T., Davis, R. J. & Stamm, W. E. 1992. Evaluation of New Anti-Infective Drugs for the Treatment of Urinary Tract Infection. *Clinical Infectious Diseases,* 15**,** S216-S227.

Sabir, S., Anjum, A. A., Ijaz, T. & Ali, M. A. 2014. Isolation and antibiotic susceptibility of *E. coli* from urinary tract infections in a tertiary care hospital. *Pakistan journal of medical sciences,* 30**,** 389.

Saldaña, Z., De La Cruz, M. A., Carrillo-Casas, E. M., Durán, L., Zhang, Y., Hernández-Castro, R., Puente, J. L., Daaka, Y. & Girón, J. A. 2014. Production of the *Escherichia coli* common pilus by uropathogenic *E. coli* is associated with adherence to HeLa and HTB-4 cells and invasion of mouse bladder urothelium. *PloS one,* 9**,** e101200-e101200.

Salvador, E., Wagenlehner, F., Köhler, C.-D., Mellmann, A., Hacker, J., Svanborg, C. & Dobrindt, U. 2012. Comparison of asymptomatic bacteriuria *Escherichia coli* isolates from healthy individuals versus those from hospital patients shows that long-term bladder colonization selects for attenuated virulence phenotypes. *Infection and immunity,* 80**,** 668-678.

Sana, T., Rami, K., Racha, B., Fouad, D., Marcel, A., Hassan, M., Sani, H. & Monzer, H. 2011. Detection of genes TEM, OXA, SHV and CTX-M in 73 clinical isolates of

Escherichia coli producers of extended spectrum Beta-lactamases and determination of their susceptibility to antibiotics. *Int Arab J Antimicrob Agents,* 1**,** 1-6.

Sauer, F. G., Remaut, H., Hultgren, S. J. & Waksman, G. 2004. Fiber assembly by the chaperone–usher pathway. *Biochimica et Biophysica Acta (BBA)-Molecular Cell Research,* 1694**,** 259-267.

Scaletsky, I. C., Fabbricotti, S. H., Carvalho, R. L., Nunes, C. R., Maranhao, H. S., Morais, M. B. & Fagundes-Neto, U. 2002. Diffusely adherent *Escherichia coli* as a cause of acute diarrhea in young children in Northeast Brazil: a case-control study. *Journal of clinical microbiology,* 40**,** 645-648.

Schembri, M. A. & Klemm, P. 2001. Biofilm formation in a hydrodynamic environment by novel FimH variants and ramifications for virulence. *Infection and immunity,* 69**,** 1322-1328.

Schroeder, M., Brooks, B. & Brooks, A. J. G. 2017a. The complex relationship between virulence and antibiotic resistance. 8**,** 39.

Schroeder, M., Brooks, B. D. & Brooks, A. E. 2017b. The Complex Relationship between Virulence and Antibiotic Resistance. *Genes,* 8**,** 39.

Schubert, S., Cuenca, S., Fischer, D. & Heesemann, J. 2000a. High-pathogenicity island of Yersinia pestis in Enterobacteriaceae isolated from blood cultures and urine samples: prevalence and functional expression. *The Journal of infectious diseases,* 182**,** 1268-1271.

Schubert, S., Cuenca, S., Fischer, D. & Heesemann, J. 2000b. High-pathogenicity island of Yersinia pestis in enterobacteriaceae isolated from blood cultures and urine samples: prevalence and functional expression. *J Infect Dis,* 182**,** 1268-71.

Schwartz, D. J., Chen, S. L., Hultgren, S. J. & Seed, P. C. 2011. Population dynamics and niche distribution of uropathogenic *Escherichia coli* during acute and chronic urinary tract infection. *Infection and immunity,* 79**,** 4250-4259.

Shaik, S., Ranjan, A., Tiwari, S. K., Hussain, A., Nandanwar, N., Kumar, N., Jadhav, S., Semmler, T., Baddam, R. & Islam, M. A. 2017. Comparative Genomic Analysis of Globally Dominant ST131 Clone with Other Epidemiologically Successful Extraintestinal Pathogenic *Escherichia coli* (ExPEC) Lineages. *mBio,* 8**,** e01596-17.

Sheikh, M., Khan, M., Khatoon, A. & Arain, G. 2000. Incidence of urinary tract infection during pregnancy. *Eastern Mediterranean health journal,* 6**,** 265-271.

Shon, A. S., Bajwa, R. P. & Russo, T. A. 2013. Hypervirulent (hypermucoviscous) Klebsiella pneumoniae: a new and dangerous breed. *Virulence,* 4**,** 107-18.

Siegfried, L., Kmeťová, M., Puzova, H., Molokáčová, M. & Filka, J. J. J. O. M. M. 1994. Virulence-associated factors in *Escherichia coli* strains isolated from children with urinary tract infections. 41**,** 127-132.

Skaar, E. P. 2010. The battle for iron between bacterial pathogens and their vertebrate hosts. *PLoS Pathog,* 6**,** e1000949.

Slater, B. S., Clabots, C., Porter, S., Johnston, B. D., Johnson, J. R., Kisiela, D., Sokurenko, E. V., Davis, G., Price, L. B., Aziz, M., Debroy, C., Pomputius, W., Ender, P. T., Cooperstock, M., Banerjee, R. & Miller, S. 2016. Household Clustering of *Escherichia coli* Sequence Type 131 Clinical and Fecal Isolates According to Whole Genome Sequence Analysis. *Open Forum Infectious Diseases,* 3.

Smelov, V., Naber, K. & Johansen, T. E. B. 2016a. Improved classification of urinary tract infection: future considerations. *European Urology Supplements,* 15**,** 71-80.

Smelov, V., Naber, K. & Johansen, T. E. B. 2016b. Improved classification of urinary tract infection: future considerations. 15**,** 71-80.

Smith, Y. C., Rasmussen, S. B., Grande, K. K., Conran, R. M. & O'brien, A. D. 2008. Hemolysin of Uropathogenic *Escherichia coli* Evokes Extensive Shedding of the Uroepithelium and Hemorrhage in Bladder Tissue within the First 24 Hours after Intraurethral Inoculation of Mice. *Infection and Immunity,* 76**,** 2978-2990.

SNYDER, J. A., HAUGEN, B. J., BUCKLES, E. L., LOCKATELL, C. V., JOHNSON, D. E., DONNENBERG, M. S., WELCH, R. A. & MOBLEY, H. L. 2004. Transcriptome of uropathogenic *Escherichia coli* during urinary tract infection. *Infection and immunity,* 72**,** 6373-6381.

Sohail, M., Khurshid, M., Saleem, H. G. M., Javed, H. & Khan, A. A. 2015. Characteristics and Antibiotic Resistance of Urinary Tract Pathogens Isolated From Punjab, Pakistan. *Jundishapur journal of microbiology,* 8**,** e19272-e19272.

Sokurenko, E. V., Vogel, V., Thomas, W. E. J. C. H. & Microbe 2008. Catch-bond mechanism of force-enhanced adhesion: counterintuitive, elusive, but… widespread? 4**,** 314-323.

Soto, S. M. 2014. Importance of biofilms in urinary tract infections: new therapeutic approaches. *Advances in Biology,* 2014.

Spangler, B. D. 1992. Structure and function of cholera toxin and the related *Escherichia coli* heat-labile enterotoxin. *Microbiological reviews,* 56**,** 622-647.

Spurbeck, R. R. & Mobley, H. L. 2013. Uropathogenic *Escherichia coli*. *Escherichia coli: pathotypes and principles of pathogenesis,* 275.

Spurbeck, R. R., Stapleton, A. E., Johnson, J. R., Walk, S. T., Hooton, T. M. & Mobley, H. L. 2011. Fimbrial profiles predict virulence of uropathogenic *Escherichia coli* strains: contribution of ygi and yad fimbriae. *Infection and immunity,* 79**,** 4753-4763.

Stamm, W. E. 1982. Recent developments in the diagnosis and treatment of urinary tract infections. *Western Journal of Medicine,* 137**,** 213.

Steigedal, M., Marstad, A., Haug, M., Damås, J. K., Strong, R. K., Roberts, P. L., Himpsl, S. D., Stapleton, A., Hooton, T. M., Mobley, H. L. T., Hawn, T. R. & Flo, T. H. 2014. Lipocalin 2 imparts selective pressure on bacterial growth in the bladder and is elevated in women with urinary tract infection. *Journal of immunology (Baltimore, Md. : 1950),* 193**,** 6081-6089.

Strömberg, N., Nyholm, P.-G., Pascher, I. & Normark, S. 1991. Saccharide orientation at the cell surface affects glycolipid receptor function. *Proceedings of the National Academy of Sciences,* 88**,** 9340-9344.

Struve, C. & Krogfelt, K. A. 1999. In vivo detection of *Escherichia coli* type 1 fimbrial expression and phase variation during experimental urinary tract infection. *Microbiology,* 145**,** 2683-2690.

Suits, M. D., Lang, J., Pal, G. P., Couture, M. & Jia, Z. J. P. S. 2009. Structure and heme binding properties of *Escherichia coli* O157: H7 ChuX. 18**,** 825-838.

Suits, M. D., Pal, G. P., Nakatsu, K., Matte, A., Cygler, M. & Jia, Z. J. P. O. T. N. A. O. S. 2005. Identification of an *Escherichia coli* O157: H7 heme oxygenase with tandem functional repeats. 102**,** 16955-16960.

Svanborg Eden, C., Jodal, U., Hanson, L., Lindberg, U. & Sohl Åkerlund, A. 1976. Variable adherence to normal human urinary-tract epithelial cells of *Escherichia coli* strains associated with various forms of urinary-tract infection. *The Lancet,* 308**,** 490-492.

Tandogdu, Z. & Wagenlehner, F. M. 2016a. Global epidemiology of urinary tract infections. *Curr Opin Infect Dis,* 29**,** 73-9.

Tandogdu, Z. & Wagenlehner, F. M. 2016b. Global epidemiology of urinary tract infections. *Current opinion in infectious diseases,* 29**,** 73-79.

Tanvir, R., Hafeez, R. & Hasnain, S. 2012. Prevalence of multiple drug resistant *Escherichia coli* in patients of urinary tract infection registering at a diagnostic laboratory in Lahore Pakistan. *Pak J Zool,* 44**,** 707-12.

Tarchouna, M., Ferjani, A., Ben-Selma, W. & Boukadida, J. 2013. Distribution of uropathogenic virulence genes in *Escherichia coli* isolated from patients with urinary tract infection. *International Journal of Infectious Diseases,* 17**,** e450-e453.

T**erlizzi, M. E., Gribaudo, G. & Maffei, M. E.** 2017a. UroPathogenic *Escherichia coli* (UPEC) Infections: Virulence Factors, Bladder Responses, Antibiotic, and Non-antibiotic Antimicrobial Strategies. *Frontiers in Microbiology,* 8**,** 1566.

Terlizzi, M. E., Gribaudo, G. & Maffei, M. E. 2017b. UroPathogenic *Escherichia coli* (UPEC) Infections: Virulence Factors, Bladder Responses, Antibiotic, and Non-antibiotic Antimicrobial Strategies. 8.

ThANASSI, D. G., BLISKA, J. B. & CHRISTIE, P. J. 2012. Surface organelles assembled by secretion systems of Gram-negative bacteria: diversity in structure and function. *FEMS Microbiol Rev,* 36**,** 1046-82.

Thompson, J. M., Jones, H. A. & Perry, R. D. 1999. Molecular Characterization of the Hemin Uptake Locus (hmu) from Yersinia pestis and Analysis ofhmu Mutants for Hemin and Hemoprotein Utilization. *Infection and Immunity,* 67**,** 3879.

Throup, J. P., Koretke, K. K., Bryant, A. P., Ingraham, K. A., Chalker, A. F., Ge, Y., Marra, A., Wallis, N. G., Brown, J. R., Holmes, D. J., Rosenberg, M. & Burnham, M. K. 2000. A genomic analysis of two-component signal transduction in Streptococcus pneumoniae. *Mol Microbiol,* 35**,** 566-76.

Thumbikat, P., Berry, R. E., Zhou, G., Billips, B. K., Yaggie, R. E., Zaichuk, T., Sun, T.-T., Schaeffer, A. J. & Klumpp, D. J. 2009. Bacteria-induced uroplakin signaling mediates bladder response to infection. *PLoS pathogens,* 5**,** e1000415.

Torres, A. G. & Payne, S. M. J. M. M. 1997. Haem iron-transport system in enterohaemorrhagic *Escherichia coli* O157: H7. 23**,** 825-833.

Totsika, M., Moriel, D. G., Idris, A., Rogers, B. A., Wurpel, D. J., Phan, M. D., Paterson, D. L. & Schembri, M. A. 2012a. Uropathogenic *Escherichia coli* mediated urinary tract infection. *Curr Drug Targets,* 13**,** 1386-99.

Totsika, M., Wells, T. J., Beloin, C., Valle, J., Allsopp, L. P., King, N. P., Ghigo, J.-M. & Schembri, M. A. 2012b. Molecular characterization of the EhaG and UpaG trimeric autotransporter proteins from pathogenic *Escherichia coli*. *Applied and environmental microbiology,* 78**,** 2179-2189.

Touati, D. 2000. Iron and oxidative stress in bacteria. *Archives of biochemistry and biophysics,* 373**,** 1-6.

Toutain, C. M., Caizza, N. C., Zegans, M. E. & O'toole, G. A. 2007. Roles for flagellar stators in biofilm formation by Pseudomonas aeruginosa. *Research in microbiology,* 158**,** 471-477.

Trautner, B. W. & Darouiche, R. O. 2004. Role of biofilm in catheter-associated urinary tract infection. *American journal of infection control,* 32**,** 177-183.

Triveda, L. & Gomathi, S. 2016. Detection of biofilm formation among the clinical isolates of Enterococci: An evaluation of three different screening methods. *Int. J. Curr. Microbiol. App. Sci,* 5**,** 643-650.

Turnidge, J. D., Gottlieb, T., Mitchell, D. H., Coombs, G. W., Daley, D. A. & Bell, J. M. J. C. D. I. Q. R. 2014. Community-onset Gram-negative Surveillance Program annual report, 2012. 38**,** E49-E53.

Uhlén, P., Laestadius, Å., Jahnukainen, T., Söderblom, T., Bäckhed, F., Celsi, G., Brismar, H., Normark, S., Aperia, A. & Richter-Dahlfors, A. 2000. α-Haemolysin of uropathogenic *E. coli* induces Ca 2+ oscillations in renal epithelial cells. *Nature,* 405**,** 694-697.

Ulett, G. C., Totsika, M., Schaale, K., Carey, A. J., Sweet, M. J. & Schembri, M. A. 2013. Uropathogenic *Escherichia coli* virulence and innate immune responses during urinary tract infection. *Current Opinion in Microbiology,* 16**,** 100-107.

Ullah, A., Shah, S. & Almugadam, B. 2018. Prevalence of symptomatic urinary tract infections and antimicrobial susceptibility patterns of isolated uropathogens in kohat region of Pakistan. *MOJ Biol Med,* 3**,** 85-89.

Ullah, F., Malik, S. & Ahmed, J. 2009. Antibiotic susceptibility pattern and ESBL prevalence in nosocomial *Escherichia coli* from urinary tract infections in Pakistan. *African Journal of Biotechnology,* 8.

Väisänen, V., Tallgren, L., Helena Mäkelä, P., Källenius, G., Hultberg, H., Elo, J., Siitonen, A., Svanborg-Edén, C., Svenson, S. & Korhonen, T. 1981. Mannose-resistant haemagglutination and P antigen recognition are characteristic of *Escherichia coli* causing primary pyelonephritis. *The Lancet,* 318**,** 1366-1369.

Valdebenito, M., Crumbliss, A. L., Winkelmann, G. & Hantke, K. 2006. Environmental factors influence the production of enterobactin, salmochelin, aerobactin, and yersiniabactin in *Escherichia coli* strain Nissle 1917. *Int J Med Microbiol,* 296**,** 513-20.

Valle, J., Mabbett, A. N., Ulett, G. C., Toledo-Arana, A., Wecker, K., Totsika, M., Schembri, M. A., Ghigo, J.-M. & Beloin, C. 2008. Upag, A New member of the

trimeric autotransporter family of adhesins in uropathogenic *Escherichia coli*. *Journal of bacteriology,* 190**,** 4147-4161.

Varani, A. M., Siguier, P., Gourbeyre, E., Charneau, V. & Chandler, M. 2011. ISsaga is an ensemble of web-based methods for high throughput identification and semi-automatic annotation of insertion sequences in prokaryotic genomes. *Genome Biology,* 12**,** R30.

Velasco, M., Horcajada, J. P., Mensa, J., Martinez, A. M., Vila, J., Martinez, J. A., Ruiz, J., Barranco, M., Roig, G. & Soriano, E. 2001. Decreased Invasive Capacity of Quinolone-Resistant *Escherichia coli* in Patients with Urinary Tract Infections. *Clinical Infectious Diseases,* 33**,** 1682-1686.

Vielva, L., De Toro, M., Lanza, V. F. & De La Cruz, F. 2017. PLACNETw: a web-based tool for plasmid reconstruction from bacterial genomes. *Bioinformatics,* 33**,** 3796-3798.

Vigil, P. D., Alteri, C. J. & Mobley, H. L. 2011. Identification of in vivo-induced antigens including an RTX family exoprotein required for uropathogenic *Escherichia coli* virulence. *Infection and immunity,* 79**,** 2335-2344.

Virkola, R., Westerlund, B., Holthöfer, H., Parkkinen, J., Kekomäki, M. & Korhonen, T. K. 1988. Binding characteristics of *Escherichia coli* adhesins in human urinary bladder. *Infection and immunity,* 56**,** 2615-2622.

Visvikis, O., Boyer, L., Torrino, S., Doye, A., Lemonnier, M., Lorès, P., Rolando, M., Flatau, G., Mettouchi, A. & Bouvard, D. 2011a. *Escherichia coli* Producing CNF1 Toxin Hijacks Tollip to Trigger Rac1-Dependent Cell Invasion. *Traffic,* 12**,** 579-590.

Visvikis, O., Boyer, L., Torrino, S., Doye, A., Lemonnier, M., Lorès, P., Rolando, M., Flatau, G., Mettouchi, A., Bouvard, D., Veiga, E., Gacon, G., Cossart, P. & Lemichez, E. 2011b. *Escherichia coli* Producing CNF1 Toxin Hijacks Tollip to Trigger Rac1-Dependent Cell Invasion. *Traffic,* 12**,** 579-590.

Vranes, J., Schonwald, S. & Zagar, Z. 1994. [Relation between P-fimbriae and resistance to amoxicillin, carbenicillin and tetracycline in uropathogenic strains of *Escherichia coli*]. *Lijec Vjesn,* 116**,** 178-81.

Walk, S. T., Alm, E. W., Calhoun, L. M., Mladonicky, J. M. & Whittam, T. S. 2007. Genetic diversity and population structure of *Escherichia coli* isolated from freshwater beaches. *Environ Microbiol,* 9**,** 2274-88.

Wandersman, C. & Stojiljkovic, I. J. C. O. I. M. 2000. Bacterial heme sources: the role of heme, hemoprotein receptors and hemophores. 3**,** 215-220.

Wang, A., Wang, Q., Kudinha, T., Xiao, S. & Zhuo, C. 2016. Effects of Fluoroquinolones and Azithromycin on Biofilm Formation of Stenotrophomonas maltophilia. *Scientific reports,* 6.

Warren, J. W., Mobley, H. L. & Trifillis, A. L. 1988. Internalization of *Escherichia coli* into human renal tubular epithelial cells. *J Infect Dis,* 158**,** 221-3.

Wattam, A. R., Abraham, D., Dalay, O., Disz, T. L., Driscoll, T., Gabbard, J. L., Gillespie, J. J., Gough, R., Hix, D., Kenyon, R., Machi, D., Mao, C., Nordberg, E. K., Olson, R., Overbeek, R., Pusch, G. D., Shukla, M., Schulman, J., Stevens, R. L., Sullivan, D. E., Vonstein, V., Warren, A., Will, R., Wilson, M. J. C., Yoo, H. S., Zhang, C., Zhang, Y. & Sobral, B. W. 2014. PATRIC, the bacterial bioinformatics database and analysis resource. *Nucleic Acids Research,* 42**,** D581-D591.

Wattam, A. R., Davis, J. J., Assaf, R., Boisvert, S., Brettin, T., Bun, C., Conrad, N., Dietrich, E. M., Disz, T. & Gabbard, J. L. 2016. Improvements to PATRIC, the all-bacterial bioinformatics database and analysis resource center. *Nucleic acids research,* 45**,** D535-D542.

Watts, R. E., Totsika, M., Challinor, V. L., Mabbett, A. N., Ulett, G. C., De Voss, J. J., Schembri, M. A. J. I. & Immunity 2012. Contribution of siderophore systems to growth and urinary tract colonization of asymptomatic bacteriuria *Escherichia coli*. 80**,** 333-344.

Welch, R. A., Burland, V., Plunkett, G., 3rd, Redford, P., Roesch, P., Rasko, D., Buckles, E. L., Liou, S. R., Boutin, A., Hackett, J., Stroud, D., Mayhew, G. F., Rose, D. J., Zhou, S., Schwartz, D. C., Perna, N. T., Mobley, H. L. T., Donnenberg, M. S. & Blattner, F. R. 2002. Extensive mosaic structure revealed by the complete genome sequence of uropathogenic *Escherichia coli*. *Proceedings of the National Academy of Sciences of the United States of America,* 99**,** 17020-17024.

WiLES, T. J., KULESUS, R. R. & MULVEY, M. A. 2008a. Origins and virulence mechanisms of uropathogenic *Escherichia coli*. *Experimental and molecular pathology,* 85**,** 11-19.

Wiles, T. J., Kulesus, R. R. & Mulvey, M. A. 2008b. Origins and virulence mechanisms of uropathogenic< i> *Escherichia coli</i>*. *Experimental and molecular pathology,* 85**,** 11-19.

Woodford, N., Carattoli, A., Karisik, E., Underwood, A., Ellington, M. J. & Livermore, D. M. 2009. Complete nucleotide sequences of plasmids pEK204, pEK499, and pEK516, encoding CTX-M enzymes in three major *Escherichia coli* lineages from the

United Kingdom, all belonging to the international O25:H4-ST131 clone. *Antimicrob Agents Chemother,* 53**,** 4472-82.

World Health Organization %J Who: Geneva, S. 2017. WHO publishes list of bacteria for which new antibiotics are urgently needed.

World Health Organization %J World Health Organization, G., Switzerland. ACCESSED 2016. Antimicrobial resistance. Draft global action plan on antimicrobial resistance. Report by the secretariat. 24.

Wu, X.-R., Kong, X.-P., Pellicer, A., Kreibich, G. & Sun, T.-T. J. K. I. 2009. Uroplakins in urothelial biology, function, and disease. 75**,** 1153-1165.

Xie, B., Zhou, G., Chan, S.-Y., Shapiro, E., Kong, X.-P., Wu, X.-R., Sun, T.-T. & Costello, C. E. J. J. O. B. C. 2006. Distinct Glycan Structures of Uroplakins Ia and Ib structural basis for the selective binding of FimH adhesin to uroplakin Ia. 281**,** 14644-14653.

Yamamoto, S., Terai, A., Yuri, K., Kurazono, H., Takeda, Y. & Yoshida, O. 1995. Detection of urovirulence factors in *Escherichia coli* by multiplex polymerase chain reaction. *FEMS Immunology and Medical Microbiology,* 12**,** 85-90.

Yun, K. W., Kim, H. Y., Park, H. K., Kim, W. & Lim, I. S. 2014. Virulence factors of uropathogenic *Escherichia coli* of urinary tract infections and asymptomatic bacteriuria in children. *Journal of Microbiology, Immunology and Infection,* 47**,** 455-461.

Zdziarski, J., Svanborg, C., Wullt, B., Hacker, J. & Dobrindt, U. 2008. Molecular Basis of Commensalism in the Urinary Tract: Low Virulence or Virulence Attenuation? *Infection and Immunity,* 76**,** 695-703.

Zhang, J., Zheng, B., Zhao, L., Wei, Z., Ji, J., Li, L. & Xiao, Y. 2014. Nationwide high prevalence of CTX-M and an increase of CTX-M-55 in *Escherichia coli* isolated from patients with community-onset infections in Chinese county hospitals. *BMC Infectious Diseases,* 14**,** 659.

Zhang, L. & Foxman, B. 2003. Molecular epidemiology of *Escherichia coli* mediated urinary tract infections. *Frontiers in bioscience: a journal and virtual library,* 8**,** e235-44.

Zhao, L., Gao, S., Huan, H., Xu, X., Zhu, X., Yang, W., Gao, Q. & Liu, X. 2009. Comparison of virulence factors and expression of specific genes between uropathogenic *Escherichia coli* and avian pathogenic *E. coli* in a murine urinary tract infection model and a chicken challenge model. *Microbiology,* 155**,** 1634-1644.

Zong, Z. 2013. Complete sequence of pJIE186-2, a plasmid carrying multiple virulence factors from a sequence type 131 *Escherichia coli* O25 strain. *Antimicrobial Agents and Chemotherapy,* 57**,** 597-600.

Zowawi, H. M., Harris, P. N. A., Roberts, M. J., Tambyah, P. A., Schembri, M. A., Pezzani, M. D., Williamson, D. A. & Paterson, D. L. 2015. The emerging threat of multidrug-resistant Gram-negative bacteria in urology. *Nature Reviews Urology,* 12**,** 570.